The regulation of cellular microRNAs during KSHV lytic replication

Becky Ann Foster

Submitted in accordance with the requirements for the degree of

Doctor of Philosophy

The University of Leeds

Faculty of Biological Sciences

School of Molecular and Cellular Biology

February 2022

The candidate confirms that the work submitted is her own and that appropriate credit has been given where reference has been made to the work of others.

Acknowledgements

First of all, I would like to express my gratitude to my supervisor Professor Adrian Whitehouse for all his support during my time in his research group. His guidance throughout my PhD studies has been invaluable.

I've met some of the most amazing friends while being at Leeds, including those of the Whitehouse group. Thank you for making my time here that much more enjoyable. I've had some of the best times with you guys and while I know that they'll be more, I already miss seeing you guys every day!

Many thanks to the University of Leeds NGS facility and Ummey Hany for carrying out the miR-Seq and Dr Anthony Anene at the Queens Mary University of London (QMUL) for performing miRNA bioinformatics analysis.

I would also like to thank the BBSRC and the University of Leeds for partly funding this work for the last 4 (and a bit) years.

To my family, I'm extremely grateful for all the help you've given me over the many, many years I've spent studying. It has ultimately contributed to getting me to this point and I will always appreciate that so much.

Finally, a massive thank you to Dan. Both your support and comfort throughout my PhD has helped me more than you can imagine. I'm very much looking forward to what's next ... and one of your Margs!

Abstract

Kaposi's sarcoma-associated herpesvirus (KSHV) is a human tumour virus and the causative agent of Kaposi's sarcoma (KS), as well as multiple lymphoproliferative diseases. As is characteristic of all herpesviruses, KSHV can undergo both latent and lytic replication cycles. During latent infection, viral gene expression is limited, enabling persistence of the viral genome. Whereas lytic replication is characterised by the abundant transcription of viral genes, and the production and release of infectious virions. Interestingly, both of these cycles are important for KSHV pathogenesis.

Viruses have developed numerous mechanisms to manipulate host mRNA expression. Indeed, the dysregulation of cellular miRNAs has emerged as a common mechanism utilised by viruses to influence the host cell transcriptome during infection.

In chapter 3, the differential expression of cellular miRNAs was investigated following KSHV lytic reactivation. Notably miR-142-3p and miR-25-p were found to be downregulated. Importantly, overexpression of these miRNAs had a significant impact on KSHV lytic replication, culminating in a substantial reduction in the production of infectious virions.

In Chapter 4, GPRC5A was identified as a direct target of miR-142-3p, with the KSHV-mediated downregulation of miR-142-3p thought to contribute to the upregulation of GPRC5A expression during KSHV lytic replication. Subsequent analysis implicated GPRC5A in the regulation of actin dynamics as well as a potential involvement in lipid raft stability. Both of which may enhance viral egress and dissemination.

Finally, in Chapter 5 investigations were undertaken to determine the potential mechanisms involved in the regulation of miR-142-3p expression. Results highlighted ORF50 and ADAR editing as potential factors involved in the downregulation of miR-142-3p following KSHV lytic reactivation.

To summarise, this study identifies a number of previously unidentified host cell interactions during KSHV lytic replication, which could prove valuable targets for the development of novel therapeutic approaches.

Contents

List of figures

List of tables

Abbreviations

%	percentage
~	approximately
>	more than
°C	degrees Celsius
α	Alpha
β	beta
γ	gamma
ε	epsilon
κ	kappa
µg	microgram
µl	microlitre
µm	micrometre
µM	micromolar

293T	HEK 293T
8-Aza	8-Azaadenosine
A	Amp
AD	Alzheimer's disease
ADAR	Adenosine deaminases acting on RNA
AGO	Argonaute
AIDS	Acquired immune deficiency syndrome
AP	Adaptor protein
AP-MS	Affinity purification- Mass spectrometry
APP	Amyloid precursor protein
APS	Ammonium Persulfate
ARID3B	AT-Rich Interaction Domain 3B
ART	Anti-retroviral therapies
ASO	Antisense oligonucleotide
ATG	Autophagy Related
ATCC	American Type Culture Collection
ATP	Adenosine triphosphate
BACE1	Beta-secretase 1
BARTs	BamHI A rightward transcripts
BCA	Bicinchoninic acid
BCBL	Body cavity-based lymphoma
bp	Base pair
BSA	Bovine serum albumin
BVDV	Bovine Virus Diarrhoea Virus
bZIP	Basic leucine zipper domain
C/EBPα	CCAAT/enhancer-binding protein alpha
cDNA	Complementary DNA

CDS	Coding DNA sequence
C.elegans	*Caenorhabditis elegans*
CCR4-NOT	Catabolite repression 4- negative on TATA-less
CCV	Channel Catfish Herpesvirus
CDK6	Cyclin Dependent Kinase 6
CGI	CpG island
ChIP	Chromatin immunoprecipitation
circRNA	Circular RNA
CLL	Chronic lymphoid leukaemia
CMV	Cytomegalovirus
CPM	Counts per million
CR2	Complement receptor type 2
CRC	Colorectal Cancer cells
CTL	Cytotoxic T cell
CXCL8	C-X-C Motif Chemokine Ligand 8
DCP2	Decapping mRNA 2
DC-SIGN	DC-specific intercellular adhesion molecule-3 grabbing nonintegrin
DDX6	DEAD-Box Helicase 6
DE	Delayed early
DENV	Dengue virus
DGCR8	DiGeorge syndrome critical region 8
DLBCL	Diffuse large B-cell lymphoma
DLL4	Delta Like Canonical Notch Ligand 4
DMEM	Dulbecco's modified Eagles medium
DNMT	DNA (cytosine-5)-methyltransferase
DMSO	Dimethylsulphoxide
DNA	Deoxyribonucleic acid
DNase	Deoxyribonuclease
Dox	Doxycycline hyclate
ds	Double stranded
dT	Deoxythymidine
DTT	Dithiothreitol
EBNA	Epstein-Barr nuclear antigen
EBV	Epstein-Barr virus
EC	Endothelial cell
ECL	Enhanced chemiluminescence
EDTA	Ethylenediaminetetraacetic acid disodium salt
eIF4E	Eukaryotic Translation Initiation Factor 4E
EphA2	Ephrin receptor tyrosine kinase A2
EV71	Enterovirus 71
EZH2	Enhancer of zeste homolog 2
F-actin	Filamentous actin
FBS	Foetal bovine serum

FC	Fold- change
FDA	Food and drug administration
FLIP	FLICE-inhibitory protein
FLOT	Flotillin
g	Gram
g	Gravitational force
GaHV	Gallid herpesvirus
GAPDH	Glyceraldehyde 3-phosphate dehydrogenase
gB	Glycoprotein B
GFP	Green Fluorescent Protein
gH	Glycoprotein H
gL	Glycoprotein L
gM	Glycoprotein M
gN	Glycoprotein N
gp	Glycoprotein
GPRC5A	G Protein-Coupled Receptor Class C Group 5 Member A
GTP	Guanosine triphosphate
H3K9	Histone H3 lysine 9
HA	Hemagglutinin
HAART	Highly active antiretroviral therapy
HBV	Hepatitis B virus
HCl	Hydrochloric acid
HCC	Hepatocellular carcinoma
HCMV	Human cytomegalovirus
HCV	Hepatitis C virus
HDAC5	Histone deacetylase 5
HEK	Human embryonic kidney
HFF	Human foreskin fibroblast
HHV	Human herpesvirus
HIF	Hypoxia-inducible factor
HITS-CLIP	High-throughput sequencing of RNA isolated by crosslinking immunoprecipitation
HIV	Human immunodeficiency virus
HLA	Human leukocyte antigen
HPV	Human papillomavirus
HRE	Hypoxia response element
HRP	Horseradish peroxidase
hrs	Hours
HS	Heparan sulphate
Hsa	human
HSC70	Heat shock cognate 71 kDa protein
HSPA1A	Heat Shock Protein Family A (Hsp70) Member 1A
HSP90	Heat shock protein 90

HSUR	Herpesvirus saimiri U RNA
HSV	Herpes simplex virus
HT	High- throughput
HVS	Herpesvirus saimiri
IAV	Influenza virus
ICP	Infected-cell polypeptide
ICTV	International Committee on Taxonomy of Viruses
IE	Immediate early
IgG	Immunoglobulin G
IFN	Interferon
IFNAR	IFN alpha receptor
IKK	IκB kinase
IL-10	Interleukin-10
IL-6	Interleukin-6
IM	Infectious mononucleosis
IR	Internal repeat
IRAK	Interleukin-1 receptor associated kinase
IRES	Internal ribosome entry site
IRF	Interferon regulatory factor
IRIS	Immune reconstitution inflammatory syndrome
ISG	Interferon stimulated gene
JAK	Janus Kinase
JC	John Cunningham
JEV	Japanese encephalitis virus
Kb	Kilobase
Kbp	Kilobase pair
KD	Knockdown
KDM6A	Lysine Demethylase 6A
KICS	KSHV inflammatory cytokine syndrome
KS	Kaposi's Sarcoma
KSHV	Kaposi's Sarcoma associated herpesvirus
L	Late
LAMP	Latency-associated membrane protein
LANA	Latency-associated nuclear antigen
LAR	Latency associated region
LATs	Latency-associated transcripts
LEC	Lymphatic endothelial cell
LLB	Leeds Lysis Buffer
LMO3	LIM Domain Only 3
LMP	Latent membrane proteins
LNA	Locked nucleic acid
LncRNA	Long non-coding RNA
LPD	lymphoproliferative disorder

LTAg	Large T antigen
LTR	Long terminal repeat
Luc	Luciferase
MALAT1	Metastasis associated lung adenocarcinoma transcript 1
MASP	Mannan-binding lectin serine protease
MCC	Merkle cell carcinoma
MCD	Multicentric Castleman's disease
MCF-7	Michigan Cancer Foundation-7
MCMV	Murine cytomegalovirus
MCV	Merkel cell polyomavirus
MDV	Marek's disease virus
MICB	MHC Class I Polypeptide-Related Sequence B
miDGE	miRNA discovery by forced genomic expression
miRDE	microRNA decay element
mins	minutes
miRNA	MicroRNA
miR-Seq	miRNA sequencing
ml	Millilitre
mM	Millimolar
MRE	miRNA response element
mRNA	Messenger RNA
MSP	Methylation specific PCR
MTA	mRNA transcript accumulation
m6A	N^6-Methyladenosine
n	Sample size
NaCl	Sodium chloride
NcRNA	Non-coding RNA
NaF	Sodium fluoride
Na4O7P2	Sodium pyrophosphate
Nef	Negative Regulatory Factor
NFTs	Neurofibrillary tangle
NF-κB	Nuclear factor kappaB
NGS	Next generation sequencing
NK	Natural killer
nm	Nanometre
nM	Nanomolar
NPC	Nuclear pore complex
nts	Nucleotides
OBP	Ori-lyt binding protein
OCT4	Octamer-binding transcription factor 4
ORF	Open reading frame
Ori-Lyt	Lytic origin of DNA replication
Ori-P	Latent origin of DNA replication

O/N	Overnight
p	P-value
P bodies	Processing bodies
PAGE	Polyacrylamide gel electrophoresis
PAN	Polyadenylated nuclear
PARCLIP	Photoactivatable ribonucleoside-enhanced crosslinking and immunoprecipitation
PAZ	Piwi Argonaut and Zwille
PBS	Phosphate buffered saline
PCBP2	Poly (RC) Binding Protein 2
PCR	Polymerase chain reaction
pds	Partially double stranded
PEL	Primary effusion lymphoma
PKM1	Pyruvate kinase M
PML	Progressive multifocal leukoencephalopathy
PNS	Peripheral nervous system
Poly(A)	Polyadenylated
POU5F1	POU class 5 homeobox 1
Pre-miRNA	Precursor miRNA
Pri-miRNA	Primary miRNA
PTL	Post- transplant lymphoma
PTLDs	Post-transplant lymphoproliferative diseases
PyVs	Polyomaviruses
qPCR	Quantitative PCR
RA	Rheumatoid arthritis
RAC1	Ras-related C3 botulinum toxin substrate 1
RBP-jκ	Recombination signal-binding protein 1 for J-kappa
RDA	Representational difference analysis
RhoA	Ras homolog family member A
RIIID	RNase III domain
RING	Really interesting new gene
RLU	Relative light unit
RISC	RNA-induced silencing complex
RNA	Ribonucleic acid
RNAi	RNA interference
RNAP	RNA polymerase II
RNase	Ribonuclease
ROCK	Rho-associated protein kinase
RPM	Revolutions per minute
RPMI	Roswell Park Memorial Institute medium
RRE	RTA response element
RT	Reverse transcription
RTA	Replication and transcription activator

Secs	Seconds
Scr	Scrambled control siRNA
SD	Standard deviation
SDS	Sodium dodecyl sulphate
SND1	Staphylococcal nuclease domain-containing protein 1
SNP	Single nucleotide polymorphism
SOX	Shutoff and exonuclease
SP1	Specificity protein 1
SPFH	Stomatin/prohibitin/flotillin/HflK/HflC
SSA	Sub-Saharan Africa
STAT	Signal Transducer and Activator of Transcription
TAR	Trans-activation response
TBS	Tris buffered saline
TCR	T cell receptor
TDMD	Target RNA-directed miRNA degradation
TEMED	N-N-N'-N'-tetramethylethylenediamine
TF	Transcription factor
TNF	Tumor necrosis factor
TNTase	Terminal transferase
TPM1	Tropomyosin 1
TR	Terminal repeat
TRAF	Tumor necrosis factor receptor–associated factor
TRBP	Transactivation response element RNA-binding protein
Tris	Tris(hydroxymethyl)aminoethane
TSS	Transcription start site
U_L	Unique long region
USA	United States of America
U_S	Unique short region
UTR	Untranslated region
V	Volts
v/v	Volume per volume
VV	Vaccinia virus
vFLIP	Viral FLICE inhibitory protein
vIL-6	Viral interleukin 6
vIRF	Viral interferon regulatory factor
v-miRNA	Virally-encoded miRNA
VSV	Varicella-zoster virus
WT	Wild-type
w/v	Weight per volume
Xbp	X-box binding protein
XPO5	Exportin 5
XRN1	Exoribonuclease

Nucleic acid bases

A	Adenine
C	Cytosine
G	Guanine
T	Thymine
I	Inosine
U	Uracil

Amino acids

Alanine	Ala	A
Arginine	Arg	R
Asparagine	Asn	N
Aspartate	Asp	D
Cysteine	Cys	C
Glutamate	Glu	E
Glutamine	Gln	Q
Glycine	Gly	G
Histidine	His	H
Isoleucine	Ile	I
Leucine	Leu	L
Lysine	Lys	K
Methionine	Met	M
Phenylalanine	Phe	F
Proline	Pro	P
Serine	Ser	S
Threonine	Thr	T
Tryptophan	Trp	W
Tyrosine	Tyr	Y
Valine	Val	V

Chapter 1

~

Introduction

1 Introduction

1.1 *Herpesviridae*

1.1.1 Classification of Herpesviruses

Herpesviruses are a large, distinct class of viruses that share common virion architecture and morphology. All members of the *Herpesvirales* order developed from a common primordial ancestor and the point of evolutionary divergence is estimated to be approximately 180-220 million years ago (McGeoch et al., 1995).

The International Committee of the Taxonomy of Viruses (ICTV) first established the genus *Herpesvirus* in 1971. However, following the recommendation of the Herpesvirus study group, the ICTV elevated the *Herpesviridae* to order and subsequently became known as *Herpesvirales* in 2009, which contained three virus families. The revised *Herpesviridae* maintained mammal, avian and reptile viruses while herpesviruses of fish and amphibians and those of invertebrates were separated into *Alloherpesviridae* and *Malacoherpesviridae,* respectively (Summarised in table 1.1) (Davison et al., 2009). These alterations became increasingly necessary owing to the discovery of large genetic distance between members of the former *herpesviridae*; indeed, fish and mollusc herpesviruses are only distantly related to those of birds and mammals (Fauquet et al., 2005).

Table 1.1. The Herpesvirales overview

Family	Animal	Number of members
Herpesviridae	Mammals, avian and reptile	115
Alloherpesviridae	Bony fish and Amphibians	13
Malacoherpesviridae	Mollusc and sea snail	2

Original classification was primarily based on biological properties including host range, site of infection, cytotoxicity, and length of reproduction cycle (Roizmann et al., 1992). However, following advancements in genome sequencing, that assignment shifted towards genome comparison (Davison et al., 2009).

As of February 2022, ICTV states that the *Herpesvirales* order contains 130 species that are distributed across three families (ictvonline.org). The largest of these families; the

Herpesviridae is further separated into three distinct subfamilies the *Alpha-*, *Beta-* and *Gammaherpesvirinae* **(Figure 1.1)** (Matthews, 1979).

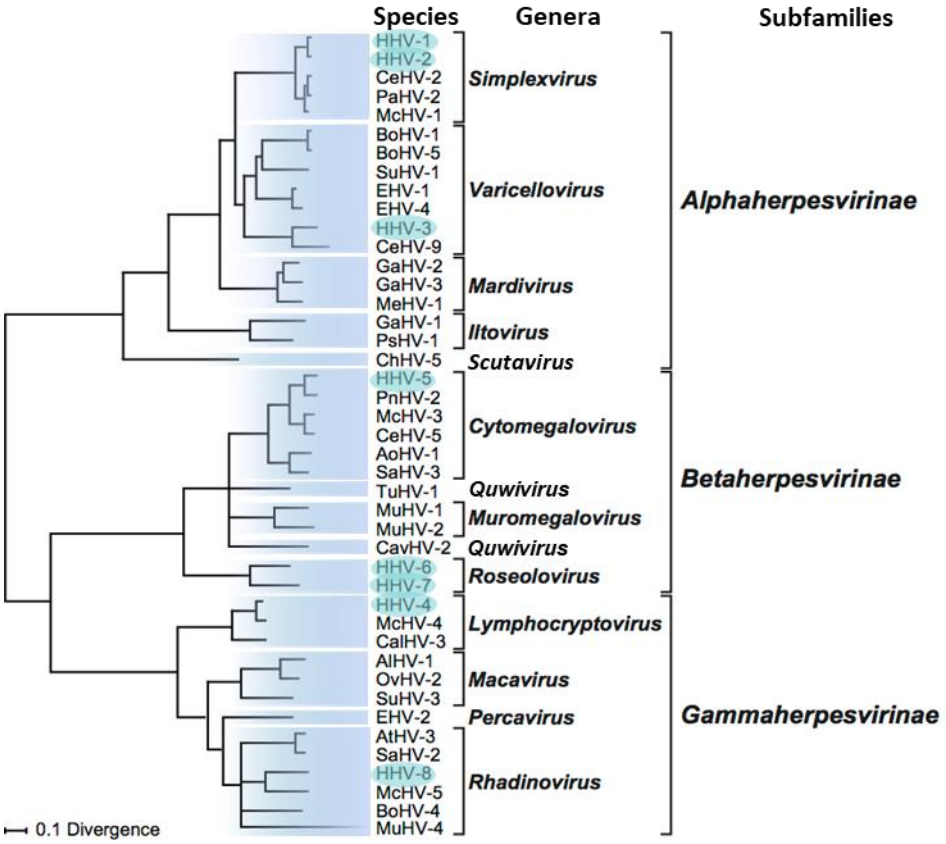

Figure 1.1 Phylogenetic tree of the *Herpesviridae*. A Phylogenetic tree of select members of the *Herpesviridae* based of amino acid sequence alignment. Human herpesviruses including Kaposi's sarcoma-associated herpesvirus (KSHV, HHV-8) are highlighted in green. Adapted from (McGeoch et al., 2008).

1.1.1.1 *Alphaherpesvirinae*

Herpesviruses belonging to the *Alphaherpesvirinae* possess a number of features that distinguish them from those of other subfamilies, including a broad host range and a rapid replication cycle (Whitley and Roizman, 2001). Furthermore, *Alphaherpesvirinae* establish latency in neuronal cells, predominantly primary sensory ganglia while lytic replication often takes place in epidermal cells (Stevens and Cook, 1971). The most clinically relevant members of the *Alphaherpesvirinae* include herpes Simplex virus (HSV) I and II (human herpes [HHV] 1/2) and varicella-Zoster virus (VSV, HHV-3), which belong to the *Simplexvirus* and *Varicellovirus* genus, respectively. HSV 1/2 can cause both orolabial and genital herpes, while VSV is the causative agent of chickenpox in children

and shingles in adults. Additionally, the *Alphaherpesvirinae* contains a number of important animal pathogens, including Marek's disease virus (MDV, GaHV-2) of the *Mardivirus* genus, which causes a commercially important neoplastic disease in chickens and turkeys (Biggs, 2001).

1.1.1.2 *Betaherpesvirinae*

In contrast to members of the *Alphaherpesvirinae*, those belonging to the *Betaherpesvirinae* are noted for having a restricted host range and a relatively slow reproduction cycle. Betaherpesviruses also primarily establish latent infection in secretory glands (Whitley, 1996). Moreover, infected cells are often found to be enlarged forming characteristic cytomegaly, which is exemplified by human cytomegalovirus (HCMV, HHV-5). The *Betaherpesvirinae* includes three other human herpesviruses; HHV-6A, HHV-6B and HHV-7 of the *Roseolovirus* genus.

1.1.1.3 *Gammaherpesvirinae*

Members belonging to the *Gammaherpesvirinae* have a narrow host range, only infecting those that belong to the family or order of its natural host. Latent infection of gammaherpesviruses occurs in lymphoblastoid cells primarily T or B lymphocytes, while certain members of this subfamily are able to lytically replicate in epithelial cells and fibroblasts (Flaño et al., 2002) (Li et al., 1992). The *Gammaherpesvirinae* currently contains two important human pathogens; Epstein-Barr virus (EBV, HHV-4) and Kaposi's sarcoma-associated herpesvirus (KSHV, HHV-8), which are members of the *lymphocrytovirus* and *Rhadinovirus* genus, respectively.

1.1.2 Virion structure

Members of the *Herpesvirales* order share a unique virion architecture and morphology **(Figure 1.2)**, indeed prior to advancements in genome sequencing these common structural features were used in their taxonomic classification (Davison et al., 2009). Herpesviruses have a large, linear, double stranded (ds) DNA genome that is packaged into an icosahedral capsid (Furlong et al., 1972). The icosahedron structure, possessing T=16 symmetry, is formed from 162 capsomers and has a final diameter of ~125-130 nm. A single pentameric capsomere, located at the icosahedral 5-fold symmetry axis is replaced by the so-called portal vertex, which allows both DNA egress and packaging (Cardone et al., 2007). In addition to the nucleocapsid, virions consist of two other distinct structures, tegument, and the viral envelope. Tegument, an amorphous proteinaceous layer surrounds the viral capsid and proteins within the tegument are thought to have diverse roles in host cell shut, reactivation from latency, immune evasion and capsid transport (Kelly et al., 2009). While the viral envelope contains several virally-encoded glycoproteins which perform important viral entry functions, facilitating both host cell attachment and membrane fusion events (Mettenleiter et al., 2009). Due to the varying thickness of the tegument layer, the final size of virions varies from 100-300 nm in diameter.

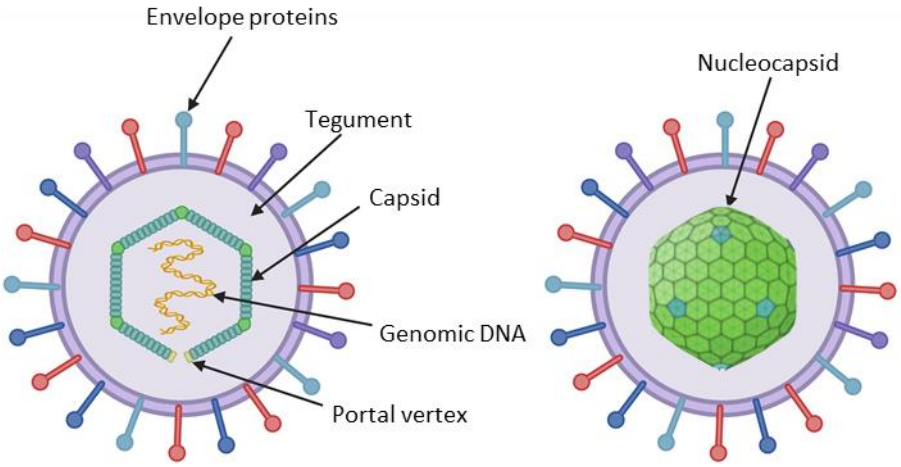

Figure 1.2 Herpesvirus virion structure. A schematic of a herpesvirus virion with key structural components indicated. Figure adapted from Viral structures and antibodies, abcam®.

1.1.3 Genomic structure

The genetic material of herpesviruses comprises of a single, linear dsDNA and depending on the species can range from 125-291 kbp (Honess, 1984). *Herpesviridae* genomes can be classified into six distinct types based on the organisation of unique and direct or inverted repeat sequences **(Figure 1.3)** (McGeoch et al., 2008)(Davison, 2007).

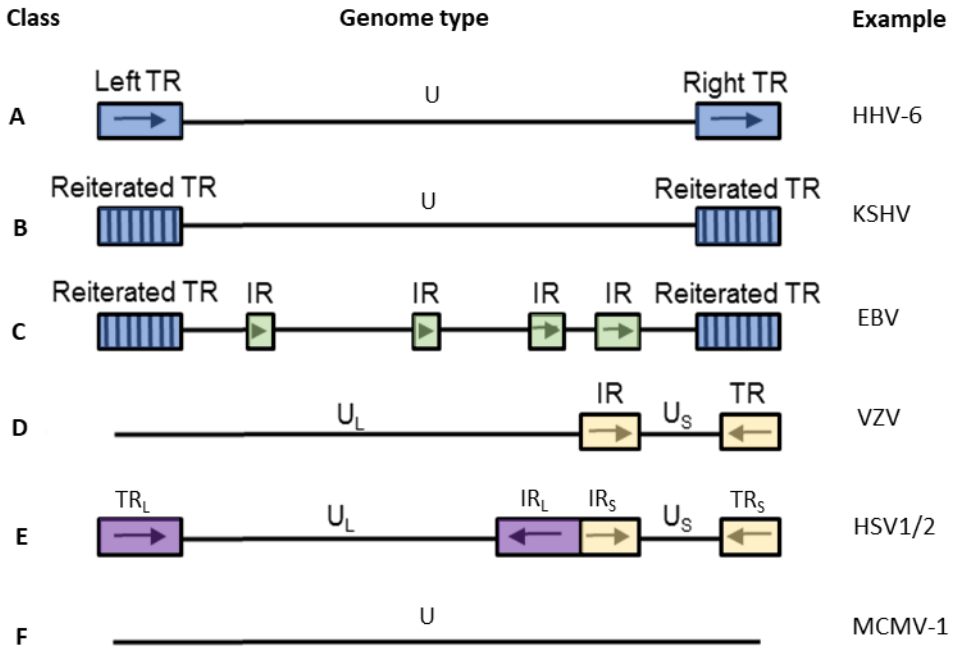

Figure 1.3 Types of herpesvirus genome arrangements. The genomes of different herpesviruses exist in six distinct arrangements. All contain a unique region that is represented by a line, while various repeat regions are indicated by colour coded boxes. Direct repeats (Blue), Inverted repeats (yellow). The orientation of the gene element is indicated by an arrowhead. Abbreviations: TR - terminal repeat; IR – internal repeat; U_L – unique long region; U_S – unique short region; HHV-6- Human herpesvirus 6; KSHV- Kaposi associated herpesvirus; EBV- Epstein Barr virus; VZV-Varicella zoster virus; HSV1/2- Herpes simplex virus 1 and 2; MCMV-1- Murine cytomegalovirus 1. Adapted from (McGeoch et al., 2008).

The class A genome contains a central unique region that is flanked by two large identical terminal repeats (TR). These direct repeats can range from ~30 bp to several kbp. This genome class was first described for Channel Catfish Herpesvirus (CCV) (Chousterman et al., 1979) and the Betaherpesvirus HHV-6 has since been recognized as a member (Lindquester and Pellet, 1991). Class B genomes are characteristic for the majority of the *Gammaherpesvirinae,* including KSHV (Russo et al., 1996). These genomes contain a central unique region with direct terminal repeats however they are tandemly repeated

sequences of varying copy number ranging from 0.8- 2.3 kbp. Genomes of Class C are similar to those of class B however in addition to tandemly repeated terminal sequences they also contain several unrelated internal repeats (IR), which are located throughout the unique genome region. The gammaherpesvirus, EBV has this arrangement (Given and Kieff, 1979). Class D genomes characteristically contain a unique long (U_L) and unique short (U_S) sequence, which are created by two inverted repeats, one located internally and the other at a terminus. VZV provides an example of a class D genome (Dumas et al., 1981). The class E genome was first described for HSV-1 and represents the most complex genome structure (Sheldrick and Berthelot, 1975). This genome is similar to class D however the U_L and U_S are flanked by distinct inverted repeat sequences. In contrast class F genomes are relatively simple and contain no extended DNA repeat sequences. This class is represented by MCMV-1, a member of the *Betaherpesvirinae* (Roizmann et al., 1981).

Notably, all genome classes are found throughout the *Alpha-*, *Beta-* and *Gammaherpesvirinae* indicating evolutionary relatedness does not correlate with genome classification.

1.1.4 Lifecycle

The herpesvirus lifecycle is initiated following the attachment of an infectious virion to the surface of its target cell (summarised in **figure 1.4**). This interaction is mediated by multiple virally-encoded glycoproteins that protrude the viral envelope. There are three glycoproteins that are considered both necessary and essential for herpesvirus entry, unsurprisingly these are conserved across the *Herpesvirales* order. Glycoproteins gH, gL and gB, form two core glycoprotein complexes which are required for all entry and fusion events (Möhl et al., 2019) (Nishimura and Mori, 2019). The gHgL complex can directly interact with host cell receptors during entry and appears necessary for the activation of gB facilitated plasma membrane fusion **(Figure 1.5a)**. Alternatively, some host cell receptors are only considered binding receptors and function to increase the concentration of virions attached to the surface of a target cell, greatly increasing entry efficiency. Proteoglycans represent a commonly utilised cellular entry receptor. Indeed,

the glycosaminoglycan, heparan sulphate (HS) mediates the binding of both KSHV and HSV-1 (Akula et al., 2001).

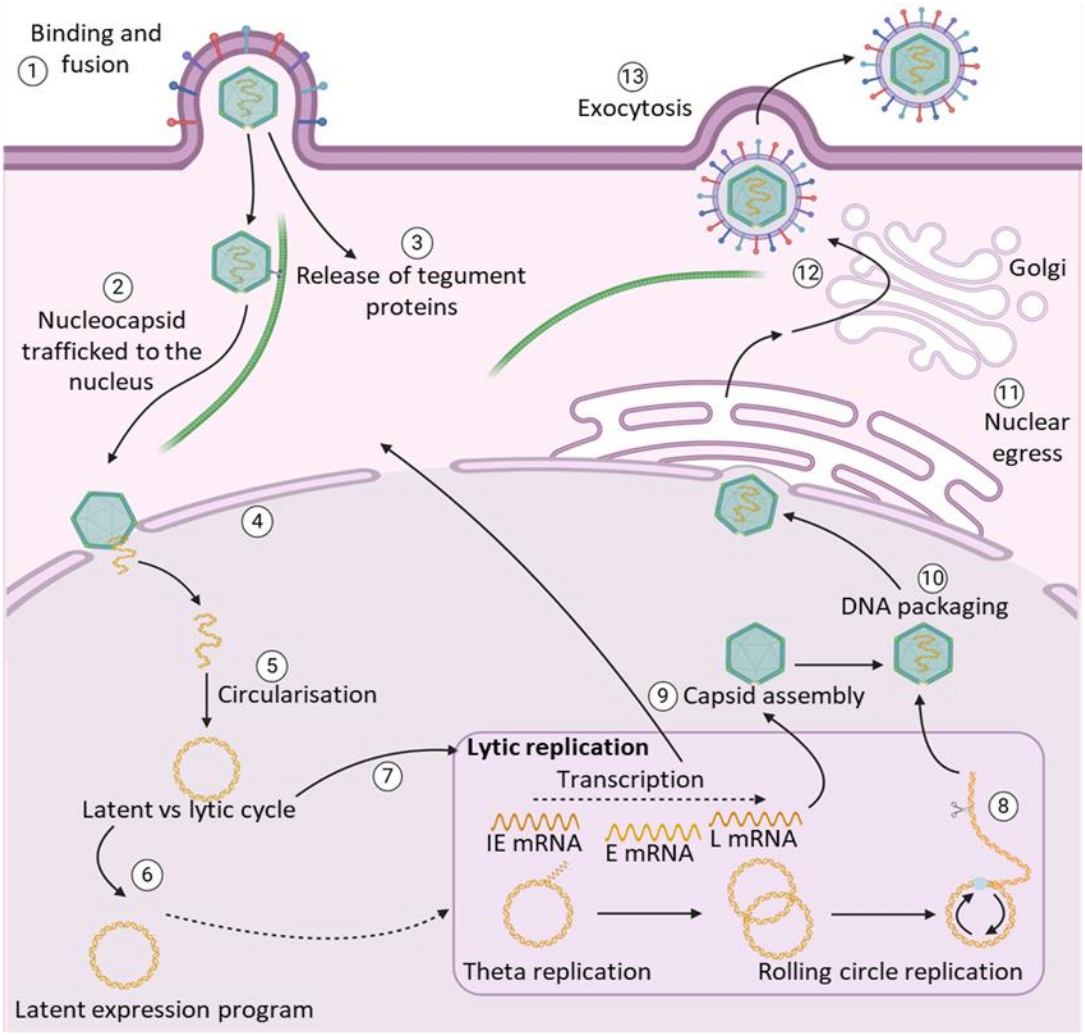

Figure 1.4 Herpesvirus lifecycle. 1. Herpesvirus biphasic lifecycle begins following binding and entry into its target host cell. 2. The nucleocapsid and tegument proteins are released into the cytoplasm. 3. The nucleocapsid is trafficked along the microtubule network to the nucleus (Döhner et al., 2002). 4. Here the nucleocapsid interacts with the nuclear pore complex, releasing the viral genome into the nucleus. 5. The viral genome immediately circularises (Mabit et al., 2002). Herpesviruses can then enter two distinct lifecycles: latent or lytic replication cycle 6. Following the initiation of latent infection, viral gene expression is restricted to the expression of a number of latency associated expression programs. 7. Latency infection is reversible, and herpesvirus can undergo reactivation, leading to the lytic replication cycle. During the lytic cycle, three successive transcription phases occur leading to the expression of immediate early (IE), delayed early (DE), and late (L) transcripts which are subsequently trafficked to the cytoplasm and translated into viral proteins (Zhu, Cusano and Yuan, 1999). 8. The viral genome then undergoes rolling circle replication, producing concatemers which are subsequently processed into monomers (Homa and Brown, 1997). 9. Viral capsid proteins are also assembled in the nucleus. 10. The viral genome is packaged into capsid. 11. The newly assembled nucleocapsid buds from the nucleus, gaining a primary envelope, the capsid is deenveloped in the cytoplasm and the tegument layer is added. 12. The nucleocapsid is reenveloped (Mettenleiter, 2002). 13. Mature virions are released via exocytosis resulting in the lysis of cells.

Furthermore, the gHgL complex can mediate the assembly of larger entry complexes, recruiting additional non-conserved viral proteins that interact with specific cellular receptors. This in part is thought to explain the cellular/tissue tropism that is observed across the different subfamilies of herpesviruses. Moreover, depending on the herpesvirus and cell type some herpesviruses use endocytosis to enter their target cell, where membrane fusion occurs following entry and subsequent to the acidification of the endosomal compartment **(Figure 1.5b)** (Miller and Hutt-Fletcher, 1992).

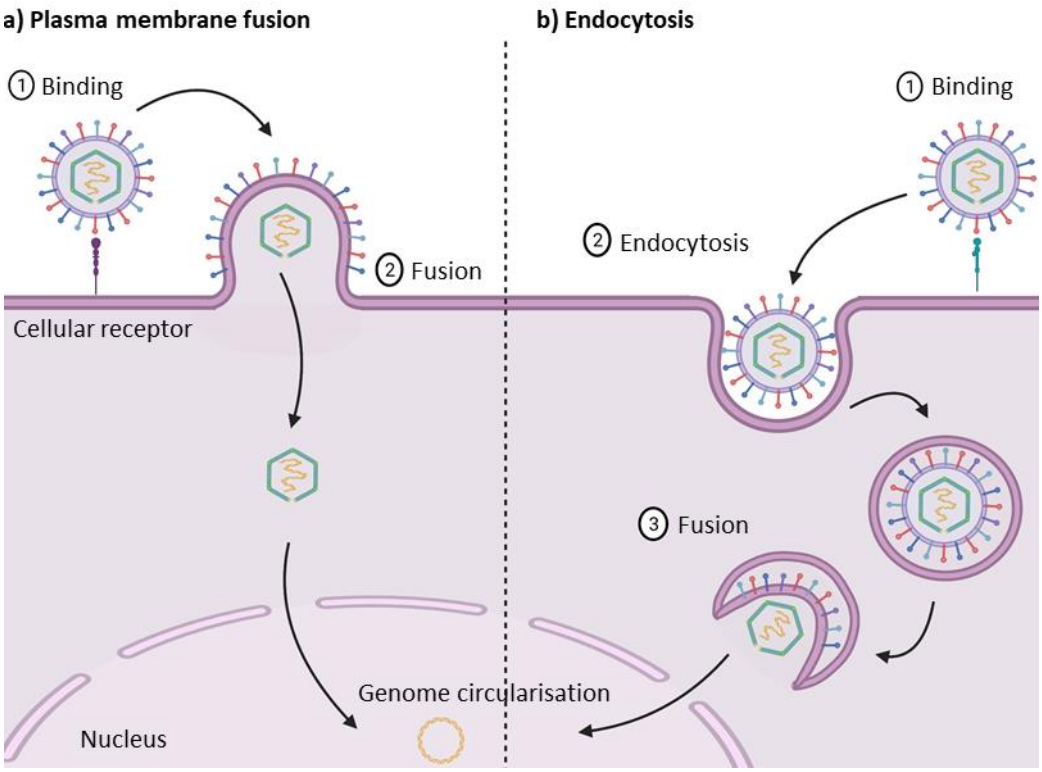

Figure 1.5 Herpesvirus entry mechanisms. Herpesviruses utilise two major mechanisms to enter their target host cell a) Herpesviruses can enter the cell through binding and fusion of the viral envelope at the plasma membrane. b) Alternatively, they can enter cells via the endocytic pathway where pH-dependent fusion of the viral envelope and vesicular envelope occurs in the cytoplasm (Miller and Hutt-Fletcher, 1992). Ultimately the viral nucleocapsid is released into the cytoplasm, where it is trafficked to the nucleus. The viral genome enters the nucleus where it immediately circularises (Mabit et al., 2002).

Subsequent to membrane fusion, the viral capsid and tegument is released into the cytoplasm of the cell. The uncoated capsid is then trafficked along the microtubule network to the nuclear membrane by the dynein/dynactin motor protein complex (Sodeik et al., 1997) (Döhner et al., 2002). The capsid binds the nuclear pore complex

(NPC), and viral DNA is released into the nucleus where it immediately circularises (Mabit et al., 2002).

Next, herpesviruses can enter two distinct phases, that of latency or lytic replication.

1.1.4.1 Latency

Herpesviruses rely on latency to establish a long-term persistent infection and depending on the virus is established in a specific cell type. During latency, the viral genome persists as a non-integrated nuclear episome, and viral gene expression is largely restricted, permitting a few latency associated transcripts and several virally-encoded microRNAs (Collins and Medveczky, 2002) (Griffiths and Whitehouse, 2007). Furthermore, no infectious progeny virions are produced (Kaschka-Dierich et al., 1982)

Latency-associated transcripts (LATs) often encode multifunctional proteins that are involved in preventing apoptosis, persistence of the viral genome and immune evasion (Croen, 1991) (Friborg et al., 1999). In addition to LATs, herpesviruses rely on numerous virally-encoded miRNAs (v-miRNAs) and host cell factors to establish latency. Indeed, the importance of the host immune system itself has long been recognised in establishing and maintaining latent infection. Epigenetic mechanisms including specific methylation of viral genes has also been reported (Lieberman, 2016).

Importantly, latent infection is reversible, and herpesviruses are able to reactivate and engage in lytic replication, ultimately allowing viral persistence and dissemination (Wilson and Mohr, 2012).

1.1.4.2 Lytic replication

During lytic replication, the lytic temporal expression cascade is initiated, resulting in the expression of three successive phases: immediate early (IE), delayed early (DE) and late (L) (Zhu et al., 1999). Viral gene transcription is facilitated by cellular RNA polymerase II (RNAPII), characteristically producing 5’ capped and 3’ polyadenylated transcripts. Subsequently, viral transcripts are exported to the cytoplasm, where protein translation occurs. IE transcripts are the first to be translated and are necessary for DE gene expression. Delayed early genes not only encode a number of proteins that function in

DNA synthesis and the modulation of the host cell immune response but are also necessary for the expression of late (L) genes which encode viral structural proteins (Honess and Roizman, 1974).

DNA synthesis initially proceeds via a theta replication mechanism, allowing the circular episome to be maintained. There is a subsequent switch to rolling circle replication where the circular DNA is replicated by a viral DNA polymerase, producing long concatemers. These concatemers are subsequently processed producing viral genome monomers that are packaged into newly synthesised preformed capsids (Homa and Brown, 1997).

Both capsid assembly and viral DNA packaging occur in the nucleus. The capsid leaves the nucleus, first budding into the perinuclear space via the inner nuclear membrane, resulting in primary envelopment. The primary enveloped virion then fuses with the outer nuclear membrane, leading to de-envelopment. Once in the cytoplasm, the tegument protein layer is added, through a yet unclear mechanism and the virion re-envelope (Mettenleiter, 2002). Though this was initially thought to occur following Golgi vesicle budding, reports have since emerged suggesting the cellular endocytic network may play an important role in this process (Hollinshead et al., 2012).

Finally, mature virions are trafficked to the plasma membrane and released via exocytosis, a process that consequently leads to the lysis of host cells. While virion assembly and budding remains poorly characterised it is clear that herpesviruses utilise host cell machineries to facilitate these processes (Wang et al., 2015) (Arii, 2021).

1.2 The *Gammaherpesvirinae*

The *Gammaherpesvirinae* consist of 43 species that are divided between 7 distinct genera: *Bossavirus*, *Lymphocrytovirus*, *Macavirus*, *Manticavirus*, *Patagivirus*, *Percavirus* and *Rhadinovirus* (ictvonline.org). The genomes of *Gammaherpesvirinae* are described as co-linear due to the high similarity, observed in both genome orientation and arrangement of core genes (Albrecht and Fleckenstein, 1990). The central region is generally conserved with unique open reading frames (ORFS) distributed throughout. Furthermore, the central region is flanked by terminal repeats (TR) sequences which vary depending on the virus (Davison, 2007). Gammaherpesviruses predominantly infect and

establish latency in B and T lymphocytes though they can also undergo lytic replication within epithelial and fibroblast cells. As gammaherpesviruses establish latency in dividing lymphocytes, they must replicate and ensure segregation of the viral genome during cell division, thus allowing persistence (Cotter and Robertson, 1999). Additionally, members of the *Gammaherpesvirinae* are associated with the development of various forms of malignant disease. Indeed, human pathogens EBV and KSHV have been implicated in a number of cancers and proliferative diseases (Damania, 2004).

1.2.1 Epstein Barr virus (EBV)

Epstein Barr virus (EBV) also known as human herpesvirus 4 (HHV-4) was the first human oncogenic virus to be identified. It was originally discovered in 1964, following its isolation from lymphoblast cells taken from a Burkitt's lymphoma sample (Epstein et al., 1964). Since its discovery, EBV has now been implicated in a number of different malignancies, which are summarised below in table 1.2.

Table 1.2 EBV-associated malignancies

Associated malignancy	Name
B-cell lymphoma	Burkitt's lymphoma
	Hodgkin's lymphoma
	Post- transplant lymphoma (PTL)
T-cell lymphoma	Extranodal Natural killer/ T cell lymphoma
Carcinoma	Nasopharyngeal carcinoma
	Gastric carcinoma

The majority of EBV infections do not pose any serious health consequences, indeed >90% of adults worldwide are thought to be seropositive (De Paschale and Clerici, 2012). Primary EBV infection during early childhood usually leads to an asymptomatic infection, while initial infection during adulthood can be more severe, causing infectious mononucleosis (IM). IM or glandular fever is a self-limiting infection, characterised by flu-like symptoms and severe fatigue. Following infection of B lymphocytes (B cells), EBV undergoes an initial period of lytic replication triggering an immune response. This systemic response ultimately leads to the expansion of T lymphocytes (T cells) including EBV-specific CD8+ cytotoxic T cells that are responsible for the pathological symptoms of

IM (Callan et al., 1996). Most EBV infected cells are cleared by the immune response within a few weeks, however EBV is able to establish a latent reservoir in some cells, ensuring life-long persistence. Furthermore, EBV can infect and replicate in oral epithelial cells, contaminating saliva, thus ensuring viral transmission (Kurth et al., 2000) (Tugizov et al., 2003).

While the development of EBV-associated malignancies is rare, the dysregulation of latency and inability to control lytic replication can lead to lymphoproliferative and other diseases. Hence, immunodeficient patients invariably appear to be the most severely affected, with EBV-associated malignancies well characterised in individuals with HIV co-infection and those receiving immunosuppressive therapy following tissue or organ transplantation (Taylor and Blackbourn, 2011).

1.2.1.1 EBV lifecycle

In order to enter B cells, EBV utilises complement receptor type 2 (CR2, also known as CD21). This is in contrast to many other herpesviruses that bind and enter host cells via the proteoglycan HS. In addition to the core entry machinery, EBV expresses gp350 a glycoprotein that binds with high affinity to CR2, increasing the efficiency of B cell entry (Fingeroth et al., 1984) (Johannsen et al., 2004). Furthermore, EBV gp42 mediates human leukocyte antigen (HLA) class II binding at the surface of B cells, triggering membrane fusion (Li et al., 1995) (Borza and Hutt-Fletcher, 2002). EBV can also infect endothelial cells however this mechanism is poorly understood and proceeds in a considerably less efficient way.

Following entry, EBV undergoes a brief period of lytic replication in order to produce a pool of infectious virions, before generating a latent reservoir. EBV latency is defined by four distinct latency expression programs known as 0, I, II and III (Rowe et al., 1987) (Tempera and Lieberman, 2014). Latency III represents the broadest expression program and is the first phase of latency established following initial EBV infection. During this phase, a number of EBV nuclear antigens (EBNAs 1, 2, 3A, 3C and leader protein) are expressed along with 3 latent membrane proteins (LMP 1, 2A and 2B), and various ncRNAs including virally-encoded miRNAs (Kang and Kieff, 2015).

This initial infection triggers an immune response, which results in the clearance of most infected cells, however some cells are able to escape and ultimately lead to the formation of immortalised B cells. In order to escape further immune interference in healthy individuals, viral gene expression is sequentially downregulated leading to latency II and later latency I program expression profiles. Latency II is defined by the expression of EBNA1, LMP1 and LMP2A/B, while only a single viral gene, EBNA1 is expressed during latency I. Finally, no viral genes are expressed during Latency 0 (Young and Rickinson, 2004). EBV does however encode many ncRNAs including miRNAs that are expressed during all latency programs as well as the lytic replication cycle (Greifenegger et al., 1998). Interestingly, each latency expression program tends to be linked with different malignancies. For example, latency III is related to malignancies in immunosuppressed patients including AIDS-associated Diffuse large B cell lymphoma (DLBCL) and also post-transplant lymphoproliferative diseases (PTLDs) (Thorley-Lawson and Gross, 2004). While latency II is often associated with the development of Hodgkin's lymphoma, Nasopharyngeal carcinoma, and T/NK cell lymphomas (Pallesen et al., 1991) (Brooks et al., 1992) (Kawa et al., 2001). Furthermore, Burkitts lymphoma and gastric carcinoma are commonly linked to latency I (Rowe et al., 1987) (Sugiura et al., 1996).

Reactivation of EBV is primarily mediated by the virally-encoded transactivators BZLF1 and BRLF1, which initiate the lytic cascade (Sinclair, 2003) in a similar fashion as detailed in figure 1.4.

1.2.2 Kaposi's sarcoma-associated herpesvirus (KSHV)

KSHV, was the eighth human herpesvirus to be identified. It was first discovered in 1994 when herpesvirus-like DNA fragments were isolated from KS tumour cells (Chang et al., 1994). These fragments were found to belong to a new gammaherpesvirus, later named Kaposi's sarcoma-associated herpesvirus (KSHV). Following its identification, KSHV was found to be the causative agent of AIDS-associated KS and has since been implicated in all subtypes of KS and a number of lymphoproliferative diseases including Multicentric Castleman's disease (KSHV-MCD) and primary effusion lymphoma (PEL). Thus, KSHV is one of the seven, currently known human oncoviruses (Cesarman et al., 1995) (Soulier et al., 1995).

KSHV has a class B genome structure, consisting of a central unique coding region that is flanked by direct, tandem repeats. The length of the genome varies, ranging from approximately 165-170 kb, with the central region approximately 145 kb in length (Russo et al., 1996). The central coding region encodes 87 open reading frames (ORFs). The majority of these are conserved across other herpesviruses and are typically involved in viral gene replication and virion assembly. KSHV, however encodes over 20 unique ORFs, which carry the prefix K (Russo et al., 1996). Interestingly, KSHV also expresses several cellular homologues, presumably captured from host cells during co-evolution (Russo et al., 1996). These pirated genes appear to primarily function in preventing apoptosis and cell cycle shutdown, thereby contributing to KSHV pathogenesis (Sakakibara and Tosato, 2014). In addition, the genome contains 12 pre-miRNAs that are processed to express 25 mature miRNAs and several long ncRNAs including polyadenylated nuclear RNA (PAN) (Cai et al., 2005) (Rossetto et al., 2013). The organisation of the KSHV genome is displayed in below **figure 1.6** (Arias et al., 2014).

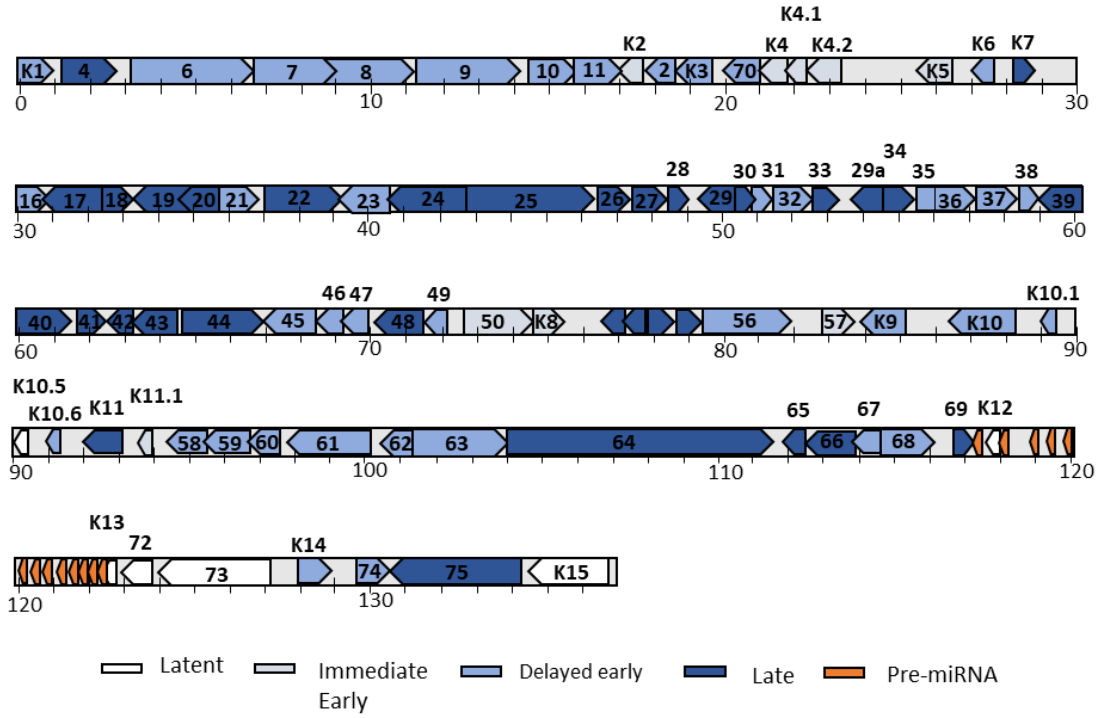

Figure 1.6 KSHV genome map. The position of open reading frames and miRNA are mapped within the KSHV genome. Latently expressed KSHV genes are indicated in white, immediate early (IE) genes are shown in light grey, while delayed early (DE) and late (L) genes are shown in light blue and dark blue respectively. The location of KSHV encoded pre-miRNAs are also indicated in orange. Adapted from (Arias et al., 2014).

While EBV infections appear to be ubiquitous across the world, this is not the case for KSHV. Sub-Saharan Africa (SSA) shows the highest prevalence of KSHV with >50% of the population sero-positive, while other regions have a lower level of seropositivity; the Mediterranean, 30% and less than 10% for parts of Europe, Asia, and the US **(Figure 1.7)** (Uldrick and Whitby, 2011)**.**

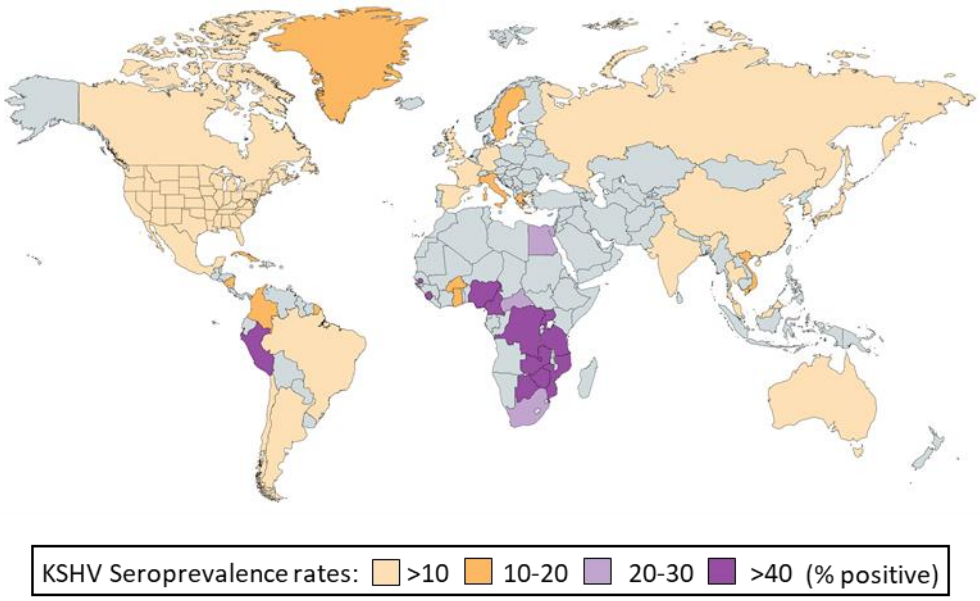

Figure 1.7 Worldwide KSHV seroprevalence rates. A map indicating the seroprevalence of KSHV infections worldwide. Seroprevalence rates are colour coded >10% (Beige), 10-20% (orange), 20-30% (light purple) and over 40% (dark purple) (Uldrick and Whitby, 2011).

A number of routes have been highlighted in KSHV transmission, though contact with contaminated saliva proves to be a common route, especially for childhood infections in parts of Africa. This occurs due to the ability of KSHV to infect and replicate in oral epithelial cells, which subsequently leads to shedding of infectious virions into saliva (Pauk et al., 2000) (Webster-Cyriaque et al., 2006). Additionally, incidences of transmission through sexual contact and blood transfusion have been reported (Kedes et al., 1996) (Whitby et al., 1995).

1.2.2.1 KSHV-associated disease

Since it was discovered to be the aetiological agent of all forms of Kaposi's sarcoma (KS), KSHV has also been implicated in other neoplastic diseases such as primary effusion

lymphoma (PEL) and multicentric Castleman disease (MCD) (Chang et al., 1994) (Cesarman et al., 1995) (Soulier, 1995).

1.2.2.1.1 Kaposi's sarcoma (KS)

The first occurrence of KS was described in healthy elderly men of Mediterranean or Middle Eastern descent, by Hungarian dermatologist, Moritz Kaposi in the late nineteenth century (Kaposi, 1872). This has since become known as classic KS and is considered a relatively benign disease. In contrast the major remaining KS subtypes, AIDS-associated KS, African endemic KS and Iatrogenic KS are much more aggressive, with tumours rapidly spreading to internal organs and lymph nodes (Ganem, 2010).

An infectious agent had long been suspected to be involved in the development of KS, however this was not confirmed until 1994 when representational difference analysis (RDA, a PCR-based technique) detected viral DNA fragments in KS biopsies, leading to the discovery of KSHV (Chang et al., 1994). Though KS incidence dropped some 80% following the introduction of anti-retroviral therapies (ART), KS remains the most common tumour affecting HIV-positive individuals. An increasing concern is also the number of HIV-KS patients experiencing a worsening disease after starting ART, attributed to developing KS-associated immune reconstitution inflammatory syndrome (KS-IRIS). KS-IRIS occurs when ART is initiated in 7%–31% of cases and is now a major contributor to KS-related deaths (Letang et al., 2013). Furthermore, the prevalence of KS is substantially higher in HIV-positive individuals compared to the general population, even in those with seemingly controlled HIV infection (Grulich et al., 2001) (Maurer et al., 2007). There is also a high prevalence of KS in Sub-Saharan Africa (SSA). Endemic KS was first described in HIV-negative children >50 years ago in Central Africa, where it is likely co-morbidities and malnutrition contributes to its development. Moreover, following a drastic increase in HIV/AIDS prevalence across SSA, epidemic, HIV-associated KS has become one of the most common cancers affecting the region (Parkin et al., 2008). Additionally, patients undergoing chemotherapy or those receiving immunosuppressive therapy following organ transplants have a higher risk of developing Iatrogenic KS (Buonaguro et al., 2003).

KS presents as multifocal cutaneous nodules that most commonly affects the lower extremities, however nodules affecting the lymph nodes, lungs and bone can also occur. Owing to the highly vascular nature of KS tumour cells, skin nodules characteristically appear dark purple as microvascular channels become filled with blood. Furthermore, spindle-like tumour cells originating from endothelial cells are a classic hallmark of KS lesions (Boshoff et al., 1995) (Gramolelli and Ojala, 2017) **(Figure 1.8)**.

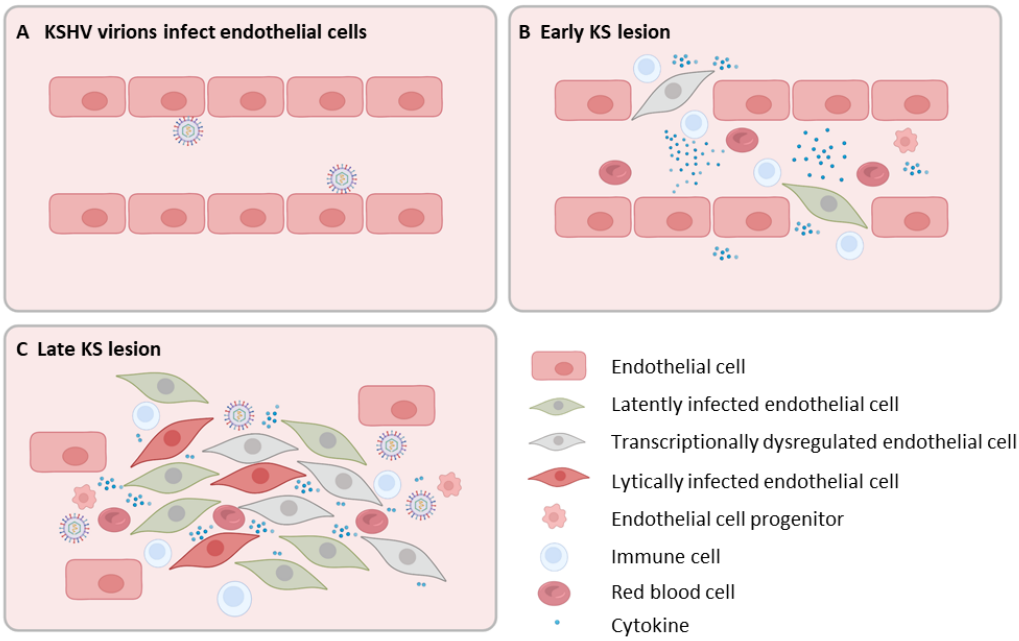

Figure 1.8 KS lesion formation. a) KSHV virions infect endothelial cells (EC) b) Early KS lesions: KSHV infected EC adopt typical spindle cell morphology. These cells release both pro inflammatory and angiogenic cytokines causing an infiltration of immune cells to the tumour site c) Late KS lesion: Tumour site is mainly composed of KSHV infected spindle cells. The majority of these at latently infected or undergoing transcriptional dysregulation while a small subset is lytically infected producing infectious virions to sustain infection. Adapted from (Gramolelli and Ojala, 2017).

Though the majority of KS tumour cells are latently infected, a small proportion of cells undergo spontaneous lytic replication. Interestingly, lytic replication appears an important factor in KS pathogenesis, this is in contrast to EBV infection, where viral latency is associated with all EBV associated malignancies (Ye et al., 2011). Lytic replication allows the dissemination and spread of mature KSHV virions from B cell latent reservoirs to other areas of the body such at endothelial cells (Staskus et al., 1997). It also sustains the population of latently-infected tumour cells that would otherwise be reduced due to the poor persistence of the KSHV episome during tumour cell division (Grundhoff and Ganem, 2004). Lytically-expressed proteins also mediate paracrine

secretion of growth and angiogenic factors, essential for tumour development (Nicholas, 2007) and induce DNA damage and genomic instability (Jackson et al., 2014).

There is currently no recognised curative treatment for KS. The progression of KS appears to be largely dependent on the host immune system. Thus, correcting and improving immune status is the initial course of treatment. Indeed, cases of long-term remission have been reported following HAART and alterations in immunosuppressive drug treatment in HIV and post-transplant patients, respectively (Martinez et al., 2006) (Stallone et al., 2005). Unfortunately, these incidences remain relatively rare. Furthermore, systemic treatment is limited by toxicity therefore new, effective approaches with fewer toxic effects are required. Encouragingly, Pomalidomide an immune modulating agent has been recognised as an effective treatment for symptomatic KS regardless of HIV status (Polizzotto *et al.*, 2016). Importantly, Pomalidomide (POMALYST®) is a well-tolerated, oral treatment which potentially provides an effective alternative KS treatment, especially in resource limited regions. In May last year it became the first FDA approved KS treatment in >20 years, though disappointingly access currently appears limited (fda.gov).

1.2.2.1.2 Primary effusion lymphoma (PEL)

Soon after it was identified to be the causative agent of KS, KSHV was also linked to primary effusion lymphoma (PEL) (Cesarman et al., 1995). PEL, previously known as body cavity-based lymphoma (BCBL) is a relatively rare, high-grade non-Hodgkin's lymphoma. While PEL has on occasion been shown to effect immunocompetent individuals, it is most commonly associated with end stage AIDS (Ascoli et al., 1999) (Nador et al., 1996). PEL occurs following lymphomatous effusion to serosal cavities, primarily pleural, but also pericardia, peritoneal and joints (Nador et al., 1996). There is currently no effective treatment for PEL. While some individuals have been shown to respond to chemo/ immunomodulation therapy, survival rates are generally very poor, and even with therapeutic intervention median survival is approximately 6 months (Khoury et al., 2018).

PEL derived cell lines are commonly used in the laboratory, as well as being fully immortalised these cells are also latently-infected with KSHV and therefore prove extremely useful in KSHV study (Drexler et al., 1998).

1.2.2.1.3 KSHV-associated Multicentric Castleman's disease (KSHV-MCD)

KSHV-associated multicentric Castleman's disease (KSHV-MCD) is a rare, extremely aggressive B cell lymphoproliferative disorder (LPD). MCD can occur in HIV-negative individuals however it is appreciated that most cases of MCD occur in AIDS patients. Furthermore, 100% of these cases show co-infection with KSHV, while only 40% of non-HIV cases are associated with KSHV infection (Soulier et al., 1995). Clinical presentation of all forms of MCD are similar, with patients displaying common systemic inflammation symptoms including fever, fatigue, and cachexia along with lymphadenopathy. Indeed, MCD-derived tumour cells show elevated pro-inflammatory cytokine expression specifically vIL-6, a virally-encoded homologue of cellular IL-6 (Oksenhendler et al., 2000). Moreover, vIL-6 has been shown to activate the expression of cellular IL-6 and IL-10, which further contribute to the pathological symptoms of KSHV-MCD. It is therefore thought vIL-6 plays a pivotal role in KSHV-MCD development (Suthaus et al., 2012).

1.2.2.1.4 KSHV-associated inflammatory cytokine syndrome (KICS)

KSHV-associated inflammatory cytokine syndrome (KICS) is a recently recognised disease. It was first described following observations that some KSHV-infected patients displayed inflammatory symptoms similar to that of KSHV-MCD in the absence of MCD pathology (Uldrick et al., 2010). Indeed, KICS is associated with high systemic KSHV lytic replication along with significantly elevated serum levels of vIL-6, hIL-6, and IL-10 comparable to KSHV-MCD patients (Polizzotto *et al.*, 2016). Though some cases appear to have been successfully treated with immunomodulatory therapy, the reported mortality rate of KICS is ~60% (Polizzotto *et al.*, 2016).

1.2.2.2 KSHV lifecycles

KSHV can infect a number of different cell types, including endothelial cells, monocytes, and keratinocytes. B cells however provide the major reservoir for latent KSHV infection (Ganem, 2007). The mechanism of KSHV entry is cell type specific, but usually involves a multistep process, where various viral glycoproteins interact with host cell receptors, facilitating attachment at the plasma membrane and membrane fusion. In addition to core entry glycoproteins, gB, gH and gL, KSHV also expresses a number of additional glycoproteins that aid both host cell attachment and fusion. These include gM, gN, ORF4 and the KSHV specific glycoprotein K8.1A. Like other herpesviruses gH and gL form a non-covalently linked complex. The gHgL complex and gB interact with ORF4 and K8.1A respectively, mediating HS binding (Birkmann et al., 2001). KSHV, therefore appears to utilise ubiquitous proteoglycan HS as an initial binding receptor on most target cells. Additionally, integrins have also been implicated in KSHV attachment and entry. For example, α4β1, αvβ3 and αvβ5 have well established roles in HFF, HEK 293, Vero and monocytes entry (Akula et al., 2002) (Garrigues et al., 2008). Indeed, glycoprotein gB contains the integrin RGD binding motif (Russo et al., 1996). Furthermore, DC-SIGN and EphA2R have been found to mediate B cell and endothelial cell entry, respectively (Rappocciolo et al., 2008) (Bandyopadhyay et al., 2014). To summarise KSHV entry involves numerous virus glycoprotein and host cell surface interactions that ultimately facilitate attachment, fusion, and the internalisation of KSHV in a cell dependent manner.

Following entry, KSHV is rapidly trafficked along the microtubule network to the nucleus. At the nuclear membrane, the viral capsid interacts with the nuclear pore complex, and the viral genome is translocated into the nucleus. Here, the linear DNA genome immediately circularises, forming a non-integrated episome (Collins and Medveczky, 2002).

1.2.2.2.1 Latency

In order to escape immune clearance and ensure viral persistence, KSHV establishes a latent infection in B cells. During latency, viral gene expression is restricted to several latency associated transcripts (LATs) along with a number of virally-encoded miRNAs (v-

miRNAs). In addition to KSHV encoded LATs, a number of virus host cell interactions prove important for maintaining latent infection.

Only seven LATs are expressed during latent infection. Three latent genes, LANA, v-Cyclin, and v-FLIP are located within a single cluster and are transcribed from the same LTc promoter, producing a polycistronic mRNA which subsequently undergoes alternative splicing (Jeong et al., 2004) (Dittmer et al., 1998). The latency-associated nuclear antigen (LANA) represents the most abundantly expressed latent protein. LANA is a multifunctional protein that not only plays a crucial role in maintaining latent infection but also functions in viral genome persistence and KSHV pathogenesis. To ensure genome persistence in a dividing B cell population, the viral genome must first undergo DNA replication. Latent DNA replication proceeds from origin of plasmid replication sites (*Ori-P*) located within TR regions of the viral genome. LANA binds these sites where is recruits and mediates the assembly of cellular DNA replication machinery in a cell cycle dependent manner (Ohsaki et al., 2009). Importantly, LANA also tethers the viral genome to the host chromosome, allowing segregation between daughter cells during mitosis (**Figure 1.9**) (Ballestas et al., 1999).

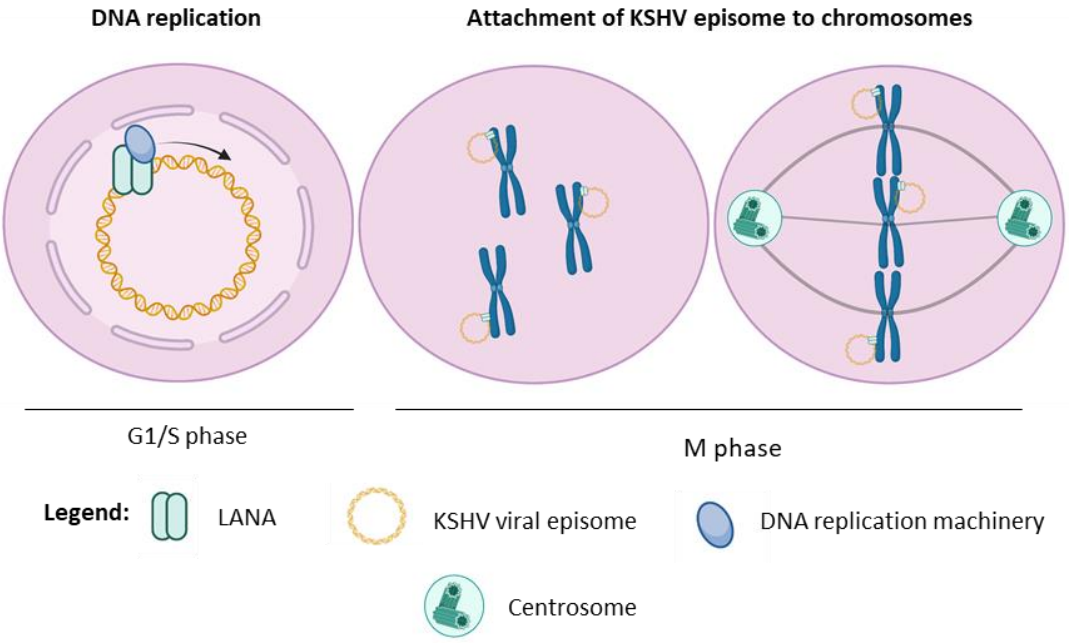

Figure 1.9 Functions of KSHV LANA during DNA replication and mitosis. LANA binds *Ori-P* sites located within the viral genome, where it recruits DNA replication machinery (Ohsaki et al., 2009). Furthermore, during mitosis LANA directs the attachment of the viral episome to host chromosomes, ensuring persistence (Ballestas et al., 1999). Adapted from (Ballestas et al., 1999).

Additional functions of LANA include the transcriptional regulation of both viral and cellular genes (Renne et al., 2001). For example, LANA has been reported to bind and repress the expression of several lytic KSHV genes, notably ORF50 the lytic transactivator. Ultimately inhibiting the lytic expression cascade and maintaining latent infection. Furthermore, LANA directly binds and inhibits the transcriptional activity of TP53, a key tumour suppressor protein, leading to abnormal cellular proliferation and thus promoting KSHV tumorigenesis (Friborg et al., 1999). The latently expressed viral homologue of cyclin-D, v-Cyclin maintains many cellular functions of its cellular counterpart. Thus, v-Cyclin primarily regulates cell cycle progression, where it drives G1/S phase transition via the constitutive activation of CDK6, thereby promoting cellular proliferation (Van Dross et al., 2005). KSHV expresses another viral homologue, v-FLIP (FADD-like interleukin-1-β–converting enzyme [FLICE/caspase 8]-inhibitory protein) during latency. KSHV v-FLIP directly interacts with NEMO, the regulatory subunit of the IκB kinase (IKK) complex, which ultimately leads to the inhibition of apoptosis through the activation of NF-κB (Liu et al., 2002) (Matta et al., 2003).

KSHV expresses 4 further proteins during latent infection: Kaposin, v-IRF2, LAMP and LANA2. There are 3 known isoforms of Kaposin (A, B and C) which are all expressed from the K12 locus. While little is known about the function of Kaposin C, Kaposin A and B have both been implicated in promoting inflammation and consequently KS development. Kaposin A activates ERK1/2 MAP kinase signalling, leading to the expression of proinflammatory cytokines while Kaposin B activates the p38/MK2 pathway and stabilises cytokine mRNA (Muralidhar et al., 1998) (McCormick and Ganem, 2005). Likewise, LAMP has been shown to promote a pro-inflammatory cytokine microenvironment (Pietrek et al., 2010). KSHV latent proteins also act to suppress host antiviral immune responses. KSHV homologue, Interferon regulatory factor 2 (v-IRF2) dysregulates the expression of antiviral interferons through the inhibition of IRF1-mediated transcriptional activity (Burysek et al., 1999). Finally, LANA2 also known as v-IRF3, is specifically expressed in latently infected B cells. LANA2 not only disrupts antiviral IFN expression but also inhibits apoptosis through p53 inhibition (Lubyova and Pitha, 2000) (Rivas et al., 2001). Due to a degree of leaky expression, a number of genes primarily expressed during lytic replication have also been found to be transcribed at low levels during latent infection including ORFK1, ORF4, K14, vIL-6 and ORF59 (Chandriani et al., 2010). However, their role in latency is poorly defined.

Finally, numerous virally-encoded miRNAs are abundantly expressed during latency. Most appear to function in maintaining latent infection however this with be explored further in section 1.4.

1.2.2.2.2 Lytic replication

Importantly, latent infection is reversible, and reactivation initiates the lytic replication cycle. During the lytic cycle, KSHV lytic genes are abundantly expressed in a temporal cascade, leading to viral progeny being assembled and released. This proves critical for both viral persistence and dissemination. Furthermore, KSHV lytic replication is associated with KSHV pathogenesis, unlike other herpesviruses where latent infection appears key.

The switch between KSHV latent and lytic lifecycles is complex. The immediate early transcript ORF50, encodes the replication and transactivator (RTA) protein. RTA is the first viral protein to be expressed following KSHV lytic reactivation and its role in both lytic gene transactivation and DNA replication is well established (Lukac et al., 1999) (Deng et al., 2000) (Wu et al., 2001). Indeed, RTA expression alone is both necessary and sufficient to induce the KSHV lytic cycle (Lukac et al., 1998) (Lukac et al., 1999). Various factors including environmental stressors like hypoxia and physiological changes such as immunosuppression and coinfection have been shown to initiate KSHV lytic reactivation through the induction of RTA (Davis et al., 2001) (Ye et al., 2011). During hypoxia, hypoxia inducible factors (HIFs) are produced. RTA along with many other lytic genes, contain hypoxia response elements (HRE) within their promoters (Haque et al., 2003). Indeed, HIF1 directly binds the RTA promoter, inducing its transcription, leading to the activation of the lytic gene expression cascade (Davis et al., 2001) (Haque et al., 2003). Furthermore, hypoxia induces the expression of the X-box protein 1 (XBP-1), another transactivator of RTA expression (Dalton-Griffin et al., 2009). Interestingly, B cell differentiation stimulates the expression of XBP-1, a factor that is also reported to lead to KSHV lytic reactivation (Wilson et al., 2007). Furthermore, classical KS tumours predominantly present on extremities, indicating that hypoxia may contribute to tumorigenesis (Davis et al., 2001).

1.2.2.2.2.1 RTA mechanisms of transcriptional activation

There are three distinct mechanisms by which RTA can mediate viral gene transcription: directly, cooperatively or through repressor degradation via its intrinsic E3 ligase activity **(Figure 1.10)**. Similar to cellular transcription factors, RTA can directly bind gene promoters in a sequence specific manner. The C terminus of RTA recognises and binds RTA response elements (RRE) within numerous lytic gene promoters, activating their transcription (Lukac, Kirshner and Ganem, 1999). For example, the expression of polyadenylated nuclear (PAN) RNA is directly induced by RTA transactivation (Chang et al., 2002). Furthermore, the RTA promoter itself contains an RRE; RTA can therefore induce its own expression in a positive feedback loop (Deng et al., 2000).

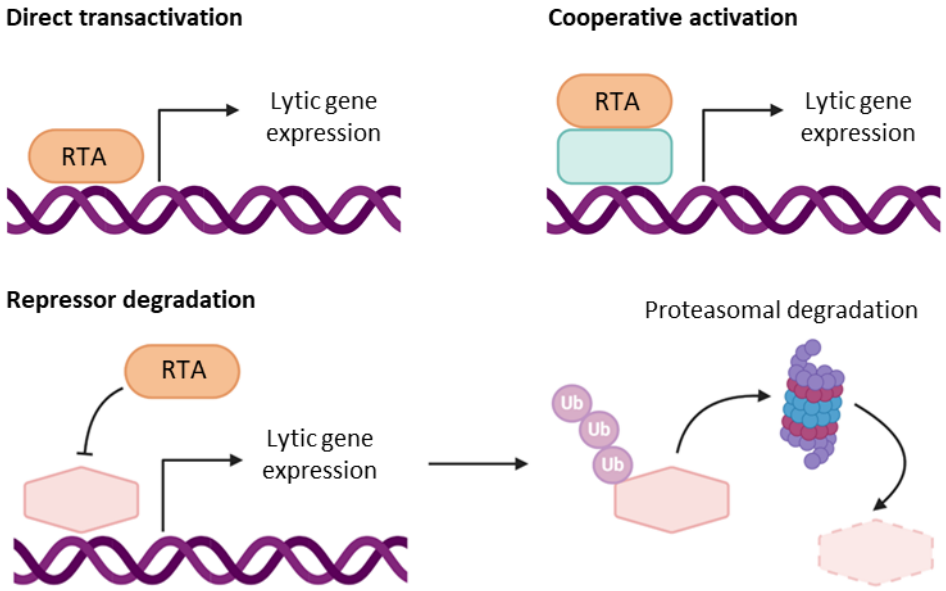

Figure 1.10 Mechanisms of RTA transactivation. RTA can transactivate lytic gene expression via three distinct mechanisms. Firstly, RTA is a transcription factor and can therefore directly bind RTA response elements (RRE) located within gene promoters (Lukac, Kirshner and Ganem, 1999). Indeed, RTA induces its own expression through direct transactivation. RTA can also stimulate the transcription of genes that do not contain RRE including ORF57 and K8 through cooperative binding. Here, RTA recruit's cellular transcription factors such as Rbp-jκ, C/EBPα and AP-1 in order to stimulate transcription (Liang et al., 2002) (Wang et al., 2003) (Wang et al., 2004a). Alternatively, RTA can direct transcriptional repressors of lytic gene expression for proteasomal degradation via its intrinsic E3 ligase activity (Yang, Yan, and Wood, 2008).

RTA can also initiate the transcription of genes that do not contain RREs via an indirect or cooperative binding mechanism. RTA can interact and recruit cellular transcription factors such as Rbp-jκ, C/EBPα and AP-1 to activate the expression of certain genes (Liang

et al., 2002) (Wang et al., 2003) (Wang *et al.*, 2004a). The expression of viral genes ORF57 and K8 are induced through this mechanism.

RTA also possesses intrinsic E3 ubiquitin ligase activity (Yang et al., 2008). Consequently, RTA is able to induce the degradation of lytic gene transcriptional repressors such as Hey1. Hey1 competitively binds the ORF50 promoter during latency, ultimately inhibiting RTA protein expression. However, following lytic reactivation and the induction of RTA expression, RTA directs Hey1 is for proteasomal degradation (Gould et al., 2009).

1.2.2.2.2.2 RTA and DNA replication

In addition to promoting lytic gene expression, RTA also mediates lytic DNA replication. Lytic phase DNA replication is initiated at lytic origin (*ori-Lyt*) sites and proceeds via a rolling circle mechanism. RTA binds *ori-Lyt* sites via an RRE and together with K-bZIP (K8), another virally-encoded *ori-Lyt* binding protein (OBP) mediates the recruitment and assembly of replication complexes (Wu et al., 2001) (Wang *et al.*, 2004b) (AuCoin et al., 2002). K-bZIP is unable to directly bind *ori-Lyt* sites, and instead utilises the cellular C/EBPα protein to associate with these sites (Wu et al., 2001) (Wang *et al.*, 2004b). In contrast to DNA synthesis during latency (maintenance), lytic phase replication proceeds via a virally-encoded DNA polymerase. Lytic DNA replication produces a long head-to-tail concatemeric DNA molecule that is subsequently cleaved into monomers within the TR region during genome packaging. Interestingly, KSHV DNA replication is coupled with late gene transcription, as inhibitors of viral DNA polymerase also prevent late gene expression (Tang et al., 2004).

1.2.2.2.2.3 The role of ORF57 in lytic replication

In addition to RTA, ORF57 another immediate early gene is crucial for efficient lytic replication and infectious virion production (Han and Swaminathan, 2006). The expression of ORF57 also known as the mRNA transcript accumulation (MTA) protein is indirectly induced by RTA.

ORF57 is a multifunctional protein that ultimately promotes the expression of viral genes through its interaction with numerous cellular factors. Several functions of ORF57 have

been described including its involvement in promoting RNA stability, RNA splicing and translation (Majerciak and Zheng, 2015). KSHV is a nuclear replicating virus, which relies on cellular export pathways to transport its mRNAs into the cytoplasm. The human transcription/ export (hTREX) complex predominantly mediates the export of host mRNAs, and its recruitment is dependent on successful splicing/ maturation of pre-mRNAs (Reed and Hurt, 2002). This process is subject to several control mechanisms, with unsuccessfully processed transcripts ultimately being degraded (Fasken and Corbett, 2009). As KSHV expresses numerous intronless (non-spliced) transcripts it utilises the intron containing ORF57 protein to circumvent host mediated RNA decay pathways and promote the accumulation of viral intronless genes. For example, through its cooperative binding with the cellular polyadenylate-binding protein cytoplasmic 1 (PABCP1) protein, ORF57 protects PAN from nuclear degradation (Massimelli et al., 2011). Additionally, ORF57 appears to promote the splicing of viral mRNAs containing suboptimal introns including ORF50 and K8 (Majerciak et al., 2008). Indeed, ORF57 promotes K8 splicing, directly interacting, and inhibiting SRSF3, a cellular splicing factor that suppresses K8 splicing (Majerciak et al., 2014). Finally, while ORF57 is predominantly located in the nucleus, a small proportion is present in the cytoplasm where it interacts with PYM, a cellular scaffold protein presumably to promote the translation of viral intronless mRNAs (Boyne et al., 2010).

1.3 Cellular miRNAs

MicroRNAs (miRNA) are key regulators of cellular gene expression. These highly conserved, small non-coding RNAs (~22 nts in length) post-transcriptionally regulate the expression of endogenous messenger RNAs (mRNAs). Since their discovery in *Caenorhabditis elegans* (*C. elegans*) in 1993, miRNAs they have been identified in plants, animals, and viruses (Lee et al., 1993). To date, >2600 miRNAs have been identified in the human genome and collectively are thought to regulate ~60% of all cellular mRNAs (miRBase v.22). It is therefore unsurprising that miRNAs have been shown to play critical roles in a wide range of biological processes, including development, metabolism, apoptosis, and immune function (Mehta and Baltimore, 2016). The importance of miRNAs in the maintenance of homeostatic cell function is further highlighted by ever-

increasing evidence, linking the dysregulation of miRNA expression and human disease (Sayed and Abdellatif, 2011) (Peng and Croce, 2016).

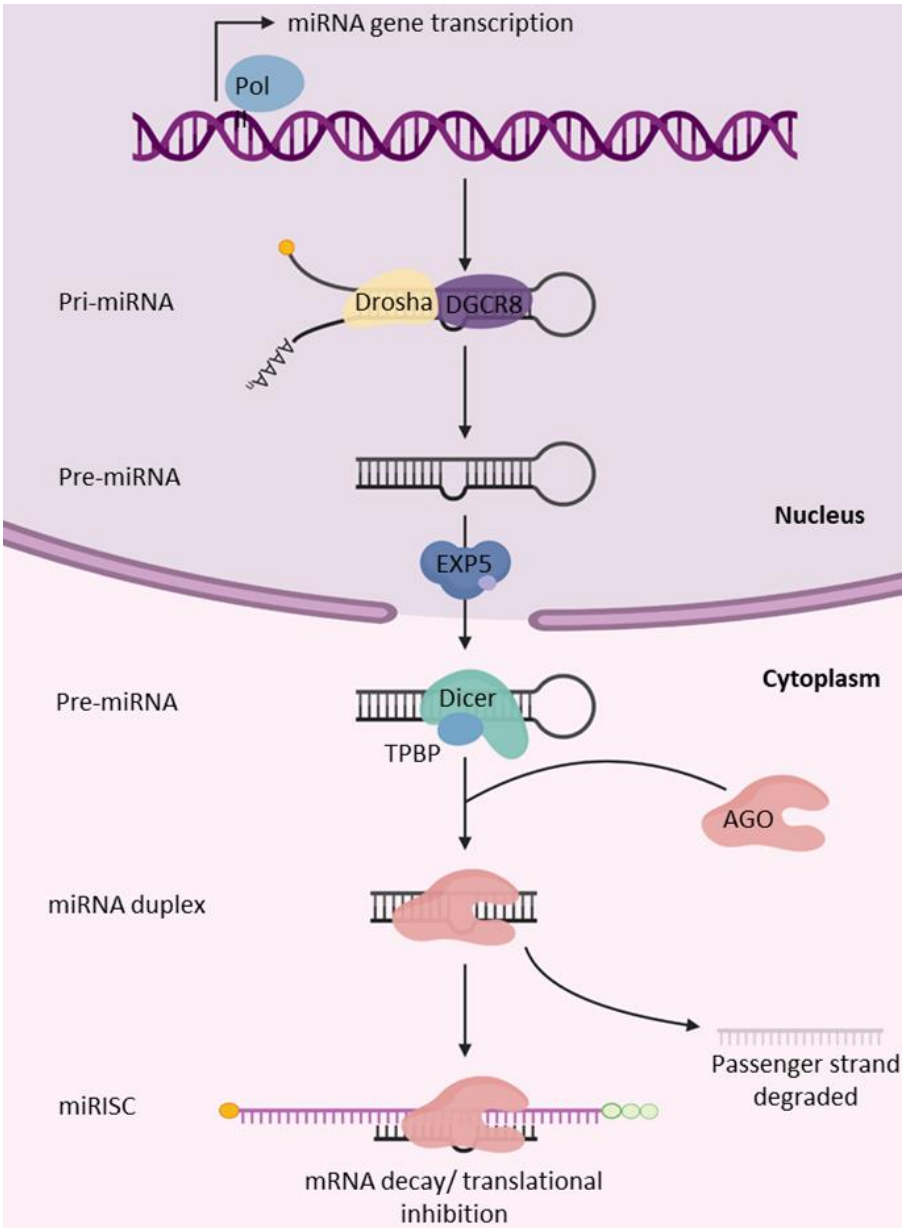

Figure 1.11 The canonical pathway of miRNA biogenesis. RNAPII, mediates miRNA genes transcription, producing long pri-miRNAs (Lee et al., 2004). Pri-miRNAs then undergo nuclear processing by the microprocessor, a complex that consists of Drosha, and its cofactor DGCR8 (Han et al., 2004). Microprocessor cleavage results in the generation of pre-miRNA, which are recognised by XPO5 and actively exported to the cytoplasm (Yi et al., 2003). Cytoplasmic processing is mediated by Dicer and produces a miRNA duplex, that interacts with AGO proteins forming pre-RISC. Guide strand selection by AGO proteins results in the removal of the passenger strand, generating an active RISC (Hu et al., 2009). The guide strand leads RISC to a subset of specific mRNA targets, determined through complementary base pairing. The recognition of target mRNA, results in the silencing of gene expression through a combination of mRNA decay and translational repression (Braun et al., 2012) (Humphreys et al., 2005) (Peterson et al., 2006).

1.3.1 Canonical miRNA biogenesis

The production of an active, mature miRNA first requires a series of processing events that occur in both the nucleus and the cytoplasm. While many non-canonical miRNA biogenesis pathways have been described, canonical processing involving the nuclear microprocessor complex remains the most utilised method of miRNA synthesis and is summarised above **(Figure 1.11)**.

1.3.1.1 Transcription of miRNA genes

MiRNA biogenesis begins with the transcription of miRNA genes, which are located throughout the genome. Indeed, both intragenic and intergenic miRNAs have been reported. A significant percentage of human miRNAs are intragenic and are transcribed largely from intronic but also exonic regions of host coding genes (França et al., 2017). Intragenic miRNAs are believed to be co-transcribed with their host gene, thus sharing regulatory and expression patterns of the respective mRNA. Alternatively, intergenic genes are located between genes and are thought to utilise distinct promoters (Hinske et al., 2014). To date, a limited number of miRNA promoter regions have been fully annotated, with relatively few transcription start sites (TSSs) actually confirmed.

While RNA Polymerase III has been reported to transcribe a subset of miRNA genes, RNA polymerase II (RNAPII) facilitates the transcription of the majority of miRNAs (Borchert et al., 2006) (Lee et al., 2004). RNAPII transcription produces a 5' capped, polyadenylated primary miRNA (pri-miRNA) transcript, that folds to form a characteristic stem loop structure (Lee et al., 2004). The stem-loop structure of pri-miRNAs typically consist of 5' and 3' single stranded RNA segments, a stem of approximately 33 nucleotides (nts), where mature miRNA sequences are located, and a terminal hairpin loop (Cai et al., 2004).

Following miRNA gene transcription, pri-miRNAs are co-/post transcriptionally processed in the nucleus.

1.3.1.2 Nuclear processing and export

The first step of miRNA maturation occurs within the nucleus, where pri-miRNAs undergo processing by the RNase III endonuclease, Drosha (Lee et al., 2003). Drosha mediates the cleavage of pri-miRNAs via two tandem RNase III domains (RIIIDs) which interact intramolecularly, to form two nearby catalytic active sites (Blaszczyk et al., 2001). Drosha is unable to mediate pri-miRNA processing alone and recruits the RNA binding protein DiGeorge syndrome critical region gene 8 protein (DGCR8), which provides additional binding to pri-miRNAs and directs Drosha cleavage (Han et al., 2004). The Drosha-DGCR8 complex is also known as the microprocessor complex and together recognises the stem-loop structures of pri-miRNA. While the specific elements required for microprocessor recognition remain to be fully determined, some pri-miRNA sequence identifiers have been described. These include a UG and CNNC motif located at the basal junction and an UGUG motif with the apical terminal loop (highlighted in **figure 1.12**) (Auyeung et al., 2013).

Furthermore, DGCR8 is known to recognise N^6-methyladenosine (m6A) GGAC reader bound sequences within pri-miRNA, subsequently promoting pri-miRNA processing (Alarcón et al., 2015) (Dang et al., 2020). Following recognition and binding, Drosha cleaves both strands of the pri-miRNA at the stem of the hairpin structure, approximately 22 bp and 11 bp away from the apical and basal junctions, respectively **(Figure 1.12)**. Ultimately leading to the release of an approximately 70 nt stem loop precursor miRNA (pre-miRNA). Drosha cleavage characteristically generates a two nt 3' overhang on the pre-miRNA which is important for subsequent nuclear export.

Exportin 5 (XPO5), a member of the nuclear transport family interacts with the GTP binding protein Ran to form a transport complex that recognises dsRNA stem loop structures containing a 2 nt, 3' overhang, such as those present in pre-miRNA (Yi et al., 2003) (Lund et al., 2004). XPO5 subsequently interacts with nucleoporin proteins at the nuclear membrane to actively translocate the miRNA complex through the nuclear pore complex (NPC) (Bohnsack et al., 2004). Once in the cytoplasm GTP is hydrolysed, resulting in disassembly of the complex and the release of pre-miRNA into the cytosol.

Additional functions have also been ascribed to XPO5, including the protection of pre-miRNAs from nucleolytic degradation. This is supported by observations that XPO5 inhibition not only reduced mature miRNA expression but also that of nuclear pre-miRNA, suggesting XPO5 may provide functions beyond that of nuclear export (Yi et al., 2003). Following nuclear export, pre-miRNAs are subjected to additional maturation steps and the cytoplasm.

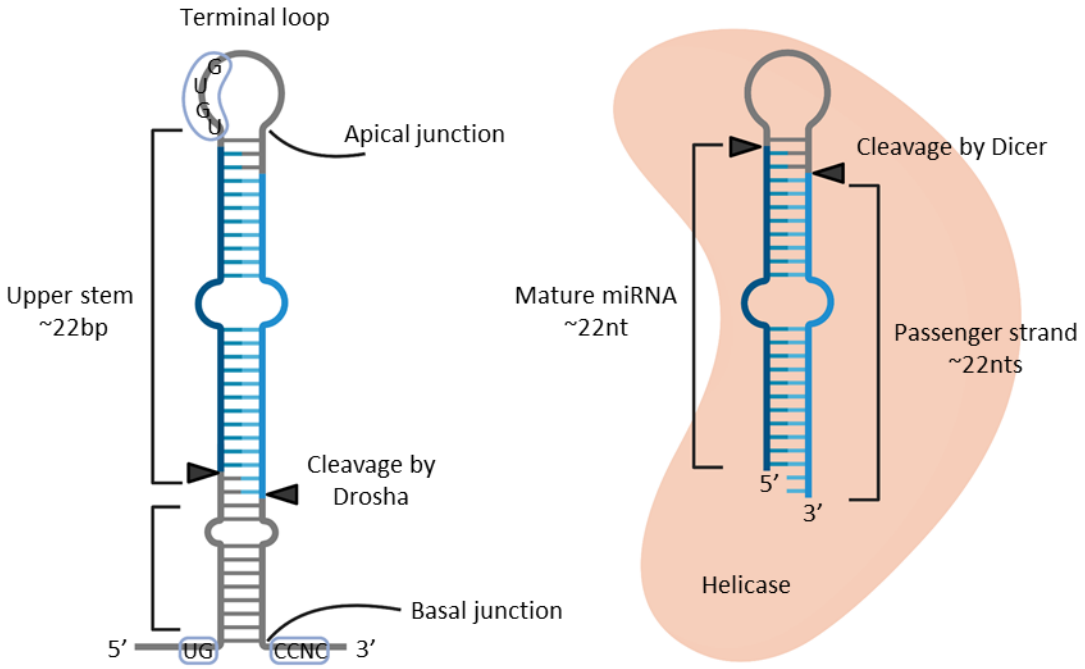

Figure 1.12 Cleavage sites of primary and precursor miRNA. The ribonuclease Drosha cleaves primary miRNA ~11 bp away from the basal junction, while also cleaving ~22 bp away from the apical junction (Han et al., 2004). Following nuclear export precursor miRNA are recognised and cleaved by Dicer. Dicer cleaves pre-miRNA at the base of the terminal loop, generating a miRNA duplex. Adapted from (Ha and Kim, 2014).

1.3.1.3 Cytoplasmic processing by Dicer

Cytoplasmic processing of pre-miRNAs is mediated by the RNase III endonuclease, Dicer. Dicer contains a central PAZ domain which recognises and binds the 3' overhang, produced during Drosha processing of the pri-miRNA (Park et al., 2011) (Tian et al., 2014). Additional binding of pre-miRNAs is provided by an N-terminal helicase domain, which recognises its terminal loop structure (Tsutsumi et al., 2011).

Dicer interacts with two ds RBD proteins, TAR RNA binding protein (TRBP) and protein activator of PKR (PACT). Though neither appear to be essential for the processing activity

of Dicer, TRBP regulates the processing efficiency of a subset of pre-miRNAs (Lee *et al.*, 2013). Dicer cleaves pre-miRNA just after the terminal loop, generating a ~22 nts miRNA duplex, which is then loaded onto Argonaute (AGO) proteins, with the help of HSC70/HSP90 chaperones in an ATP-dependent manner (Iwasaki et al., 2010) **(Figure 1.12)**.

The human AGO protein family consists of four AGO proteins (AGO1-4). AGO2 is the only human AGO that possesses intrinsic endonuclease activity, which is facilitated by its PIWI domain (Song et al., 2004). AGO proteins are a key component of the RNA-induced silencing complex (RISC), which ultimately mediates the silencing of target mRNA expression (Boland et al., 2011).

1.3.1.4 Recognition of mRNA targets and gene silencing

The interaction of miRNA duplexes with AGO proteins, leads to the assembly of pre-RISC, as guide strand selection and the removal of the passenger strand must first occur to generate mature RISC. Guide strand selection is determined by AGO proteins and ultimately directs RISC to target mRNAs. Selection usually based on the thermostability of the miRNA duplex and the strand with the most unstable 5' end is usually selected. Furthermore, Ago proteins favour guide strands with a 5' U at the first nt position (Hu et al., 2009). The passenger strand is consequently removed and rapidly degraded, the removal mechanism of the passenger strand depends on the complementarity of the central region of the miRNA duplex. If the duplex is matched at its centre, direct cleavage can occur by AGO2, the strand is then released and further degraded by the endonuclease C3PO (X. Ye et al., 2011).

However, most human miRNA duplexes contain central mismatches, therefore an alternative mechanism known as unwinding is used to mediate passenger strand removal. Unwinding is facilitated by multiple cellular helicases, which results in the miRNA duplex strand separation, followed by release and degradation of the passenger strand (Yoda et al., 2010) (Leuschner et al., 2006). Interestingly, strand selection is not an entirely strict process, and although one strand is typically more biologically active than the other, both strands of the miRNA duplex can be incorporated into RISC and contribute to gene silencing. The proportion of the strand incorporated into RISC

appears to alter considerable between different cell types and indeed the cellular environment (Meijer et al., 2014).

Following the generation of a mature RISC (miRISC), the post-transcriptional silencing of specific target mRNAs is initiated. Target recognition is guided by complementary base pairing, primarily between the 5' seed sequence of miRNA (2-8 nts) and target sites which are commonly located in the 3' UTR of mRNAs known as miRNA response elements (MREs) (Lewis et al., 2003). However, functional MREs within the 5' UTR and coding region of mRNAs have also been reported (Lee et al., 2009) (Hausser et al., 2013). Furthermore, studies have identified various non-canonical modes of binding through seed-like motifs and bulges (Helwak et al., 2013). If complete complementarity exists between a miRNA and its mRNA target, the mRNA undergoes direct cleavage by AGO2. This is a common method of silencing observed in plants however it is rarely seen in humans (Axtell et al., 2011). Silencing instead occurs through a combination of translational repression and mRNA destabilisation, which ultimately leads to mRNA decay **(Figure 1.13)** (Ipsaro and Joshua-Tor, 2015).

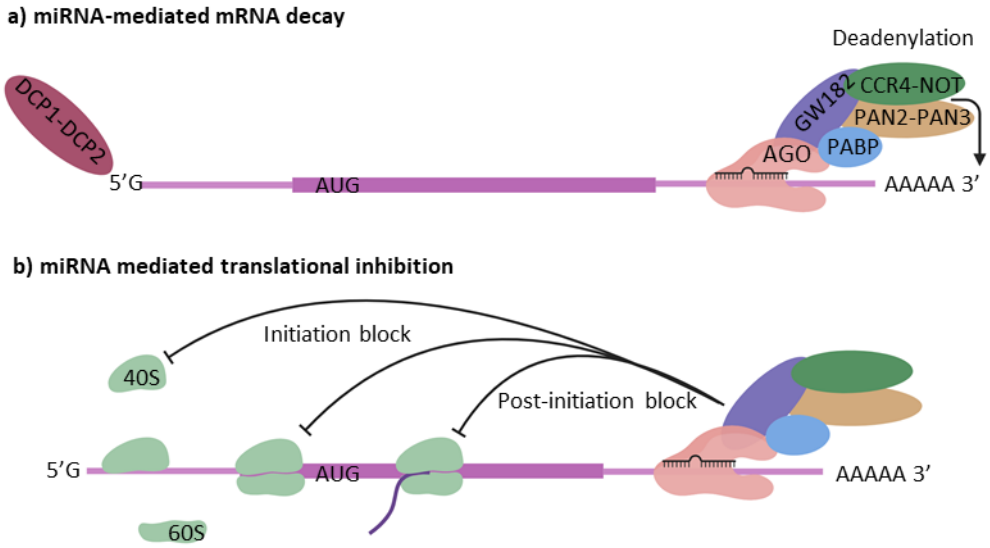

Figure 1.13 Mechanisms of miRNA-mediated silencing. miRNA mediated gene silencing primarily occurs through two mechanism: translational repression and mRNA decay. **a)** miRISC interaction with GW182 leads to the recruitment of deadenylase complexes; CCR4-NOT and PAN2-PAN3, leading to the deadenylation of the poly(A) tail (Behm-Ansmant et al., 2006). Subsequently the 5' cap is removed by the DCP1-DCP2 decapping complex. Finally, mRNA degradation is facilitated by the exoribonuclease, XRN1 (Braun et al., 2012). **b)** Translational repression: The miRISC inhibits translational initiation, restricting eIF4E cap recognition while also inhibiting the recruitment of both the 40S and 60S ribosomal subunits which ultimately prevents the formation of the 80S ribosomal complex (Humphreys et al., 2005). Post-iniation steps may also be inhibited by miRISC, leading to ribosomal elongation arrest (Petersen et al., 2006).

To facilitate translational repression and mRNA decay, AGO proteins interact with various adaptor proteins namely, GW182, which subsequently enables the recruitment of different effector proteins including those of the 5'-3' mRNA decay pathway. GW182, a well-known binding partner of AGO recruit's RISC to cytoplasmic processing bodies (P bodies), where it directs the function of PAN2-PAN3 and CCR4-NOT. These deadenylases remove the poly(A) tail of mRNAs which are then decapped by decapping protein 2 (DCP2) and its cofactor, the DEAD box RNA helicase, DDX6 (Behm-Ansmant et al., 2006) **(Figure 1.13a)**. The final step of the cellular 5'-3' mRNA decay pathway is the degradation of processed mRNA by the 5'-3' exoribonuclease, XRN1, ultimately preventing protein translation of mRNA transcripts (Braun et al., 2012). In addition to mRNA decay, miRNA target recognition can lead to translational repression, the mechanism of this however remains unclear **(Figure 1.13b)**. Indeed, the step at which translational repression occurs remains a subject of debate. It was originally thought that recruitment of RISC to P-bodies, which lack translational machinery, caused translation repression. However, in the absence of GW182 and thus P-body recruitment, translational repression was still observed suggesting repression is mediated by an alternative mechanism (Chu and Rana, 2006). Some have proposed that miRNAs can prevent the assembly and function of the eukaryotic initiation factor 4E complex (eIF4E), thereby inhibiting translational initiation (Humphreys et al., 2005), while others suggest miRNAs repress the elongation step of translation (Petersen et al., 2006). Interestingly, evidence continues to emerge implicating miRNAs in functions beyond gene silencing, including transcriptional activation within the nucleus (Vasudevan and Steitz, 2007) (Xiao et al., 2017).

1.3.2 Regulation of miRNA expression and function

Due to the extensive regulatory nature of miRNAs, it is unsurprising that they themselves are subject to tight regulatory control. Indeed, regulatory mechanisms across all stages of miRNA biogenesis have been described including those at the level of transcription, processing, and miRNA stability, which all contribute to the spatiotemporal regulation of miRNA (Ha and Kim, 2014).

1.3.2.1 Transcriptional regulation

Transcription of miRNA genes is primarily facilitated by RNAPII; thus, miRNA gene expression can be greatly influenced by the expression of RNAPII-associated transcription factors (TFs). These include p53 and ZEB1/2 that positively and negatively regulate miRNA gene expression, respectively. The expression level of TFs represents a key regulatory mechanism between different cell types and tissues. Furthermore, miRNAs often form regulatory feedback loops with TFs, therefore participating in their own regulation (Kim et al., 2007). Epigenetic changes such as DNA methylation and histone modifications have also been reported to influence the transcription of miRNA genes (Glaich et al., 2019) (Konno et al., 2019).

1.3.2.2 miRNA processing

The production of mature miRNAs is a multi-step process, facilitated by various protein complexes and RNA binding protein (RBP) cofactors. Regulation of the expression, nuclear location, and activity of all these elements therefore affects mature miRNA expression. Efficient Drosha processing of pri-miRNAs is critical for mature miRNA production. Multiple mechanisms are reported to control Drosha processing. For example, Drosha and its cofactor DGCR8 engage in an autoregulatory loop, to control expression ratios in the cell. While DGCR8 stabilises Drosha expression, Drosha directs DGCR8 for degradation through cleavage of hairpins present in DGCR8 mRNA (Han et al., 2009). This is necessary as excessive DGCR8 inhibits Drosha processing (Gregory et al., 2004). Furthermore, binding of haem stimulates DGRC8 dimerization and promotes an active structural confirmation that mediates pri-miRNA processing (Faller et al., 2007). Cytoplasmic Dicer is also subject to regulation. TRBP, its cofactor leads to the accumulation of Dicer, with a reduction of TRBP negatively affecting the stability of Dicer and therefore pre-miRNA processing. Indeed, the importance of TRBP is further highlighted by the high level of mutations within the TRBP gene and thus impairment of Dicer processing being implicated in a number of human carcinomas (Qin et al., 2020). Furthermore, post-translational modification including phosphorylation and acetylation has been demonstrated to affect protein stability, nuclear localisation, and processing activity of miRNA biogenesis components (Tang et al., 2013) (Tang et al., 2010) (Tu et al., 2015)

1.3.2.3 miRNA editing

Adenosine deaminases acting on RNA (ADAR) enzymes mediate adenosine (A) to inosine (I) editing of dsRNA molecules, with editing sites primarily located within Alu elements (Chung et al., 2018) **(Figure 1.14)**. ADARs have been reported to target both pri-miRNA and pre-miRNA affecting Drosha and Dicer processing respectively. For example, editing of pri-miR-142 inhibits Drosha cleavage and ultimately leads to the degradation of pri-miR-142 by Tudor-SN (SND1) (Yang et al., 2006). Alternatively, ADAR editing of pri-miR-151 has been shown to inhibit cytoplasmic processing of pre-miR-151 by Dicer (Kawahara, Zinshteyn, Chendrimada, et al., 2007). Furthermore, editing within the mature miRNA seed sequence has important implications, ultimately altering target genes that are regulated (Kawahara, Zinshteyn, Sethupathy, et al., 2007).

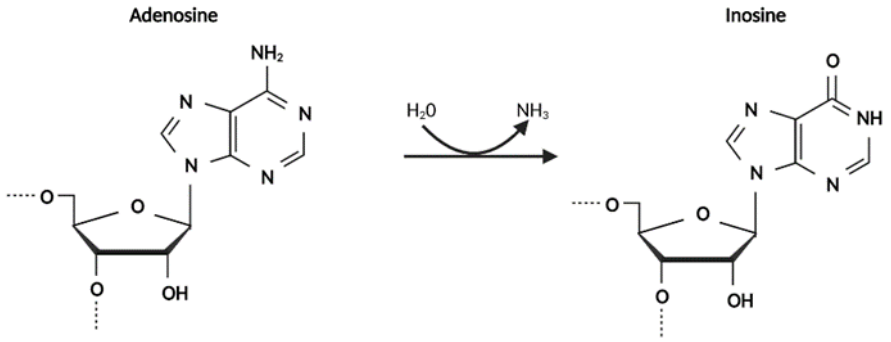

Figure 1.14 ADAR deaminases mediate A-to-I editing by deamination. Schematic showing a deamination reaction.

1.3.2.4 miRNA stability, turnover and sponging

The cellular environment is ever changing. Mechanisms that regulate the stability and turnover of mature miRNAs are therefore necessary in order to respond to both physiological and environmental changes rapidly. Modifications to the 3' end of miRNAs, AGO and target RNAs have all been shown to affect miRNA stability and turnover (Liang et al., 2020) (Gutiérrez-Vázquez et al., 2017). Interestingly, target RNAs have emerged as a mechanism utilised by viruses to target specific miRNAs for degradation and will be explored in further detail in section 1.4.2.3. Furthermore, various ncRNA species, including circRNAs and lncRNAs have been implicated in regulating miRNA function, by acting as molecular sponges and preventing target mRNA silencing (Panda, 2018).

1.3.3 Dysregulation of miRNA and disease

MiRNAs are involved in the regulation of a diverse number of biological processes, the association of aberrant miRNA expression with many human diseases is therefore unsurprising (Tüfekci et al., 2014) (Paul et al., 2018). Indeed, miRNA dysfunction has been linked to the development of neurological disorders, autoimmune inflammatory diseases, and cancer. The use miRNAs as potential biomarkers for such diseases have therefore been thoroughly investigated and several miRNA-based diagnostic tests are currently clinically available (Condrat et al., 2020) (Wang et al., 2018) (Bonneau et al., 2019). Furthermore, given the multifactorial nature of these human disorders, miRNA targeted therapies have emerged as a promising therapeutic strategy, with numerous clinical trials ongoing (Hanna et al., 2019) (Winkle et al., 2021).

1.3.3.1 Neurological disorders

The dysfunction of miRNAs has been implicated in a number of psychiatric and neurological disorders including Alzheimer's disease, epilepsy, Parkinson's disease, and schizophrenia (Juźwik et al., 2019). Alzheimer's disease (AD), a major neurological disorder is characterised by progressive memory loss and cognitive impairment. These hallmark symptoms of AD are primarily caused by the accumulation of β-amyloid plaques and intracellular neurofibrillary tangles (NFTs) that lead to the deterioration of neurons in the brain (Lane et al., 2018). Many miRNAs are expressed in the central nervous system (CNS), having pivotal roles in neuronal development and brain function. Dysregulation of these miRNAs has been implicated in the development and pathogenesis of AD, directly contributing to toxic Aβ accumulation, aggregation of hyperphosphorylated tau and neuroinflammation (summarised in **figure 1.15**) (Wang et al., 2019b) (Zhao et al., 2020) (Hussein and Magdy, 2021).

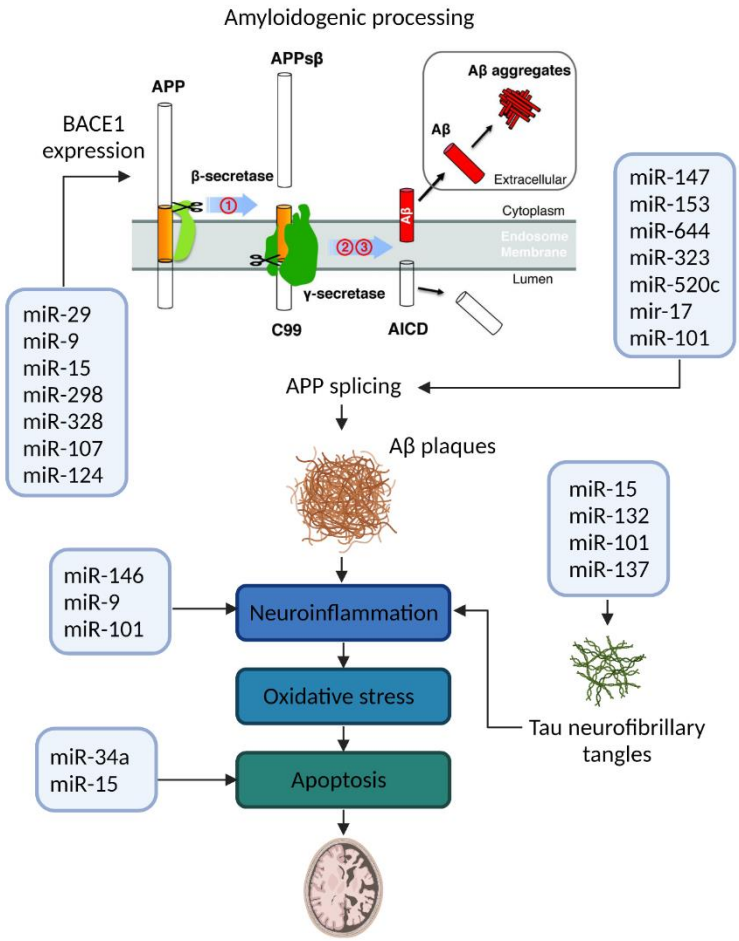

Figure 1.15 Dysregulation of miRNA in Alzheimer's disease. Examples of miRNAs involved in toxic Aβ accumulation, neurofibrillary formation, neuroinflammation and apoptosis are highlighted. Adapted from (Zhao et al., 2020) and (Hussein and Magdy, 2021).

1.3.3.2 Autoimmune inflammatory disease

Autoimmune inflammatory diseases, such as Rheumatoid arthritis (RA), have also been linked to abnormal miRNA expression. RA is a systemic disease, characterised by severe inflammation and destruction of joints. A number of miRNAs are dysregulated in RA patient samples, the majority being involved in B-cell activation and the production of inflammatory cytokines (Buckland, 2010). Interestingly, single-nucleotide polymorphisms (SNPs) have also been discovered in a number of miRNA genes, linked to increased RA risk. For example, an SNP has been found within the miR-499 gene, a miRNA that regulates a number of genes involved in several inflammation pathways including TNF-α signalling pathway (Hashemi et al., 2013).

1.3.3.3 Cancer

Cancer is one of the leading causes of death in humans, causing an estimated 10 million deaths worldwide in 2020 (Sung et al., 2021). MiRNAs have been implicated in both the formation and development of cancer. Some miRNAs may act as tumour suppressors while others possess oncogenic properties. Interestingly, this appears to be tissue type dependent, with some miRNA carrying out different, even opposing functions in different cell types (Gaur et al., 2007).

MicroRNAs were first linked to cancer development in 2004. This was following observations that the 13gq14 chromosomal region is often deleted in chronic lymphoid leukaemia (CLL) cells. Attempts were subsequently made to identify tumour suppressor genes located within this region, resulting in the discovery of miR-15a and miR-16-1. These miRNAs target the anti-apoptotic protein, BCL2, thus inducing apoptosis. Indeed BCL2 is overexpressed in many malignancies including leukaemia and solid tumours (Cimmino et al., 2005) (Calin et al., 2008). Since, many other miRNAs have been linked to the regulation of apoptosis including the upregulation of anti-apoptotic factors, suppression of pro-apoptotic proteins and the inhibition of death receptor signalling. Furthermore, increasing evidence continues to highlight the critical role that miRNAs have in regulating cancer hallmarks including resisting apoptosis, sustaining proliferation signalling, evading growth suppression, activating invasion/metastasis, and inducing angiogenesis (Peng and Croce, 2016).

Interestingly, miRNAs have also been implicated in chemoresistance, targeting drug resistance-related genes. For example, miR-21 is frequently upregulated in the breast cancer cell line, MCF-7 and has been shown to affect the susceptibility of cells to doxorubicin treatment (Wang et al., 2011).

The functional role of miRNAs in the development of cancer has led to considerable research into their use as potential therapeutic tools. Indeed, numerous, miRNA-based cancers therapies are currently under development, including mesomiR-1, a miR-16 mimic based targomiR which performed well during phase I clinical trials (van Zandwijk et al., 2017).

1.4 Viruses and miRNA

The diversity and extensive regulatory nature of miRNAs makes them extremely useful tools for viruses. Thus, viruses not only encode their own miRNAs but often manipulate host cell miRNAs to create a favourable cellular environment to enhance the progression of their lifecycle.

1.4.1 Virally-encoded miRNA

In 2004 the first virally-encoded miRNA (v-miRNA) was discovered in EBV (Pfeffer et al., 2004). Subsequently numerous v-miRNA have been identified across many different virus families. V-miRNAs not only allow viruses to simultaneously control numerous cellular pathways but also directly regulate viral factors, aiding viral persistence. Furthermore, v-miRNAs require less coding capacity and prove less immunogenic than viral proteins. As viruses do not express their own miRNA processing machinery, they hijack that of their host cell, with v-miRNA predominantly being transcribed by RNAPII and processed by Drosha and Dicer in the nucleus and cytoplasm respectively (Bartel, 2004) (Carthew and Sontheimer, 2009).

1.4.1.1 DNA viruses

Collectively, DNA viruses including members of the *Herpesviridae, Polyomaviridae, Papillomaviridae* have been shown to encode over 500 v-miRNAs (miRBase.org). DNA viruses tend to lead to long-term persistent infections; thus, miRNAs provide a means to regulate a diverse set of biological processes found at the host-virus interface.

1.4.1.1.1 Herpesviridae

The majority of viral miRNAs that have so far been identified, are encoded by members of the herpesvirus family. Furthermore, all human herpesviruses except VZV have been found to express v-miRNA (Skalsky and Cullen, 2010).

Herpesvirus miRNAs not only target cellular mRNAs but also their own, indicating that viral miRNAs not only manipulate the host cell environment but directly function in the

viral lifecycle. In 2004 the first virally-encoded miRNA was identified in the gammaherpesvirus, EBV (Pfeffer et al., 2004). Subsequently a total of 44 EBV miRNAs have been identified, that are processed from 25 pre-miRNAs (Man Wang et al., 2019). These miRNAs are encoded by two clusters, the larger BART cluster encodes 40 miRNAs, while the remaining miRNAs are encoded by the smaller BHFR1 cluster **(Figure 1.16)** (Pfeffer et al., 2004) (Cai et al., 2006). EBV miRNAs are expressed throughout the EBV lifecycle, where they play key roles in maintaining latency, immune suppression, and apoptosis (Kang et al., 2015).

KSHV encodes a total of 25 mature miRNAs that originate from 12 different pre-miRNAs. The majority of these pre-miRNAs are transcribed from the latency associated region (LAR) located between Kaposin (K12) and ORF71, however pre-K10 and K12 are encoded within the Kaposin gene itself **(Figure 1.16)** (Gottwein et al., 2006)**.** Accordingly, all KSHV-encoded miRNAs are abundantly expressed during latent infection, however expression of KSHV miRNAs originating from pre-K10 and K12 are further enhanced during lytic replication (Gottwein et al., 2006). Many KSHV miRNAs function in maintaining viral latency. In fact, miR-K12-7, K12-9 and K9-5p directly target the expression of the viral RTA transcript in order to suppress lytic reactivation (Bellare and Ganem, 2009). Alternatively, other KSHV miRNAs repress the expression of cellular factors in order to promote latent infection. For example, miR-K12-1 targets IκBα, an inhibitor of NF-κB signalling, promoting NF-κB dependent latency as well as cell survival pathways (Lei et al., 2010). KSHV miRNAs also interfere with host cell immunity including Type 1 IFN signalling a major antiviral response. KSHV miRNA miR-K12-11 directly targets IκB kinase epsilon (IKKε), a crucial regulator of IFN signalling that mediates the transcription of a subset of IFN responsive genes (Liang et al., 2011). Alternatively, other KSHV v-miRNA directly contribute to KSHV-associated pathogenesis including miR-K5 which targets the expression of tumour suppressor tropomyosin 1 (TPM1), increasing angiogenesis (Kieffer-Kwon et al., 2015).

In addition to gammaherpesviruses, members of both the *Alpha*- and *Betaherpesvirinae* encode miRNAs. Alphaherpesviruses, HSV-1/2 predominantly express miRNAs that promote latent infection while HCMV (Betaherpesvirus) expresses miRNAs throughout

the virus lifecycle that are involved in immune evasion, cell cycle control and also enhancing HCMV virulence (Pfeffer et al., 2005) (Hancock et al., 2017).

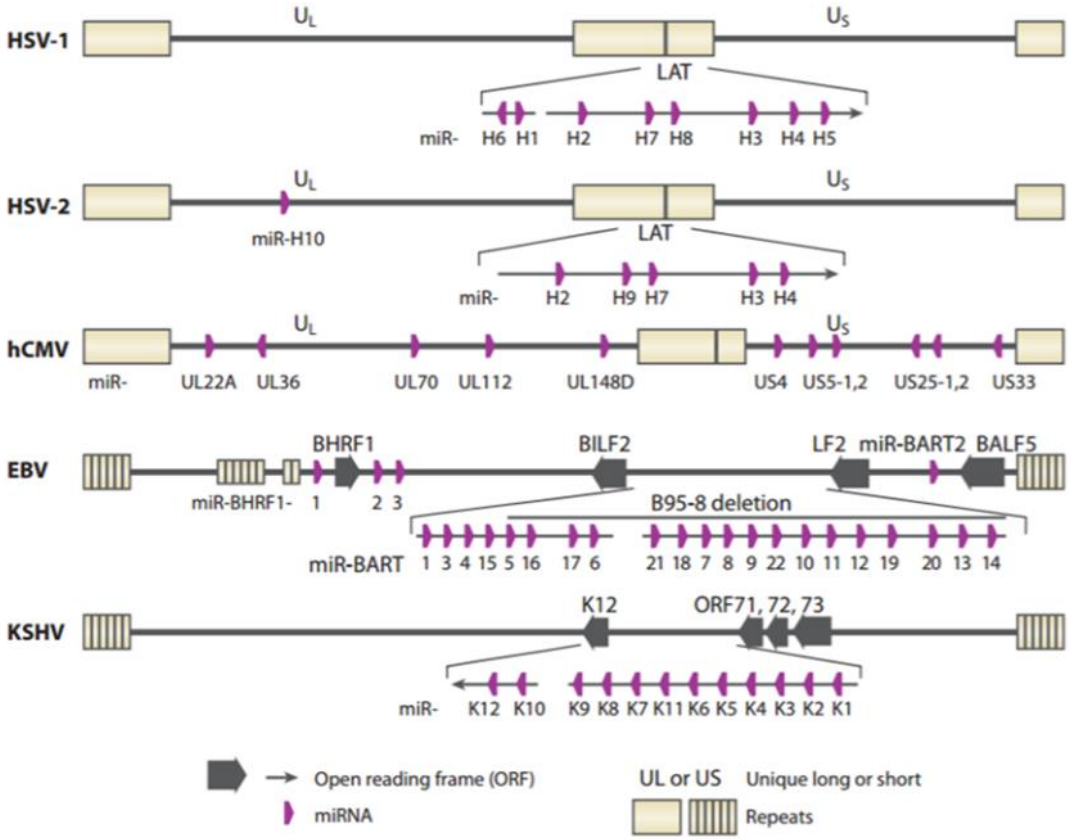

Figure 1.16 Human herpesvirus encoded pre-miRNA. Schematic showing the genomic position of pre-miRNAs for a subset of human herpesviruses. Multiple mature miRNAs can be processed from a single pre-miRNA (Taken from Skalsky and Cullen 2010).

1.4.1.1.2 Polyomaviridae

Human Polyomaviruses (PyVs) are associated with serious disease in immunosuppressed individuals. Important members of this order include the betapolyomviruses JC virus (JCV) and BK virus (BKV) which are associated with progressive multifocal leukoencephalopathy (PML) and neuropathy, respectively (Dalianis and Hirsch, 2013). Along with Merkel cell polyomavirus (MCV) which is the primary cause of Merkel cell carcinoma (MCC) (Liu et al., 2016). PyVs encode two mature miRNAs originating from a single pre-miRNA. While the genomic location and sequence of PyV miRNAs vary between viruses; they all appear to be involved in the cleavage of the early mRNA viral transcript. The early region of the PyV genome encodes regulatory proteins including the large T antigen (LTAg) which is involved in cytotoxic T lymphocyte (CTL) recognition.

Furthermore, MCV-miR-M1 has recently been shown to hinder neutrophil immune responses through the direct targeting of SP100 which ultimately leads to a decrease in the secretion of the chemoattractant, CXCL8 (Akhbari et al., 2018). PyV miRNAs are therefore considered to function in the autoregulation of viral replication as well as the suppression of immune responses, promoting viral latency and persistence (Seo et al., 2009) (Broekema and Imperiale, 2013).

1.4.1.1.3 Papillomaviridae

The *Papillomaviridae* is a large family of viruses, to date over 200 human papillomaviruses (HPV) have been identified. Most result in asymptomatic or benign infections however some HPVs are associated with the development of high-grade lesions and malignancy. Indeed, most cervical cancers are linked to HPV-16 and HPV-18 infection (Crosbie et al., 2013). While PV-encoded miRNAs had long been predicted and PV-derived small RNAs described, evidence of canonical papillomaviral miRNAs were not reported until 2018 (Chirayil et al., 2018). Newly developed, miRNA discovery by forced genomic expression (miDGE) technology was used to screen 73 PV genomes. This approach identified three HPV-encoded miRNAs. Similar to those of PyVs, these viral miRNAs were found to target the early region of the HPV genome. However, somewhat surprisingly high-risk HPVs were found not to express bona fide v-miRNAs, why this is the case is yet to be determined.

1.4.1.2 RNA viruses

While the existence of canonical RNA virus encoded miRNAs (rv-miRNA) remains controversial, reports of miRNA-like small RNAs continue to emerge. Numerous ideas have been proposed to address the apparent lack of bona fide rv-miRNAs expressed during RNA infection. For example, the majority of RNA viruses replicate in the cytoplasm of their host cell; thus, they may not have access to miRNA processing machinery present in the nucleus. Furthermore, RNA viruses tend to contain small genomes, therefore processing of precursor miRNA from the primary transcripts may prove detrimental to RNA viral replication (Aguado and TenOever, 2018).

Due to the development of deep sequencing technology, a number of RNA virus derived miRNA-like species have recently been discovered. So far, the majority of these have been identified in retroviruses. Interestingly, contrary to most RNA viruses' retroviruses such as HIV-1 complete viral genome replication within the nucleus, where they can utilise miRNA processing machinery to potentially express miRNA-like small RNA. Indeed, several HIV-1 encoded miRNA-like RNAs have been shown to affect HIV infection **(Figure 1.17)** (Bernier and Sagan, 2018)**.**

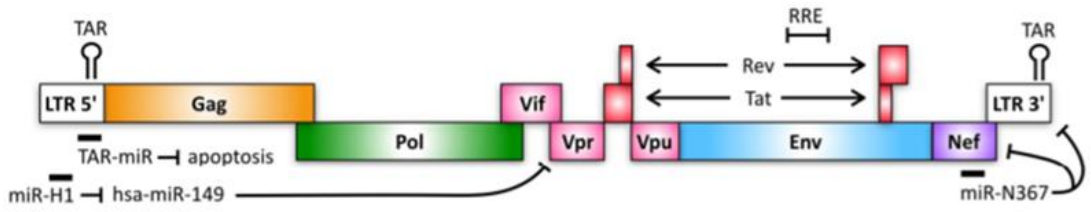

Figure 1.17 miRNA like RNAs and HIV genome. Several HIV encoded miRNA-like RNAs interact with cellular apoptotic factors and the viral genome itself (Taken from Berneir and Sagan, 2018).

For example, the transactivation response (TAR) element which forms a stable hairpin resembling that of pre-miRNA encodes miR-TAR-3p and miR-TAR-5p (Ouellet et al., 2008). These miRNAs have since been shown to target apoptotic genes such as ERCC1 and IER3, ultimately enhancing HIV infection (Klase et al., 2009). Similarly, HIV-1 miR-H1 has been shown to inhibit apoptosis, while also promoting the degradation of cellular miR-149 which targets Vpr, a HIV accessory protein (Kaul et al., 2009). Finally, the negative regulatory factor (Nef) derived miRNA, miR-N367, targets Nef itself, inhibiting HIV-1 transcription (Omoto et al., 2004).

Similarly, influenza (IAV) of the *Orthomyxoviridae* is a nuclear replicating RNA virus. H5N1, a subtype of IAV is associated with systemic inflammatory syndrome, characterised by the rapid production of antiviral cytokines and immune cell activation. This leads to a so called 'cytokine storm' and results in a high level of mortality (Watanabe et al., 2012). H5N1 encodes a single miRNA-like small RNA, miR-HA-3p, that is processed from a viral stem-loop containing RNA precursor using host cell machinery. H5N1 miR-HA-3p targets Poly (RC) Binding Protein 2 (PCBP2) expression, a negative regulator of antiviral immunity and thus antiviral cytokine expression. H5N1 miR-HA-3p therefore contributes to the induction of the 'cytokine storm' and mortality of H5N1 infection (Li et al., 2018).

1.4.2 Viruses and the dysregulation of cellular miRNAs

Viral infections also aberrantly affect the expression of cellular miRNAs, which can be ascribed to viral factors modifying the cellular environment but also host antiviral responses to infection.

1.4.2.1 Herpesvirus and latency

In addition to encoded v-miRNAs herpesviruses also take advantage of cellular miRNA to promote viral latency. Two cellular miRNAs have been implicated in promoting HSV-1 latency: miR-101 and miR-138. ICP4, an IE protein encoded by HSV-1 directly binds the promoter and induces the transcription of miR-101 (Wang *et al.*, 2021). Mitochondrial ATP synthase subunit β (ATP5B) is a direct target of miR-101 and has previously been reported to activate lytic infection. Moreover, the downregulation of ATP5B blocks DNA packaging and capsid formation, seemingly limiting the energy that is available for these processes (Zheng et al., 2011). Additionally, ICPO a viral transactivator of lytic gene expression is a direct target of miR-138 (Pan et al., 2014). Similarly, miR-320d, miR-498 and miR-1258 have all been reported to bind the 3' UTR of the KSHV lytic transactivator, RTA (Yan et al., 2013) (Yan et al., 2014).

1.4.2.2 Global downregulation of cellular miRNAs

Viruses can have a global impact on cellular miRNA expression; indeed, many viruses have been reported to directly target and inhibit the miRNA biogenesis machinery. For example, Vaccinia virus (VV) a large DNA virus that replicates within the cytoplasm of cells, causes a dramatic reduction in host cell miRNA expression (Grinberg et al., 2012). VV downregulates Dicer expression, a key component in the generation of mature miRNAs. This is achieved through the viral protease, I7, which directly mediates the degradation of Dicer (Chen et al., 2015). Furthermore, VV encodes VP55, a poly(A) polymerase which 3' polyadenylates host miRNAs and directs them for proteosomal degradation (Backes et al., 2012). Notably, VV genes contain long 3' UTRs that may contain potential miRNA binding sites. Therefore, to avoid degradation of its viral genes, it is thought that VV globally downregulates host miRNA expression.

1.4.2.3 Selective degradation of antiviral cellular miRNAs

Viruses have also developed multiple sophisticated methods to selectively target the expression of specific miRNAs that hinder their replication and survival (Cazalla et al., 2010). Notably, the production of target RNAs that recognise cellular miRNAs has emerged as a novel mechanism to trigger miRNA degradation and turnover. This process is known as target RNA-directed miRNA degradation (TDMD) and involves the active degradation of mature miRNAs through extensive base pairing at the 3'end of target miRNA. TDMD was first described in *Drosophila* but has since been identified as a mechanism employed by certain viruses to target specific miRNAs for degradation (Ameres et al., 2010). During TDMD target-miRNA binding differs from that of canonical miRNA binding allowing target RNAs to escape silencing and instead direct miRNA for degradation **(Figure 1.18)**.

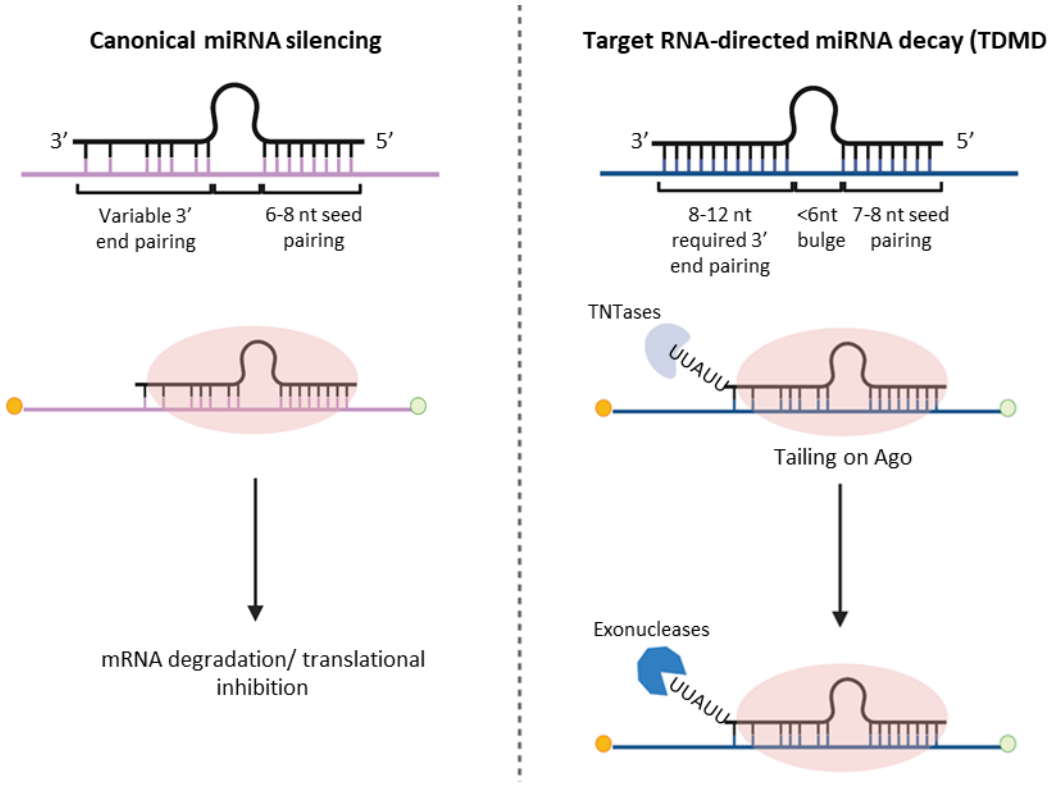

Figure 1.18 Target RNA-directed miRNA decay (TDMD). The architectures of target RNA binding to miRNA differs from that of canonical miRNA binding. Indeed significant 3' end pairing is required for TDMD while partial 3' end binding is sufficient for miRNA mediated silencing (de la Mata et al., 2015). This allows target RNA to escape miRNA silencing and instead direct miRNA degradation. Extensive 3' pairing subsequently leads to tailing by TNTases and exonuclease degradation of miRNA (Haas et al., 2016).

While only partial 3' end binding of a target mRNA is needed for canonical miRNA silencing, significant 3' end base pairing is required for TDMD (de la Mata et al., 2015). This subsequently leads to the addition of non-templated nts (tailing) to the 3' end of miRNA by cellular terminal nucleotidyl transferases (TNTases) (Haas et al., 2016). Tailed miRNAs are consequently subject to decay by 3-5' exonucleases.

Herpesvirus Saimiri (HVS) was the first virus found to utilise TDMD. HVS produces several small nuclear, U-rich ncRNAs (HSURs) during latent infection, with HSUR1 triggering TDMD of mature miR-27 (Cazalla et al., 2010). HITS-CLIP, revealed the functional relevance of selective miR-27 degradation by HVS, identifying regulators of T cell receptor (TCR) signalling as mRNA targets (Guo et al., 2014). HVS shows cellular tropism for T cells, thus it is proposed HVS degrades miR-27 in order to sustain TCR signalling, thereby promoting T cell proliferation, and permitting its propagation. Human cytomegalovirus (HCMV) also uses TDMD to selectively degrade members of the miR-17~92 cluster (Lee *et al.*, 2013). Interestingly, HCMV encoded IE1 and IE2 first induce the transcription of the miR-17~92 cluster before a miRNA decay element (miRDE) encoded by clinical strains of HCMV mediates the decay of miR-17 and miR-20a post-transcriptionally. While the specific mechanisms by which miR-17 and miR-20a degradation proves beneficial for HCMV infection remain to be determined, inhibition of miR-17 degradation results in reduced viral DNA synthesis and delayed virion production during lytic infection (Lee *et al.*, 2013). Furthermore, TDMD machinery appears to be entirely provided by the host cell and hijacked by viruses. This was demonstrated by reports that the expression of m169, a target RNA produced by murine cytomegalovirus (MCMV) alone was sufficient to direct miR-27 degradation (Libri et al., 2012).

TDMD therefore appears to be a strategy exploited by certain viruses in order to inhibit the expression miRNAs that possess antiviral properties.

1.4.2.4 Proviral miRNA that inhibit antiviral host factors

The expression of specific cellular miRNAs can also prove beneficial for viruses. Indeed, viruses have been found to upregulate proviral miRNA that inhibit the expression of antiviral host cell factors. Type I IFN represents a major arm of host antiviral immune responses to infection. Accordingly, many viruses selectively enhance the expression of cellular miRNAs that inhibit components of this pathway. Notably, HSV-1 promotes the

upregulation of miR-23a to target the expression of IFN regulatory factor (IRF1) (Ru et al., 2014). Similarly, DENV, JEV and VSV have all been found to target IL-1 receptor associated kinase 1 (IRAK1), IRAK2 and TNF receptor associated factor 6 (TRAF6) expression through the induction of miR-146a expression. Ultimately, the inhibition of key type I IFN components, supresses the production of antiviral interferon stimulated genes (ISGs) and impairs the hosts ability to effectively respond to viral infection, consequently promoting both viral survival and propagation (Wu et al., 2013) (Sharma et al., 2015) (Hou et al., 2009).

1.4.2.5 Proviral miRNA that directly interact with viral genome

Cellular miRNAs have also been reported to exert proviral functions through direct interaction with viral genomes. For example, canonical miRNA binding sites have been found in the UTRs of the *Flaviviridae* members Hepatitis C virus (HCV) and Bovine Virus Diarrhoea Virus (BVDV) and promote viral RNA accumulation (Jopling et al., 2005) (Scheel et al., 2016).

The 5' UTR of the HCV genome is highly structured and contains an internal ribosome entry site (IRES) important for HCV cap-independent translation initiation (Otto and Puglisi, 2004). This 5' UTR also contains two tandem miR-122 binding sites, where miR-122 binding results in a 3' overhang (Machlin et al., 2011). While the exact mechanisms by which miR-122 binding aids the accumulation of viral RNA remain to be determined, it is reported to protect viral RNA from decay and promote HCV-IRES formation **(Figure 1.19)** (Sedano and Sarnow, 2014) (Amador-Cañizares, 2018).

The 5' terminus of the HCV genome contains a triphosphate moiety; however it appears that miR-122 binding and subsequent AGO recruitment masks this feature, preventing recognition by cellular pyrophosphatases such as DOM32 and DUSP II (Amador-Cañizares, 2018). Ultimately, a monophosphate at the 5' end would leave the HCV genome vulnerable to degradation by cellular 5' exonucleases (Sedano and Sarnow, 2014). Additionally, miR-122 binding initiates a conformational changes, promoting HCV-IRES formation and therefore RNA translation (Schult et al., 2018). Furthermore, sequestration of miR-122 leads to the de-repression of its canonical host mRNA targets, including PKM1 and MASP1. Both are known to be upregulated during hepatocellular carcinoma (HCC), suggesting that the sustained expression of miR-122 targets contribute

to the oncogenic potential of HCV (Luna et al., 2015). Interestingly, miR-122 binding sites are present in the genomes of other Hepaciviruses, suggesting it may represent a conserved mechanism by which they increase viral RNA expression (Sagan et al., 2013). Due to the clear importance of miR-122 during HCV infection and potentially other hepaciviruses, targeting its expression may represent a potential therapeutic strategy. Indeed, Miravirsen, a LNA miR-122 inhibitor is currently in phase II of clinical trials for the treatment of HCV infection (Chakraborty et al., 2021).

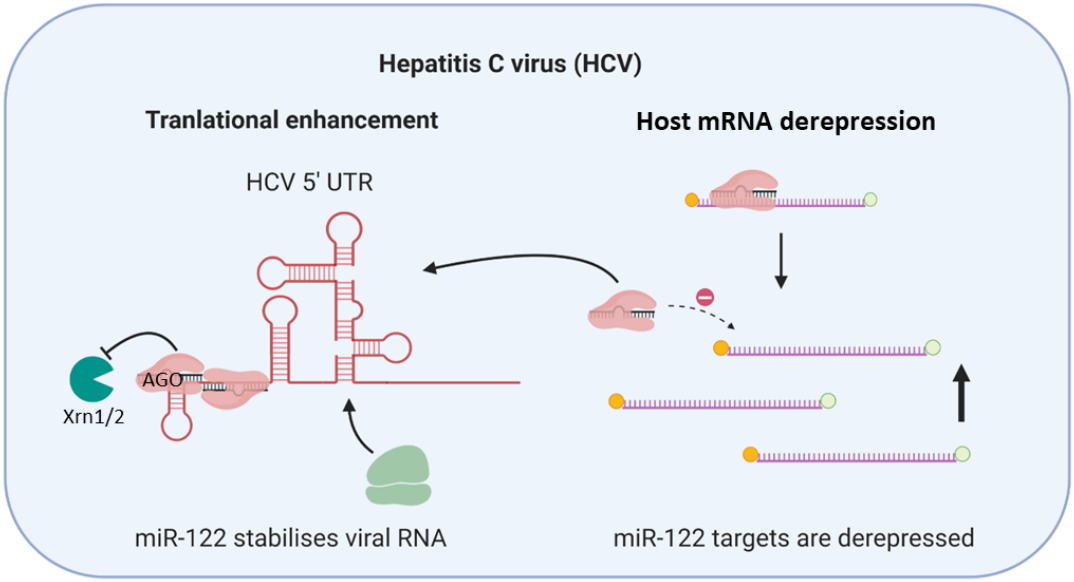

Figure 1.19 miR-122 directly interacts with the HCV genome. miR-122 directly binds to the 5' UTR of the HCV genome. Here miR-122 recruits AGO which ultimately protects the genome from cellular pyrophosphatases and subsequent degradation by exonucleases (Amador-Cañizares, 2018) (Sedano and Sarnow, 2014). Binding of miR-122 also facilitates HCV-IRES formation, enhancing viral translation (Schult et al., 2008). Furthermore, the sequestration of miR-122 by the HCV genome leads to the derepression of its cellular mRNA targets (Luna et al., 2015).

1.5 Thesis aims

The initial aim of this thesis was to investigate the importance of cellular miRNAs during lytic KSHV infection. Chapter 3 aimed to identify cellular miRNAs that are dysregulated during lytic KSHV infection. To this end, miRNA sequencing was used, and numerous miRNAs were shown to be differentially expressed following KSHV lytic reactivation. The dysregulation of several miRNAs was confirmed including the downregulation of miR-142-3p and miR-25-5p during lytic infection of TREx BCBL-1 cells. Furthermore, reintroducing the expression of these miRNAs inhibited viral infection, particularly the production of infectious virions, indicating that KSHV actively promotes the downregulation of these miRNAs.

Chapter 4 explored the identification of cellular mRNA targets, whose expression was increased by the downregulation of miR-142-3p during lytic KSHV infection. Multiple miRNA target prediction programmes were utilised to identify potential miR-142-3p mRNA targets. Mimic and 3' UTR luciferase assays confirmed that GPRC5A is a direct target of miR-142-3p. GPRC5A depletion resulted in a decrease in infectious virion production, a similar phenotype was also observed following miR-142-3p overexpression.

Finally, chapter 5 aimed to elucidate potential mechanisms by which KSHV mediates the downregulation of cellular miRNAs during lytic replication. Efforts focused on transcriptional and pri-miR-142 processing mechanisms such as methylation, editing and alterations in transcription factors.

In summary, these findings highlight how KSHV is able to exploit cellular miRNAs in order to promote KSHV lytic infection. Ultimately, increasing our understanding of these interactions may lead to the discovery of novel therapeutic approaches for the treatment of KSHV-associated diseases. As KSHV commonly causes malignant disease, research into pathways utilised by these pathogens may also prove beneficial in elucidating mechanisms of cancer development.

Chapter 2

~

Material and Methods

2. Materials and Methods

2.1 Materials

2.1.1 Chemicals

Unless stated otherwise, chemicals were obtained from Sigma Aldrich®, Thermo Fisher Scientific or VWR International.

2.1.2 Cell culture reagents

Cell culture reagents were obtained as indicated in table 2.1.

Table 2.1: List of cell culture reagents and their suppliers

Reagent	Supplier
Dulbecco's Modified Eagle's Medium (DMEM)	Gibco™
RPMI1640	Gibco™
Foetal bovine serum (FBS)	Gibco™
Penicillin/streptomycin	Gibco™
Hygromycin B	Thermo Fisher Scientific
Puromycin	Thermo Fisher Scientific
Doxycycline hyclate	Sigma-Aldrich®
Phosphate buffered saline (PBS)	Lonza
Trypsin-EDTA	Gibco™
Opti-MEM™	Gibco™
Lipofectamine™ RNAiMAX	Thermo Fisher Scientific
Lipofectamine™ 2000	Thermo Fisher Scientific

2.1.3. Enzymes

All enzymes used and their supplier are listed in the table below (Table 2.2).

Table 2.2: List of enzymes and their suppliers

Enzyme	Supplier
DNA-free™ DNA Removal (DNase I treatment)	Invitrogen™
LunaScript™ Reverse transcription SuperMix	New England Biolabs (NEB)
miScript II Reverse transcription	QIAGEN
Proteinase K	QIAGEN

T4 RNA ligase	Illumina
Antarctic phosphatase (AnP)	New England Biolabs (NEB)

2.1.4 Antibodies

All primary antibodies, their working dilution and suppliers are indicated in table 2.3.

Table 2.3: List of primary antibodies, working dilution and suppliers

Antibody	Origin	Working dilution		Supplier	Identity
		WB	IF		
Anti-ADAR1	Rabbit	1:500	-	Proteintech®	14330-1-AP
Anti-ADAR2	Rabbit	1:500	-	Proteintech®	22248-1-AP
Anti-DNMT1	Rabbit	1:500	-	Proteintech®	24206-1-AP
Anti-GAPDH	Mouse	1:5000	-	Abcam	ab126605
Anti-GFP	Mouse	1:1000	-	Living Colours®	632381
Anti-GPRC5A	Rabbit	1:500	-	Atlas Antibodies	HPA007928
Anti- HSPA1A	Rabbit	1:1000	-	Aviva Systems Biotech	ARP33096
Anti-K8.1A			-		
Anti-OCT4	Mouse	1:5000	-	Proteintech®	60242-1-Ig
Anti-ORF57	Mouse	1:1000	1:500	Santa Cruz Biotech	sc-135746
Anti-ORF59	Rabbit	1 1000	-	Gift from Britt Glaunsinger. University of California, Berkley	-
Anti-ORF65	Rabbit	1:500	-	Discovery® Antibodies	Crb2005224
Anti- SND1	Rabbit	1: 1000	-	Proteintech®	60265–1-Ig
Anti-STAT6	Mouse	1:1000	-	Proteintech®	66717-1-Ig

Secondary Horseradish peroxidase (HRP)-conjugated anti-mouse and anti-rabbit IgG antibodies were purchased from Dako and used for western blotting at a 1:5000 dilution. Secondary Alexa Fluor® 488 and 594- conjugated IgG used for confocal microscopy were purchased from Life Technologies and used at a dilution of 1:500.

2.1.5 Oligonucleotides

Oligonucleotide primers used for qPCR were purchased from IDT or Sigma-Aldrich®, while universal reverse and mature miScript miRNA primers assays were obtained from QIAGEN.

2.1.5.1 qPCR primers

The sequence of primers used to assess mRNA levels (viral and cellular) and miRNA expression are detailed table 2.4 and 2.5 respectively.

Table 2.4: List of oligonucleotides and their sequences

Primer	Forward sequence (5'-3')	Reverse sequence (5'-3')
ADCY9	CTCAAAACGGCTGCCAAGACGA	GAGAAGTCTGACTGTTGGTGAGC
ARID3B	CCTGGAGTGATGATGCAGATGG	GACGAAGAGGTCATCCAGGAAC
ATG16L1	CTACGGAAGAGAACCAGGAGCT	CTGGTAGAGGTTCCTTTGCTGC
ATG5	GCAGATGGACAGTTGCACACAC	GAGGTGTTTCCAACATTGGCTCA
CCNT2	GGCTGCAAAAGTGGAAGAACAGG	CCAGTTCTTGAGTCTGTTGAAGG
DNMT1	AGGTGGAGAGTTATGACGAGGC	GGTAGAATGCCTGATGGTCTGC
GAPDH	TGTGGTCATGAGTCCTTCCACGAT	AGGGTCATCATCTCTGCCCCCTC
GPRC5A	CCTTTCCCTGTTGGTGATTCT	AGACATTGACGTTGGTCCTATTC
HMBG1	GATCCCAATGCACCCAAGAG	GGGCGATACTCAGAGCAGAAGA
HSPA1A	CGACCTGAACAAGAGCATCA	AAGATCTGCGTCTGCTTGGT
HSPA1B	ACCTTCGACGTGTCCATCCTGA	TCCTCCACGAAGTGGTTCACCA
IL-10	TCTCCGAGATGCCTTCAGCAGA	TCAGACAAGGCTTGGCAACCCA
IL-6	TCTGCGCAGCTTTAAGGAGT	GACCAGAAGAAGGAATGCCCA
K8.1A	CCACCAAGAGGACCACACATTC	CACACAAAGTCTGGCATGGTTCTC
KDM6A	CGTGTCGTATCAGCAGGAAA	CACCCCAGTAACCTTCAGCA
LMO3	TCTGAGGCTCTTTGGTGTAACG	CCAGGTGGTAAACATTGTCCTTG
MALAT1	GAATTGCGTCATTTAAAGCCTAGTT	GTTTCATCCTACCACTCCCAATTAAT
OCT4-	TATTCAGCCAAACGACCATCT	TCAGCTTCCTCCACCGACTT
ORF21	CCCTGAGGAGAGGAAACCACTAAC	CCGACTGGCAAAAATGCTGC
ORF50	ATGACAAGGGTAAGAAGCTTCGG	ACTGGTAGAGTTGGGCCTTCAGTT
ORF47	CGCGGTCGTTCGAAGATTGGG	CGAGTCTGACTTCCGCTAACA
ORF57	GCCATAATCTAAGCGTACTGG	GCAGACAAATATTGCGGTGT
ORF59	CCGATCGTGGAAAGGTAGGA	ATGTACTCGACGCTGGCATA
ORF65	AAGGTGAGAGACCCCGTGAT	TCCAGGGTATTCATGCGAGC
RAC1	CCTGATGCAGGCCATCAAG	AGTAGGGATATATTCTCCAGGAAATGC
STAT6	CCTTGGAGAACAGCATCCCTG	GCACTTCTCTGTGACAGAC
TAB2	TATTCAGCACCTCACGGACCCT	CTTTGAAGTCGTTCCATTCTGGC
vIL-6	GGCATCTGCAAGGGTATTCT	AAATCCTATTAACCCGCAGTGAT

Table 2.5 List of primers used to assess miRNA expression

Primer	Target sequence	Accession number
miR-128-1-5p	CGGGGCCGUAGCACUGUCUGAGA	MIMAT0026477
miR-142-3p	UGUAGUGUUUCCUACUUUAUGGA	MIMAT0000434
miR-142-5p	CAUAAAGUAGAAAGCACUACU	MIMAT0000433
miR-191-3p	GCUGCGCUUGGAUUUCGUCCCC	MIMAT0001618
miR-21-3p	CAACACCAGUCGAUGGGCUGU	MIMAT0004494
miR-21-5p	UAGCUUAUCAGACUGAUGUUGA	MIMAT0000076
miR-23a-5p	GGGGUUCCUGGGGAUGGGAUUU	MIMAT0004496
miR-25-5p	AGGCGGAGACUUGGGCAAUUG	MIMAT0004498
miR-3609	CAAAGUGAUGAGUAAUACUGGCUG	MIMAT0017986
miR-4516	GGGAGAAGGGUCGGGGC	MIMAT0019053
miR-92a-1-5p	AGGUUGGGAUCGGUUGCAAUGCU	MIMAT0004507

2.1.5.3 Cloning primers

Primer sequences used for molecular cloning are shown below in table 2.6. All cloning primers were purchased from IDT.

Table 2.6 List of cloning primers and their sequences

Primer	Forward sequence (5'-3')	Reverse sequence (5'-3')
GPRC5A 3'UTR	AAAAAACTCGAGTCCACATCAAAT GAACATTGG	AAAAAAGCGGCCGCTGAGGGCTAAA ACTGAAATG
psiCHECK ™-2	-	GAGGACGCTCCAGATGAAATG

2.1.6 miRNA mimics

All miRNA mimics were obtained from Applied Biological Materials Inc and are shown in the table below (Table 2.7).

Table 2.7 List of miRNA mimics and their suppliers

miRNA mimic	Supplier	Catalogue number
miR-142-3p	Applied Biological Material Inc (abm)	MCH01312
miR-25-5p	Applied Biological Material Inc (abm)	MCH01623

2.1.7 Plasmid

All plasmid constructs used in this study were kind gifts from collaborators or already present in the Whitehouse laboratory (Table 2.8).

Table 2.8 List of plasmid constructs and their suppliers

Plasmid	Supplier	Identifier
plenti-CMV-GPRC5A	Oliver Manners (Whitehouse laboratory)	-
psiCHECK™-2	Dr. James Boyne (Leeds Beckett University)	C8021
psiCHECK™-2-3'UTR GPRC5A	Cloned from psiCHECK™-2	-
GFP-ORF50	Dr. James Boyne (Whitehouse laboratory)	-

2.2 Methods

2.2.1 Molecular cloning

2.2.1.1 Bacterial cell culture and cryopreservation

All work using live bacterial cells were performed in a sterile environment. A sterile flame and sterile tips were used to prevent contamination. Autoclaving at 121°C, 1 hour (hr) was used to sterilise culture medium and agar. For long-term storage, transformed *E. coli* were frozen at -80°C as a glycerol stock in 1 ml lysogeny broth (LB) medium [0.5% yeast extract, 1% (w/v) tryptone, 0.5 (w/v) NaCl] containing 25% glycerol.

2.2.1.2 Transformation of *E. coli* DH5α

For each transformation, 50 µl of competent *E. coli* DH5α cells were thawed on ice. Cells were mixed with 1 ng plasmid DNA and incubated for 30 minutes (mins) on ice. Cells were then subjected to heat shock at 42°C for 30 seconds (secs) before being immediately returned to ice for 5 mins for cooling. Following the addition of 450 µl of SOC medium (NEB), cultures were incubated with shaking (180 rpm) at 37°C for 1 hr. Next cultures were spread onto agar plates [1.5% (w/v) in LB medium] containing ampicillin or kanamycin (50 µg/ml) and incubated at 37°C overnight.

2.2.1.3 Plasmid purification

Single colonies or glycerol stocks were used to inoculate 10 ml LB containing 50 µg/ml ampicillin or kanamycin where appropriate and incubated overnight at 37°C with shaking (180 rpm). Bacterial cells were then pelleted, and the supernatant removed following centrifugation at 4,500 x *g* for 5 mins. Next, plasmid DNA was purified using a Monarch® Plasmid Miniprep Kit (NEB) according to manufacturer's instructions. In brief, bacterial cell pellets were resuspended in 200 µl B1 buffer and vortexed to ensure complete resuspension. Following the addition of 200 µl B2 buffer, samples were inverted several times and incubated for 1 min. Next 400 µl B3 buffer was added, samples were again inverted several times to allow mixing and incubated for 2 mins. Samples were subsequently centrifuged for 5 mins at 16000 x *g* and the supernatant transferred to spin columns. Spin columns were then centrifuged for 1 min and the flow-through discarded. Following to sequential addition of plasmid wash buffer 1 (200 µl) and wash buffer 2 (400 µl), columns were centrifuged for 1 min and the flow-through discarded. Columns were then transferred to a clean 1.5 ml microcentrifuge tube and 30 µl of water added. Following a 1 min incubation, samples were centrifuged for 1 min. All centrifugation steps were carried out at 16000 x *g* at room temperature unless otherwise stated. DNA concentrations were assessed using a NanoDrop ND-1000 spectrophotometer (NanoDrop technologies). Purified plasmid DNA was stored at -20°C.

2.2.1.4 Cloning

The 3' UTR of GPRC5A was cloned into the psiCHECK™-2 vector plasmid. NCBI AceView was first used to identify the 3' UTR of GPRC5A and appropriate primers designed. The 3' UTR of GPRC5A was then amplified from TREx BCBL-1 Rta cDNA using Q5 high fidelity 2x master mix (NEB). The following master mix was added to an appropriate volume of cDNA and nuclease free water making a final reaction volume of 25 µl:

12.5 µl Q5 High-Fidelity 2x Mater mix

1.25 µl 10 µM Forward primer

1.25 µl 10 µM Reverse primer

The following cycling conditions were used: initial denaturation at 98°C for 30 secs, followed by 35 cycles of denaturation at 98°C for 10 secs, annealing at 60-72°C for 20

secs and extension at 72°C for 20-30 sec/kb. A final extension step was then performed at 72°C for 2 mins.

A double digestion reaction was set up containing 1 µg plasmid DNA, 2 µl 10x CutSmart™, 1 µl XhoI, 1 µl Not1-HF and made up to 20 µl using nuclease free water. The digestion reaction was incubated at 37°C for 1 hr, followed by 65°C for 20 mins. Following plasmid digestion, a phosphatase reaction was performed using the NEB alkaline phosphatase kit (NEB). Digested plasmid DNA was incubated with 2 µl 10x Antarctic Phosphatase Reaction Buffer, 1 µl Antarctic Phosphatase and nuclease free water making a final reaction volume of 20 µl. The reaction mixture was incubated at 37°C for 30 mins, followed by a heat-inactivation step at 80°C for 2 mins. Subsequently a ligation reaction containing the following was set up:

5 µl 10x T4 DNA ligase buffer

100 ng plasmid DNA

16 ng insert DNA

1 µl T4 DNA ligase

Finally, nuclease free water was added to make a final reaction volume of 50 µl. The ligation reaction was incubated at 16°C overnight before being used to transform competent *E. coli* DH5α as described above in section 2.2.1.2.

2.2.2 Mammalian cell culture

2.2.2.1 Cell lines

Human embryonic kidney (HEK) 293T (referred to as 293T) cells obtained from the American Type Culture Collection (ATCC) and were used in plasmid transfection and reinfections assays. TREx BCBL-1 Rta cells (human B-cell lymphoma derivative, latently infected with KSHV) were a kind gift from J. U. Jung (University of Southern California, USA) (Nakamura, 2003). These cells contain an inducible Myc-RTA expression construct and were therefore used in experiments to access KSHV lytic replication. GPCR5A knockdown TREx BCBL-1 Rta cells were generated by Oliver Manners (Whitehouse laboratory).

2.2.2.2 Cell maintenance

TREx BCBL-1 Rta cells were cultured in Roswell Park Memorial Institute 1640 growth medium (RPMI1640) supplemented with 10% (v/v) heat inactivated foetal bovine serum (FBS), 1% (v/v) penicillin/ streptomycin (known as complete RPMI1640). Additionally, TREx BCBL-1 Rta cells were kept under Hygromycin B selection (100 µg/ml). HEK 293T (293T) cells were maintained in Dulbecco's Modified Eagle's Medium (DMEM), also containing 10% (v/v) FBS, and 1% (v/v) penicillin/streptomycin (here after referred to as complete DMEM). GPRC5A knockdown TREx BCBL-1 Rta cell were maintained in complete RPMI and kept under both Hygromycin B selection (100 µg/ml) and puromycin (3 µg/ml). All cells incubated at 37°C in the presence of 5% CO_2. Cells were split every 2-3 days upon reaching appropriate confluency. 293T cells were trypsinized (1 ml, 0.05% (v/v) trypsin in PBS) to dissociate adherent cells before being resuspended in 10 ml complete DMEM to inactivate the trypsin. These cells were then split 1:10 in a new flask in complete DMEM. TREx BCBL-1 Rta were cultured in suspension and split 1:4 into complete RPMI1640 growth medium.

2.2.2.3 Cell counting

Cells were counted for cell seeding at concentrations as required. Following collection of cell suspensions in a falcon tube, 1 ml of cells was transferred to a 1.5 ml microcentrifuge tube. A volume of 10 µl was then added to a sterile haemocytometer and cells counted using a light microscope (Leica Microsystems). The number of cells/ml was then calculated.

2.2.2.4 Transient transfection

For transient transfection, 293T cells were transfected using Lipofectamine™ 2000 (Thermo Fisher Scientific) 24 hrs after seeding, according to manufacturer's instructions at variable concentrations. For example, 1 µg of plasmid DNA was added to 100 µl Opti-MEM™, similarly 4 µl of Lipofectamine™ 2000 was added to 100 µl of Opti-MEM™. Both mixtures were incubated for 5 mins at room temperature before being combined and incubated for a further 20 mins at room temperature. Following incubation, the combined solution was added to 293T cells, dropwise. Cells were then harvested or analysed 24 hrs post transfection.

2.2.2.5 miRNA mimic treatment

For miRNA mimic assays cells were transfected using Lipofectamine™ RNAiMAX (Thermo Fisher Scientific), following manufacturer's instructions. In short, 4 µl Lipofectamine RNAiMAX was used to transfect TREx BCBL-1 Rta cells with specific miRNA mimics at a final concentration of 100 nM. Cells were incubated at 37°C for 24 hrs, then reactivated as described below (section 2.2.3.1). Cells were collected 24 hrs post reactivation and used for analysis of protein by western blotting (described in sections 2.2.4.1- 2.2.4.3) and RNA by quantitative reverse transcriptase PCR (qRT-PCR) as described below in sections 2.2.5.1- 2.2.5.4.

2.2.2.6 8-Azadenosine treatment

TREx BCBL-1 Rta cells were treated with varying concentrations of 8-Azaadenosine (0-125 nM) (Cambridge Bioscience) for 1 hr before lytic KSHV replication was induced. It was dissolved in DMSO and 1 µl of the working solution was added per ml of media. A total of 0.1% (v/v) DMSO was therefore used.

2.2.2.7 Cell sample collection

Following collection, cell samples were centrifuged at 500 x *g* for 3 mins and the supernatant removed. Cell pellets were stored at -80°C until required.

2.2.3 Virus based assays

2.2.3.1 Induction of KSHV lytic replication

Viral replication in TREx BCBL-1 Rta cells were induced by adding 2 µg/ml doxycycline hyclate (Sigma-Aldrich®) to media. Viral protein and RNA expression studies were performed at 8, 16 and 24 hrs post induction. Viral reinfection studies however were performed 72 hrs after induction.

2.2.3.2 KSHV replication assay

To assess viral load within cells following treatment with miRNA mimics/ inhibitors, TREx BCBL-1 Rta cells were seeded into 12 well plates. Cells were then treated as described

above in section 2.2.2.5 before being induced (as described in section 2.2.3.1). Following a 72 hrs incubation, cells were harvested. Cells were centrifuged at 500 x *g* for 5 mins at 4°C, the supernatant was removed. Cells were then resuspended in PBS, before being spun again at 500 x *g* for 5 mins. The QIAamp DNA mini kit (QIAGEN) was subsequently used to purify both viral and cellular DNA, according to manufacturer's instructions. Cells were lysed using QIAGEN protease and buffer AL, at 56°C for 10 mins. Following the addition of ethanol, the mixture was added to a QIAquick spin column and spun at 6,000 x *g* for 1 min at room temperature. The flow through was discarded, before centrifugation was repeated following the addition of AW1 buffer. The flow through was again discarded and AW2 buffer added to the column, before being spun at 16,000 x *g* for 3 mins at room temperature. The column was then transferred to a 1.5 ml microcentrifuge tube and 50 µl distilled water added. The column was then spun at 6,000 x *g* for 1 min at room temperature to elute the DNA, which was subsequently stored at -20°C. Levels of viral and cellular DNA were quantified by qPCR (as described below in section 2.2.5.4).

2.2.3.3 KSHV reinfection assay

To assess the production of infectious virions, TREx BCBL-1 Rta cells were first seeded into 12 well plates before being treated with miRNA mimic and induced as described in section 2.2.2.5 and 2.2.3.1 respectively. Cells were incubated for 72 hrs before being harvested; cells were spun at 500 x *g* for 5 mins at 4°C. The supernatant was then mixed with complete DMEM (1:1) and added to previously seeded, confluent 293T cells. Cells were incubated for 48 hrs, washed with PBS, and then harvested. Total RNA was extracted using TRIzol™ Reagent (Invitrogen™), and then analysed using quantitative reverse transcriptase PCR (qRT-PCR) as described below in sections 2.2.4.1-2.2.4.4. Like cellular mRNA, viral mRNA was normalised against GAPDH, (a house keeping gene) and quantified using the comparative *C*T method as previously described (Baquero-Perez et al., 2019).

2.2.4 Analysis of proteins

2.2.4.1 Production of protein lysates

Cells were washed with PBS and lysed in 100 µl Leeds lysis buffer (LLB) (25 mM glycerol phosphate, 20 mM Tris, 150 mM NaCl, 1 mM EDTA, 1% Triton X-100, 10% glycerol, 50 mM NaF, 5 mM Na4O7P2, pH 7.4) supplemented with Roche cOmplete™ protease inhibitor cocktail (Sigma-Aldrich®) at the recommended concentration. If necessary, the protein concentration of cell lysates was assessed using a Pierce™ Bicinchoninic acid (BCA) Protein assay kit (Thermo Fisher Scientific) according to manufacturer's instructions. In a 96-well plate, 10 µl of protein sample or Bovine serum albumin (BSA) standards were added to 190 µl of pre-diluted BCA working reagent containing BCA reagent A and B (50:1, Reagent A: B) in duplicate. Following a 15 min incubation at 37 °C, absorbance was measures at 562 nm using an Infinite® F50 Robotic microplate reader (Tecan).

2.2.4.2 SDS-PAGE electrophoresis

Protein samples were separated using sodium dodecyl sulphate (SDS)-polyacrylamide gel electrophoresis (PAGE). Protein lysates were mixed with 2 x SDS loading buffer [100 mM Tris/HCl, pH 6.8, 4% (w/v) SDS, 20% (v/v) glycerol, 10 mM DTT, 0.25% (w/v) bromophenol blue] (1:1) and boiled for 10 mins at 95°C. Samples were then loaded along with Precision Plus Protein™ Dual Colour Standards (Bio-Rad Laboratories) on 10-15% polyacrylamide gels, where appropriate. Proteins were resolved through polyacrylamide gels containing a 5% stacking gel [5% (v/v) acrylamide/bis-acrylamide 37.5:1, 125 mM Tris/HCl; pH 6.8, 0.1% (w/v) SDS, 0.08% (v/v) APS, 0.008% (v/v) TEMED] and a 10-15% resolving gel [10-15% (v/v) acrylamide/bis-acrylamide 37.5:1 (Severn Biotech Ltd), 375 mM Tris/HCl; pH 8.8, 0.1% (w/v) SDS, 0.12% (v/v) APS, 0.012% TEMED (v/v)]. Gels were run at 180 V for ~60 mins in running buffer containing 25 mM Tris, 192 mM Glycine and 0.1 % (w/v) SDS.

2.2.4.3 Western blot analysis

Following SDS-PAGE, protein samples were subsequently transferred onto nitrocellulose Amersham™ Protran 0.45 µM membranes (GE Healthcare) using a Trans-Blo t® Turbo System™ (Bio-Rad Laboratories). The transfer took place at a standard setting

of 25 V, 1 A for 30 mins. Transfer buffer containing 20% (v/v) methanol, 25 mM Tris, 192 mM glycine was used. Non-specific binding of membranes was blocked with 10% (w/v) dried skimmed milk powder (Marvel) in TBS-T [150 mM NaCl, 50 mM Tris/HCl pH 7.5, 1% (v/v) Tween-20] for 1 hr at room temperature on a rocking platform. Following this the membranes were incubated with primary antibody in 5% (w/v) dried skimmed milk powder (Marvel) in TBS-T for 1 hr at room temperature on a rocking platform or overnight (O/N) at 4°C on a roller. Membranes were then washed three times for 5 mins in TBS-T. Primary antibodies were labelled with appropriate horseradish peroxidase (HRP) conjugated secondary antibodies and washed four times for 5 mins again in TBS-T. All membranes were visualised using the enhanced chemiluminescence (ECL) blotting system (Promega) and imaged using a G: BOX Chemi XX6 and XX9 gel doc system (Syngene).

2.2.4.4 Immunofluorescence microscopy

To assess proteins by confocal microscopy, cells were seeded into 12-well plates onto poly-L-lysine (Sigma-Aldrich®) coated sterile glass coverslips. Coverslips were treated with poly-L lysine for 5 mins before being washed with sterile PBS. After 3 hrs, cells were reactivated for 24 hrs. Cells were then washed in 0.5 ml of PBS and then fixed with 4% v/v formaldehyde for 15 mins at room temperature. Formaldehyde was removed and discarded; cells were then washed three times with 0.5 ml PBS. Next cells were permeabilised using 1% (v/v) Triton-X100 in PBS for 15 mins at room temperature, followed by three PBS washes. Non-specific binding was then blocked by adding 1% (w/v) BSA in PBS to cells, cells were then incubated for 1 hr at 37°C. The blocking buffer was removed, and cells were subsequently incubated with primary antibody in PBS containing 1% BSA (w/v) for 1 hr at 37°C in a humidity chamber. Following the removal of primary antibody, cells were washed three times with PBS and Alexa Fluor®-conjugated secondary antibodies added (Thermo Fisher Scientific). Rhodamine phalloidin-TRITC dye (Thermo Fisher Scientific) was also added at the same time as secondary antibodies (1 in 1000). Cells were again incubated for 1 hr at 37°C in a humidity chamber. Secondary antibodies were removed before cells were washed three times with PBS and coverslips mounted onto microscope slides using Hard-set Antifade Mounting Medium with DAPI (VECTASHIELD®). Cells were stored in a sealed slide box at

4°C until there were visualised using an LSM microscope (ZEISS). Images were later analysed using the Zen 2 Blue edition (ZEISS) software.

2.2.4.5 3' UTR Luciferase assay

A luciferase reporter assay was performed 24 hrs post transfection as detailed in section 2.2.2.4 using the Dual-luciferase Reporter (DLR™) Assay System (Promega) as per manufacturer's instructions. In short, 100 µl of 1x passive lysis buffer was added to each well of the culture plate and incubated at room temperature on a rocking platform for 15 mins. Following incubation, the culture plate was placed at -20°C overnight. Next, 10 µl of each sample was transferred to a white 96-well plate in triplicate. Next, 50 µl LARII was added to each sample and luminescence measured using A FLUOstar OPTIMA plate reader (BMG LABTECH). Next, 50 µl of Stop & Glo® reagent was added and luminescence again measured. Data was then accessed through the OPTIMA data analysis programme and transferred to Microsoft Excel.

2.2.5 Analysis of mRNA

2.2.5.1 Total RNA isolation

Cells were washed with PBS before total RNA was extracted using TRIzol™ Reagent (Invitrogen) according to manufacturer's instructions. For TRIzol™ extraction, 1 ml of TRIzol™ Reagent was added to each sample, mixed, and incubated at room temperature for 5 mins, 200 µl chloroform was then added and mixed vigorously for 15 secs, before being incubated for 2 mins at room temperature. To achieve phase separation samples were centrifuged at 12000 x *g* for 15 mins at 4°C. The upper aqueous phase containing RNA was then transferred to a new microcentrifuge tube and mixed with 500 µl of isopropanol. Samples were then mixed and incubated at room temperature for 10 mins, RNA was then pelleted via centrifugation at 4°C at 12000 x *g* for 10 mins. The supernatant was then removed and discarded; the RNA pellet was washed in 1 ml 75% ethanol and centrifuged at 7500 x *g* for 5 mins at 4°C. The supernatant was again discarded, and RNA allowed to air dry at room temperature. The RNA was resuspended 20 µl nuclease free water.

2.2.5.2 DNAse treatment

Total RNA isolated via TRIzol™ Reagent was treated with DNA-*free*™ Kit (Invitogen) to remove residual DNA from samples following manufacturer's instructions. DNA digestion was performed by adding 2 µl of 10 x DNase I buffer and 1 µl of DNase I to each sample and incubating at 37 °C for 30 mins. Following this 2.3 µl of DNase inactivating reagent was gently mixed with samples for 2 mins at room temperature. Samples were then centrifuged at 7500 x *g* for 1.5 mins at room temperature and the RNA containing supernatant was transferred to a new microcentrifuge tube. The RNA was then stored at -80 °C until further use.

2.2.5.3 Reverse transcription

Purified total RNA was quantified using a NanoDrop ND-1000 (NanoDrop Technologies). Following quantification of purified total RNA, 1 µg RNA was reverse transcribed using the LunaScript™ RT SuperMix Kit (New England Biolabs), according to manufacturer's instructions. The appropriate volume of RNA was added to 4 µl of 5x LunaScript RT SuperMix, nuclease free water was then added to make a final reaction volume of 20 µl. The mixture was incubated at 25°C for 2 mins, followed by heating at 55°C for 10 mins, before a final incubation at 95°C for 1 min to inactivate the reverse transcriptase. This was done using a thermocycler. The cDNA was then stored at -20°C.

2.2.5.4 Quantitative polymerase chain reaction (qPCR)

Changes in transcript abundance of endogenous cellular and viral mRNAs were quantified using qPCR with the GoTaq qPCR Master Mix kit (Promega), performed according to manufacturer's instructions using a Rotor-Gene Q 6000 Real-Time PCR machine (QIAGEN). The following master mix was added to 2 µl of cDNA:

10 µl 2x GoTaq® qPCR Master Mix

1 µl 10 µM sequence specific forward and reverse primer mix

7 µl nuclease free water

A standard 40-cycle, three-step melt program was used with the following steps: denaturation at 95°C for 15 secs, annealing at 60°C for 30 secs, following by an elongation

step at 72°C for 20 secs. Data acquisition was acquired during the elongation step of each cycle, analysed using RotorGene Q 6000 software 1.7 and exported to Microsoft excel. Samples were normalised to the housekeeping gene GAPDH and relative changes in abundance calculated for each sample using the comparative *C*T method.

2.2.6 miRNA sequencing

2.2.6.1 Preparation of samples for miRNA sequencing

For miRNA sequencing (miR-Seq), cells were seeded into 6 well plates. Cells were reactivated as described in section 2.2.3.1. Cells were harvested at 0, 16 and 24 hrs post reactivation and centrifuged at 500 x *g* for 5 mins at 4°C, the supernatant was then removed and discarded. Total RNA isolation was then performed on samples as described in section 2.2.5.1. To ensure, necessary RNA integrity, samples were analysed using an Agilent High Sensitivity D1000 Screen Tape Station.

2.2.6.2 miRNA sequence library preparation

Small RNA libraries were generated from 1 µg total RNA using the TruSeq® Small RNA Library Prep Kit according to maufacturers instructions (Illumina). Small RNA libraries were prepared at the University of Leeds, NGS facility by Technical Specialist Ummey Hany. In brief, RA5 and RA3 adaptors were added to the 5' and 3' of RNA molecules present in each sample using T4 RNA ligase respectively. Next, reverse transcription using specific adaptor primers was followed by PCR amplification. A different index primer was also used to ensure the differentiation of each sample following sequencing. Samples were run on an Agilent Technologies 2000 Bioanalyzer, to confirm adapter ligation. Small RNA libraries were then purified using gel extraction and again run on an Agilent High Sensitivity D1000 Screen Tape Station for quality control analysis of final libraries. Subsequently, these small RNA libraries were sequenced using a HiSeq (Illumina) sequencing platform.

2.2.7. Analysis of mature miRNA expression

2.2.7.1 Total RNA isolation

Total RNA extraction for miRNA analysis was extracted either using TRIzol™ Reagent (as described in section 2.2.5.1) or using the miRNeasy mini kit (QIAGEN) following manufacturer's instructions. For miRNeasy mini kit extraction 700 µl QIAzol Lysis Reagent was added to each sample and homogenised for 5 mins at room temperature, then 140 µl of chloroform was added and samples were vigorously shaken for 15 secs. Samples were incubated at room temperature for 3 mins and then centrifuged for 15 mins at 12,000 x *g* at 4°C. The RNA containing upper aqueous phase was transferred to a new microcentrifuge tube and mixed with 525 µl of 100% ethanol. This resulting mixture was then loaded onto a RNeasy® Mini column in a 2 ml collection tube and centrifuged at 8000 x *g* for 15 secs and the flow-through discarded. Following this 500 µl RPE buffer was washed through the RNeasy Mini column by centrifugation at 8000 x *g* for 15 secs, the flow-through was discarded. RPE buffer was again added to the RNeasy Mini column and centrifuged at 8000 x *g* for 2 mins. The RNeasy Mini column was transferred into a new 2 ml collection tube and centrifuged at full speed for a further 1 min. Subsequently the RNeasy Mini column was transferred to a new 1.5 ml microcentrifuge tube, 30 µl of RNase free water was then added to the RNeasy Mini column membrane and centrifuged for 1 min at ≥8000 x *g* to elute RNA.

2.2.7.2 miScript reverse transcription

For mature cellular miRNA analysis, 1 µg total RNA was reverse transcribed using the miScript II RT Kit (QIAGEN), according to manufacturer's instructions. The following master mix was added to the appropriate volume of RNA and nuclease free water making a final reaction volume of 20 µl:

4 µl 5x miScript HiFlex Buffer

2 µl 10x miScript Nucleics Mix

2 µl miScript Reverse Transcriptase Mix

The mixture was then incubated at 37°C for 60 mins. To inactivate the reverse transcriptase the samples were then incubated at 95°C for 5 mins, before the cDNA was stored at -20°C.

2.2.7.3 miScript qPCR

The miScript SYBR® Green PCR kit (QIAGEN) was used to quantify mature miRNA, according to manufacturer's instructions using a Rotor-Gene Q 6000 Real-Time PCR machine (QIAGEN) in combination with mature miRNA primer assays purchased from QIAGEN. The following master mix was added to 2 µl cDNA:

10 µl 2x QuantiTect SYBR Green PCR Master Mix

2 µl 10x miScript primer assay (miRNA specific forward primer)

2 µl 10x µM Universal reverse primer

4 µl Nuclease free water

A 40 cycle three-step melt program was then used with the following parameters: denaturation at 94°C for 15 secs, annealing at 55°C for 30 secs, and elongation at 70°C for 30 secs. Data was acquired the elongation step of each cycle and analysed using Rotor-Gene Q 6000 Series software 1.7 (QIAGEN). Samples were normalised to RNU6-1 (U6), a small nucleolar housekeeping RNA and relative abundance calculated using the comparative *C*T method.

2.2.8 Bioinformatics and statistics

2.2.8.1 miR-Seq analysis

MiR-Seq bioinformatic analysis was performed by Dr. Anthony Anene, Queens Mary University of London (QMUL). Sequencing reads were aligned to the homo sapien hg38 (GRCh38/hg38) genome using Bowtie 2 (V.2.4.2) (Bolger et al., 2014) (Langmead and Salzberg, 2012). Expression levels were subsequently normalised and differential expression (DE) calculated at 0, 16 and 24 hrs timepoints using Limma R package (Anders et al., 2015). Transcripts with at least 1 CPM in 3 samples were used to reduce false discovery rates in the DE analysis.

2.2.8.2 Gene Ontology analysis

Gene Ontology (GO) gene enrichment analysis was performed using PANTHER.db (pantherdb.org), resulting in a list of enriched biological processes that were subsequently presented as a pie chart using Microsoft Excel.

2.2.8.3 Statistical analysis

Quantified data was analysed for statistical significance using student's unpaired T test unless otherwise stated. Differences were deemed significant when $p<0.05$, asterisks were used to denote the level of significance where *=$p<0.05$, **p=<0.01 and ***=$p<0.001$.

2.2.8.4 Image generation

All graphs and tables were generated in Microsoft Excel, while scientific diagrams were drawn using BioRender unless otherwise stated.

Chapter 3

~

Cellular miRNAs are dysregulated during KSHV lytic replication

3. Cellular miRNAs are dysregulated during KSHV lytic replication

3.1 Introduction

The role of miRNAs as master regulators of post transcriptional gene expression is now largely appreciated. These small non-coding RNA molecules recognise complementary mRNA targets and direct their degradation or translational repression. The production of an active mature miRNA is a multistep process, that begins with the transcription of a long primary transcript in the nucleus (Lee et al., 2004). Next, the ribonuclease enzyme Drosha and its co-factor DGRC8 cleave pri-miRNA, releasing an ~70 nt pre-miRNA hairpin (Han et al., 2004). Pre-miRNA molecules are subsequently recognised and actively exported through the nuclear pore complex by Exportin 5 to the cytoplasm (Yi et al., 2003). In the cytoplasm, pre-miRNAs undergo further processing by a second ribonuclease, Dicer. Dicer cleavage generates a double stranded miRNA duplex that is loaded onto AGO proteins with the help of HSC70/HSP90 chaperones (Park et al., 2011) (Iwasaki et al., 2010). Here, guide strand selection occurs, and a mature RISC formed. The guide strand ultimately directs mature RISC to a specific subset of mRNAs and promotes their degradation or translational inhibition (Behm-Ansmant et al., 2006) (Humphreys et al., 2005).

Several viruses, including those belonging to the *herpesviridae,* hijack the miRNA biogenesis pathway to produce their own v-miRNAs. Indeed, KSHV expresses 25 mature v-miRNAs that primarily function in maintaining latent infection and immune evasion (Skalsky and Cullen, 2010). Alternatively, many viruses have been reported to utilise cellular miRNAs which seemingly allows them to exploit various existing cellular networks, to promote their lifecycle. Interestingly, some viruses take advantage of TDMD to selectively degrade antiviral miRNAs. For example, HCMV encodes a miRNA decay element that mediates the post transcriptional degradation of miR—17~92 cluster members miR-17 and miR-20a, promoting viral DNA synthesis and virion production (Lee *et al.*, 2013). Cellular miRNAs can also prove beneficial during virus infection. Naturally viruses have developed mechanisms to upregulate these proviral miRNA and the upregulation of miRNAs that interfere with host antiviral immune responses appears to be a common strategy. Notably, EBV and HSV-1 target the expression of a number of interferon genes through the upregulation of miR-146a and miR-23a respectively,

impairing the host antiviral responses to infection (Rosato et al., 2012) (Ru et al., 2014). Somewhat surprisingly there are examples of viruses, namely HCV, that directly sequester cellular miRNAs to protect their viral genome. Cellular miR-122 directly binds to the 5' UTR of the HCV genome and prevents its degradation from host exonucleases. Furthermore, miR-122 binding mediates HCV IRES formation and promotes viral RNA translation (Luna et al., 2015). Little is known about the role of cellular miRNAs in KSHV lytic replication. However, due to the extensive dysregulation of cellular pathways that is observed during lytic replication, it seems likely that KSHV may take advantage of host miRNAs to simultaneously manipulate existing regulatory networks. This is especially true given the fact that most KSHV v-miRNAs are expressed and function during latent infection. Furthermore, previous data suggests that expression of ORF57 leads to the upregulation of both Exportin 5 and SMARC4 in the nucleolus following subcellular fractionation (Owen, 2015). These factors have both been found to be important in miRNA biogenesis. This suggests that ORF57 may be involved in altering cellular miRNA levels during KSHV lytic replication. Further supporting the hypothesis that KSHV utilises cellular miRNA during lytic replication.

In this results chapter miRNA sequencing (miR-Seq) was used to identify potentially dysregulated cellular miRNAs during lytic KSHV replication. A number of host miRNAs including miR-142-3p and miR-25-5p were confirmed to be dysregulated. Moreover, reintroducing the expression of these miRNAs during KSHV lytic replication appeared to disrupt viral replication and significantly inhibits the production of infectious virions.

3.2 Preparation of miRNA sequencing samples and libraries

To investigate whether cellular miRNAs are dysregulated during KSHV lytic replication, miR-Seq was performed using next generation sequencing of a small RNA library (summarised in **figure 3.1**). First, latently infected B cells (referred to as TREx BCBL-1 Rta cells) were treated with doxycycline hyclate (dox) to induce lytic replication. Samples were collected at 0 (latent control), 16 and 24 hours (hrs) post reactivation. These time points were selected as they allowed for the analysis of miRNA expression throughout the course of KSHV lytic replication. The expression of the lytic ORF57 protein was assessed using western blotting to confirm the lytic reactivation of each time point

sample **(Figure 3.1)**. Following confirmation of lytic reactivation, total RNA was extracted, and samples examined by an Agilent bioanalyzer to confirm the presence of high integrity RNA, necessary for Next generation sequencing (NGS) analysis. MiRNA sequencing libraries were then prepared using the Truseq Small RNA Library Preparation kit (Illumina), which allows for the generation of small RNA libraries directly from total RNA. In short, adaptor oligos were added to both the 5' and 3' end of each RNA molecule. Next, complementary primers were added, and RNA reverse transcribed into cDNA.

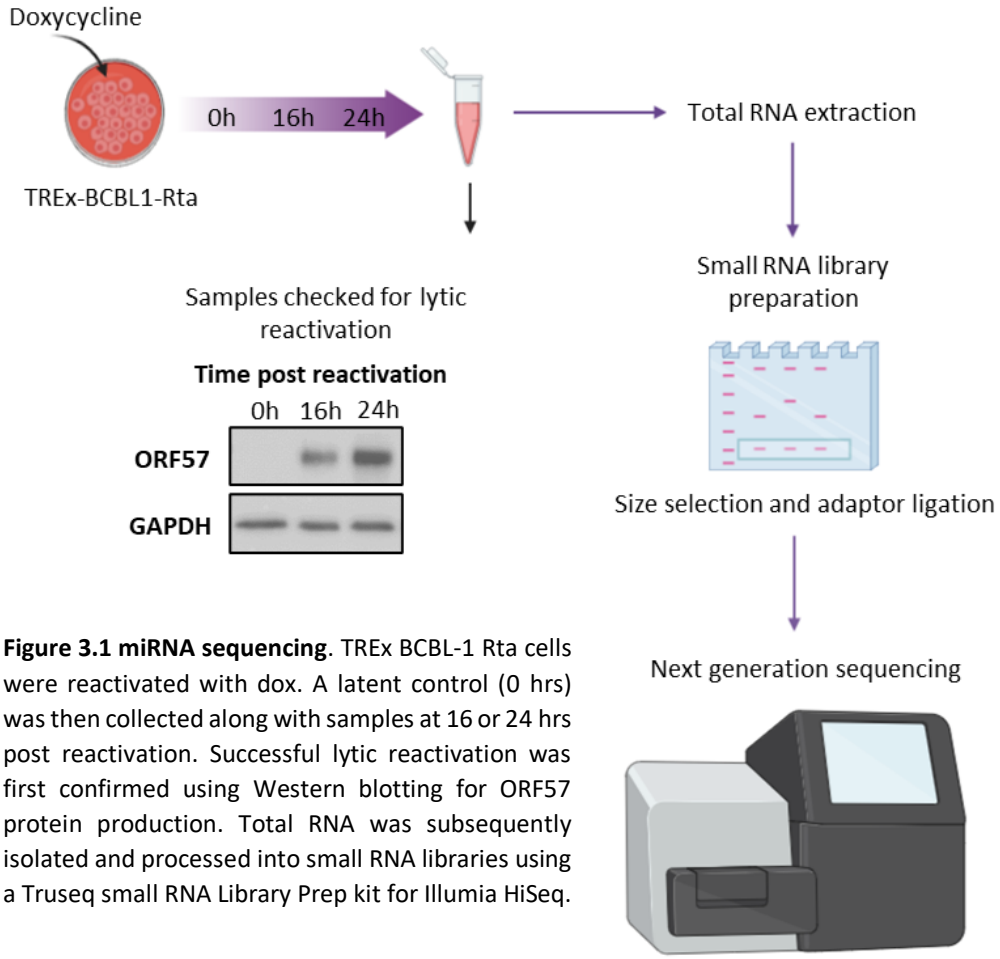

Figure 3.1 miRNA sequencing. TREx BCBL-1 Rta cells were reactivated with dox. A latent control (0 hrs) was then collected along with samples at 16 or 24 hrs post reactivation. Successful lytic reactivation was first confirmed using Western blotting for ORF57 protein production. Total RNA was subsequently isolated and processed into small RNA libraries using a Truseq small RNA Library Prep kit for Illumia HiSeq.

Samples were subsequently amplified using PCR and each library accessed using an Agilent High sensitivity D1000 Screen Tape station **(Figure 3.2)**. Next gel-electrophoresis and size-based selection was performed, selecting miRNAs that were ~160 bp in length with the addition of adaptor sequences. Quality control of libraries along with miRNA sample enrichment were confirmed using a bioanalyzer. The libraries were then

sequenced using an Illumina HiSeq at the University of Leeds, NGS facility by Technical Specialist, Ummey Hany.

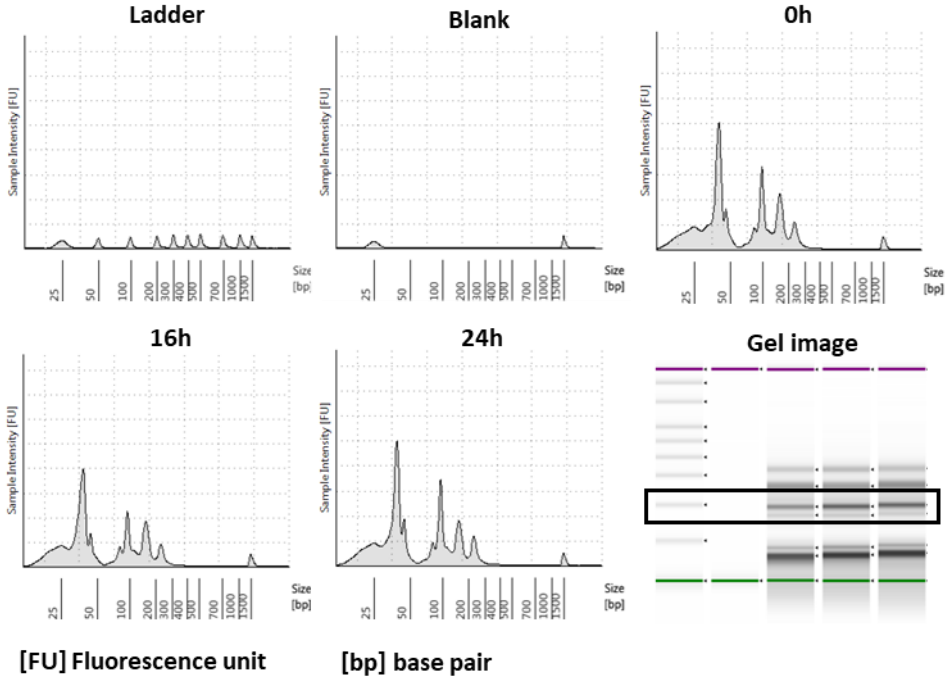

Figure 3.2 Preparation of small RNA sequencing libraries from TREx BCBL-1 Rta at 0, 16 and 24 hrs post reactivation. Total RNA was extracted from TREx BCBL-1 Rta samples, small RNA libraries were generated using an Illumina® TruSeq® Small RNA Library Prep Kit. Samples were then accessed using an Agilent High Sensitivity D1000 Screen Tape Station. Gel electrophoresis and size-based extraction (indicated) was subsequently performed.

3.3 KSHV dysregulates cellular miRNA expression

Sequencing reads produced by miR-Seq were processed and aligned to the *Homo sapien* hg38 (GRCh38/hg38) genome using Bowtie2 (V 2.4.2) (Bolger et al., 2014) (Langmead and Salzberg, 2012). Read expression levels were generated and normalised by counts per million (CPM) and differential expression (DE) calculated at 0, 16 and 24 hrs timepoints using Limma R package (Anders et al., 2015). Only transcripts with at least 1 CPM were used to reduce false discovery rates in the DE analysis. All processing and bioinformatics analysis was performed by Dr. Anthony Anene, Queens Mary University of London (QMUL). MiRNAs that consistently showed the greatest dysregulation across the different timepoints are displayed in figure 3.3 (Harper et al., 2022).

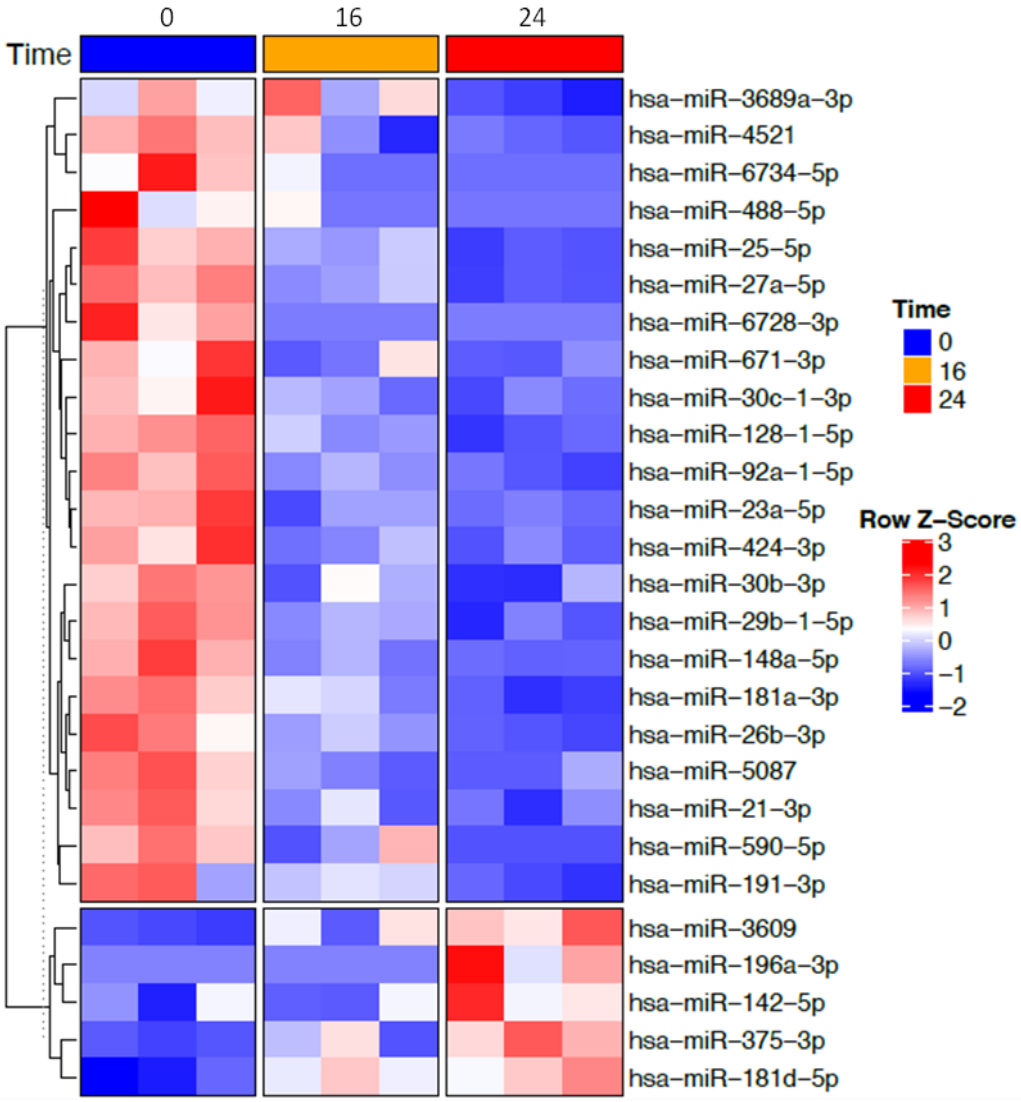

Figure 3.3. Identification of mature miRNAs altered during lytic KSHV infection. Small RNA libraries prepared from TREx BCBL-1 Rta cells at 0 (latent), 16 and 24 hrs post reactivation were sequenced using Illumina HiSeq (n=3). Sequencing reads were aligned to the Homo sapien hg38 and compared to published miRNA annotations (this work was performed by Dr. Anthony Anene - QMUL, London). The miRNAs which were found to be significantly altered following lytic reactivation were plotted on a heatmap. Each row represents a single miRNA, while the column denotes individual samples at the indicated timepoints. The colour scale shown on the right illustrates the relative expression of the miRNA across all samples: Relative abundance is represented by colour. Red= high, blue= low (Harper et al., 2021).

While most of the miRNAs identified had not previously been identified as dysregulated during KSHV infection, the dataset was validated as results highlighted the KSHV-mediated dysregulation of miR-30 family members. KSHV has previously been shown to downregulate both miR-30b and miR-30c, to enhance the expression of Delta-like 4 (DLL4) and promote the angiogenesis of lymphatic endothelial cells (LECs) (Bridge et al.,

2012). Furthermore, the dataset highlighted the downregulation of both miR-27 and miR-26b, which have reported antiviral properties and are downregulated by other herpesviruses (Cazalla et al., 2010) (Liu et al., 2018). The downregulation of these miRNAs by KSHV is therefore unsurprising and may represent a conserved strategy.

To validate the dysregulated miRNA expression profiles observed in the miR-Seq data, the highly sensitive and specific miScript PCR system was used to detect and quantify mature miRNA expression levels **(Figure 3.4).** The miScript PCR system involves the polyadenylation and cDNA conversion of miRNA using an oligo-dT primer, that contains a universal tag at its 5' end. A universal reverse primer that recognises this tag along with a specific miRNA forward primer is then used to quantify mature miRNA by qPCR.

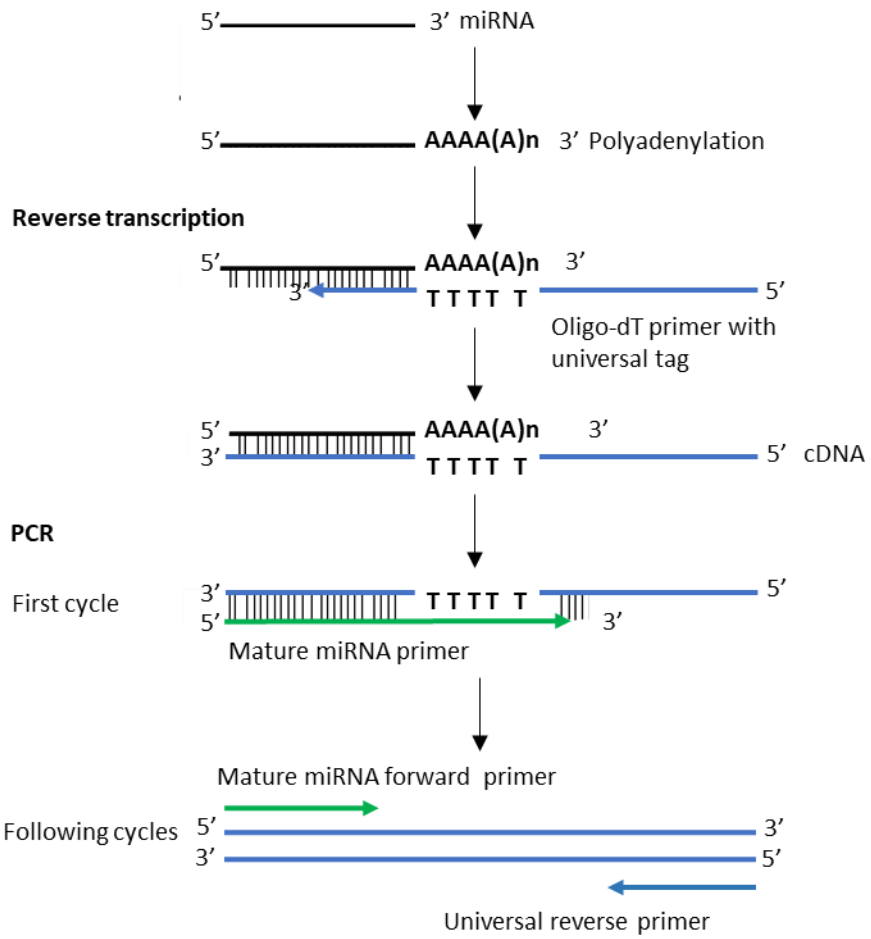

Figure 3.4 miScript qRT-PCR quantifies mature miRNA expression. Following total RNA extraction, cellular miRNAs are first polyadenylated before being converted into cDNA via reverse transcription using oligo-dT primers. This cDNA template can then be used to quantify mature miRNA levels via quantitative PCR using a universal reverse primers and a miRNA specific forward primer.

The miScript PCR system was used to determine the expression levels of miRNAs identified in the available miR-Seq data but also interesting examples from the literature, at 0, 16 and 24 hrs post reactivation. Cellular miRNAs found to be downregulated are displayed in figure 3.5.

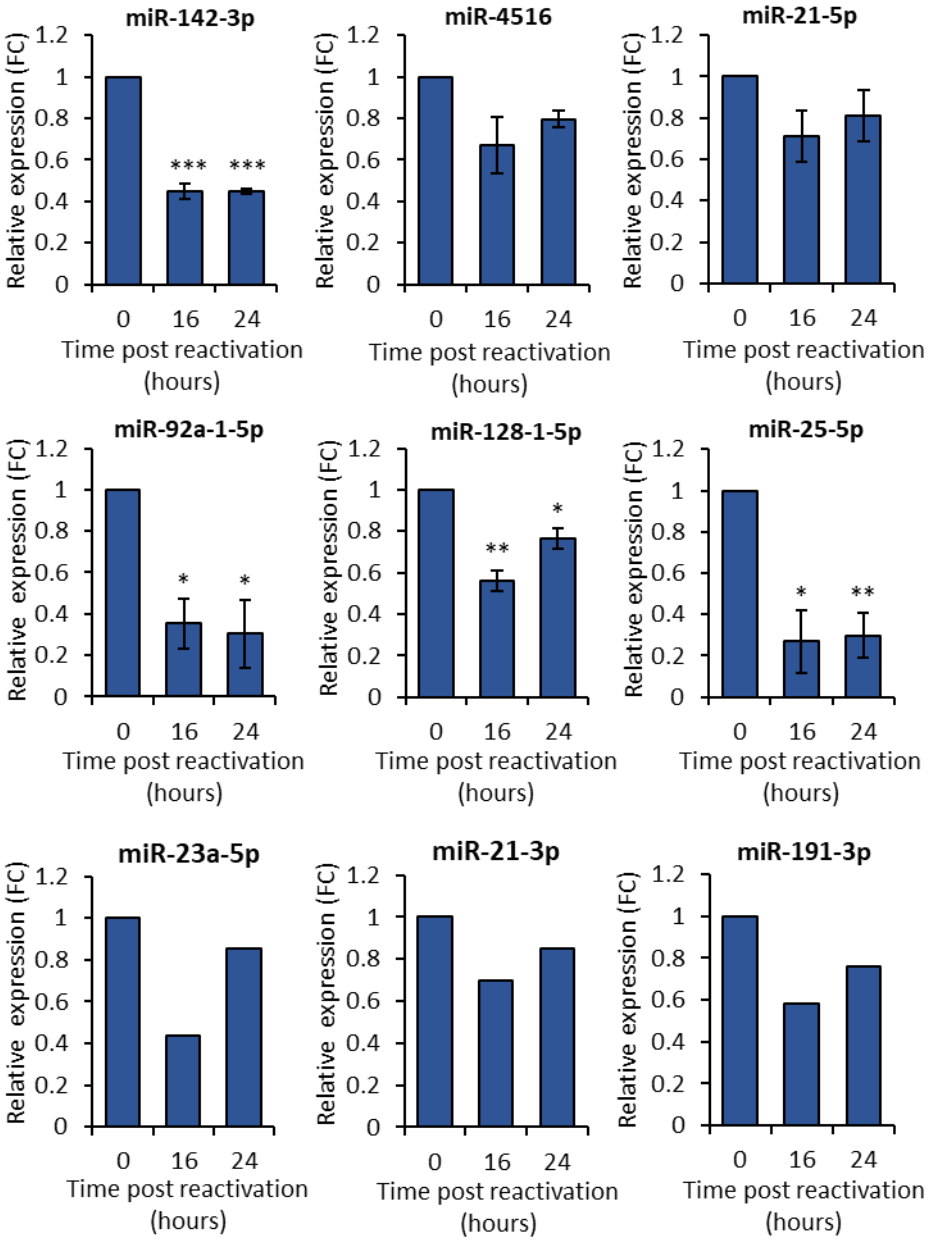

Figure 3.5 Validation of potentially downregulated cellular miRNAs following KSHV reactivation in TREx BCBL-1 Rta cells. The expression of a number of potentially downregulated miRNAs were assessed following lytic reactivation. Total RNA was extracted from TREx BCBL-1 Rta cells at 0 (latent control), 16 and 24 hrs post reactivation, and subsequently reverse transcribed into cDNA using the miScript RT assay. Quantitative qPCR was then performed in order to quantify mature miRNAs using specific miRNA primers, with U6 being used as a normalisation control. Error bars= ±SD, $p<0.001$= ***, $p<0.01$= **, $p<0.05$= * compared with 0 hr latent control sample.

Alternatively, the expression of miRNAs thought to be upregulated in the miR-Seq data are shown in figure 3.6.

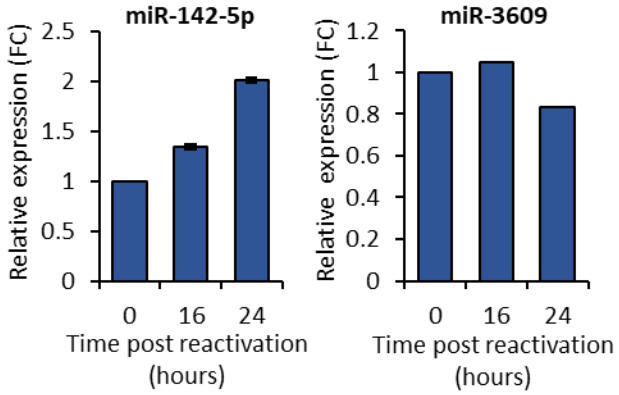

Figure 3.6 Validation of potentially upregulated cellular miRNAs following KSHV reactivation. The expression of potentially upregulated miRNAs was assessed following lytic reactivation. TREx BCBL-1 Rta cells were reactivated for 0h (latent), 16 and 24 hrs (lytic). Total RNA was extracted, and reverse transcribed using the miScript RT assay. Quantitative qPCR was subsequently performed using specific miRNA primers as indicated. U6 was used as a normalisation control. Error bars= ±SD.

A number of miRNAs consistently showed similar trends to those observed in the miR-Seq data, especially miR-25-5p and miR-92a-1-5p. Furthermore, miR-142-3p a miRNA identified in a previous miR-Seq data set that is known to be highly expressed in PEL cells was significantly downregulated following KSHV lytic replication.

3.4 Synthetic miRNA mimics specifically upregulate miRNA expression

To assess the potential importance of miR-142-3p and miR-25-5p during KSHV lytic replication, synthetic miRNA mimics were utilised to reverse the effect of their virus-mediated downregulation. Synthetic miRNA mimics are double stranded RNA fragments that imitate the function of endogenous mature miRNA duplexes. These molecules function similarly to endogenous miRNAs, predominantly binding the 3' UTR of target genes to reduce their expression via mRNA degradation or translation inhibition **(Figure 3.7)** (Hum et al., 2021). Furthermore, mimics also contain modifications to increase their stability making them useful tool for assessing miRNA gene regulation.

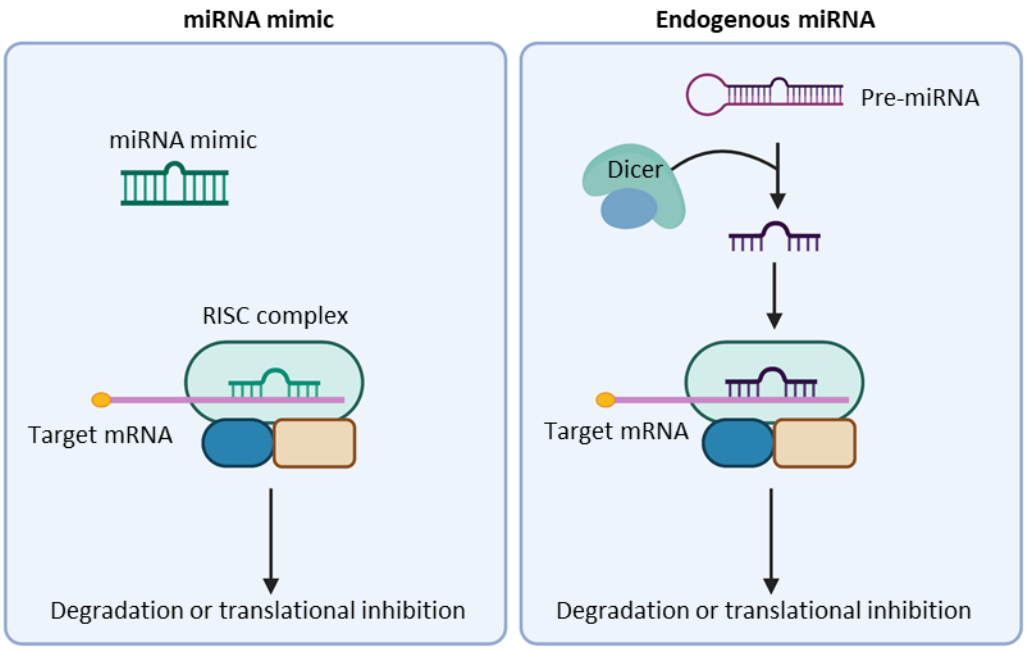

Figure 3.7 miRNA mimic function. miRNA mimics can be used to enhance miRNA expression that is potentially lost following viral reactivation, subsequently leading to the degradation or translational inhibition of target mRNA. Adapted from (Hum et al., 2021).

First, the effect of introducing specific miRNA mimics on the expression of previously validated downregulated cellular miRNAs was assessed. Where appropriate TREx BCBL-1 Rta cells were transfected with increasing concentrations of a scrambled control or specific miRNA mimic as indicated. Samples were subsequently collected at 0, 24 and 48 hrs post transfection. Next, total RNA extraction and miScript qRT-PCR was performed as previously described. Importantly, synthetic miRNA mimics were shown to specifically upregulate the expression of their target miRNAs. Indeed, miR-142-3p and miR-25-5p mimics specifically increased the expression of miR-142-3p **(Figure 3.8a)** and miR-25-5p respectively **(Figure 3.8b).**

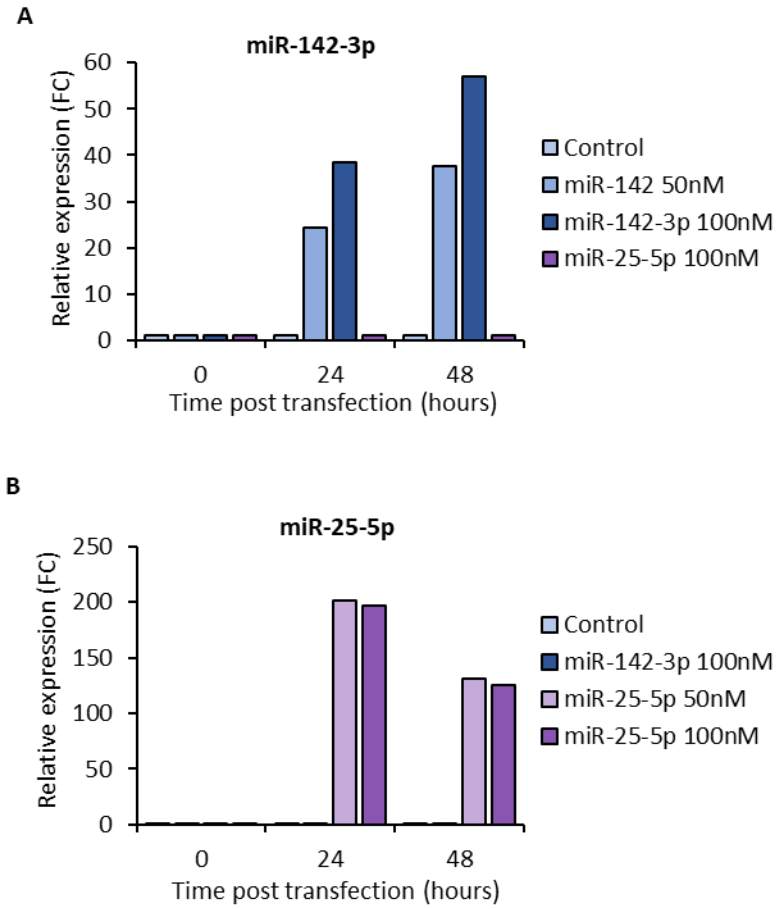

Figure 3.8 Over-expression of miRNA mimics specifically and efficiently upregulate target miRNA expression. Time course of (a) miR-142-3p and (b) miR-25-5p levels following miRNA mimic treatment in TREx BCBL-1 Rta cells. Cells were transfected with either a scramble siRNA (control) or miRNA mimics specific for miR-142-3p or miR-25-5p at the concentrations indicated. Samples were collected at 0, 24 or 48 hrs post transfection and total RNA extracted. Following extraction, RNA was reverse transcribed using the miScript RT II kit and qPCR performed using specific miR-142-3p and miR-25-5p primers.

These results suggest that miRNA mimics can be used to successfully overexpress miR-142-3p and miR-25-5p specifically and therefore investigate the role of these miRNA in KSHV lytic replication.

3.5 Over-expression of miR-142-3p following lytic reactivation has a detrimental effect on viral gene and protein expression

Given that miRNAs post-transcriptionally regulate target mRNAs, several KSHV mRNAs and proteins were assessed following the over-expression of miR-142-3p using qRT-PCR and protein immunoblotting, respectively.

TREx BCBL-1 Rta cells were first treated with a specific miR-142-3p mimic or scrambled control for 24 hrs. Cells were subsequently reactivated to induce lytic replication for a further 24 hrs, samples were then collected, and total RNA extraction performed. The expression of various KSHV mRNAs with expression profiles across the entire lytic expression cascade (early, delayed early and late) were assessed **(Figure 3.9)**. Results showed that the majority of KSHV mRNAs examined appeared to be somewhat diminished following miR-142-3p mimic treatment, however ORF57 and K8.1A gene expression did not appear to be significantly affected when compared to the scrambled control.

To investigate whether the downregulation of viral gene expression observed following miR-142-3p mimic treatment led to a decrease in viral protein production, the expression of early/delayed early proteins **(Figure 3.10a)** and late viral proteins were also assessed **(Figure 3.10c)** using western blotting. Densitometry analysis revealed that over-expression of the miR-142-3p mimic resulted in a reduction of ~30-40% for all the viral proteins examined **(Figure 3.10b and d).** Interestingly, while little downregulation of ORF57 and K8.1A was observed at a gene expression level, miR-142-3p mimic treatment did appear to significantly affect their protein levels. This possibly highlights the different mechanisms that miRNAs can utilise to silence the expression of their targets. Indeed, in addition to promoting mRNA degradation, miRNAs can also inhibit the translation of specific targets.

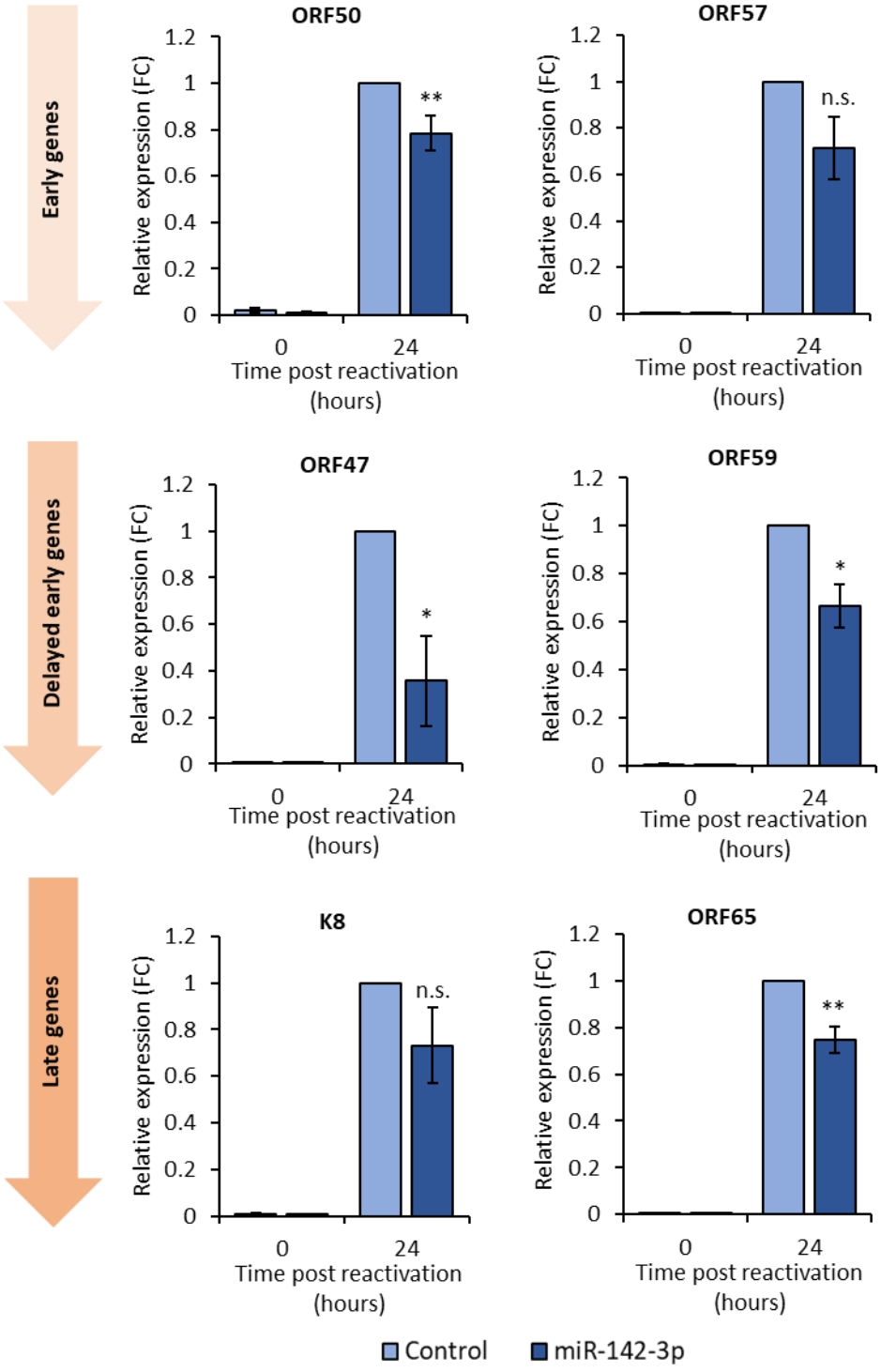

Figure 3.9 Reduction of KSHV gene expression following miR-142-3p mimic treatment. TREx BCBL-1 Rta cells were transfected with scramble siRNA (control), or a miR-142-3p specific miRNA mimic. 24 hrs post transfection, lytic replication was induced for 0 (latent) or 24 hrs (lytic) using dox. Following sample collection, total RNA was reverse transcribed, and qPCR performed using specific primer for a variety of viral genes as indicated. Error bars= ±SD, $p<0.01$= **, $p<0.05$= * when compared with scramble control (n=3).

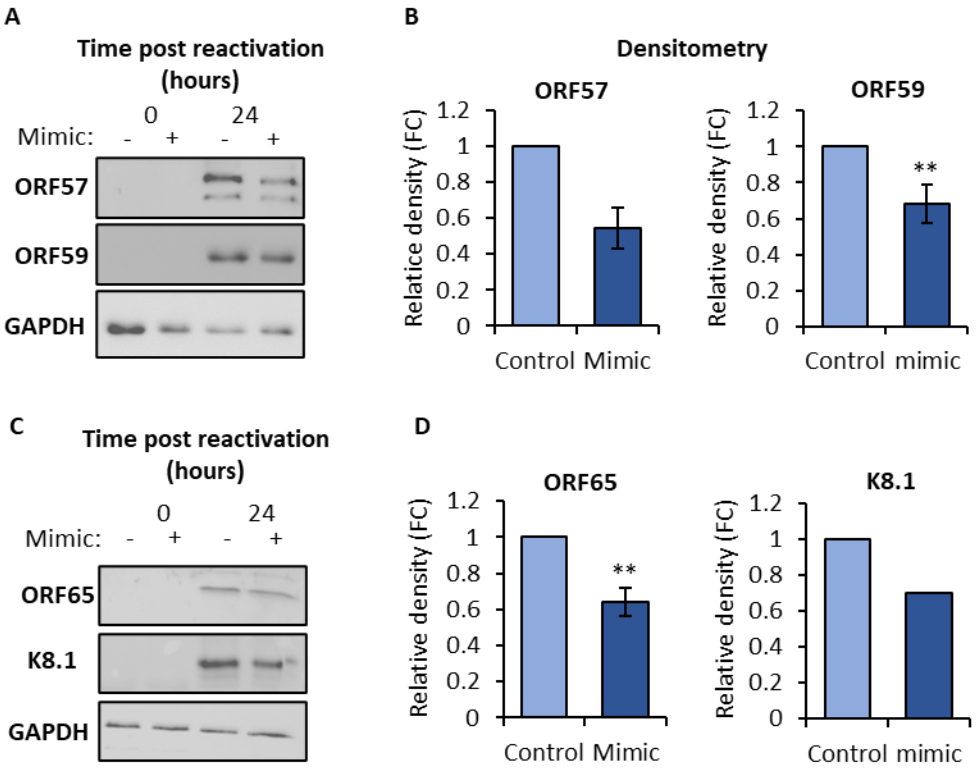

Figure 3.10 Over-expression of the miR-142-3p mimic reduced viral protein expression. (a) TREx BCBL-1 Rta cells transfected with a scramble control or a miR-142-3p specific mimic were either left uninduced (0h, latent) or treated with dox to induce KSHV lytic replication (24 hrs). Protein lysates were harvested and the expression of (a) early and delayed early (ORF57 and ORF59) KSHV proteins were accessed using immunoblotting. (b) Densitometry analysis was performed to calculate the relative expression of ORF57 and ORF59 in each sample following reactivation. (c) ORF65 and K8 (late protein) expression was also accessed and (d) densitometry performed. Error bars= ±SD, $p<0.01$= ** compared to reactivated control sample.

3.6 Expression of miR-142-3p does not affect viral load following KSHV lytic replication

In order to assess the effect of miR-142-3p upregulation on viral DNA replication, TREx BCBL-1 Rta cells were treated with a scrambled control or the synthetic mimic for 24 hrs. Cells were then treated to induce lytic replication; a latent control was also included. 72 hrs post reactivation samples were collected, and total DNA extracted. Subsequently, qPCR was performed to assess viral DNA levels using both KSHV ORF57 and ORF47 as viral genome markers. GAPDH was used as a normalisation control **(Figure 3.11)**. The overexpression of miR-142-3p did not appear to have a significant effect on viral load.

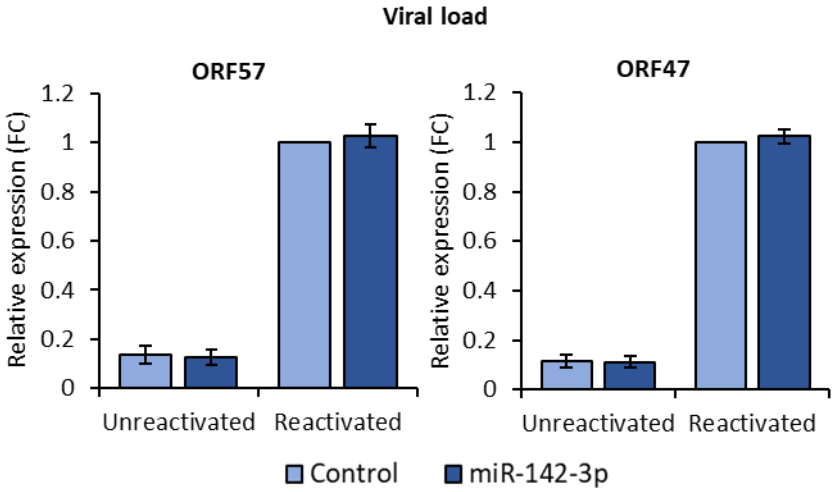

Figure 3.11 Overexpression of the miR-142-4p mimic does not appear to affect viral load following lytic reactivation. TREx BCBL-1 Rta cells were transfected with scrambled control or miR-142-3p mimic for 24 hrs. Cells were then reactivated using dox to induce lytic replication or left untreated. 72 hrs post reactivation samples were collected, and DNA harvested. Viral load was assessed using qPCR against ORF57 and ORF47. GAPDH was used as a control. Error bars= ±SD (n=3).

3.7 Expression of miR-142-3p significantly reduces infectious virion production

To investigate whether overexpression of miR-142-3p had an effect on the production of infectious virions, a viral reinfection assay was performed. TREx BCBL-1 Rta cells were transfected with a miR-142-3p specific miRNA mimic or scrambled control for 24 hrs before being reactivated for 72 hrs. The viral supernatants containing KSHV virions were then used to infect naïve HEK 293T cells (293T). 48 hrs post infection, 293T cells were collected, and total RNA extracted. Next, qPCR was performed in order to assess the expression of viral genes including ORF57 and ORF47, with GAPDH being used as a normalisation control **(Figure 3.12)**.

Results showed that reinfection of 293T cells using supernatant from miR-142-3p mimic treated cells resulted in an ~50% reduction in ORF57 expression when compared to the control. Similarly, a ~70% reduction was observed in ORF47 expression. This suggests miR-142-3p overexpression reduces infectious virion production.

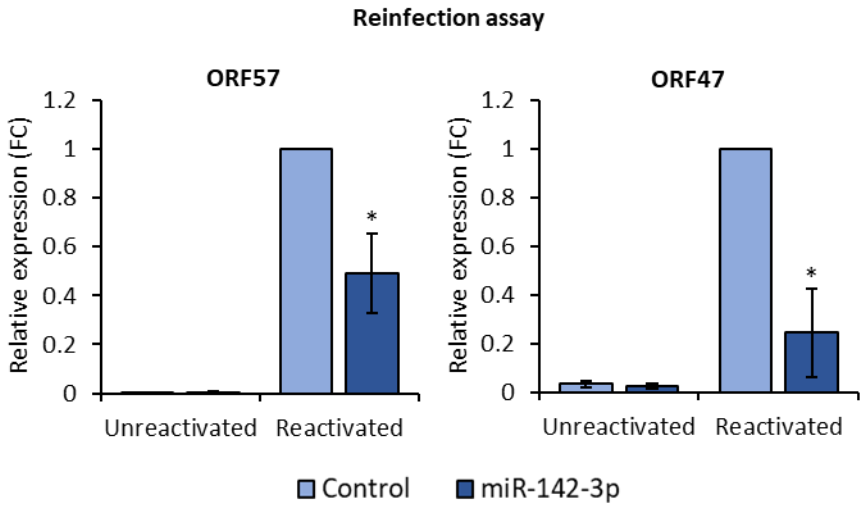

Figure 3.12 Overexpression of the miR-142-3p mimic decreases the production of KSHV virions. TREx BCBL-1 Rta cells were transfected with scrambled control or miR-142-3p mimic. 24 hrs post transfection, cells were treated with dox to induce KSHV lytic replication or left untreated for a latent control. After 72 hrs, supernatant was collected and added to naïve 293T cells. 48 hrs post reinfection, total RNA was harvested. Following reverse transcription, qPCR was performed to assess ORF57 and ORF47. GAPDH was used as a normalisation control. Error bars= ±SD, $p<0.05$= * when compared to reactivated control sample (n=3).

3.8 Expression of miR-25-5p appears to affect viral load and significantly reduces infectious virion production

The effect of miR-25-5p overexpression on KSHV lytic infection was also examined. To this end, KSHV endpoint assays were performed to assess viral load and infectious virion production following miR-25-5p mimic treatment **(Figure 3.12).**

TREx BCBL-1 Rta cells were treated with a miR-25-5p mimic or scrambled control for 24 hrs, following this cells were reactivated to induce lytic replication. TREx BCBL-1 Rta cells were collected, and viral load assessed. Following DNA extraction, qPCR was performed to measure viral load using KSHV ORF57 and ORF47 as genome markers **(Figure 3.12a)**. In addition, at 72 hrs post reactivation the supernatant containing infectious virions were used to infect naïve 293T cells for 48 hrs. 293T cells were harvested 48 hrs post infection and total RNA extracted. Next, reverse transcription was performed, and qPCR used to assess the expression of ORF57 and ORF47, as a marker of infectious virions produced **(Figure 3.12b).**

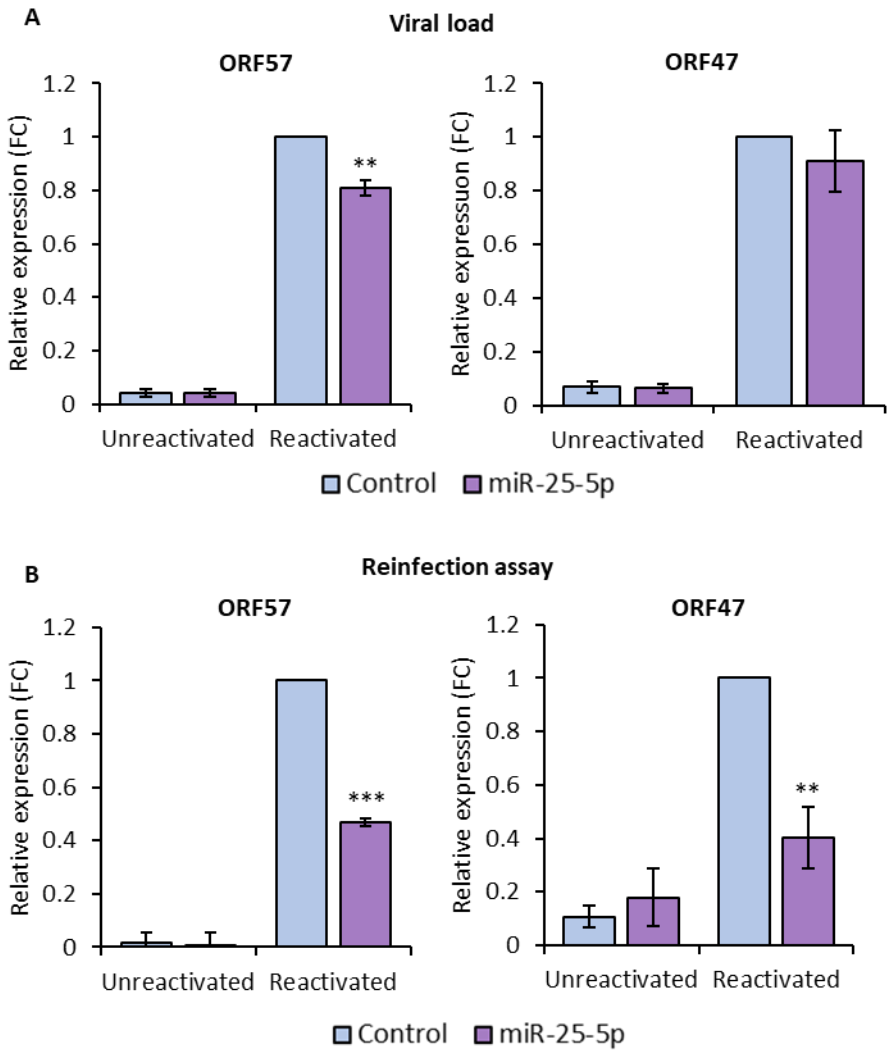

Figure 3.13 Over-expression of the miR-25-5p mimic does not appear to affect viral load but does decrease the production of infectious virion particles. TREx BCBL-1 Rta cells were transfected with scramble control or miR-25-5p mimic. 24 hrs post transfection were reactivated using dox or left untreated as latent control. (a) 72 hrs post reactivation cells were collected, and DNA harvested. Viral load was assessed using qPCR against ORF57 and ORF47. (b) Supernatant was also collected and used to infect naive 293T cells. 48 hrs post reinfection, total RNA was collected and transcribed. qPCR was performed to assess the expression of ORF57 and ORF47, GAPDH was used as a normalisation control. Error bars= SD, $p<0.01$= **, $p<0.001$= *** when compared to reactivated control (n=3).

The overexpression of miR-25-5p appears does not appear to have a significant effect on overall viral load, as indicated by varying effects on the viral genome markers ORF57 and ORF47. In contrast, reinfection of 293T cells following miR-25-5p mimic treatment resulted in a significant reduction in both ORF57 and ORF47 expression of ~50%. This suggests that miR-25-5p overexpression reduces infectious virion production during lytic KSHV infection.

3.9 Discussion

Numerous viruses have been shown to utilise cellular miRNAs to both facilitate and promote their replication (Lee *et al.*, 2013) (Ru et al., 2014) (Luna et al., 2015). Indeed, it represents an interesting host cell interaction that may lead to the identification of new antiviral drug targets. Advancements in RNA sequencing technology now allows the global, paralleled sequencing of mature miRNA. MiRNA sequencing has already proved extremely valuable in assessing miRNA regulation particularly in virus infection. This technique was therefore utilised to identify cellular miRNA that are altered following KSHV lytic reactivation.

Here, it has been demonstrated that KSHV is able to dysregulate the expression levels of various host cell miRNAs during KSHV lytic replication. Specifically, a number of cellular miRNA were confirmed to dysregulated, including miR-142-3p and miR-25-5p which were found to be significantly downregulated. While miR-142-3p did not appear in the miR-Seq data produced during this research, its absence could be explained by biases introduced at the library preparation or sequencing stage

Synthetic miRNA mimics have been used to successfully overexpress miRNA in numerous studies (Genz et al., 2019). Here specific miR-142-3p and miR-25-5p miRNA mimics were also shown to upregulate the expression of their respective miRNAs both efficiently and specifically. They were therefore deemed appropriate tools to further investigate the importance of miR-142-3p and miR-25-5p during lytic KSHV infection. Notably, the over-expression of these miRNAs appears to negatively affect KSHV lytic replication, significantly reducing infectious virion production, as measured by reinfection of naïve 293T cells. These results therefore suggest that these miRNAs direct the degradation or translational inhibition of mRNA targets important in the production and/ or release of infectious virions. Moreover, it indicates that the downregulation of these miRNAs is promoted by the virus itself and is not as a cellular antiviral response to infection.

As the manipulation of host cell miRNAs continues to emerge as a widespread strategy employed by numerous viruses, targeting these interactions represents an intriguing antiviral approach. miRNA expression is commonly cell type/tissue specific thus similar experiments in other cell types are needed to investigate the therapeutic potential of

targeting these miRNA-lytic KSHV cycle interactions. Indeed, KSHV infects both B cells and endothelial cells (Chen and Lagunoff, 2005) (Carroll et al., 2004).

Finally, other miRNAs found to be dysregulated in the present study still remain to be functionally characterised.

Chapter 4

~

The downregulation of miR-142-3p during KSHV lytic replication contributes to the increase in target cellular mRNAs

4. The downregulation of miR-142-3p during KSHV lytic replication contributes to the increase in target cellular mRNAs

4.1 Introduction

Regulating the expression levels of mRNA is fundamental in controlling gene expression. Naturally, the abundance of mRNA is controlled by multiple mechanisms at various stages of mRNA maturation, including transcription, export and mRNA stability (Boo and Kim, 2020). While mRNA regulation is pivotal for maintaining cellular homeostasis, viruses have also developed numerous mechanisms to manipulate host mRNA expression. Indeed, KSHV ORF37 encodes an exonuclease, termed SOX, which facilitates the widespread degradation of cytoplasmic mRNA as part of a host cell shutoff mechanism during infection (Glaunsinger and Ganem, 2004). Furthermore, KSHV ORF10 has recently been implicated in blocking the nuclear export of specific cellular mRNAs (Gong et al., 2016). This clearly demonstrates the importance of host mRNA manipulation during virus infection. Viruses also take advantage of miRNA function in order to alter host mRNA expression, not only encoding their own miRNAs but also utilising that of the host (Bruscella et al., 2017). Cellular miRNAs regulate numerous mRNA targets, exploiting these miRNAs allow viruses to control a variety of cellular pathways simultaneously, ultimately creating a transcriptome that is beneficial for virus infection. Furthermore, non-canonical uses of miRNA have been reported during virus infection. For example, HCV directly sequesters miR-122 to protect its viral genome from cellular exonuclease degradation (Jopling et al., 2005) (Machlin et al., 2011).

mRNA target binding is usually facilitated by an ~8 nt seed region located at the 5' end of the miRNA (Lewis et al., 2003). Additional pairing beyond that of the seed site has however been reported to support miRNA target binding. While miRNAs tend to bind complementary sequences in the 3' UTR of their respective target mRNAs, examples of CDS and 5' UTR binding have also binding described (Duursma et al., 2008) (Lytle et al., 2007). Furthermore, non-canonical modes of binding through bulges and other structures have been reported, highlighting the complexity of miRNA target recognition (Helwak et al., 2013). Nevertheless, target recognition by miRNA directs the degradation and/or the translational repression of mRNAs through the recruitment of a variety of

effector proteins including those of the 5'-3' mRNA decay pathway (Behm-Ansmant et al., 2006).

Given the extensive regulatory nature of miRNA, initial identification of potential miRNA targets largely relies on computational predictive tools. Indeed, several different bioinformatic software's currently exist. While vast improvements have been made to these tools in recent years, challenges remain leading to frequent false predictions (Bartel, 2018). These predictive programs however remain useful in selecting promising candidates for further experimental validation.

In this chapter, multiple computational target prediction programmes were used in combination with previously validated targets to identify potential miR-142-3p mRNA targets in TREx BCBL-1 Rta cells. Next, the functional validity of these candidates was assessed using synthetic miRNA mimics and 3' UTR luciferase assays. Results indicate that KSHV-mediated downregulation of miR-142-3p contributes to the upregulation of a selection of host mRNAs during KSHV lytic replication, particularly GPRC5A. This is reinforced by additional experiments showing depletion of GPRC5A is detrimental to KSHV lytic replication.

4.2 Identifying potential viral targets of miR-142-3p

Due to the downregulation of viral mRNA transcripts following over-expression of the miR-142-3p mimic (section 3.5), it was initially investigated if any KSHV lytic mRNAs could potentially represent direct targets of miR-142-3p. Interestingly, PARCLIP data has previously identified miR-142-3p binding sites in multiple latent KSHV genes including LANA, v-Cyclin, and v-FLIP, leading to speculation that miR-142-3p may function in fine tuning expression during latent infection. Additionally, a binding site was also found in the 3' UTR of vIL-6, a viral homologue of cellular IL-6, known to promote KSHV pathogenesis (Gottwein et al., 2011). While vIL-6 is expressed during latency, its expression and that of its cellular counterpart are greatly upregulated following lytic reactivation. Furthermore, miR-142-3p has previously been demonstrated to engage in a regulatory feedback loop with cellular IL-6. Here, IL-6 expression promotes the methylation of the miR-142-3p promoter, whilst miR-142-3p binds the 3' UTR of IL-6, directing its degradation/translational inhibition (Chiou et al., 2013). However, results

showed no significant effect on the expression of either vIL-6 or IL-6 following miR-142-3p mimic overexpression during lytic replication (data not shown), which may be complicated by the fact that KSHV ORF57 is also known to directly bind and promote the stability of these mRNAs. In fact, ORF57 binding has already been shown to disrupt miRNA targeting of both vIL-6 and IL-6 (Kang et al., 2011). Interestingly, a miR-142-3p site was located within the ORF57 binding region, thus ORF57 binding may also prevent miR-142-3p binding and consequently the silencing of these mRNAs.

4.3 Identifying potential cellular targets of miR-142-3p

The functional characterisation of miRNA targets first begins with the identification of potential candidates, this is subsequently followed by extensive experimental confirmation (outlined in **figure 4.1**).

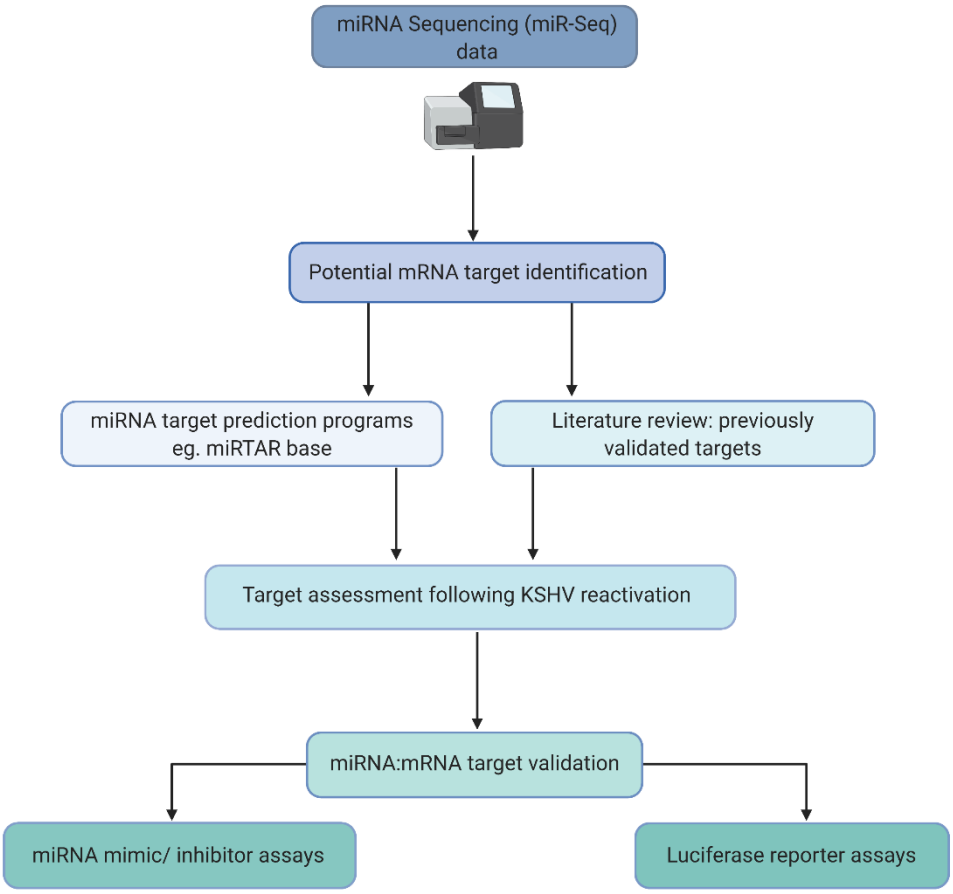

Figure 4.1 miRNA target identification. Schematic outlining the pipeline for the identification of cellular miRNA targets

To identify likely cellular mRNA targets of miR-142-3p, multiple target prediction tools were utilised in combination with previously validated targets. Common hits from predictive bioinformatic tools including miRTarBase (miRTarBase.edu), TargetScan (targetscan.org) and miRWALK (mirwalk.de) were combined with previously published examples (pubmed.ncbi) to generate a list of potential miR-142-3p targets. Gene ontology analysis was performed on these candidates using PANTHER 16.0 and is shown in figure 4.2.

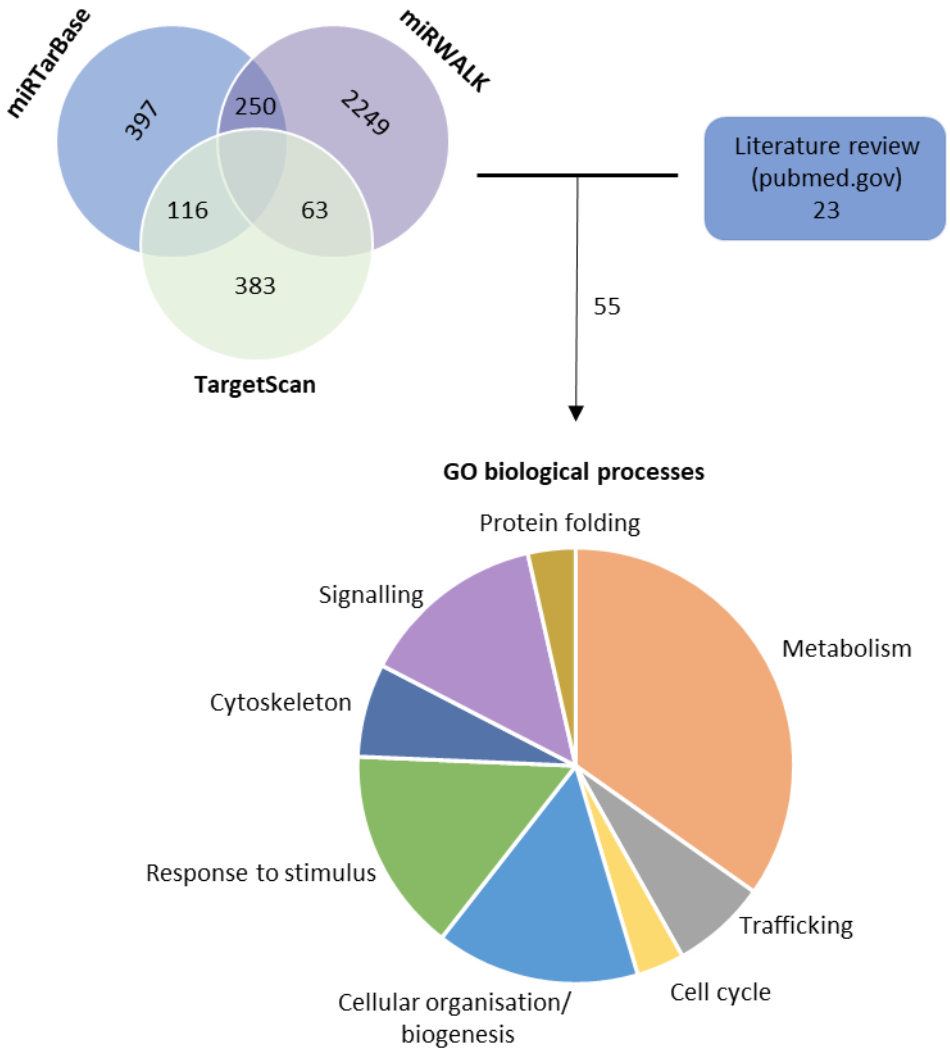

Figure 4.2 Gene ontology analysis for predicted miR-142-3p-targets. Predicted targets with a higher level of experimental evidence were supplemented with literature examples to create a list of potential miR-142-3p targets. Gene ontology analysis was subsequently performed on 55 potential cellular targets (pantherdb.org) and enriched GO terms according to biological processes are shown.

Interestingly, many of the enriched GO biological processes identified seem favourable to productive virus infection. For example, KSHV is known to reprogram metabolic

processes of infected cells, seemingly to compensate for energy demands associated with viral replication and infectious virion production (Sanchez et al., 2017) (Li and Gao, 2021). Furthermore, many viruses including KSHV, have been shown to hijack the cytoskeleton to not only facilitate viral entry but also intracellular transport of viral components and viral egress (Taylor et al., 2011).

Given that miR-142-3p expression is downregulated, potential mRNA targets would be expected to be upregulated following lytic reactivation. A panel of potential targets, randomly selected from the list of previously curated cellular targets were therefore assessed during KSHV lytic replication. To this end, TREx BCBL-1 Rta cells were treated with doxycycline to induce lytic reactivation and samples collected at 0 (latent control), 16 and 24 hrs. Following sample collection, total RNA was extracted, and reverse transcription performed. Subsequently, qPCR was used to measure the expression of miR-142-3p target genes as indicated.

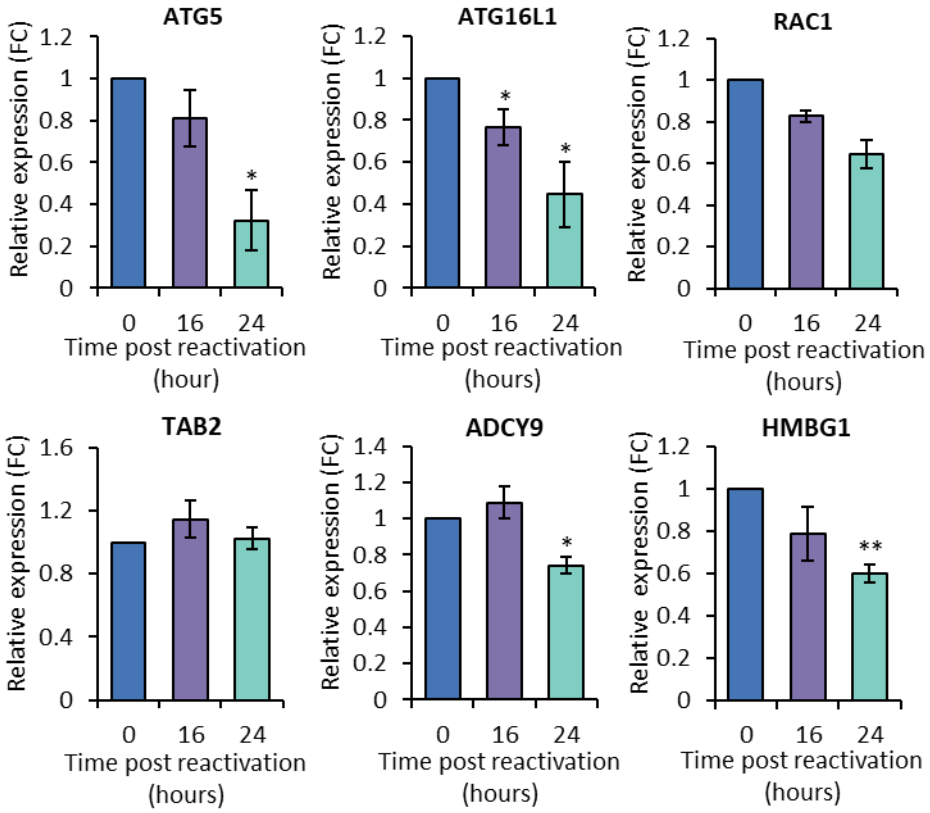

Figure 4.3 Gene expression of potential miR-142-3p targets following lytic KSHV reactivation. The expression of a number of potential cellular mRNA targets of miR-142-3p was assessed following reactivation. TREx BCBL-1 Rta cells were treated to induce lytic replication. Samples were collected at 16 and 24 hrs post reactivation. A 0 hr, latent control was also included. Total RNA was then extracted, and reverse transcription performed. Subsequently qPCR was used to assess the expression of mRNA targets using relevant primers. Error bars= ±SD, $p<0.001$= ***, $p<0.01$= **, $p<0.05$= * compared with 0 hr latent control sample (n=3).

Genes that were not found to be upregulated following reactivation are shown above in figure 4.3. This downregulation is likely due to the activity of the exonuclease, SOX, which leads to cytoplasmic degradation of mRNA and host cell shutoff (Glaunsinger and Ganem, 2004).

Notably, several mRNAs were shown to be significantly upregulated following KSHV reactivation are shown below in figure 4.4.

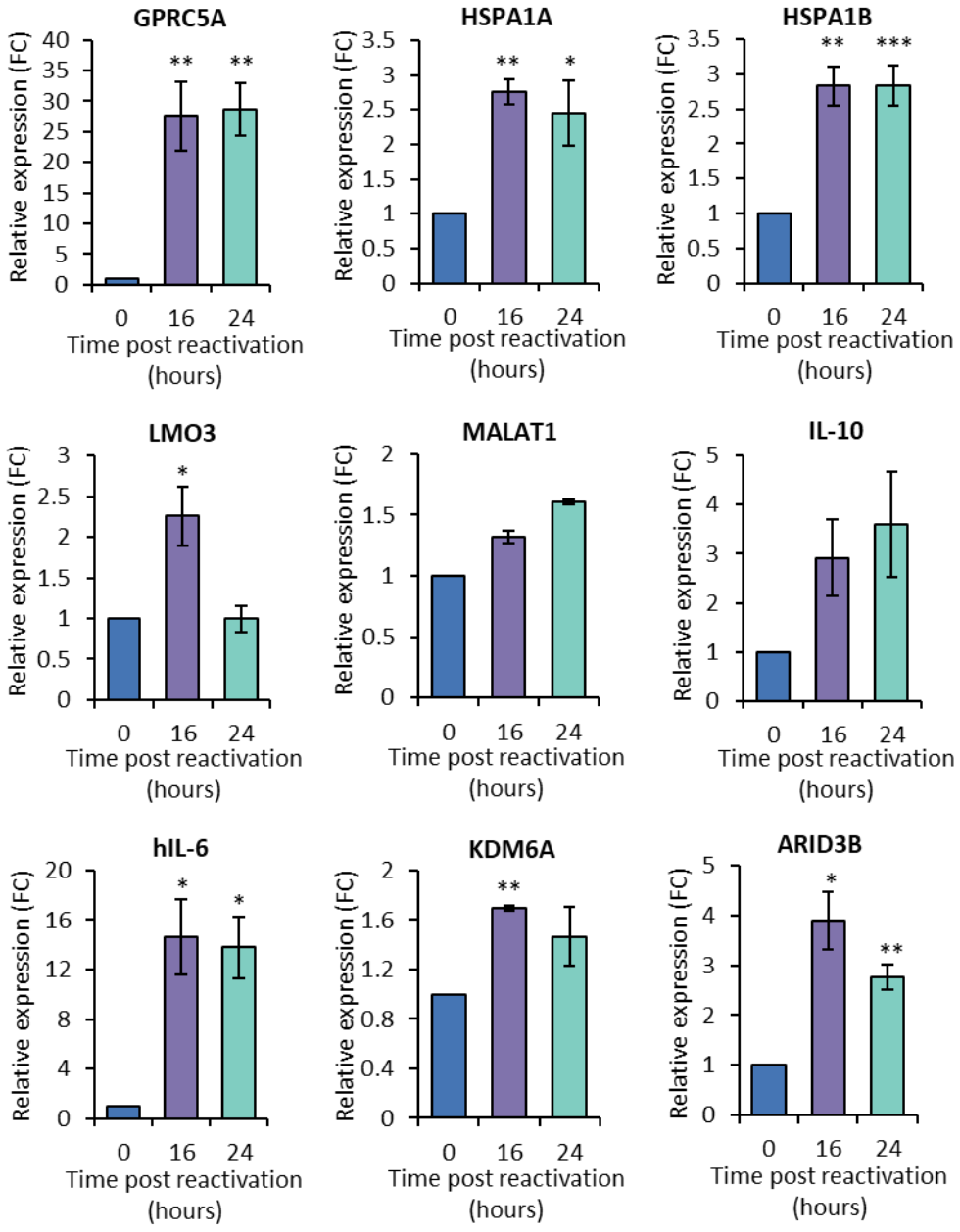

Figure 4.4 Gene expression of potential miR-142-3p targets following KSHV reactivation. The expression of potential miR-142-3p cellular mRNA targets were examined. Total RNA was extracted from TREx BCBL-1 Rta cells at 0 (latent control), 16 and 24 hrs post reactivation. Total RNA was subsequently reverse transcribed, and qPCR performed using specific mRNA primers. Error bars= ±SD, $p<0.01$= **, $p<0.05$= * compared with 0 hr latent control sample (n=3).

These mRNAs may therefore be regulated by KSHV-mediated downregulation of miR-142-3p.

In order to assess whether an upregulation of cellular mRNA target expression also led to an increase in protein expression, immunoblotting was used to assess select targets following lytic reactivation. Reactivated TREx BCBL-1 Rta cells were collected at 0 (latent control), 16 and 24 hrs. Protein lysates were harvested, and immunoblotting was used to analyse the expression of GPRC5A and HSPA1A **(Figure 4.5)**. Results showed that the expression of GPRC5A was significantly increased following KSHV reactivation, however, little change in HSPA1A protein expression was observed.

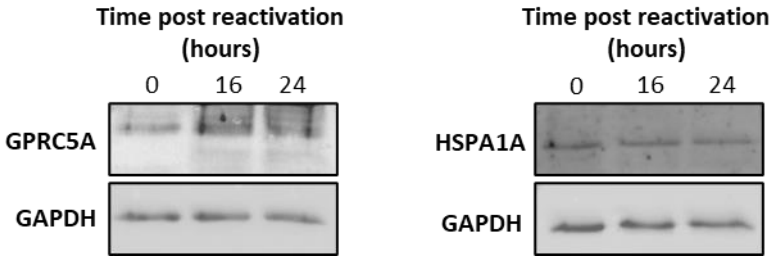

Figure 4.5 Protein expression of potential miR-142-3p targets following lytic KSHV reactivation. TREx BCBL-1 Rta cells were left uninduced (latent control) or reactivated for 16 and 24 hrs. Following sample collection protein lysates were harvested and the expression of GPRC5A and HSPA1A assessed using immunoblotting.

4.4 Expression of miR-142-3p following KSHV lytic replication downregulates select targets

To investigate whether mRNAs found to be upregulated during lytic infection were in fact potential targets of miR-142-3p, their expression was assessed using both qPCR and immunoblotting, following overexpression of the miRNA mimic. TREx BCBL-1 Rta cells were treated with a specific miR-142-3p mimic or scrambled control for 24 hrs. 24 hrs post transfection cells were reactivated to induce lytic replication for a further 24 hrs. Following sample collection, total RNA was extracted, and qPCR performed to assess the expression of candidate miR-142-3p targets **(Figure 4.6)**. Interestingly, the expression of GPRC5A, HSPA1A and HSPA1B were all significantly downregulated following miR-142-3p mimic overexpression, with a reduction of ~50-60% in gene expression being observed. These results suggested that GPRC5A, HSPA1A, HSPA1B, MALAT1 and ARID3B may be specific miR-142-3p targets during KSHV lytic replication.

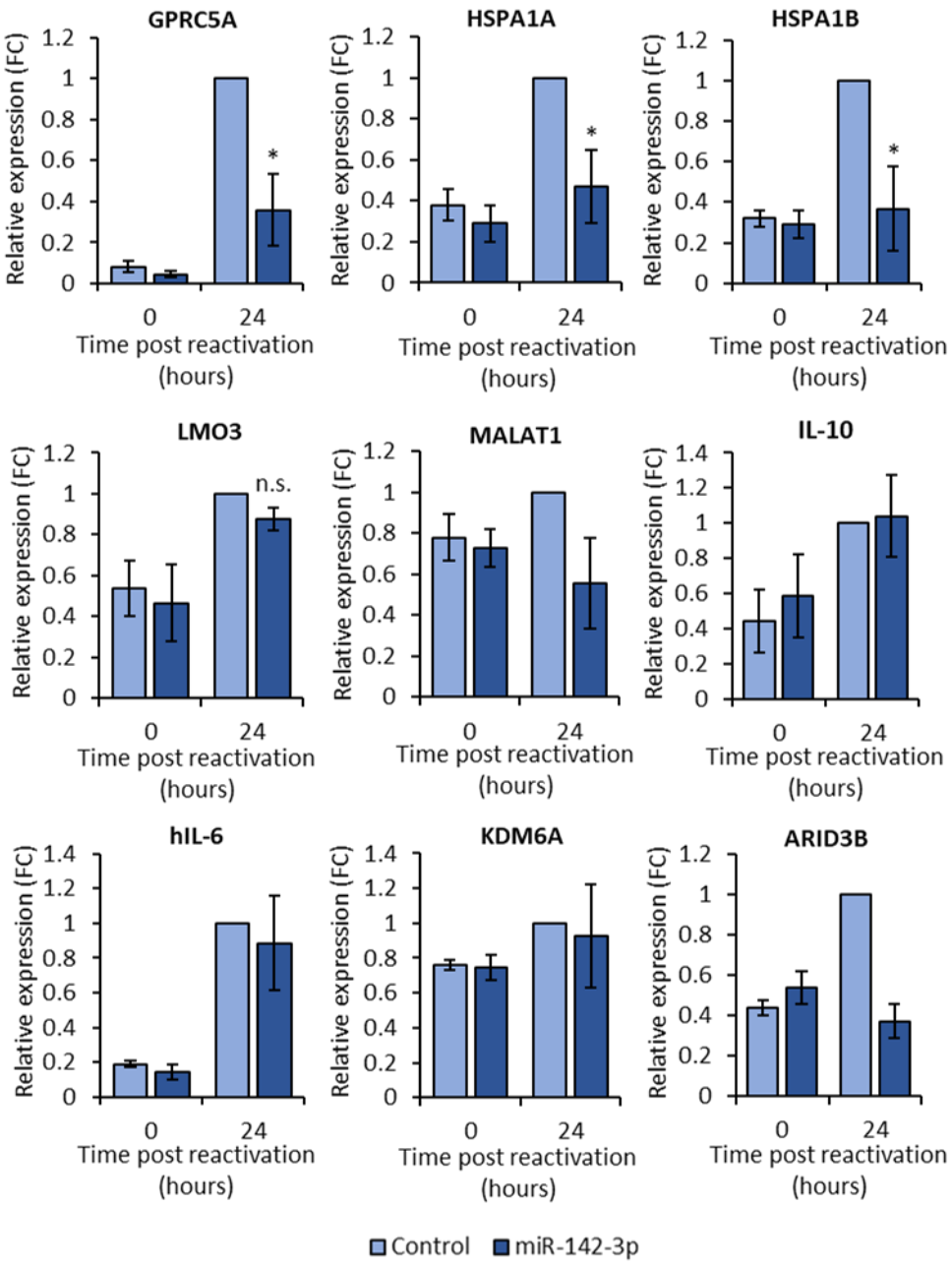

Figure 4.6 Gene expression of miR-142-3p targets following miR-142-3p mimic treatment. TREx BCBL-1 Rta cells were transfected with a miR-142-3p mimic or a scrambled control for 24 hrs. Following 24 hrs post transfection, cells were reactivated to induce KSHV lytic replication. Samples were collected 24 hrs post reactivation and total RNA extracted. After reverse transcription, qPCR was performed using primers for a variety of genes as indicated. Error bars= ±SD, $p<0.05$=* compared to 24 hr control (n=3).

MiRNA gene silencing via mRNA decay or translational inhibition will ultimately lead to a reduction in protein expression level of cellular targets. Thus, the protein expression of GPRC5A and HSPA1A were assessed following miR-142-3p mimic overexpression.

Following miR-142-3p mimic treatment and lytic reactivation, protein lysates were collected as previously described. The expression of GPRC5A and HSPA1A were then assessed using immunoblotting, with GAPDH being used as a loading control **(Figure 4.7)**.

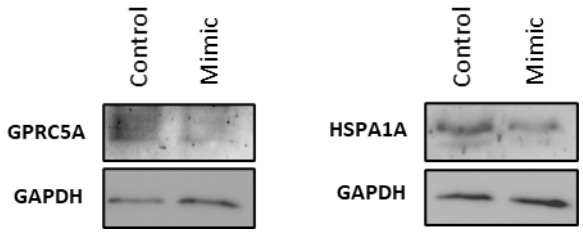

Figure 4.7 Protein expression of miR-142-3p mRNA targets following mimic treatment. TREx BCBL-1 Rta cells were transfected with a scrambled control or a specific miR-142-3p mimic. 24 hrs post transfection, lytic replication was induced. Samples were collected 24 hrs post reactivation and protein lysates harvested. Immunoblotting was then used to assess the protein expression of GPRC5A and HSPA1A.

Results show the protein expression of both GPRC5A and HSPA1A were significantly reduced following the overexpression of miR-142-3p when compared to control cells. Taken together, these results suggest that KSHV is able to influence the expression of host miRNAs to tailor host gene expression. Indeed, the downregulation of miR-142-3p during lytic replication appears to contribute to the increased levels of some cellular mRNAs, particularly GPRC5A.

4.5 GPRC5A knockdown affects KSHV lytic protein expression

In order to investigate the significance of KSHV-mediated miR-142-3p downregulation leading to GPRC5A upregulation following lytic reactivation, a stable GPRC5A knockdown (KD) cell line was generated using lentivirus-mediated shRNA delivery. In brief, lentiviruses expressing specific GPRC5A shRNAs were generated and used to transduce TREx BCBL-1 cells, ultimately leading a reduction in both GPRC5A mRNA and protein expression. Plasmid creation and lentivirus transductions were performed by Oliver Manners. Prior to further experimental use, effective GPRC5A depletion was first confirmed using qPCR. Following total RNA extraction from both scrambled control and GPRC5A KD cells, qPCR was performed to assess GPRC5A gene expression with GAPDH being used as a normalisation control **(Figure 4.8a)**.

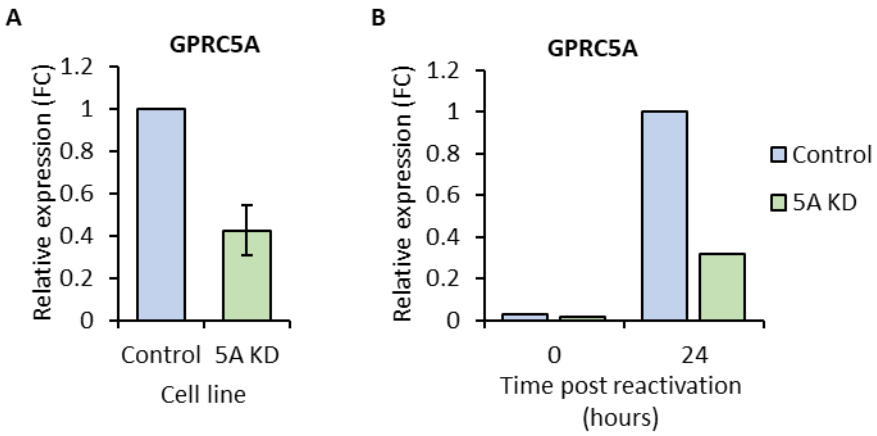

Figure 4.8 Confirmation of GPRC5A knockdown. (a) Total RNA was harvested from control and stable GPRC5A knockdown (KD) cells. Following extraction, RNA was reverse transcribed, and qPCR used to assess the expression of GPRC5A. Errors bars= ±SD compared to control sample (n=2). (b) Control and 5A KD cells were reactivated for 24 hrs before total RNA extraction was performed (n=1). qPCR was then performed to assess GPRC5A expression. GAPDH was used as a normalisation control.

Results showed that GPRC5A expression was significantly reduced in knockdown cells compared to that of the control line, with a reduction of ~60% being observed. Importantly, GPRC5A expression remain depleted following lytic KSHV reactivation **(Figure 4.8b)**.

Next, the effect of GPRC5A KD on KSHV lytic replication was examined. To this end, control and GPRC5A KD cell lines were either left untreated (latent control) or reactivated for 24 hours. Following sample collection, protein lysates were harvested, and viral protein expression assessed using immunoblotting **(Figure 4.9)**. A significant reduction in both early **(Figure 4.9a)** and late **(Figure 4.9b)** viral proteins was observed following GPRC5A KD when compared to control cells. Densitometry measurements highlight that the expression of early ORF57 protein was reduced by ~60%. Similarly, the expression of late proteins K8.1A and ORF65 was diminished ~60-70%. This suggests that GPCR5A is required for efficient KSHV lytic replication.

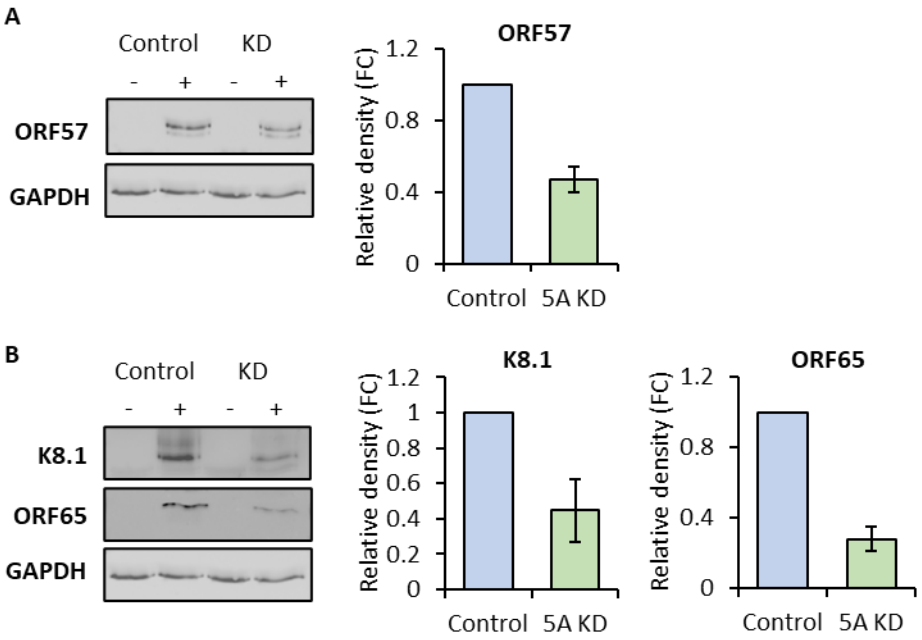

4.9 GPRC5A Knockdown reduces viral protein expression. Control and GPRC5A KD cells were reactivated to induce KSHV lytic replication. 24 hrs post reactivation, protein lysates were harvested. Immunoblotting was subsequently used to assess the expression of (a) the early protein, ORF57 and (b) late proteins; K8.1 and ORF65. Densitometry was also performed on western blots in both (a) and (b) using ImageJ software. Error bars= ±SD compared to reactivated control sample (n=2).

4.6 GPRC5A knockdown reduces viral load and the infection of naïve cells following lytic infection

To assess the effect of GPRC5A KD on KSHV DNA replication, control and GPRC5A KD cells were treated with dox to induce lytic replication. Samples were collected 72 hrs post reactivation and total DNA extracted. Following DNA extraction, qPCR was used to assess viral DNA levels using KSHV ORF57 and ORF47 as genome markers, with GAPDH being used as a normalisation control **(Figure 4.10)**. Results show KD of GPRC5A led to a significant decrease in viral load following lytic replication, resulting in an ~40% reduction of viral genomes.

Moreover, to investigate if GPRC5A knockdown reduces the production of infectious virions, a viral reinfection assay was performed. Control and GPRC5A KD cells were treated to induce lytic replication. 72 hrs post induction, supernatant containing KSHV virions was collected and used to infect naïve 293T cells. Infection was allowed to proceed for 48 hrs, after which 293T cells were collected and total RNA harvested.

Following reverse transcription, qPCR was performed to assess the expression of both ORF57 and ORF47 **(Figure 4.11)**.

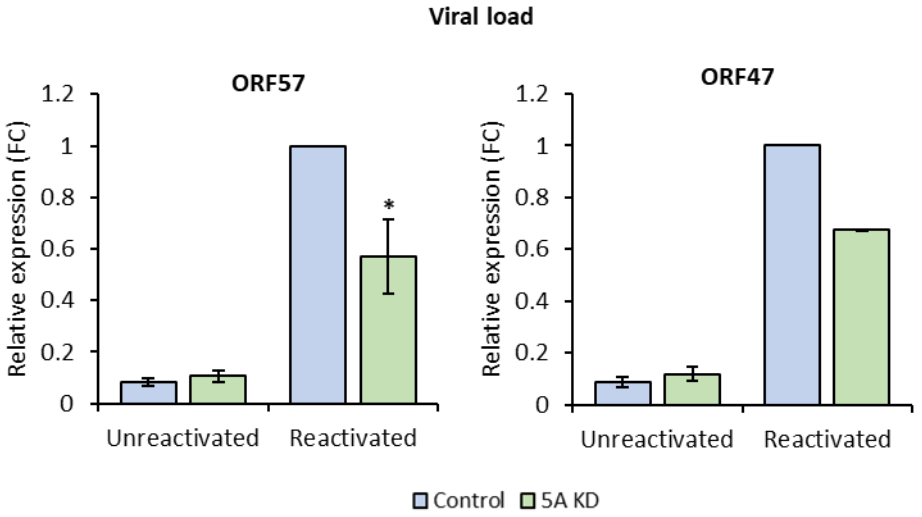

Figure 4.10 GPRC5A Knockdown reduces viral load following lytic reactivation. GPRC5A KD and control cells were reactivated to induce lytic KSHV replication for 72 hrs. Samples were collected and DNA harvested. Viral load was examined using qPCR, with viral ORF57 (n=3) and ORF47 (n=2) DNA levels being assessed. GAPDH was used as a normalisation control. Error bars= ±SD, p< 0.05= * compared to reactivated control.

Figure 4.11 GPRC5A Knockdown reduces infectious virion infectivity of naïve cells. Control and GPRC5A knockdown cell lines were reactivated to induce lytic infection for 72 hrs. After 72 hrs, supernatants containing KSHV virions were collected and added to naïve 293T cells. After 48 hrs cells were collected, and total RNA extracted. qPCR was used to assess both ORF57 and ORF47 expression, with GAPDH being used as a normalisation control. Error bars= ±SD (n=2).

The infection of naïve 293T cells was significantly diminished following infection with supernatant taken from GPRC5A knockdown cells, compared to the scrambled control cells. Notably, GPRC5A KD supernatant resulted in an ~ 90% reduction in viral gene expression when compared to the control supernatant.

Taken together these results indicate that GPRC5A depletion significantly effects KSHV lytic replication, ultimately leading to a substantial reduction in infectious virion production, a phenotype also observed following miR-142-3p mimic overexpression.

4.7 GPRC5A is a direct target of miR-142-3p

While the overexpression of miR-142-3p led to a significant reduction in GPRC5A expression, it remained to be fully determined whether GPRC5A was in fact a direct target of miR-142-3p. To address this a 3' UTR luciferase assay was utilised **(Outlined in figure 4.12)**.

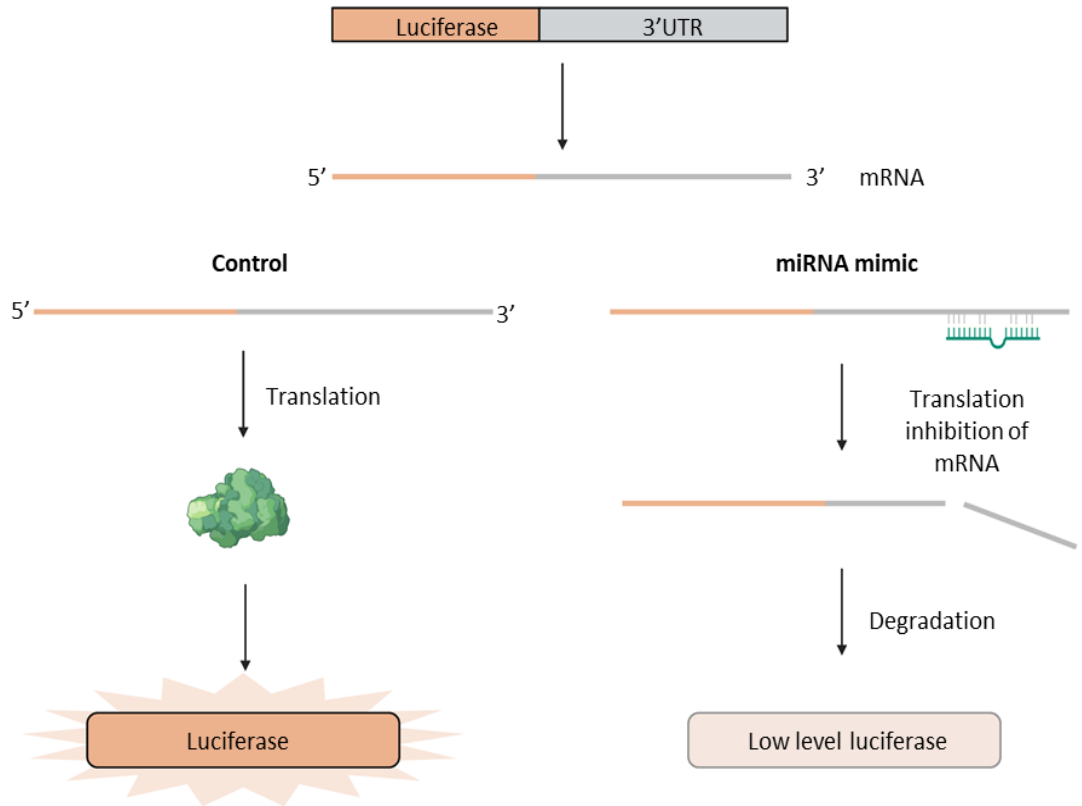

4.12 3'UTR luciferase assay. Schematic diagram outlining a 3' UTR luciferase assay. The DNA sequence containing the potential 3' untranslated region (UTR) binding site of the target gene is cloned into a luciferase reporter. Ultimately leading to the transcription of a fusion transcript containing luciferase and the 3' UTR miRNA binding site. The recombinant plasmid is transfected into cells along with a specific miRNA mimic. The binding of the miRNA mimic binds and represses the translation of the luciferase reporter protein, reducing the luminescence produced.

To identify any potential miR-142-3p binding sites within the GPRC5A gene, the predictive software; miRWALK was used (mirwalk.de). A potential binding site was found to be located within the 3'UTR of GPRC5A **(Figure 4.13a)**.

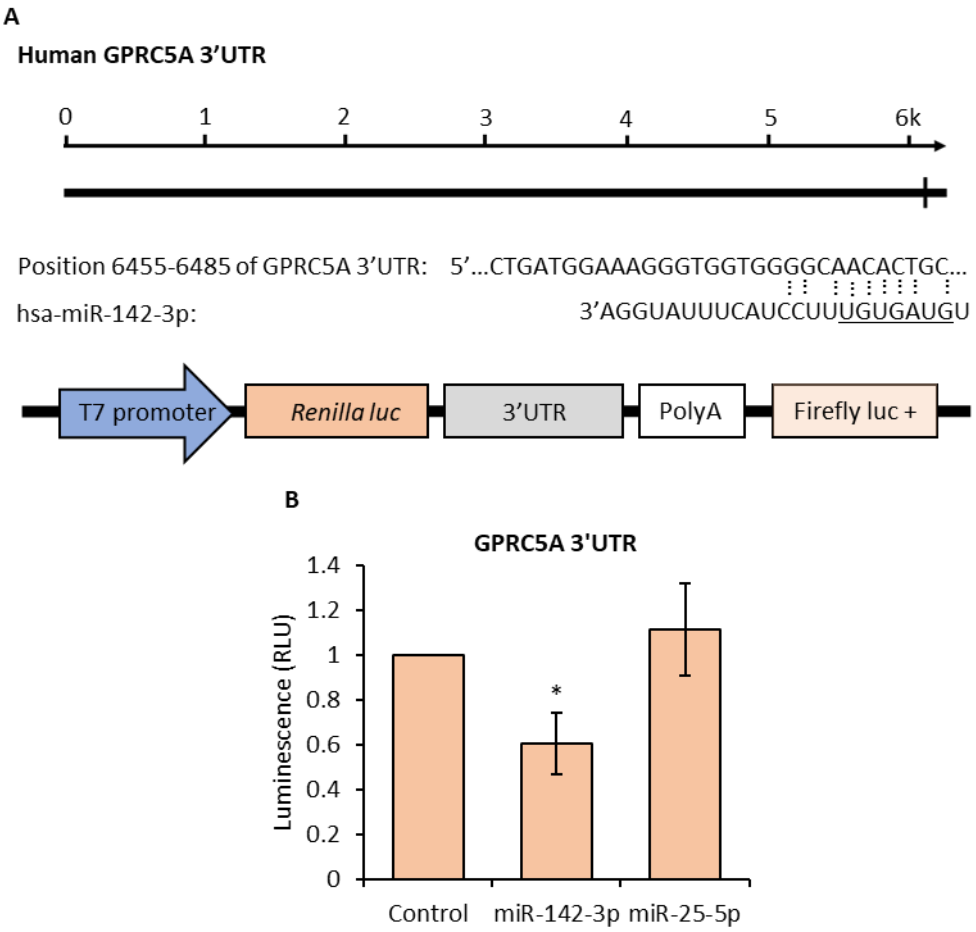

Figure 4.13 GPRC5A is a direct target of miR-142-3p. (a) Schematic representation of the GPRC5A 3' UTR. Below, the predicted binding site of miR-142-3p is indicated. (b) A dual luciferase reporter plasmid expressing the 3' UTR region of GPRC5A containing a potential miR-142-3p binding site was co-transfected into 293T cells with a scrambled control or miR-142-3p mimic. 24 hrs post transfection, luminescence of both the *Renilla* and firefly reporter genes were sequentially assessed using a FLUOstar optima plate reader. *Renilla* luciferase activity was normalised to that of the firefly reporter. Error bars= ±SD, $p<0.05$= * compared to control (n=3).

The 3' UTR was subsequently cloned into a dual luciferase reporter plasmid (Promega) and co-transfected into 293T cells with either a scrambled control or miR-142-3p mimic. Cells were also co-transfected with a miR-25-5p mimic, a miRNA that is not predicted to bind the 3' UTR region of GPCR5A. 24 hrs post transfection luminescence was analysed

using a FLUOstar optima plate reader. Firefly luminescence was used as a normalisation control **(Figure 4.13b)**.

Results show luminescence was significantly decreased following co-transfection with a miR-142-3p mimic compared to that of the scrambled control or the miR-25-5p mimic. These results indicate that GRPC5A is a direct mRNA target of miR-142-3p.

4.8 Investigating the potential function of GPRC5A during KSHV lytic infection

While GPRC5A has been found to be dysregulated in many diseases including cancer, very little is known about its precise molecular function. It has however been reported to affect the activity of small GTPases, with GPRC5A KD leading to a decrease in the activity of Rho GTPases, specifically RhoA and RAC1 which are notably involved in the assembly of actin structures including stress fibres, lamellipodia and filopodia. Additionally, GPRC5A was found to be abundant in membrane protrusions containing F-actin (Bulanova et al., 2017). Interestingly, the importance of the actin cytoskeleton for viral infection is well documented and has been found critical for numerous processes including viral entry, assembly, egress and dissemination (Taylor, Koyuncu and Enquist, 2011). Indeed, KSHV ORF21 has been implicated in the induction of actin stress fibres, during lytic replication via a RhoA-ROCK dependent mechanism (Gill et al., 2015). It was therefore hypothesised that GPRC5A may be involved in actin remodelling following KSHV lytic reactivation.

Following observations that GPRC5A KD led to a decrease in KSHV lytic protein expression (section 4.5), the expression of ORF21 was first assessed following KSHV lytic reactivation in 5A KD cells. In the absence of an available ORF21 antibody, qPCR was used to assess ORF21 gene expression **(Figure 4.14)**.

Interestingly, the expression of ORF21 appears to be downregulated in 5A knockdown compared to control cells, with a reduction of ~35% being observed.

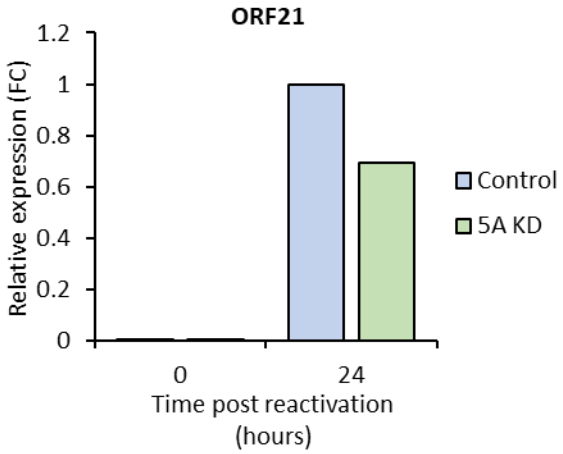

Figure 4.14 GPRC5A knockdown appears to reduce ORF21 expression. GPRC5A knockdown cells were reactivated, and samples collected after 24 hrs. Following total RNA extraction, reverse transcription was performed, and qPCR used to assess the expression of ORF21 (n=1).

Following this observation and the previously documented involvement of GPRC5A in the regulation of actin dynamics, immunofluorescence and confocal microscopy were used to examine F-actin in control and 5A KD cells following lytic reactivation. To this end, control and 5A KD cells were reactivated for 24 hrs and stained with rhodamine conjugated phalloidin to visualise actin filaments **(Figure 4.15)**.

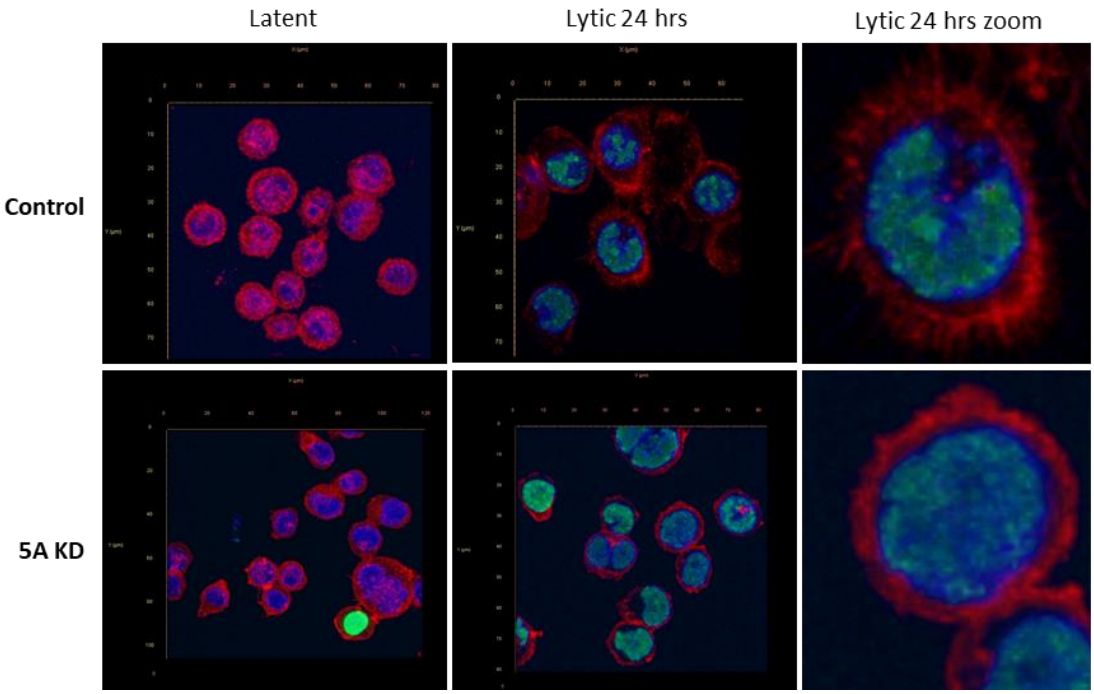

Figure 4.15 Filamentous actin staining of control and GPRC5A KD cells. Confocal Z stack images of control and 5A KD cells at 0 (latent) and 24 hrs post reactivation immunostained using anti-ORF57 (green), rhodamine- phalloidin (TRITC, red) for actin filament staining and DAPI for nuclear DNA staining (blue).

Interestingly, F-actin protrusions appeared less pronounced following reactivation of 5A KD cells compared to that of control cells. This suggests the assembly of actin membrane protrusions may be somewhat impaired in 5A KD cells.

Unfortunately, initial attempts to assess the phosphorylation of RhoA and RAC1 following reactivation of control and 5A KD cells were unsuccessful and requires further optimisation.

4.9 Discussion

Though our understanding of mechanisms which regulate miRNA-mRNA interactions has increased in recent years, identification of miRNA targets remains challenging. Indeed, a single miRNA is thought to be able to regulate the expression of hundreds of mRNA targets simultaneously. Furthermore, this target transcriptome can differ between different cell types and cellular environments providing an additional layer of complexity to target identification (Nam et al., 2014) (Sakakibara and Tosato, 2014). As it is unfeasible to validate every potential target in the laboratory, several bioinformatic programmes have been developed. These computational tools each employ different predictive algorithms and can be used to select initial target candidates. While vast improvements have been made to miRNA target predictive software, they are not without their limitations and false positives remain common (Bartel, 2018). Indeed, many cellular targets were assessed during this research project that did not prove to be significant targets of miR-142-3p, highlighting the importance of thorough experimental validation. Given time and resources alternative methods such as Argonaute-crosslinking and immunoprecipitation (AGO-CLIP) could have been used in order to map miRNA-binding sites. Indeed, utilising AGO-CLIP would not only aid in the identification of significant miR-142-3p targets but also identify alterations in miRNA targeting of the cellular transcriptome globally following KSHV lytic replication (Chi et al., 2009).

Nevertheless, this study did identify a number of potential mRNA targets of miR-142-3p, specifically GPRC5A which was confirmed as a direct target using a 3' UTR luciferase assay. Moreover, GPRC5A depletion inhibited KSHV lytic replication, culminating in a significant decrease in infectious virion production. Interestingly, a similar phenotype was observed following miR-142-3p overexpression.

G protein-coupled receptor class C group 5 member A (GPCR5A), also known as Retinoic acid induced protein 3 belongs to the G protein-coupling receptor (GPCR) superfamily. GPCRs are a diverse family of receptors, involved in numerous physiological processes (Syrovatkina et al., 2016). Given their extensive physiological functions, abnormal GPCR expression/activation is frequently linked to the development and progression of cancer. Indeed GPRC5A, a type C orphan receptor has been reported to exert both tumour suppressive and oncogenic affects in different types of cancer (Zhou and Rigoutsos, 2014). While mechanisms underpinning GPRC5A function remain poorly understood, GPRC5A has previously been found to abundantly localise with membrane protrusions containing F-actin. Furthermore, GPRC5A was also reported to regulate the activity of small GTPases, namely RhoA and RAC1 which are involved in the assembly of actin structures (e.g stress fibres) (Bulanova et al., 2017).

The importance of the actin cytoskeleton in viral infection is well described and has been implicated in a number of crucial processes, from viral entry to viral egress and dissemination (Taylor, Koyuncu and Enquist, 2011). Interestingly, lytic KSHV ORF21 was found to induce actin stress fibres and cell blebbing, indicated the importance of actin remodelling during lytic replication (Gill et al., 2015). Rhodamine conjugated phalloidin was therefore utilised in order to investigate actin remodelling in GPRC5A KD cells in combination with fluorescent microscopy. Phalloidin conjugates offer a convenient, highly efficient way to probe filamentous actin and have been used previously in numerous research studies (Lozano-Romero et al., 2020) (Salinas-Vera et al., 2019). While further investigation is required, membrane protrusions containing F-actin appeared to be somewhat impaired in GPRC5A KD cell compared to control cells, suggesting GPRC5A may be involved actin remodelling following lytic reactivation.

Increasing evidence suggests that some viruses induce actin protrusions in order to facilitate efficient viral egress and dissemination (Sattentau, 2008). For example, the alphaherpesvirus, HSV promotes the formation of actin protrusions through the activity of its viral kinase, US3 and is considered necessary for effective cell to cell spreading (Favoreel et al., 2005). Interestingly, the expression of KSHV viral kinase, ORF21 appeared to be somewhat reduced following lytic reactivation of GPRC5A KD compared to that of control cells. While the downregulation of ORF21 requires confirmation this suggests that impaired actin remodelling and subsequently viral egress/ dissemination could

potentially contribute to a decrease in viral reinfection of 293Ts observed when using supernatant from GPRC5A KD cells.

Future experiments should aim to assess the activity of the small GTPases RhoA and RAC1 in GRPC5A KD cells. While optimisation of phospho antibodies remains necessary, alternative methods to assess levels of active GTP-bound RhoA and RAC1 could be utilised. Indeed, a Small GTPase Combo Activation Assay Kit to selectively pull-down active forms of RhoA and RAC1, followed by western blot analysis could be performed as previously described (Bulanova et al., 2017). It would also be of interest to assess whether treatment with RhoA and RAC1 inhibitors results in a similar phenotype observed following GPRC5A KD.

Moreover, miR-142-3p has been reported to target a number of other key regulators of the actin cytoskeleton including ROCK2, a downstream effector of RhoA signalling (Liu et al., 2014). Thus, miR-142-3p may target the expression of multiple components of RhoA signalling and is downregulated by KSHV during lytic replication in order to promote actin remodelling and thus efficient viral replication and egress. These potential interactions should therefore be confirmed and subsequently characterised using both mimic and overexpression studies.

Furthermore, proteomic analysis carried out in the Whitehouse laboratory identified members of the flotillin family as potential interactors of GPRC5A following reactivation (unpublished data). FLOT 1 and 2 are lipid raft scaffolding proteins and as such have been implicated in cellular adhesion, endocytosis, and signal transduction (Bodin et al., 2014) (Otto and Nichols, 2011) (Sugawara et al., 2007). Interestingly, while clustering of FLOT proteins is dependent on oligomerisation, organisation, and stability of these microdomains at the plasma membrane is reliant on F-actin. Indeed, FLOT2 was found to directly interact with actin filaments via its SPFH domain (Langhorst et al., 2007).

The interaction between GPRC5A and FLOT 1 and 2 have since been validated (unpublished Whitehouse group data), thus disrupting GPRC5A-FLOT binding as well as GPRC5A actin remodelling could have an impact not only on lipid raft stability but also signal transduction. Interestingly, the importance of lipid rafts for multiple viral processes including viral replication, virion assembly and budding is well established. In fact, lipid rafts have been proven crucial for KSHV egress (Wang et al., 2015).

Nevertheless, the physiological importance of GPRC5A and its interaction during lytic replication require further investigation. Future experiments should therefore not only aim the establish the functional role of GPRC5A in viral egress but also that of intracellular signalling which could prove beneficial for KSHV viral replication.

Chapter 5

~

Investigating the regulation of miR-142-3p during KSHV lytic replication

5. Investigating the regulation of miR-142-3p during KSHV lytic infection

5.1 Introduction

The expression of miRNAs is controlled by various regulatory mechanisms. Indeed, all stages of miRNA biogenesis are subject to regulation, including transcription, processing and miRNA stability (Ha and Kim, 2014). These mechanisms ultimately contribute to the spatiotemporal expression of miRNAs and prove extremely important in responding to the dynamic environment of cells. Furthermore, viruses are known to subvert these regulatory processes in order to manipulate miRNA expression and therefore the transcriptome of their host cells.

Similar to protein coding genes, the transcription of primary miRNA transcripts is influenced by epigenetic mechanisms such as DNA methylation and also transcription factor binding. Interestingly, CpG islands (CGI's) have been found to colocalise with the promoters and transcription start sites (TSS) of numerous miRNA genes, including miR-142 (Morales, Monza and Navarro, 2017) (Skårn et al., 2013). Methylation of these genes tends to result in transcriptional repression, following reduced affinity of transcription factor (TF) binding and the formation of chromatin-modifying repression complexes (Glaich et al., 2019).

Intergenic miRNA, such as miR-142, are located between genes and are considered to be independent transcription units that utilise distinct promoters (Hinske et al., 2014). While only a limited number of miRNA promoters have been fully annotated, several TFs have been found to influence miR-142 expression, with both positive and negative regulators being described. For example, Octamer- binding transcription factor-4 (OCT4) also known as POU domain, class 5 transcription factor 1 (POU5F1), has previously been reported to negatively impact expression of miR-142-3p in colon cancer cells (Shen et al., 2013). BCL6 also supresses miR-142 expression, recruiting enhancer of zeste homolog 2 (EZH2) and histone deacetylase 5 (HDAC5) to the miR-142 promoter, thereby increasing H3K27 methylation and decreasing H3K9/K14 acetylation, consequently inhibiting miR-142 gene transcription (Ding et al., 2020). Similarly, IL-6 induces both the expression and nuclear localisation of DNMT1 which ultimately mediates the hypermethylation of the miR-142-3p promoter. Furthermore, DNMT1 appears to facilitate the methylation of SP1

binding sites in the promoter, a positive regulator of miR-142-3p expression (Chiou et al., 2013). TFs have also been implicating in promoting miRNA transcription. For example, STAT6 has been reported to positively regulate miR-142 promoter activity (Su et al., 2015). Interestingly, KSHV RTA mediates the ubiquitylation of STAT6, promoting its proteosomal degradation. Moreover, the proteosomal degradation of STAT6 proves important not only for lytic KSHV reactivation but also that of other human herpesviruses (Gu et al., 2018).

Expression of miRNAs can also be regulated post-transcriptionally, with regulatory mechanisms affecting processing, export, and mature miRNA stability being described (Ha and Kim, 2014). Interestingly, editing by ADAR deaminases affects processing of both pri-miRNAs and pre-miRNAs (Kawahara, Zinshteyn, Chendrimada, et al., 2007). Indeed, ADAR editing of pri-miR-142 by ADAR1/2 has previously been shown to inhibit Drosha cleavage, leading to its degradation by Tudor-SN (SND1) (Yang et al., 2006). SND1 possess exonuclease activity and preferentially targets hyper edited RNA, containing multiple I: U/ U: I pairs (Scadden, 2005). Alternatively, target RNA mediated TDMD and 5'-3' exonuclease degradation of mature miRNAs has previously been described (Fuchs Wightman et al., 2018). Furthermore, the expression of mature miRNAs is also regulated by a variety of 3' end post transcriptional modifications, with methylation, adenylation and uridylation reported to affect miRNA stability and turnover (Liang et al., 2020) (Rodríguez-Galán et al., 2021) (Gutiérrez-Vázquez et al., 2017).

Viruses have been found to employ a variety of mechanisms to dysregulate miRNA expression. Indeed, some have been found to alter methylation and the expression of miRNA transcription factors, ultimately affecting miRNA gene transcription. For example, Enterovirus 71 (EV71) inhibits the expression of the miR-17~92 cluster by promoting the methylation of its promoter through the upregulation of DNMT3B (Fu et al., 2019). While HPV has been found to dysregulate the expression of multiple miRNAs by targeting miRNA TF's. E6, a major HPV oncoprotein, mediates the downregulation of miR-34a, by destabilising its positive regulator, TP53 (Wang et al., 2009).

Virally-encoded factors have been reported to directly interact with miRNA promoters. Indeed, HSV-1 encoded ICP4, directly binds to the miR-101 promoter and induces its transcription (Wang *et al.*, 2021). Similarly, HCMV induces the transcription of the miR-17~92 cluster via the expression of both IE1 and IE2, before selectively degrading miR-

17 and miR-20a. Degradation of these miRNA occurs through TDMD mediated by a HCMV- encoded miRNA decay element (miRDE) (Lee *et al.*, 2013). Alternatively, VV post-transcriptionally modifies host miRNAs, directing their polyadenylation and therefore promoting a global degradation of cellular miRNAs (Backes et al., 2012).

In this chapter, potential mechanisms involved in the regulation of miR-142-3p expression were investigated. Results show that expression levels of pri-miR-142 were reduced following lytic reactivation, suggesting a change in transcription, processing or primary transcript stability leads to the downregulation of miR-142-3p. Mechanism affecting miRNA gene transcription and pri-miR-142 processing were therefore preliminarily examined including methylation, ADAR editing and the influence of both negative and positive TFs.

5.2 Primary miR-142 transcript levels are reduced following KSHV lytic reactivation

The production of a mature miRNA molecule begins with the transcription of a primary miRNA transcript, typically ~1000 nts in length (Lee et al., 2004). To assess whether an alteration in pri-miR-142 levels contributes to the downregulation of mature miR-142-3p expression following lytic reactivation, pri-miR-142 levels were examined. To this end, TREx BCBL-1 Rta cells were induced to reactivate lytic infection and samples collected at 0, 16 and 24 hrs. Subsequent to total RNA extraction and reverse transcription, qPCR was used to measure pri-miR-142 levels. GAPDH was used as a normalisation control **(Figure 5.2)**. The expression of pri-miR-142 was significantly reduced following reactivation, with a reduction of ~ 60 and 70% being observed at 16 and 24 hrs respectively.

The observed reduction in pri-miR-142 levels could be due to changes in primary transcript transcription, degradation of pri-miR-142 or even alterations in its processing. Some of these regulatory mechanisms were therefore further explored in the sections below.

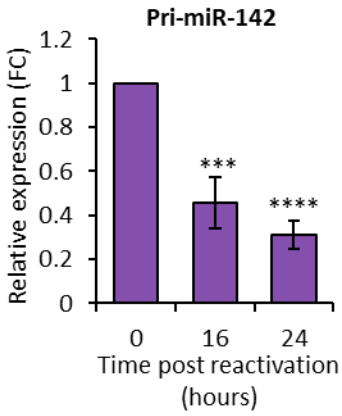

Figure 5.1 The expression of pri-miR-142 is significantly reduced following reactivation of lytic infection. TREx BCBL-1 Rta cells were treated to induce lytic replication. Total RNA extraction was performed on 0 (latent), 16 and 24 hr samples. Following, reverse transcription, qPCR was performed to assess the expression of pri-miR-142 transcript levels. GAPDH was used as a normalisation control. Error bars= ±SD, p< 0.001 ***, p< 0.0001 **** compared to 0 hr sample (n=5).

5.3 Investigating the role of methylation in the regulation of miR-142 expression

miR-142-3p is known to be abundantly expressed in hematopoietic cells compared to other cell lines (Ramkissoon et al., 2006). Methylation appears to be a common mechanism in the regulation of miR-142 expression, it was therefore hypothesised that reduced pri-miR-142 expression following lytic reactivation may be due to changes in the methylation status of the miR-142 promoter. Attempts were therefore made to assess its methylation status during KSHV lytic replication.

As low expression of miR-142-3p in 293T cells has previously been linked to methylation, this cell line was first investigated as a possible positive control for subsequent methylation PCR. Total RNA was extracted from both TREx BCBL-1 Rta and 293T cells. Following appropriate reverse transcription, qPCR was then used to determine levels of pri-miR-142 **(Figure 5.2a)** and miR-142-3p **(Figure 5.2b)** as previously described. GAPDH and U6 were used as normalisation controls for pri-miR-142 and miR-142-3p, respectively. The expression of both pri-miR-142 and mature miR-142-3p appears to be much lower in 293T cells compared to that of TREx BCBL-1 Rta cells.

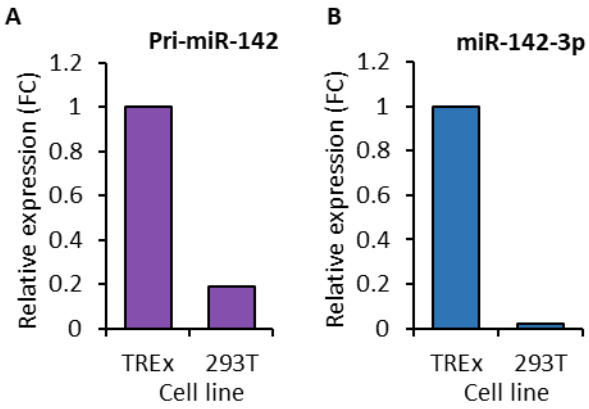

Figure 5.2 Pri-miR-142 and miR-142-3p expression is lower in 293T cells. Total RNA was extracted from TREx BCBL-1 Rta and 293T cells (a) subsequent to reverse transcription, qPCR was performed to examine pri-miR-142 expression. GAPDH was used as a normalisation control (b) miScript RT was performed and qPCR used to analyse the expression of miR-142-3p, with U6 being used as a normalisation control (n=1).

Furthermore, regulatory factors, BCL6 and DNMT1 which have previously been reported to promote miR-142 promoter methylation were assessed and appeared to be upregulated in 293T cells **(Figure 5.3)**. Therefore, to determine if an alteration in BCL6 and DNMT1 expression could potentially promote the methylation of miR-142 during KSHV lytic replication, their expression was assessed following lytic reactivation **(Figure 5.4)**.

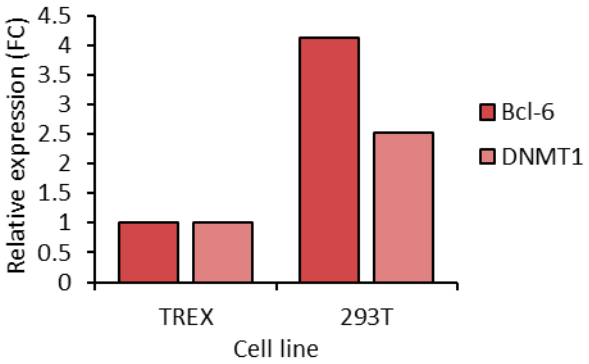

Figure 5.3 The expression of BCL6 and DMNT1 is upregulated in 293T cells. Following total RNA extraction from TREx BCBL-1 Rta and 293T cells, reverse transcription was performed. qPCR was then used to assess the expression of BCL6 and DNMT1. GAPDH was used as a normalisation control (n=1).

To this end, samples were collected at 0, 8, 16 and 24 hrs and total RNA extracted. Following reverse transcription, qPCR was used to examine the expression of both BCL6 and DNMT1 **(Figure 5.4a and b)**. Additionally, immunoblotting was used to assess

DNMT1 protein expression and densitometry subsequently performed **(Figure 5.4c and d)**. GAPDH was used as a normalisation control. Unfortunately, time constraints did not allow for the assessment of BCL6 protein levels in the present study.

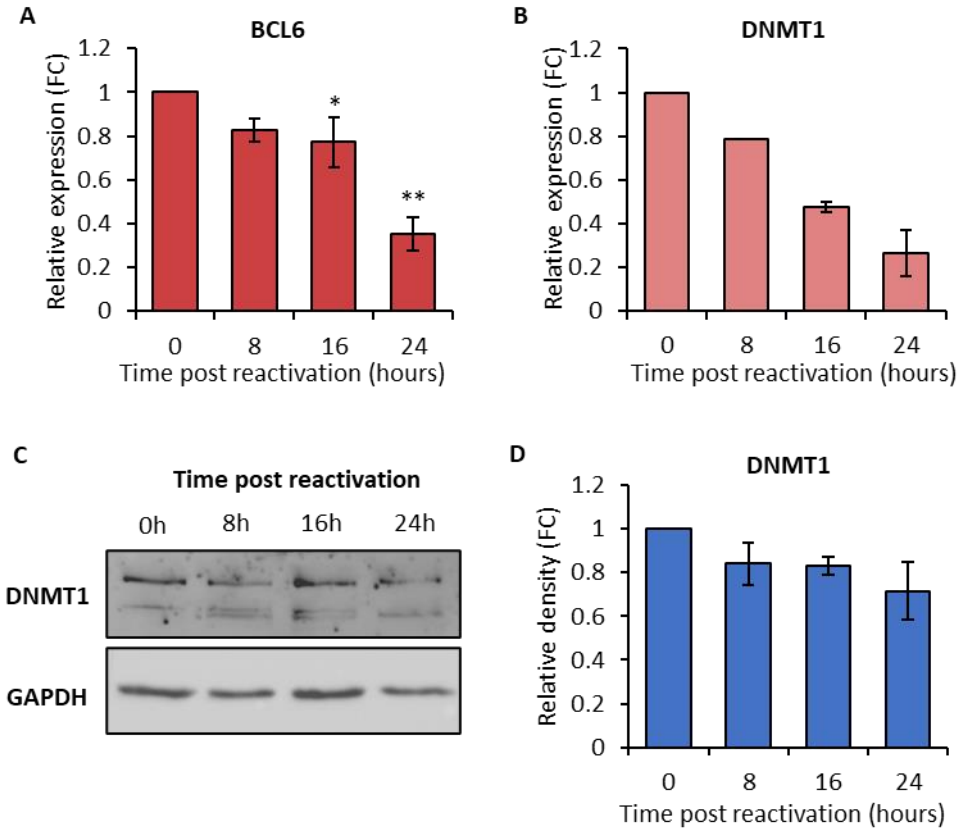

Figure 5.4 The expression of BCL6 and DNMT1 expression following KSHV lytic reactivation. Samples were collected at 0, 8, 16 and 24 hrs post reactivation. Subsequent to total RNA extraction and reverse transcription (a) BCL6 (n=3) and (b) DNMT1 expression were assessed using qPCR. GAPDH was used as a normalisation control. (c) Immunoblotting was used examine DNMT1 protein expression, with GAPDH being used as a normalisation control (n=2). (d) ImageJ was used to perform densitometry on the blot in c). Error bars= ±SD, $p<0.01$= **, $p<0.05$= *, when compared to 0 hr latent control sample.

Surprisingly, gene expression of both BCL6 and DNMT1 appeared to be downregulated following lytic reactivation, with a reduction of ~20% at 8 hrs increasing to ~60% at 24 hrs post reactivation. DNMT1 protein expression however appeared to be less affected, with only a slight reduction in protein levels observed.

While an increase in DNMT1 protein expression was not seen following KSHV lytic reactivation, IL-6 which was confirmed to be upregulated in section 4.3 has also been shown to induce the nuclear localisation of DNMT1. Thus, attempts were made to

perform methylation specific PCR following KSHV lytic reactivation. Initial efforts however were unsuccessful and further optimisation is required. Alterations in miR-142 promoter methylation during KSHV lytic infection cannot therefore currently be ruled out and requires further investigation due to time constraints.

5.4 Investigating the role of ADAR editing in pri-miR-142 regulation

ADAR1 and ADAR2 have previously been reported to inhibit the Drosha processing of pri-miR-142, subsequently leading to its degradation by SND1. Indeed, edited pri-miR-142 contains several I: U/ U: I sites, which proves favourable for SND1 cleavage. Sites within the pri-miR-142 transcript previously found to be edited by ADAR 1 and ADAR 2 are shown below in figure 5.5 (Yang et al., 2006). Interestingly, both ADAR editing and SND1 have previously been found to be essential for KSHV lytic replication (Zhang et al., 2020) (Baquero-Perez et al., 2019).

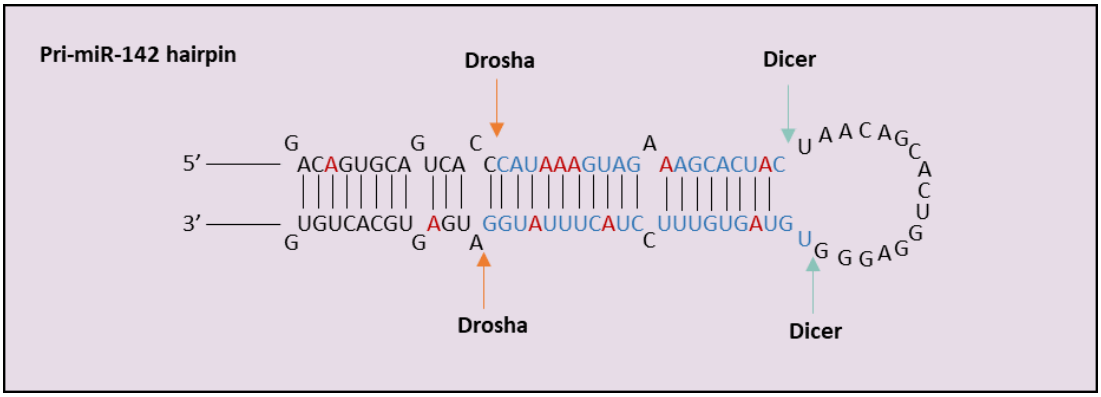

Figure 5.5 ADAR editing of pri-miR-142. Previously reported A-to-I editing sites of pri-miR-142 are indicated in red. Mature miRNA sequences processed from the primary hairpin are shown in blue, Drosha and Dicer cleavage sites are represented by orange and green arrows respectively. Adapted from (Yang et al., 2006).

It was therefore investigated if ADAR editing of pri-miR-142 and consequently its degradation by SND1 could be responsible for the reduction in pri-miR-142 levels observed following lytic reactivation **(Figure 5.6)**. To this end, TREx BCBL-1 Rta cell protein lysates were collected subsequent to lytic reactivation as previously described. Immunoblotting was then used to assess the protein expression of ADAR1, ADAR2 and

SND1 with GAPDH being used as a normalisation control **(Figure 5.6a)**. Densitometry performed using ImageJ is shown in figure 5.6b, c and d.

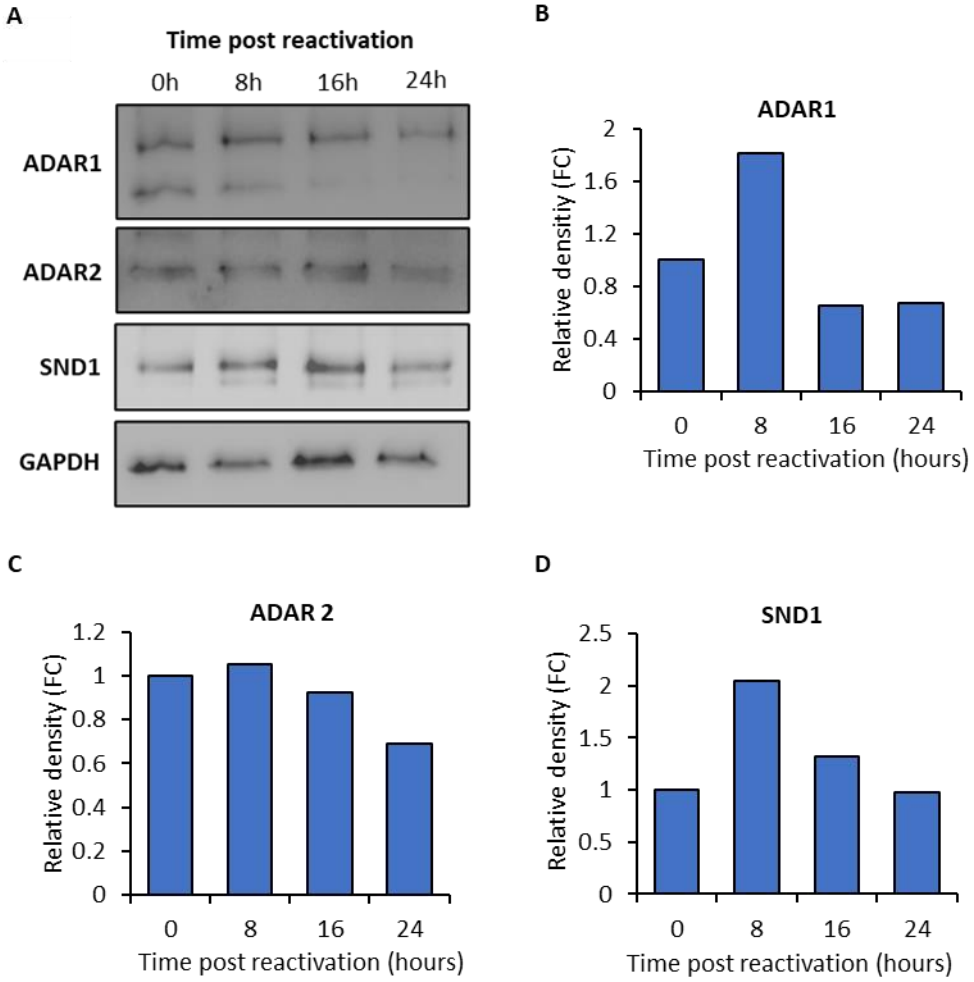

Figure 5.6 ADAR1 and SND1 protein level appear to be upregulated at 8 hrs post reactivation. TREx BCBL-1 Rta cells were reactivated, and samples collected at 0, 8, 16 and 24 hrs post reactivation (a) Following protein extraction, immunoblotting was used to assess the protein levels of ADAR1/2 and SND1. GAPDH was used as a loading control. Blots are representative of a single biological replicate Densitometry was subsequently performed on the blot in (a) for (b) ADAR1, (c) ADAR2 and (d) SND1 using ImageJ (n=1).

Results showed that expression of both ADAR1 and SND1 appeared to be slightly upregulated 8 hrs post reactivation before returning or dropping below latently expressed levels at 16 and 24 hrs. An increase can be observed for both ADAR1 and SND1 at 8 hrs. In contrast, ADAR2 expression does not appear to be significantly affected following lytic reactivation.

To further test if ADAR editing potentially contributes to the downregulation of miR-142-3p following lytic reactivation, 8-Azaadenosine (8-Aza), a selective adenosine analogue was used to inhibit the editing activity of ADAR1 **(Figure 5.7)** (Ramírez-Moya et al., 2020). TREx BCBL-1 Rta cells were treated with increasing concentrations of 8-Aza for 1 hr prior to reactivation for 24 hrs. Samples were then collected and total RNA extracted. Following miScript RT, qPCR was used to assessed then expression of miR-142-3p with U6 being used a normalisation control **(Figure 5.7)**.

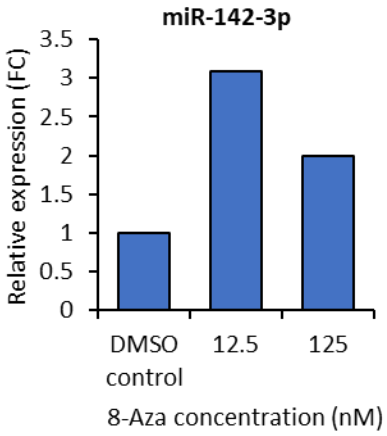

Figure 5.7 Inhibition of ADAR1 activity appears to increase miR-142-3p expression. TREx BCBL-1 Rta cells were treated with increasing concentrations of 8-Aza for 1 hour before being reactivated for 24 hrs. A DMSO control was also included. Following sample collection, total RNA was extracted and miScript RT performed. qPCR was then used to assess the expression miR-142-3p and U6 used as a normalisation control (n=1).

Interestingly, preliminary results suggest that 8-Aza treatment increases miR-142-3p expression. While further analysis is required this suggests that ADAR editing could potentially contribute the downregulation of miR-142-3p following lytic reactivation.

5.5 Investigating the role of transcription regulators in miR-142-3p expression

In addition to epigenetic mechanisms, TF binding is also known to regulate the transcription of miRNA (Ha and Kim, 2014). miR-142-3p is an intergenic miRNA, located between coding loci, and therefore thought to utilise a distinct promoter and regulatory elements (Hinske et al., 2014). Information regarding miRNA TSS and promoter regions unfortunately remain limited, largely due to limitations of conventional transcriptional methods and the transient nature of pri-miRNA expression. Efforts however have been made to address these shortfalls, with recent advances in sequencing technologies leading to the improvements in predictive computational alogrithms (Wang *et al.*, 2021).

TransmiR v2.0 database (http://www.cuilab.cn/transmir) is a comprehensive database of manually literature curated TF-miRNA regulations and was used to generate a network module of TFs potentially involved in miR-142-3p regulation **(Figure 5.8)** (Tong et al., 2019)**.** Literature examples (red, arrow) are further supplemented with predicted TF-miRNA regulations from ChIP sequencing data (level 1, grey arrow), and those with additional supporting high-throughput (HT) experimental data (level 2, green arrow).

The expression profiles of miRNA and TF are widely known to be cell type specific thus extensive validation of any potential hits is necessary (Ludwig et al., 2016). The expression of certain TFs that potentially regulate miR-142 transcription were therefore first examined following KSHV lytic reactivation of TREx BCBL-1 Rta cells.

Subsequent to lytic reactivation, samples were collected at 0, 8, 16 and 24 hrs post reactivation. Total RNA and protein were then extracted, and qPCR and immunoblotting used to assess the RNA and protein levels of possible regulators, respectively.

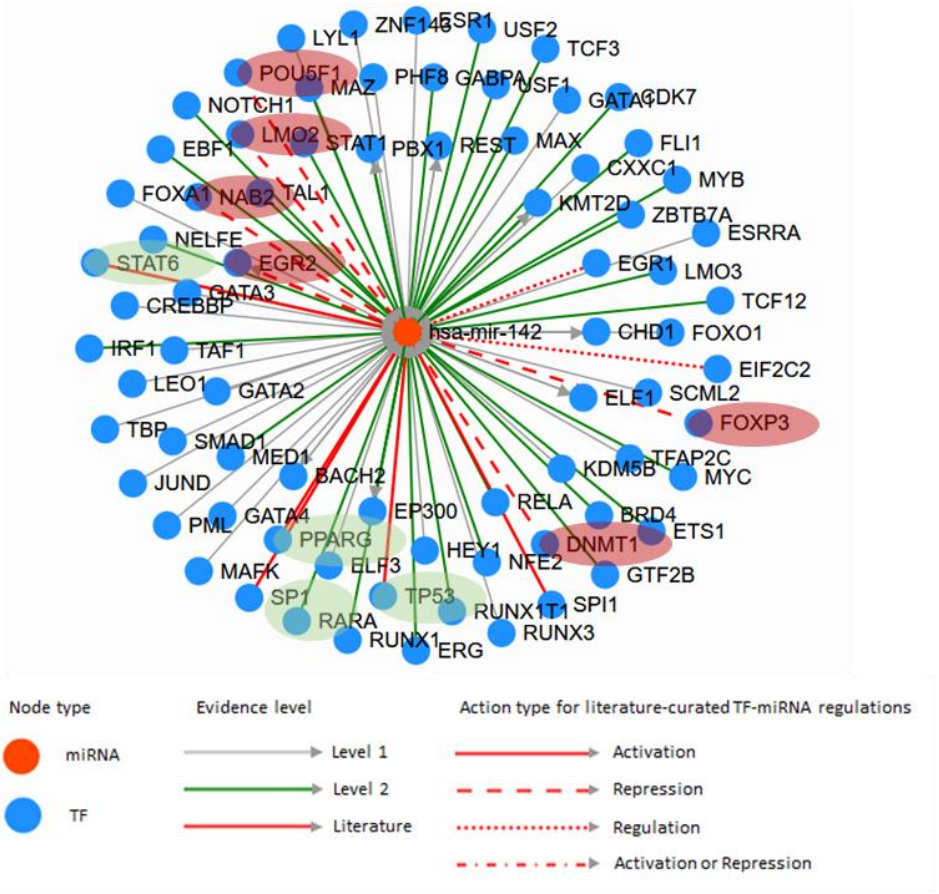

Negative regulator	Description	Reference
OCT4/A (POU5F1)	Octamer-binding transcription factor 4	Shen, 2013
DNMT1	DNA Methyltransferase 1	Chiou, 2013
EGR2	Early Growth Response 2	Lagrange, 2013
FOXP3	Forkhead box protein P3	Huang, 2008
LMO2	LIM Domain Only 2	Yuan, 2008
NAB2	NGFI-A Binding Protein 2	Lagrange, 2013

Positive regulator	Description	Reference
SP1	Specificity protein 1	Chiou, 2013
STAT6	Signal transducer and activator of transcription 6	Su, 2015
PPARγ	Peroxisome proliferator-activated receptor gamma	Yuan 2016
TP53	Tumor protein P53	Chen, 2015

Figure 5.8 Regulators of miR-142 transcription. TransmiR v2.0 (www.cuilab.cn/transmir) was used to create a network module of all transcription factors implicated in the regulation of miR-142-3p (above panel). Both predicted and literature curated TFs are shown, with literature examples highlighted. Red= negative, green= positive. Highlighted examples of negative and positive regulators are further separated into tables (below panel).

The mRNA and protein expression of OCT4 (also known as POU5F1) which has previously been reported to have a negative impact on miR-142 transcription is shown below **(Figure 5.9a and b)** (Shen et al., 2013). GAPDH was used as a normalisation control for both qPCR and immunoblotting. Densitometry was also performed using ImageJ **(Figure 5.9c)**.

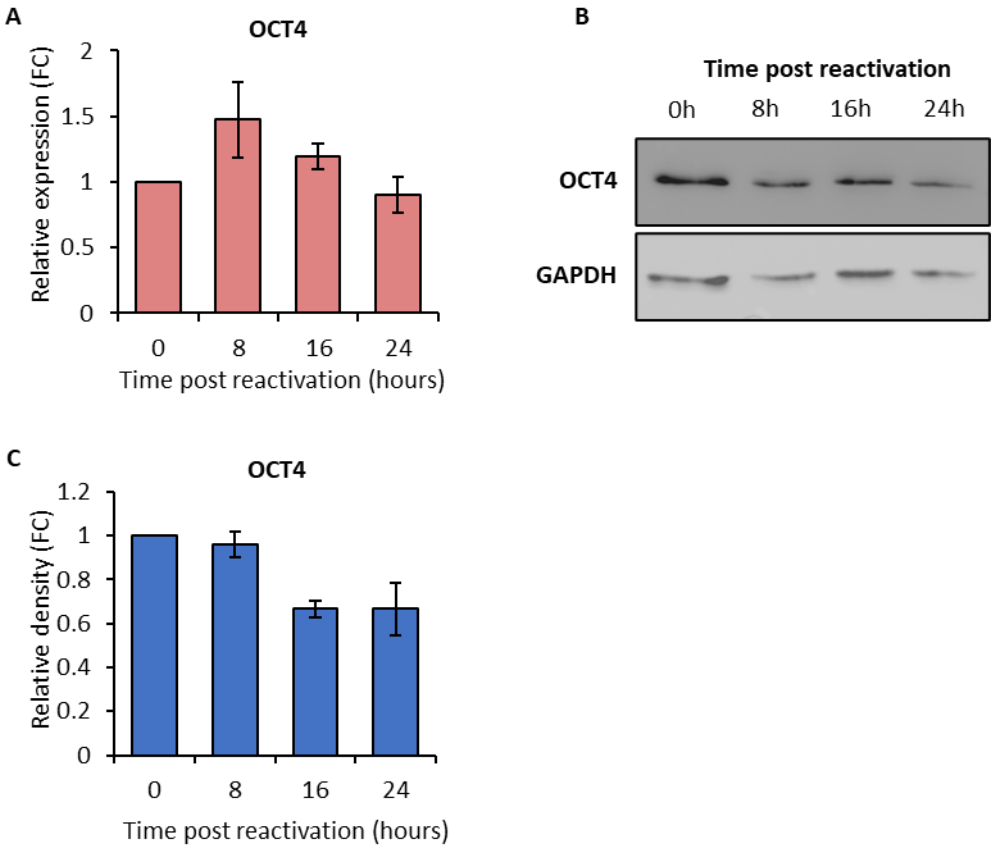

Figure 5.9 Expression of negative regulator, OCT4, following KSHV lytic reactivation. TREx BCBL-1 Rta cells were reactivated, and samples collected at 0, 8, 16 and 24 hrs. Following total RNA and protein extraction, (a) qPCR was used to OCT4 mRNA expression and (b) immunoblotting to assess OCT4 protein levels. (c) ImageJ was used to perform densitometry on blots shown in (b). GAPDH was used a normalisation control. Error bars= ±SD (n=2).

Gene expression of OCT4 did not appear to significantly alter following KSHV lytic reactivation. Similarly, 8 hrs post reactivation OCT4 protein expression remains unaffected, however, at later timepoints (16 and 24 hrs) a reduction of ~30-40% can be observed in OCT4 protein levels. This suggest that an increase in the expression of the negative regulator OCT4 is not responsible for the down regulation of miR-142-3p seen following lytic reactivation. However, an alteration in its recruitment to the miR-142 promoter cannot be ruled out without further investigation.

Other potential negative regulators of miR-142 expression such as LMO2 and its cofactor LBD1 were also assessed following lytic reactivation (data not shown) (Yuan et al., 2008). Unfortunately, while LMO2 gene expression appeared to be upregulated, transcript levels were extremely low at all timepoints investigated, thus other TFs of interest were explored.

Next, the expression of STAT6 a positive regulator of miR-142 expression was investigated following lytic reactivation **(Figure 5.10)** (Su et al., 2015). The STAT6 binding motif previously identified in the predicted promoter region of miR-142 is shown below in figure 5.10a.

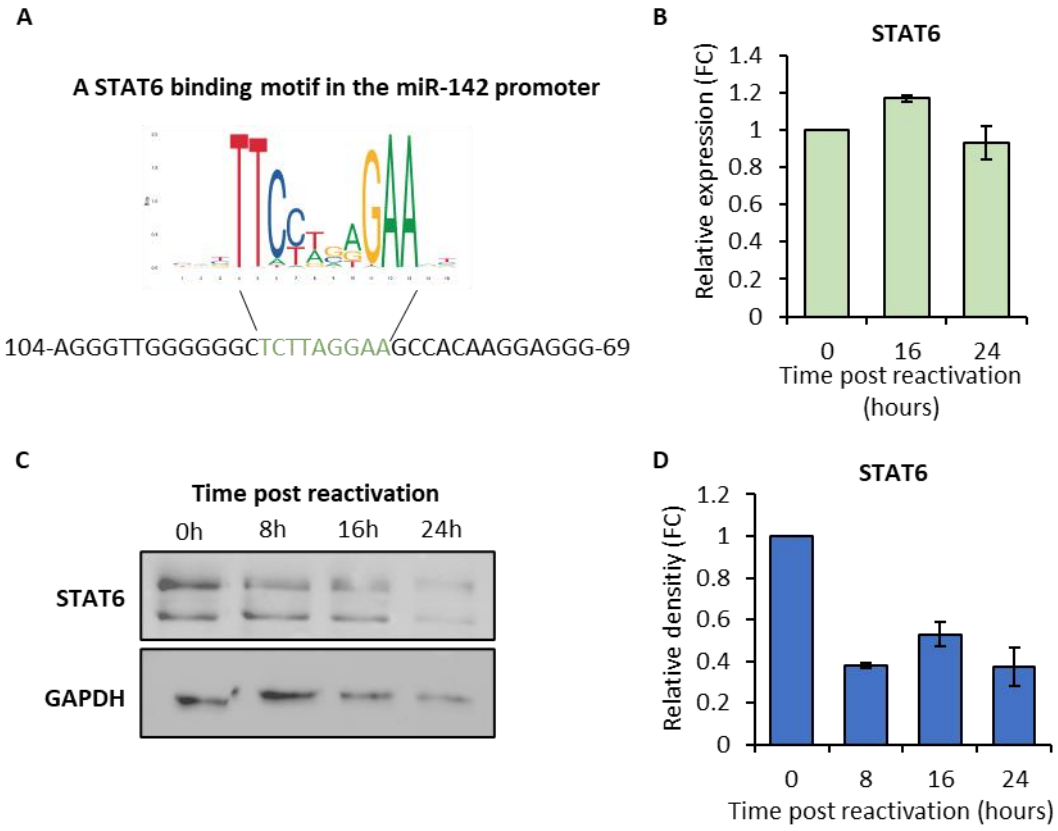

Figure 5.10 Protein expression of STAT6 appears to be downregulated following KSHV lytic reactivation. (a) A conserved STAT6 binding motif present in the miR-142 promoter predicted by JASPAR (b) TREx BCBL-1 Rta cells were collected at 0, 16 and 24 hrs post lytic reactivation, total RNA was subsequently extracted, and qPCR performed to assess STAT6 mRNA levels (c) STAT6 protein levels were also analysed using immunoblotting following lytic reactivation (blot representative of 2 replicates) (d) Densitometry using ImageJ was performed on blots shown in b. GAPDH was used as a normalisation control. Error= ±SD (n=2).

First, qPCR was used to measure STAT6 gene expression **(Figure 5.10b)** with immunoblotting then being used to assess STAT6 protein levels at 0, 8, 16 and 24 hrs post reactivation **(Figure 10.9c)**. Densitometry was subsequently performed using ImageJ **(Figure 5.10d)**. While little difference was seen at the level of STAT6 gene expression, STAT6 protein levels appear to be downregulated following KSHV lytic reactivation. A reduction of ~50-60% was observed at 8, 16 and 24 hrs post reactivation. This is consistent with previous research where RTA was found to mediate the proteosomal degradation of STAT6 (Gu et al., 2018).

To confirm a direct involvement of RTA in the proteosomal downregulation of STAT6 protein expression, 293T cells were transfected with increasing concentrations of GFP or GFP-ORF50 expressing constructs (**Figure 5.11)**.

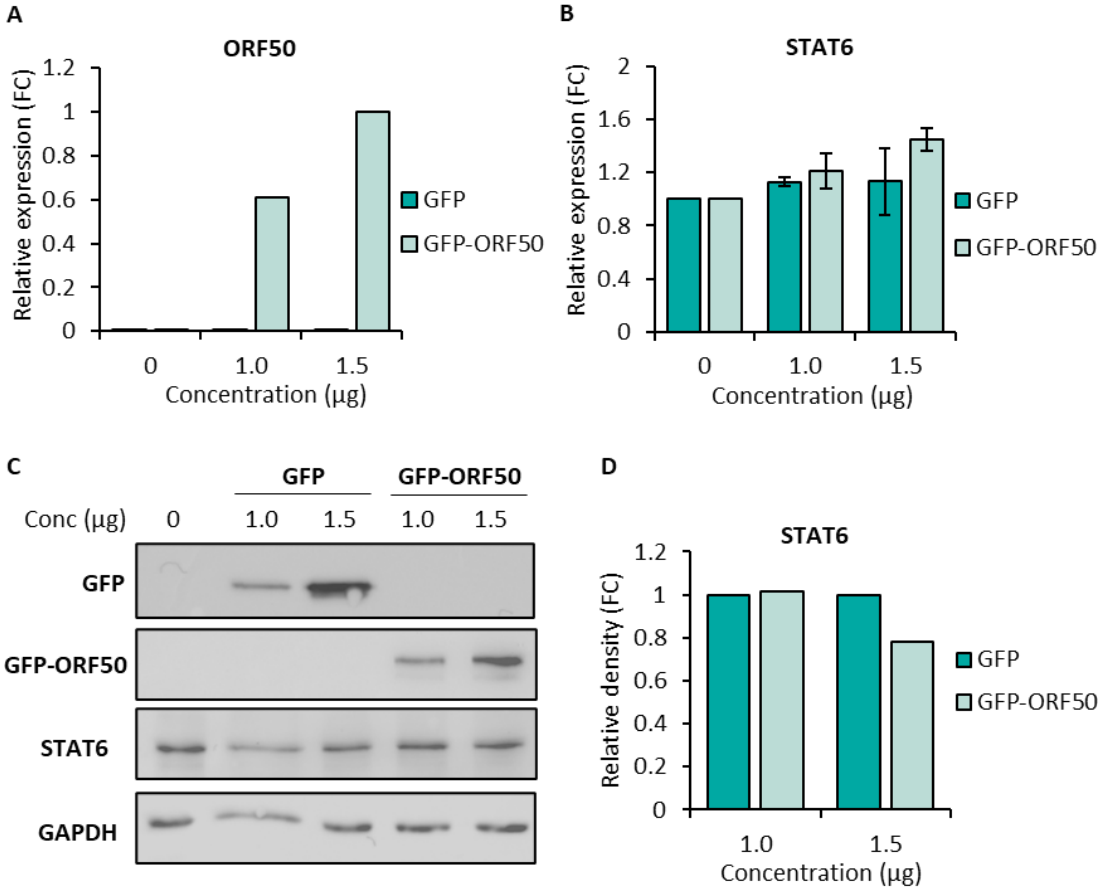

Figure 5.11 ORF50 and STAT6 expression. 293T cells were transfected with increasing concentrations of GFP or GFP-ORF50. Following total RNA extraction, qPCR was used to assess the expression of (a) ORF50 and (b) STAT6 (n=2) (c) immunoblotting was used to assess the protein expression of GFP and STAT6 d) Densitometry was performed on blots in (c) using ImageJ (n=1). GAPDH was used as a normalisation control. Error bars= ±SD.

The expression of ORF50 following transfection of a GFP-ORF50 expression construct was first confirmed using qPCR **(Figure 5.11a)**. Next STAT6 mRNA and protein expression was analysed using qPCR and immunoblotting respectively **(Figure 5.11b and c)** and ImageJ used to perform densitometry **(Figure 5.11d)**. No significant difference was observed on STAT6 gene expression following GFP-ORF50 transfection. Somewhat surprisingly, only a small reduction in STAT6 protein expression observed upon GFP-ORF50 transfection compared to control GFP transfected cells according to densitometry. No difference was seen at the lower concentration assessed.

Nevertheless, pri-miR-42-3p expression was assessed following ectopic GFP-ORF50 expression **(Figure 5.12a)**. Furthermore, the expression of GPRC5A, a direct cellular target of miR-142-3p as confirmed in section 4.7 was also assessed **(Figure 5.12b)**.

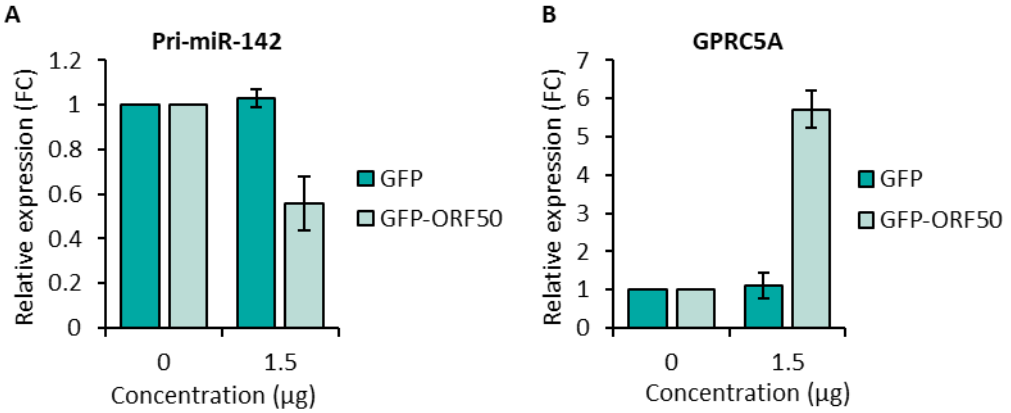

Figure 5.12 ORF50 downregulates the expression of pri-miR-142. GFP and GFP-ORF50 transfected 293T cells were collected 24 hrs post transfection and total RNA extracted. (a) pri-miR-142 and (b) GPRC5A expression levels were subsequently assessed using qPCR, with GAPDH being used as a normalisation control. Error bars= ±SD (n=2).

Results showed that pri-miR-142 expression was reduced following the transfection of GFP-ORF50 compared to GFP control transfected cells, with a decrease of ~40% being observed following transfection with 1.5 µg GFP-ORF50. Alternatively, the expression of GPRC5A was significantly upregulated, with an ~6-fold increase seen subsequent to transfection with the same concentration of GFP-ORF50. This suggest that ORF50 contributes to the reduction in pri-miR-142 levels seen following KSHV lytic reactivation.

ORF50/ RTA inherently possesses ubiquitin E3 ligase activity and has previously been implicated in the proteosomal degradation of STAT6, a positive regulator of miR-142

expression (Gu et al., 2018). While further analysis is required to test the significance of STAT6 downregulation following ORF50 expression, efforts were made to determine if the E3 ligase activity of ORF50 contributed to miR-142 downregulation. To this end, 293T cells were transfected with WT-ORF50 and the E3 ubiquitin ligase-defective mutant, ORF50-C131S. ORF50-C131S contains a cysteine (C) to serine (S) mutation at the 131 site, which is indicated in figure 5.13a. Following the confirmation of ORF50 expression for both WT-ORF50 and ORF50-C131S transfected cells **(Figure 5.13b)**, the expression of pri-miR-142 was assessed **(Figure 5.13c)**.

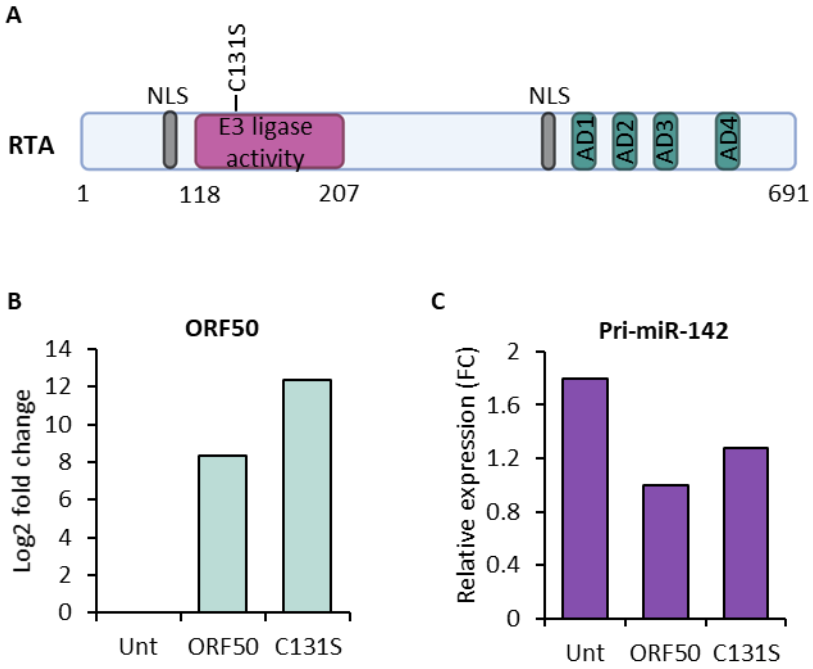

Figure 5.13 Expression of the E3 defective mutant, ORF50-C131S appears to alleviate pri-miR-142 downregulation. (a) schematic of RTA amino acid sequence with C131S mutation within the E3 ligase region indicated. NLS= nuclear localisation signal, AD= activation domain. (b) 293T cells were transfected with 1.5 µg of WT-ORF50 or ORF50-C131S, a E3 ligase defective mutant. Total RNA was subsequently extracted, and qPCR used to assess the expression ORF50. (c) pri-miR-142 levels expression was also assessed. GAPDH was used a normalisation control (n=1).

Interestingly, transfection with ORF50-C131S appeared to somewhat recover pri-miR-142 expression. Indeed, an increase of ~30% was seen following transfection of ORF50-C131S compared to that of WT-ORF50. While this may suggest that the E3 ligase activity of ORF50/RTA potentially contributes to a reduction in pri-miR-142 expression further experimental validation to confirm this result remains necessary.

5.6 Discussion

Research over the last decade has led to significant progress in our understanding of the molecular function of miRNAs, our knowledge concerning their regulation however remains limited. This is largely owed to difficulties in identifying miRNA TSS via conventional means. Indeed, the transient nature of pri-miRNA hinders the accurate identification of miRNA genes using traditional sequencing methods (Krol et al., 2010). Furthermore, inferring the location of miRNA TSS from the genomic location of mature miRNA is difficult as unlike protein coding TSS those of miRNA can be located several kb upstream (Bhattacharyya et al., 2012).

Innovative methods to identify and subsequently annotate miRNA promoters have therefore become increasingly necessary. Encouragingly, recent advancements in HT sequencing technologies have led to the development of several integrated computational predictive models (Wang et al., 2021). Indeed, chromatin immunoprecipitation (ChIP) sequencing led to the discovery of a number of chromatin modifications markers for gene transcription such as H3K27ac and H3K36me3 which are enriched at regions of active transcription and transcriptional elongation respectively (Ozsolak et al., 2008). Since multiple computational models have been developed to predict and characterise regulatory regions of pri-miRNA TSS using these markers (Barski et al., 2009) (Wang et al., 2021). Furthermore, increasingly sophisticated methods have been developed for the quantification of nascent RNA, allowing the definition of TSS at higher resolution. For example, modified global run-on sequencing (GRO-seq) and precision run-on sequencing (PRO-seq) now allow single nucleotide resolution, greatly enhancing the identification of miRNA TSS (Bouvy-Liivrand et al., 2017) (Liu et al., 2017).

Moreover, an increasing number of studies are adopting a highly integrated approach, exploiting large datasets such as those made available by the ENCODE project (Wang et al., 2021) (Turunen et al., 2021). The ENCODE consortium aims to identify functional elements in human genome providing an expansive resource for the entire scientific community. Thus ENCODE datasets prove an invalubale resource aiding the functional characterisation of pri-miRNA TSS across numerous human cell types (Turunen et al., 2021).

Investigating the regulation of miRNA expression not only allowing the identification of regulators including TF and epigenetic factors but also greatly increasing our understanding of of mechanisms underlying the regulation of miRNA expression during development and disease.

Here, TransmiR v2.0, an integrative database combining literature curated TF-miRNA hits with experimental high-throughput sequencing data (freely available at http://www.cuilab.cn/transmir) was utilised in order to identify potential regulators of miR-142 expression (Tong et al., 2019). Given the cell specificity of miRNA expression, thorough validation of potential regulators is necessary. The expression of several miR-142 regulators were thus examined following KSHV lytic reactivation including STAT6. Interestingly, STAT6 which has previously been implicated in the postive regulation of miR-142 expression, was found to be downregulated (Su et al., 2015).

This is consistent with reports that RTA facilitates the proteosomal degradation of STAT6 (Gu et al., 2018). While STAT6 protein expression appeared to be downregulated following the ectopic expression of ORF50, the significance of this downregulation remains to be determined. Nevertheless, the expression of ORF50 led to a reduction in the expression of pri-miR-142, suggesting ORF50 is in fact involved in the regulation of miR-142 following KSHV lytic reactivation. Furthermore, preliminary data suggests that the expression of an E3 defective ligase mutant somewhat alleviates the downregulation of pri-miR-142 expresson. Though thorough experimental confirmation is required, this suggests the E3 ligase activity of ORF50/RTA may be important in the regulation of pri-miR-142 regulation. Additionally, ORF50-C131S expression did not fully recover the expression of pri-miR-142 however this could be due to a redundancy within the E3 ligase domain (Gu et al., 2018).

Methylation of the miR-142 promoter has also emerged as a common mechanism regulating its expression (Morales et al., 2017). Indeed, many CpG islands have been located upstream of the prediction miR-142 TSS (Skårn et al., 2013). It was predicted that an increase in methylation of CpG nts within the promoter of miR-142 may repress its expression. Attempts were therefore made to examined the methylation status of the miR-142 promoter during KSHV lytic replication using methylation specific PCR (MSP). Unfortunately, initial efforts were unsuccessful and optimisation to address low DNA recovery rates following bisulphite conversion and primer design issues are needed.

In the absence of current MSP optimisation alternative methods including digestion-based assays could also be employed to address this (Kurdyukov and Bullock, 2016). While, most DNA methylation interrogation techniques begin with an initial bisulphite conversion step, methods utilising the selective digestion of particular endonucleases are also available. For example, HpaI digestion is inhibited by DNA methylation while the digestion activity of MspI remains unaffected (Cedar et al., 1979)

Nevertheless, the expression of factors previously found to promote the methylation of miR-142 were investigated, including DNMT1. Interestingly, IL-6 which is significantly upregulated following lytic reactivation has previously been found to induce both the expression and nuclear localisation of DNMT1 (Chiou et al., 2013). The protein expression of DNMT1 however did not appear to be significantly affected following reactivation of TREx BCBL-1 Rta cells. Still, further research is needed not only to assess the nuclear recruitment of DNMT1 but also the involvement of other potential epigenetic regulators in the methylation of the miR-142 promoter.

Post-transcriptional mechanisms have also been implicated in the regulation of miRNA. Notably, ADAR enzymes have previously been reported to edit pri-miR-142, ultimately inhibiting its nuclear processing by Drosha and promoting its degradation by SND1 (Yang et al., 2006). Intriguingly, ADAR1 and SND1 expression appeared to be upregulated at 8 hrs post reactivatavation. Futhermore, preliminary results showed that miR-142-3p expression was increased following treatment with 8-Aza, a selective ADAR inhibitor (Ramírez-Moya et al., 2020). Suggesting ADAR editing of pri-miR-142 may be involved in the regulation of miR-142-3p.

Traditionally, comparative sequencing has been used to identify candidate sites for A:I editing whereby I to G replacement occurs at corresponding sites in cDNA following RT-PCR (Wang et al., 2013). Comparative sequencing however is unable to discriminate between A:I editing sites and G residues arising from sequencing errors, thus more sophisticated methods including inosine chemical erasing (ICE) sequencing have since been developled (Sakurai et al., 2010). ICE-Seq utilises inosine cyanoethylation and RT-PCR in order to directly and accurately identify inosine residues in RNA strands. ICE-seq could therefore be used not only to assess A:I editing of pri-miR-142 following KSHV lytic reactivation but identify transcriptome-wide A:I editing sites (Okada et al., 2019) (Suzuki et al., 2015).

This research ultimately highlights the complexity surrounding the regulation of miRNA expression. Indeed, a multitude of intricate factors could collectively influence the expression of miR-142-3p following lytic reactivation, thus significant investigation remains necessary.

Chapter 6

~

Final Discussion and Future Perspectives

6. Discussion and future perspectives

The post-transcriptional regulation of mRNA is fundamental in controlling gene expression, as such mRNA abundance is subject to various regulatory mechanisms at all stages of mRNA maturation (Boo and Kim, 2020). Given the influence these mechanisms have on shaping the cellular transcriptome it is unsurprising that viruses that developed numerous methods in order to manipulate mRNA expression in order to create an environment conducive for viral replication (Glaunsinger and Ganem, 2004) (Gong et al., 2016)

Indeed, miRNAs have emerged as a common mechanism utilised by viruses to manipulate the transcriptomic landscape of cells, with many viruses not only expressing their own virally-encoded miRNAs but also developing ways to manipulate the expression of host cell miRNAs (Bruscella et al., 2017). Cellular miRNAs are able to exert both proviral and antiviral effects depending on the virus, with many viruses developing methods to upregulate and downregulate these miRNA respectively. For example, following the infection of lymphocytes, EBV upregulates miR-155 expression in order to supress innate immune responses and promote persistent infection, while other herpesviruses such HVS and HCMV employ TDMD to facilitate the degradation of antiviral miRNAs (Lu et al., 2008) (Cazalla et al., 2010) (S. Lee et al., 2013). In this research, the oncogenic gammaherpesvirus, KSHV was shown to dysregulate several cellular miRNAs, notably miR-142-3p and miR-25-5p, which were found to be significantly downregulated following KSHV lytic reactivation. Interestingly, these miRNA appear to exert an antiviral effect, with the overexpression of both miRNA having a significant impact of KSHV lytic infection and infectious virion production.

As the manipulation of host cell miRNAs continues to emerge as a widespread strategy employed by numerous viruses, targeting these interactions represents an interesting antiviral approach. Indeed, reversing miRNA dysregulation during disease through the use of antisense oligonucleotide (ASO) inhibitors and miRNA mimics has become the subject of intense research and is being explored to treat a number of human diseases. While miRNA-based therapies are yet to be approved in clinical medicine, they are the focus numerous clinical trials (Chakraborty et al., 2021).

Indeed, RNA therapies have long appeared hindered by a number of clinical challenges including targeted delivery and long-term expression and activity. As such a number of chemical modifications as well as delivery methods are now under assessment to improve both the efficacy and specificity of RNA therapeutics for future applications (reviewed in Diener et al., 2022). Excitingly, the recent FDA approval of multiple RNAi based therapies such as Patisiran and Givosiran for the treatment of hereditary transthyretin amyloidosis and acute hepatic porphyria respectively has also added promise for the development of miRNA-based therapies (Adams et al., 2018) (Balwani et al., 2020). Examples of miRNA therapies currently undergoing clinical trials are detailed below in table 6.1.

Table 6.1 miRNA therapies currently undergoing clinical trials

miRNA drug name	Target miRNA	Disease	Phase	References
Miravirsen/SPC3649	LNA-anti-miR-122	Chronic HCV	II	Van der Ree, 2014
Cobomarsen/MRG-106	LNA-anti-miR-155	Lymphoma Leukaemia	I/II	Seto, 2018
Remlarsen/MRG-201	LNA-miR-29 mimic	Keloid fibrosis	II	Gallent-Behm, 2019
MRG-110	LNA- anti-miR-92	Ischemic conditions	I	Abplanalp, 2020
MesomiR 1	LNA-miR-16 mimic	Renal cell carcinoma	I	Van Zandwijk, 2017
Lademirsen/RG-012	LNA-antimiR-21	Alport syndrome	I	Gomez, 2015
Obefazimad/ABX464	Increases miR-124	HIV	II/III	Moron-Lopez, 2021

Notably, Miravirsen (SPC3649), an antisense miR-122 inhibitor is currently being investigated as a treatment for chronic hepatitis C virus infection and has recently completed various phase I/II clinical trials (van der Ree et al., 2014) (van der Ree et al., 2016). The 5’ UTR of HCV genome contains two conserved miR-122 binding sites, with direct miR-122 binding not only conferring resistance against host nuclease degradation but also the promotion of HCV genome translation and replication (Machlin et al., 2011) (Schult et al., 2018) (Masaki et al., 2015). Additionally, Obefazimad/ABX464 an upregulator of miR-124 has recently emerged as a novel antiviral drug candidate with recent reports suggesting ABX464 is able to inhibit HIV-1 RNA biogenesis as well as total HIV reservoirs (Moron-Lopez et al., 2021).

Reversing miR-142-3p dysregulation following KSHV lytic replication could therefore provide a novel antiviral approach the infection. Furthermore, miR-142-3p is widely considered a tumour suppressor miRNA, and is often found to be downregulated in various cancers including breast, colorectal and non-small cell lung cancer (Mansoori et al., 2019) (Xu et al., 2020) (Liu et al., 2020) (Wang et al., 2017). Targeting miR-142-3p may therefore not only provide a useful strategy against KSHV and its related malignancies but also the tumorigenesis and progression of other cancers.

Chapter 4 also identified GPRC5A as a direct target of miR-142-3p while also implicating GPRC5A in the regulation of actin regulators, such as Rho GTPases. The apparent importance of these factors during KSHV replication identifies them as promising candidates for therapeutic intervention. Moreover, the importance of the actin cytoskeleton in viral infection is well-documented, thus targeting these factors could potentially represent a widespread antiviral strategy (Taylor, Koyuncu and Enquist, 2011). Encouragingly, targeting GPCRs is a well-established therapeutic method with ~34% of all FDA approved drugs directed against GPCRs (Hauser et al., 2018). Furthermore, inhibitors targeting Rho GTPase signalling networks primarily through the inhibition of RhoA signalling effectors, such as Rho-associated protein kinases (ROCKs), have emerged as a promising therapeutic approach. Indeed, two RhoA inhibitors have been FDA approved while many more are undergoing clinical trials and development for a variety of diseases including cancer (Lu et al., 2017) (Clayton and Ridley, 2020)

In chapter 5, the regulatory mechanisms effecting miR-142 expression were explored. Interestingly pri-miR-142 levels were found to be significantly reduced following KSHV lytic reactivation, thus alterations in transcription as well as processing were investigated. Notably, pri-miR-142 has previously been reported to undergo ADAR editing, which ultimately leads to its degradation by the nuclease SND1 (Yang et al., 2006). Intriguingly, preliminary data in this research suggests treatment with a selective ADAR inhibitor increases in miR-142-3p expression. While, editing of pri-miR-142 as well as its functional implications require further study (as discussed in section 5.6), this suggests that ADAR editing of pri-miR-142 following KSHV lytic reactivation may contribute to the downregulation of miR-142-3p.

Interestingly, ADAR1 has previously been identified as an important proviral factor during virus infection. Indeed, ADAR1 has been found to have a critical role innate

immune suppression, as well as promoting the replication of several viruses (Pfaller et al., 2018). For example, ADAR1 editing favours Zika replication through the suppression of PKR activation inhibiting IFN immune responses to infection (Zhou et al., 2019). Additionally, ADAR editing has also been reported to facilitate KSHV lytic reactivation through the dampening of RLR dependent signalling (Zhang et al., 2020). Modulation of innate immune via ADAR editing may therefore represent a strategy utilised by a number of viruses to aid viral replication. Moreover, aberrant ADAR editing has also been shown to promote tumorigenesis and cancer progression, which may have important implications regarding the pathogenicity of the tumour virus, KSHV (Zhang et al., 2019) (Shen et al., 2022). Previous work in the Whitehouse laboratory, also identified SND1 as a novel m6A reader, essential for KSHV lytic replication (Baquero-Perez et al., 2019). Thus, SND1 may play multiple roles during KSHV lytic infection.

In conclusion the present study identified a number of important interactions during KSHV lytic infection, while also highlighting the complexity regarding both miRNA target identification and regulatory mechanisms involved in miRNA expression. Exploiting cellular miRNAs allows viruses to harness vast regulatory potential. The characterisation of these interactions not only broadens our understanding of virus-host cellular interactions during KSHV lytic replication but also general cellular mechanisms. Further studies may therefore present these as valuable targets against KSHV-associated malignancies as well as other herpesvirus infections

References

Adams, D., Gonzalez-Duarte, A., O'Riordan, W.D., Yang, C.-C., Ueda, M., Kristen, A. V., Tournev, I., Schmidt, H.H., Coelho, T., Berk, J.L., Lin, K.-P., Vita, G., Attarian, S., Planté-Bordeneuve, V., Mezei, M.M., Campistol, J.M., Buades, J., Brannagan, T.H., Kim, B.J., Oh, J., Parman, Y., Sekijima, Y., Hawkins, P.N., Solomon, S.D., Polydefkis, M., Dyck, P.J., Gandhi, P.J., Goyal, S., Chen, J., Strahs, A.L., Nochur, S. V., Sweetser, M.T., Garg, P.P., Vaishnaw, A.K., Gollob, J.A. and Suhr, O.B. 2018. Patisiran, an RNAi Therapeutic, for Hereditary Transthyretin Amyloidosis. *The New England journal of medicine*. **379**(1), pp.11–21.

Aguado, L.C. and TenOever, B. 2018. RNA virus building blocks-miRNAs not included. *PLoS pathogens*. **14**(5), p.e1006963.

Akhbari, P., Tobin, D., Poterlowicz, K., Roberts, W. and Boyne, J.R. 2018. MCV-miR-M1 Targets the Host-Cell Immune Response Resulting in the Attenuation of Neutrophil Chemotaxis. *The Journal of investigative dermatology*. **138**(11), pp.2343–2354.

Akula, S.M., Pramod, N.P., Wang, F.Z. and Chandran, B. 2002. Integrin alpha3beta1 (CD 49c/29) is a cellular receptor for Kaposi's sarcoma-associated herpesvirus (KSHV/HHV-8) entry into the target cells. *Cell*. **108**(3), pp.407–19.

Akula, S.M., Wang, F.Z., Vieira, J. and Chandran, B. 2001. Human herpesvirus 8 interaction with target cells involves heparan sulfate. *Virology*. **282**(2), pp.245–55.

Alarcón, C.R., Lee, H., Goodarzi, H., Halberg, N. and Tavazoie, S.F. 2015. N6-methyladenosine marks primary microRNAs for processing. *Nature*. **519**(7544), pp.482–5.

Albrecht, J.C. and Fleckenstein, B. 1990. Structural organization of the conserved gene block of Herpesvirus saimiri coding for DNA polymerase, glycoprotein B, and major DNA binding protein. *Virology*. **174**(2), pp.533–42.

Amador-Cañizares, Y., Panigrahi, M., Huys, A., Kunden, R.D., Adams, H.M., Schinold, M.J. and Wilson, J.A. 2018. miR-122, small RNA annealing and sequence mutations alter the predicted structure of the Hepatitis C virus 5' UTR RNA to stabilize and promote viral RNA accumulation. *Nucleic acids research*. **46**(18), pp.9776–9792.

Ameres, S.L., Horwich, M.D., Hung, J.-H., Xu, J., Ghildiyal, M., Weng, Z. and Zamore, P.D. 2010. Target RNA-directed trimming and tailing of small silencing RNAs. *Science (New York, N.Y.)*. **328**(5985), pp.1534–9.

Anders, S., Pyl, P.T. and Huber, W. 2015. HTSeq--a Python framework to work with high-throughput sequencing data. *Bioinformatics (Oxford, England)*. **31**(2), pp.166–9.

Arias, C., Weisburd, B., Stern-Ginossar, N., Mercier, A., Madrid, A.S., Bellare, P., Holdorf, M., Weissman, J.S. and Ganem, D. 2014. KSHV 2.0: a comprehensive annotation of the Kaposi's sarcoma-associated herpesvirus genome using next-generation

sequencing reveals novel genomic and functional features. *PLoS pathogens*. **10**(1), p.e1003847.

Arii, J. 2021. Host and Viral Factors Involved in Nuclear Egress of Herpes Simplex Virus 1. *Viruses*. **13**(5).

Ascoli, V., Scalzo, C.C., Danese, C., Vacca, K., Pistilli, A. and Lo Coco, F. 1999. Human herpes virus-8 associated primary effusion lymphoma of the pleural cavity in HIV-negative elderly men. *The European respiratory journal*. **14**(5), pp.1231–4.

AuCoin, D.P., Colletti, K.S., Xu, Y., Cei, S.A. and Pari, G.S. 2002. Kaposi's sarcoma-associated herpesvirus (human herpesvirus 8) contains two functional lytic origins of DNA replication. *Journal of virology*. **76**(15), pp.7890–6.

Auyeung, V.C., Ulitsky, I., McGeary, S.E. and Bartel, D.P. 2013. Beyond secondary structure: primary-sequence determinants license pri-miRNA hairpins for processing. *Cell*. **152**(4), pp.844–58.

Axtell, M.J., Westholm, J.O. and Lai, E.C. 2011. Vive la différence: biogenesis and evolution of microRNAs in plants and animals. *Genome biology*. **12**(4), p.221.

Backes, S., Shapiro, J.S., Sabin, L.R., Pham, A.M., Reyes, I., Moss, B., Cherry, S. and TenOever, B.R. 2012. Degradation of host microRNAs by poxvirus poly(A) polymerase reveals terminal RNA methylation as a protective antiviral mechanism. *Cell host & microbe*. **12**(2), pp.200–10.

Ballestas, M.E., Chatis, P.A. and Kaye, K.M. 1999. Efficient persistence of extrachromosomal KSHV DNA mediated by latency-associated nuclear antigen. *Science (New York, N.Y.)*. **284**(5414), pp.641–4.

Balwani, M., Sardh, E., Ventura, P., Peiró, P.A., Rees, D.C., Stölzel, U., Bissell, D.M., Bonkovsky, H.L., Windyga, J., Anderson, K.E., Parker, C., Silver, S.M., Keel, S.B., Wang, J.-D., Stein, P.E., Harper, P., Vassiliou, D., Wang, B., Phillips, J., Ivanova, A., Langendonk, J.G., Kauppinen, R., Minder, E., Horie, Y., Penz, C., Chen, J., Liu, S., Ko, J.J., Sweetser, M.T., Garg, P., Vaishnaw, A., Kim, J.B., Simon, A.R., Gouya, L. and ENVISION Investigators 2020. Phase 3 Trial of RNAi Therapeutic Givosiran for Acute Intermittent Porphyria. *The New England journal of medicine*. **382**(24), pp.2289–2301.

Bandyopadhyay, C., Valiya-Veettil, M., Dutta, D., Chakraborty, S. and Chandran, B. 2014. CIB1 synergizes with EphrinA2 to regulate Kaposi's sarcoma-associated herpesvirus macropinocytic entry in human microvascular dermal endothelial cells. *PLoS pathogens*. **10**(2), p.e1003941.

Baquero-Perez, B., Antanaviciute, A., Yonchev, I.D., Carr, I.M., Wilson, S.A. and Whitehouse, A. 2019. The Tudor SND1 protein is an m6A RNA reader essential for replication of Kaposi's sarcoma-associated herpesvirus. *eLife*. **8**.

Barski, A., Jothi, R., Cuddapah, S., Cui, K., Roh, T.Y., Schones, D.E. and Zhao, K. 2009. Chromatin poises miRNA- and protein-coding genes for expression. *Genome Research*. **19**(10), p.1742.

Bartel, D.P. 2018. Metazoan MicroRNAs. *Cell*. **173**(1), pp.20–51.

Bartel, D.P. 2004. MicroRNAs: genomics, biogenesis, mechanism, and function. *Cell*. **116**(2), pp.281–97.

Behm-Ansmant, I., Rehwinkel, J., Doerks, T., Stark, A., Bork, P. and Izaurralde, E. 2006. mRNA degradation by miRNAs and GW182 requires both CCR4:NOT deadenylase and DCP1:DCP2 decapping complexes. *Genes & development*. **20**(14), pp.1885–98.

Bellare, P. and Ganem, D. 2009. Regulation of KSHV lytic switch protein expression by a virus-encoded microRNA: an evolutionary adaptation that fine-tunes lytic reactivation. *Cell host & microbe*. **6**(6), pp.570–5.

Bernier, A. and Sagan, S.M. 2018. The Diverse Roles of microRNAs at the Host–Virus Interface. *Viruses*. **10**(8).

Bhattacharyya, M., Feuerbach, L., Bhadra, T., Lengauer, T. and Bandyopadhyay, S. 2012. MicroRNA transcription start site prediction with multi-objective feature selection. *Statistical applications in genetics and molecular biology*. **11**(1), Article 6.

Biggs, P.M. 2001. The history and biology of Marek's disease virus. *Current topics in microbiology and immunology*. **255**, pp.1–24.

Birkmann, A., Mahr, K., Ensser, A., Yağuboğlu, S., Titgemeyer, F., Fleckenstein, B. and Neipel, F. 2001. Cell surface heparan sulfate is a receptor for human herpesvirus 8 and interacts with envelope glycoprotein K8.1. *Journal of virology*. **75**(23), pp.11583–93.

Blaszczyk, J., Tropea, J.E., Bubunenko, M., Routzahn, K.M., Waugh, D.S., Court, D.L. and Ji, X. 2001. Crystallographic and modeling studies of RNase III suggest a mechanism for double-stranded RNA cleavage. *Structure (London, England : 1993)*. **9**(12), pp.1225–36.

Bodin, S., Planchon, D., Rios Morris, E., Comunale, F. and Gauthier-Rouvière, C. 2014. Flotillins in intercellular adhesion - from cellular physiology to human diseases. *Journal of cell science*. **127**(Pt 24), pp.5139–47.

Bohnsack, M.T., Czaplinski, K. and Gorlich, D. 2004. Exportin 5 is a RanGTP-dependent dsRNA-binding protein that mediates nuclear export of pre-miRNAs. *RNA (New York, N.Y.)*. **10**(2), pp.185–91.

Boland, A., Huntzinger, E., Schmidt, S., Izaurralde, E. and Weichenrieder, O. 2011. Crystal structure of the MID-PIWI lobe of a eukaryotic Argonaute protein. *Proceedings of the National Academy of Sciences of the United States of America*. **108**(26), pp.10466–71.

Bolger, A.M., Lohse, M. and Usadel, B. 2014. Trimmomatic: a flexible trimmer for Illumina sequence data. *Bioinformatics (Oxford, England)*. **30**(15), pp.2114–20.

Bonneau, E., Neveu, B., Kostantin, E., Tsongalis, G.J. and De Guire, V. 2019. How close are miRNAs from clinical practice? A perspective on the diagnostic and therapeutic market. *EJIFCC*. **30**(2), pp.114–127.

Boo, S.H. and Kim, Y.K. 2020. The emerging role of RNA modifications in the regulation of mRNA stability. *Experimental & molecular medicine*. **52**(3), pp.400–408.

Borchert, G.M., Lanier, W. and Davidson, B.L. 2006. RNA polymerase III transcribes human microRNAs. *Nature structural & molecular biology*. **13**(12), pp.1097–101.

Borza, C.M. and Hutt-Fletcher, L.M. 2002. Alternate replication in B cells and epithelial cells switches tropism of Epstein-Barr virus. *Nature medicine*. **8**(6), pp.594–9.

Boshoff, C., Schulz, T.F., Kennedy, M.M., Graham, A.K., Fisher, C., Thomas, A., McGee, J.O., Weiss, R.A. and O'Leary, J.J. 1995. Kaposi's sarcoma-associated herpesvirus infects endothelial and spindle cells. *Nature medicine*. **1**(12), pp.1274–8.

Bouvy-Liivrand, M., Hernández de Sande, A., Pölönen, P., Mehtonen, J., Vuorenmaa, T., Niskanen, H., Sinkkonen, L., Kaikkonen, M.U. and Heinäniemi, M. 2017. Analysis of primary microRNA loci from nascent transcriptomes reveals regulatory domains governed by chromatin architecture. *Nucleic acids research*. **45**(17), pp.9837–9849.

Boyne, J.R., Jackson, B.R., Taylor, A., Macnab, S.A. and Whitehouse, A. 2010. Kaposi's sarcoma-associated herpesvirus ORF57 protein interacts with PYM to enhance translation of viral intronless mRNAs. *The EMBO journal*. **29**(11), pp.1851–64.

Braun, J.E., Truffault, V., Boland, A., Huntzinger, E., Chang, C.-T., Haas, G., Weichenrieder, O., Coles, M. and Izaurralde, E. 2012. A direct interaction between DCP1 and XRN1 couples mRNA decapping to 5' exonucleolytic degradation. *Nature structural & molecular biology*. **19**(12), pp.1324–31.

Bridge, G., Monteiro, R., Henderson, S., Emuss, V., Lagos, D., Georgopoulou, D., Patient, R. and Boshoff, C. 2012. The microRNA-30 family targets DLL4 to modulate endothelial cell behavior during angiogenesis. *Blood*. **120**(25), pp.5063–72.

Broekema, N.M. and Imperiale, M.J. 2013. miRNA regulation of BK polyomavirus replication during early infection. *Proceedings of the National Academy of Sciences of the United States of America*. **110**(20), pp.8200–5.

Brooks, L., Yao, Q.Y., Rickinson, A.B. and Young, L.S. 1992. Epstein-Barr virus latent gene transcription in nasopharyngeal carcinoma cells: coexpression of EBNA1, LMP1, and LMP2 transcripts. *Journal of virology*. **66**(5), pp.2689–97.

Bruscella, P., Bottini, S., Baudesson, C., Pawlotsky, J.-M., Feray, C. and Trabucchi, M. 2017. Viruses and miRNAs: More Friends than Foes. *Frontiers in microbiology*. **8**(MAY), p.824.

Buckland, J. 2010. Biomarkers: microRNAs under the spotlight in inflammatory arthritis. *Nature reviews. Rheumatology*. **6**(8), p.436.

Bulanova, D.R., Akimov, Y.A., Rokka, A., Laajala, T.D., Aittokallio, T., Kouvonen, P., Pellinen, T. and Kuznetsov, S.G. 2017. Orphan G protein-coupled receptor GPRC5A modulates integrin β1-mediated epithelial cell adhesion. *Cell adhesion & migration*. **11**(5–6), pp.434–446.

Buonaguro, F.M., Tornesello, M.L., Buonaguro, L., Satriano, R.A., Ruocco, E., Castello, G. and Ruocco, V. 2003. Kaposi's sarcoma: aetiopathogenesis, histology and clinical features. *Journal of the European Academy of Dermatology and Venereology : JEADV*. **17**(2), pp.138–54.

Burysek, L., Yeow, W.S. and Pitha, P.M. 1999. Unique properties of a second human herpesvirus 8-encoded interferon regulatory factor (vIRF-2). *Journal of human virology*. **2**(1), pp.19–32.

Cai, X., Hagedorn, C.H. and Cullen, B.R. 2004. Human microRNAs are processed from capped, polyadenylated transcripts that can also function as mRNAs. *RNA (New York, N.Y.)*. **10**(12), pp.1957–66.

Cai, X., Lu, S., Zhang, Z., Gonzalez, C.M., Damania, B. and Cullen, B.R. 2005. Kaposi's sarcoma-associated herpesvirus expresses an array of viral microRNAs in latently infected cells. *Proceedings of the National Academy of Sciences of the United States of America*. **102**(15), pp.5570–5.

Cai, X., Schäfer, A., Lu, S., Bilello, J.P., Desrosiers, R.C., Edwards, R., Raab-Traub, N. and Cullen, B.R. 2006. Epstein-Barr virus microRNAs are evolutionarily conserved and differentially expressed. *PLoS pathogens*. **2**(3), p.e23.

Calin, G.A., Cimmino, A., Fabbri, M., Ferracin, M., Wojcik, S.E., Shimizu, M., Taccioli, C., Zanesi, N., Garzon, R., Aqeilan, R.I., Alder, H., Volinia, S., Rassenti, L., Liu, X., Liu, C.-G., Kipps, T.J., Negrini, M. and Croce, C.M. 2008. MiR-15a and miR-16-1 cluster functions in human leukemia. *Proceedings of the National Academy of Sciences of the United States of America*. **105**(13), pp.5166–71.

Callan, M.F., Steven, N., Krausa, P., Wilson, J.D., Moss, P.A., Gillespie, G.M., Bell, J.I., Rickinson, A.B. and McMichael, A.J. 1996. Large clonal expansions of CD8+ T cells in acute infectious mononucleosis. *Nature medicine*. **2**(8), pp.906–11.

Cardone, G., Winkler, D.C., Trus, B.L., Cheng, N., Heuser, J.E., Newcomb, W.W., Brown, J.C. and Steven, A.C. 2007. Visualization of the herpes simplex virus portal in situ by cryo-electron tomography. *Virology*. **361**(2), pp.426–34.

Carthew, R.W. and Sontheimer, E.J. 2009. Origins and Mechanisms of miRNAs and siRNAs. *Cell*. **136**(4), pp.642–55.

Cazalla, D., Yario, T., Steitz, J.A. and Steitz, J. 2010. Down-regulation of a host microRNA

by a Herpesvirus saimiri noncoding RNA. *Science (New York, N.Y.)*. **328**(5985), pp.1563–6.

Cedar, H., Solage, A., Glaser, G. and Razin, A. 1979. Direct detection of methylated cytosine in DNA by use of the restriction enzyme MspI. *Nucleic acids research*. **6**(6), pp.2125–32.

Cesarman, E., Chang, Y., Moore, P.S., Said, J.W. and Knowles, D.M. 1995. Kaposi's sarcoma-associated herpesvirus-like DNA sequences in AIDS-related body-cavity-based lymphomas. *The New England journal of medicine*. **332**(18), pp.1186–91.

Chakraborty, C., Sharma, A.R., Sharma, G. and Lee, S.-S. 2021. Therapeutic advances of miRNAs: A preclinical and clinical update. *Journal of advanced research*. **28**, pp.127–138.

Chandriani, S., Xu, Y. and Ganem, D. 2010. The lytic transcriptome of Kaposi's sarcoma-associated herpesvirus reveals extensive transcription of noncoding regions, including regions antisense to important genes. *Journal of virology*. **84**(16), pp.7934–42.

Chang, P.-J., Shedd, D., Gradoville, L., Cho, M.-S., Chen, L.-W., Chang, J. and Miller, G. 2002. Open reading frame 50 protein of Kaposi's sarcoma-associated herpesvirus directly activates the viral PAN and K12 genes by binding to related response elements. *Journal of virology*. **76**(7), pp.3168–78.

Chang, Y., Cesarman, E., Pessin, M.S., Lee, F., Culpepper, J., Knowles, D.M. and Moore, P.S. 1994. Identification of herpesvirus-like DNA sequences in AIDS-associated Kaposi's sarcoma. *Science (New York, N.Y.)*. **266**(5192), pp.1865–9.

Chen, J.-S., Li, H.-C., Lin, S.-I., Yang, C.-H., Chien, W.-Y., Syu, C.-L. and Lo, S.-Y. 2015. Cleavage of Dicer protein by I7 protease during vaccinia virus infection. *PloS one*. **10**(3), p.e0120390.

Chi, S.W., Zang, J.B., Mele, A. and Darnell, R.B. 2009. Argonaute HITS-CLIP decodes microRNA-mRNA interaction maps. *Nature*. **460**(7254), pp.479–86.

Chiou, G.Y., Chien, C.S., Wang, M.L., Chen, M.T., Yang, Y.P., Yu, Y.L., Chien, Y., Chang, Y.C., Shen, C.C., Chio, C.C., Lu, K.H., Ma, H.I., Chen, K.H., Liu, D.M., Miller, S.A., Chen, Y.W., Huang, P.I., Shih, Y.H., Hung, M.C. and Chiou, S.H. 2013. Epigenetic regulation of the miR142-3p/interleukin-6 circuit in glioblastoma. *Molecular cell*. **52**(5), pp.693–706.

Chirayil, R., Kincaid, R.P., Dahlke, C., Kuny, C. V, Dälken, N., Spohn, M., Lawson, B., Grundhoff, A. and Sullivan, C.S. 2018. Identification of virus-encoded microRNAs in divergent Papillomaviruses. *PLoS pathogens*. **14**(7), p.e1007156.

Chousterman, S., Lacasa, M. and Sheldrick, P. 1979. Physical Map of the Channel Catfish Virus Genome: Location of Sites for Restriction Endonucleases EcoRI, HindIII, HpaI,

and XbaI. *Journal of virology*. **31**(1), pp.73–85.

Chu, C. and Rana, T.M. 2006. Translation repression in human cells by microRNA-induced gene silencing requires RCK/p54. *PLoS biology*. **4**(7), p.e210.

Chung, H., Calis, J.J.A., Hoffmann, H.-H., Rosenberg, B.R. and Correspondence, C.M.R. 2018. Human ADAR1 Prevents Endogenous RNA from Triggering Translational Shutdown.

Cimmino, A., Calin, G.A., Fabbri, M., Iorio, M. V, Ferracin, M., Shimizu, M., Wojcik, S.E., Aqeilan, R.I., Zupo, S., Dono, M., Rassenti, L., Alder, H., Volinia, S., Liu, C.-G., Kipps, T.J., Negrini, M. and Croce, C.M. 2005. miR-15 and miR-16 induce apoptosis by targeting BCL2. *Proceedings of the National Academy of Sciences of the United States of America*. **102**(39), pp.13944–9.

Clayton, N.S. and Ridley, A.J. 2020. Targeting Rho GTPase Signaling Networks in Cancer. *Frontiers in cell and developmental biology*. **8**, p.222.

Collins, C.M. and Medveczky, P.G. 2002. Genetic requirements for the episomal maintenance of oncogenic herpesvirus genomes. *Advances in cancer research*. **84**, pp.155–74.

Condrat, C.E., Thompson, D.C., Barbu, M.G., Bugnar, O.L., Boboc, A., Cretoiu, D., Suciu, N., Cretoiu, S.M. and Voinea, S.C. 2020. miRNAs as Biomarkers in Disease: Latest Findings Regarding Their Role in Diagnosis and Prognosis. *Cells*. **9**(2).

Cotter, M.A. and Robertson, E.S. 1999. The latency-associated nuclear antigen tethers the Kaposi's sarcoma-associated herpesvirus genome to host chromosomes in body cavity-based lymphoma cells. *Virology*. **264**(2), pp.254–64.

Croen, K.D. 1991. Latency of the human herpesviruses. *Annual review of medicine*. **42**, pp.61–7.

Crosbie, E.J., Einstein, M.H., Franceschi, S. and Kitchener, H.C. 2013. Human papillomavirus and cervical cancer. *Lancet (London, England)*. **382**(9895), pp.889–99.

Dalianis, T. and Hirsch, H.H. 2013. Human polyomaviruses in disease and cancer. *Virology*. **437**(2), pp.63–72.

Dalton-Griffin, L., Wilson, S.J. and Kellam, P. 2009. X-box binding protein 1 contributes to induction of the Kaposi's sarcoma-associated herpesvirus lytic cycle under hypoxic conditions. *Journal of virology*. **83**(14), pp.7202–9.

Damania, B. 2004. Oncogenic gamma-herpesviruses: comparison of viral proteins involved in tumorigenesis. *Nature reviews. Microbiology*. **2**(8), pp.656–68.

Dang, T.L., Le, C.T., Le, M.N., Nguyen, T.D., Nguyen, T.L., Bao, S., Li, S. and Nguyen, T.A. 2020. Select amino acids in DGCR8 are essential for the UGU-pri-miRNA interaction

and processing. *Communications biology*. **3**(1), p.344.

Davis, D.A., Rinderknecht, A.S., Zoeteweij, J.P., Aoki, Y., Read-Connole, E.L., Tosato, G., Blauvelt, A. and Yarchoan, R. 2001. Hypoxia induces lytic replication of Kaposi sarcoma-associated herpesvirus. *Blood*. **97**(10), pp.3244–50.

Davison, A.J. 2007. *Comparative analysis of the genomes* [Online]. Cambridge University Press. [Accessed 8 April 2020]. Available from: http://www.ncbi.nlm.nih.gov/pubmed/21348122.

Davison, A.J., Eberle, R., Ehlers, B., Hayward, G.S., McGeoch, D.J., Minson, A.C., Pellett, P.E., Roizman, B., Studdert, M.J. and Thiry, E. 2009. The order Herpesvirales. *Archives of virology*. **154**(1), pp.171–7.

Deng, H., Young, A. and Sun, R. 2000. Auto-activation of the rta gene of human herpesvirus-8/Kaposi's sarcoma-associated herpesvirus. *The Journal of general virology*. **81**(Pt 12), pp.3043–3048.

Diener, C., Keller, A. and Meese, E. 2022. Emerging concepts of miRNA therapeutics: from cells to clinic. *Trends in genetics : TIG*. **38**(6), pp.613–626.

Ding, S., Zhang, Q., Luo, S., Gao, L., Huang, J., Lu, J., Chen, J., Zeng, Q., Guo, A., Zeng, J. and Lu, Q. 2020. BCL-6 suppresses miR-142-3p/5p expression in SLE CD4+ T cells by modulating histone methylation and acetylation of the miR-142 promoter. *Cellular & molecular immunology*. **17**(5), pp.474–482.

Dittmer, D., Lagunoff, M., Renne, R., Staskus, K., Haase, A. and Ganem, D. 1998. A cluster of latently expressed genes in Kaposi's sarcoma-associated herpesvirus. *Journal of virology*. **72**(10), pp.8309–15.

Döhner, K., Wolfstein, A., Prank, U., Echeverri, C., Dujardin, D., Vallee, R. and Sodeik, B. 2002. Function of dynein and dynactin in herpes simplex virus capsid transport. *Molecular biology of the cell*. **13**(8), pp.2795–809.

Drexler, H.G., Uphoff, C.C., Gaidano, G. and Carbone, A. 1998. Lymphoma cell lines: in vitro models for the study of HHV-8+ primary effusion lymphomas (body cavity-based lymphomas). *Leukemia*. **12**(10), pp.1507–17.

Van Dross, R., Yao, S., Asad, S., Westlake, G., Mays, D.J., Barquero, L., Duell, S., Pietenpol, J.A. and Browning, P.J. 2005. Constitutively active K-cyclin/cdk6 kinase in Kaposi sarcoma-associated herpesvirus-infected cells. *Journal of the National Cancer Institute*. **97**(9), pp.656–66.

Dumas, A.M., Geelen, J.L., Weststrate, M.W., Wertheim, P. and van der Noordaa, J. 1981. XbaI, PstI, and BglII restriction enzyme maps of the two orientations of the varicella-zoster virus genome. *Journal of virology*. **39**(2), pp.390–400.

Duursma, A.M., Kedde, M., Schrier, M., le Sage, C. and Agami, R. 2008. miR-148 targets human DNMT3b protein coding region. *RNA (New York, N.Y.)*. **14**(5), pp.872–7.

Epstein, M.., Achong, B.. and Barr, Y.. 1964. VIRUS PARTICLES IN CULTURED LYMPHOBLASTS FROM BURKITT'S LYMPHOMA. *Lancet (London, England)*. **1**(7335), pp.702–3.

Faller, M., Matsunaga, M., Yin, S., Loo, J.A. and Guo, F. 2007. Heme is involved in microRNA processing. *Nature structural & molecular biology*. **14**(1), pp.23–9.

Fasken, M.B. and Corbett, A.H. 2009. Mechanisms of nuclear mRNA quality control. *RNA biology*. **6**(3), pp.237–41.

Fauquet, C., Mayo, M.A., Maniloff, J., Desselberger, U. and Ball, L.A. 2005. *Virus taxonomy: Eighth report of the international committee on taxonomy of viruses*. Elsevier/Academic Press.

Favoreel, H.W., Van Minnebruggen, G., Adriaensen, D. and Nauwynck, H.J. 2005. Cytoskeletal rearrangements and cell extensions induced by the US3 kinase of an alphaherpesvirus are associated with enhanced spread. *Proceedings of the National Academy of Sciences of the United States of America*. **102**(25), pp.8990–5.

Fingeroth, J.D., Weis, J.J., Tedder, T.F., Strominger, J.L., Biro, P.A. and Fearon, D.T. 1984. Epstein-Barr virus receptor of human B lymphocytes is the C3d receptor CR2. *Proceedings of the National Academy of Sciences of the United States of America*. **81**(14), pp.4510–4.

Flaño, E., Kim, I.-J., Woodland, D.L. and Blackman, M.A. 2002. Gamma-herpesvirus latency is preferentially maintained in splenic germinal center and memory B cells. *The Journal of experimental medicine*. **196**(10), pp.1363–72.

França, G.S., Hinske, L.C., Galante, P.A.F. and Vibranovski, M.D. 2017. Unveiling the Impact of the Genomic Architecture on the Evolution of Vertebrate microRNAs. *Frontiers in genetics*. **8**(MAR), p.34.

Friborg, J., Kong, W., Hottiger, M.O. and Nabel, G.J. 1999. p53 inhibition by the LANA protein of KSHV protects against cell death. *Nature*. **402**(6764), pp.889–94.

Fu, Y., Zhang, L., Zhang, R., Xu, S., Wang, H., Jin, Y. and Wu, Z. 2019. Enterovirus 71 Suppresses miR-17-92 Cluster Through Up-Regulating Methylation of the miRNA Promoter. *Frontiers in microbiology*. **10**(MAR), p.625.

Fuchs Wightman, F., Giono, L.E., Fededa, J.P. and de la Mata, M. 2018. Target RNAs Strike Back on MicroRNAs. *Frontiers in genetics*. **9**(OCT), p.435.

Furlong, D., Swift, H. and Roizman, B. 1972. Arrangement of herpesvirus deoxyribonucleic acid in the core. *Journal of virology*. **10**(5), pp.1071–4.

Ganem, D. 2007. *KSHV-induced oncogenesis* [Online]. Cambridge University Press. [Accessed 23 October 2021]. Available from: https://www.ncbi.nlm.nih.gov/books/NBK47373/.

Ganem, D. 2010. KSHV and the pathogenesis of Kaposi sarcoma: listening to human biology and medicine. *The Journal of clinical investigation*. **120**(4), pp.939–49.

Garrigues, H.J., Rubinchikova, Y.E., Dipersio, C.M. and Rose, T.M. 2008. Integrin alphaVbeta3 Binds to the RGD motif of glycoprotein B of Kaposi's sarcoma-associated herpesvirus and functions as an RGD-dependent entry receptor. *Journal of virology*. **82**(3), pp.1570–80.

Gaur, A., Jewell, D.A., Liang, Y., Ridzon, D., Moore, J.H., Chen, C., Ambros, V.R. and Israel, M.A. 2007. Characterization of microRNA expression levels and their biological correlates in human cancer cell lines. *Cancer research*. **67**(6), pp.2456–68.

Genz, B., Coleman, M.A., Irvine, K.M., Kutasovic, J.R., Miranda, M., Gratte, F.D., Tirnitz-Parker, J.E.E., Olynyk, J.K., Calvopina, D.A., Weis, A., Cloonan, N., Robinson, H., Hill, M.M., Al-Ejeh, F. and Ramm, G.A. 2019. Overexpression of miRNA-25-3p inhibits Notch1 signaling and TGF-β-induced collagen expression in hepatic stellate cells. *Scientific reports*. **9**(1), p.8541.

Gill, M.B., Turner, R., Stevenson, P.G. and Way, M. 2015. KSHV-TK is a tyrosine kinase that disrupts focal adhesions and induces Rho-mediated cell contraction. *The EMBO journal*. **34**(4), pp.448–65.

Given, D. and Kieff, E. 1979. DNA of Epstein-Barr virus. VI. Mapping of the internal tandem reiteration. *Journal of virology*. **31**(2), pp.315–24.

Glaich, O., Parikh, S., Bell, R.E., Mekahel, K., Donyo, M., Leader, Y., Shayevitch, R., Sheinboim, D., Yannai, S., Hollander, D., Melamed, Z., Lev-Maor, G., Ast, G. and Levy, C. 2019. DNA methylation directs microRNA biogenesis in mammalian cells. *Nature communications*. **10**(1), p.5657.

Glaunsinger, B. and Ganem, D. 2004. Lytic KSHV infection inhibits host gene expression by accelerating global mRNA turnover. *Molecular cell*. **13**(5), pp.713–23.

Gong, D., Kim, Y.H., Xiao, Y., Du, Y., Xie, Y., Lee, K.K., Feng, J., Farhat, N., Zhao, D., Shu, S., Dai, X., Chanda, S.K., Rana, T.M., Krogan, N.J., Sun, R. and Wu, T.-T. 2016. A Herpesvirus Protein Selectively Inhibits Cellular mRNA Nuclear Export. *Cell host & microbe*. **20**(5), pp.642–653.

Gottwein, E., Cai, X. and Cullen, B.R. 2006. Expression and function of microRNAs encoded by Kaposi's sarcoma-associated herpesvirus. *Cold Spring Harbor symposia on quantitative biology*. **71**, pp.357–64.

Gottwein, E., Corcoran, D.L., Mukherjee, N., Skalsky, R.L., Hafner, M., Nusbaum, J.D., Shamulailatpam, P., Love, C.L., Dave, S.S., Tuschl, T., Ohler, U. and Cullen, B.R. 2011. Viral microRNA targetome of KSHV-infected primary effusion lymphoma cell lines. *Cell host & microbe*. **10**(5), pp.515–26.

Gould, F., Harrison, S.M., Hewitt, E.W. and Whitehouse, A. 2009. Kaposi's sarcoma-

associated herpesvirus RTA promotes degradation of the Hey1 repressor protein through the ubiquitin proteasome pathway. *Journal of virology*. **83**(13), pp.6727–38.

Gramolelli, S. and Ojala, P.M. 2017. Kaposi's sarcoma herpesvirus-induced endothelial cell reprogramming supports viral persistence and contributes to Kaposi's sarcoma tumorigenesis. *Current opinion in virology*. **26**, pp.156–162.

Gregory, R.I., Yan, K.-P., Amuthan, G., Chendrimada, T., Doratotaj, B., Cooch, N. and Shiekhattar, R. 2004. The Microprocessor complex mediates the genesis of microRNAs. *Nature*. **432**(7014), pp.235–40.

Greifenegger, N., Jäger, M., Kunz-Schughart, L.A., Wolf, H. and Schwarzmann, F. 1998. Epstein-Barr virus small RNA (EBER) genes: differential regulation during lytic viral replication. *Journal of virology*. **72**(11), pp.9323–8.

Griffiths, R. and Whitehouse, A. 2007. Herpesvirus saimiri episomal persistence is maintained via interaction between open reading frame 73 and the cellular chromosome-associated protein MeCP2. *Journal of virology*. **81**(8), pp.4021–32.

Grinberg, M., Gilad, S., Meiri, E., Levy, A., Isakov, O., Ronen, R., Shomron, N., Bentwich, Z. and Shemer-Avni, Y. 2012. Vaccinia virus infection suppresses the cell microRNA machinery. *Archives of virology*. **157**(9), pp.1719–27.

Grulich, A.E., Li, Y., McDonald, A.M., Correll, P.K., Law, M.G. and Kaldor, J.M. 2001. Decreasing rates of Kaposi's sarcoma and non-Hodgkin's lymphoma in the era of potent combination anti-retroviral therapy. *AIDS (London, England)*. **15**(5), pp.629–33.

Grundhoff, A. and Ganem, D. 2004. Inefficient establishment of KSHV latency suggests an additional role for continued lytic replication in Kaposi sarcoma pathogenesis. *The Journal of clinical investigation*. **113**(1), pp.124–36.

Gu, F., Wang, C., Wei, F., Wang, Y., Zhu, Q., Ding, L., Xu, W., Zhu, C., Cai, C., Qian, Z., Yuan, Z., Robertson, E. and Cai, Q. 2018. STAT6 degradation and ubiquitylated TRIML2 are essential for activation of human oncogenic herpesvirus. *PLoS pathogens*. **14**(12), p.e1007416.

Guo, Y.E., Riley, K.J., Iwasaki, A. and Steitz, J.A. 2014. Alternative capture of noncoding RNAs or protein-coding genes by herpesviruses to alter host T cell function. *Molecular cell*. **54**(1), pp.67–79.

Gutiérrez-Vázquez, C., Enright, A.J., Rodríguez-Galán, A., Pérez-García, A., Collier, P., Jones, M.R., Benes, V., Mizgerd, J.P., Mittelbrunn, M., Ramiro, A.R. and Sánchez-Madrid, F. 2017. 3' Uridylation controls mature microRNA turnover during CD4 T-cell activation. *RNA (New York, N.Y.)*. **23**(6), pp.882–891.

Ha, M. and Kim, V.N. 2014. Regulation of microRNA biogenesis. *Nature reviews.*

Molecular cell biology. **15**(8), pp.509–24.

Haas, G., Cetin, S., Messmer, M., Chane-Woon-Ming, B., Terenzi, O., Chicher, J., Kuhn, L., Hammann, P. and Pfeffer, S. 2016. Identification of factors involved in target RNA-directed microRNA degradation. *Nucleic acids research*. **44**(6), pp.2873–87.

Han, J., Lee, Y., Yeom, K.-H., Kim, Y.-K., Jin, H. and Kim, V.N. 2004. The Drosha-DGCR8 complex in primary microRNA processing. *Genes & development*. **18**(24), pp.3016–27.

Han, J., Pedersen, J.S., Kwon, S.C., Belair, C.D., Kim, Y.-K., Yeom, K.-H., Yang, W.-Y., Haussler, D., Blelloch, R. and Kim, V.N. 2009. Posttranscriptional crossregulation between Drosha and DGCR8. *Cell*. **136**(1), pp.75–84.

Han, Z. and Swaminathan, S. 2006. Kaposi's sarcoma-associated herpesvirus lytic gene ORF57 is essential for infectious virion production. *Journal of virology*. **80**(11), pp.5251–60.

Hancock, M.H., Hook, L.M., Mitchell, J. and Nelson, J.A. 2017. Human Cytomegalovirus MicroRNAs miR-US5-1 and miR-UL112-3p Block Proinflammatory Cytokine Production in Response to NF-κB-Activating Factors through Direct Downregulation of IKKα and IKKβ. *mBio*. **8**(2).

Hanna, J., Hossain, G.S. and Kocerha, J. 2019. The Potential for microRNA Therapeutics and Clinical Research. *Frontiers in genetics*. **10**(MAY), p.478.

Haque, M., Davis, D.A., Wang, V., Widmer, I. and Yarchoan, R. 2003. Kaposi's Sarcoma-Associated Herpesvirus (Human Herpesvirus 8) Contains Hypoxia Response Elements: Relevance to Lytic Induction by Hypoxia. *Journal of Virology*. **77**(12), pp.6761–6768.

Harper, K.L., Mottram, T.J., Anene, C.A., Foster, B., Patterson, M.R., McDonnell, E., Macdonald, A., Westhead, D. and Whitehouse, A. 2022. Dysregulation of the miR-30c/DLL4 axis by circHIPK3 is essential for KSHV lytic replication. *EMBO reports*., p.e54117.

Hashemi, M., Eskandari-Nasab, E., Zakeri, Z., Atabaki, M., Bahari, G., Jahantigh, M., Taheri, M. and Ghavami, S. 2013. Association of pre-miRNA-146a rs2910164 and pre-miRNA-499 rs3746444 polymorphisms and susceptibility to rheumatoid arthritis. *Molecular medicine reports*. **7**(1), pp.287–91.

Hauser, A.S., Chavali, S., Masuho, I., Jahn, L.J., Martemyanov, K.A., Gloriam, D.E. and Babu, M.M. 2018. Pharmacogenomics of GPCR Drug Targets. *Cell*. **172**(1–2), pp.41-54.e19.

Hausser, J., Syed, A.P., Bilen, B. and Zavolan, M. 2013. Analysis of CDS-located miRNA target sites suggests that they can effectively inhibit translation. *Genome research*. **23**(4), pp.604–15.

Helwak, A., Kudla, G., Dudnakova, T. and Tollervey, D. 2013. Mapping the human miRNA interactome by CLASH reveals frequent noncanonical binding. *Cell*. **153**(3), pp.654–65.

Hinske, L.C., França, G.S., Torres, H.A.M., Ohara, D.T., Lopes-Ramos, C.M., Heyn, J., Reis, L.F.L., Ohno-Machado, L., Kreth, S. and Galante, P.A.F. 2014. miRIAD-integrating microRNA inter- and intragenic data. *Database : the journal of biological databases and curation*. **2014**.

Hollinshead, M., Johns, H.L., Sayers, C.L., Gonzalez-Lopez, C., Smith, G.L. and Elliott, G. 2012. Endocytic tubules regulated by Rab GTPases 5 and 11 are used for envelopment of herpes simplex virus. *The EMBO journal*. **31**(21), pp.4204–20.

Homa, F.L. and Brown, J.C. 1997. Capsid assembly and DNA packaging in herpes simplex virus - PubMed. *Rev Med Virol*. [Online], pp.107–122. [Accessed 23 February 2022]. Available from: https://pubmed.ncbi.nlm.nih.gov/10398476/.

Honess, R.W. 1984. Herpes simplex and 'the herpes complex': diverse observations and a unifying hypothesis. The eighth Fleming lecture. *The Journal of general virology*. **65 (Pt 12**, pp.2077–107.

Honess, R.W. and Roizman, B. 1974. Regulation of herpesvirus macromolecular synthesis. I. Cascade regulation of the synthesis of three groups of viral proteins. *Journal of virology*. **14**(1), pp.8–19.

Hou, J., Wang, P., Lin, L., Liu, X., Ma, F., An, H., Wang, Z. and Cao, X. 2009. MicroRNA-146a feedback inhibits RIG-I-dependent Type I IFN production in macrophages by targeting TRAF6, IRAK1, and IRAK2. *Journal of immunology (Baltimore, Md. : 1950)*. **183**(3), pp.2150–8.

Hu, H.Y., Yan, Z., Xu, Y., Hu, H., Menzel, C., Zhou, Y.H., Chen, W. and Khaitovich, P. 2009. Sequence features associated with microRNA strand selection in humans and flies. *BMC genomics*. **10**, p.413.

Hum, C., Loiselle, J., Ahmed, N., Shaw, T.A., Toudic, C. and Pezacki, J.P. 2021. MicroRNA Mimics or Inhibitors as Antiviral Therapeutic Approaches Against COVID-19. *Drugs*. **81**(5), pp.517–531.

Humphreys, D.T., Westman, B.J., Martin, D.I.K. and Preiss, T. 2005. MicroRNAs control translation initiation by inhibiting eukaryotic initiation factor 4E/cap and poly(A) tail function. *Proceedings of the National Academy of Sciences of the United States of America*. **102**(47), pp.16961–6.

Hussein, M. and Magdy, R. 2021. MicroRNAs in central nervous system disorders: current advances in pathogenesis and treatment. *Egyptian Journal of Neurology, Psychiatry and Neurosurgery*. **57**(1), pp.1–11.

Ipsaro, J.J. and Joshua-Tor, L. 2015. From guide to target: molecular insights into

eukaryotic RNA-interference machinery. *Nature structural & molecular biology*. **22**(1), pp.20–8.

Iwasaki, S., Kobayashi, M., Yoda, M., Sakaguchi, Y., Katsuma, S., Suzuki, T. and Tomari, Y. 2010. Hsc70/Hsp90 chaperone machinery mediates ATP-dependent RISC loading of small RNA duplexes. *Molecular cell*. **39**(2), pp.292–9.

Jackson, B.R., Noerenberg, M. and Whitehouse, A. 2014. A novel mechanism inducing genome instability in Kaposi's sarcoma-associated herpesvirus infected cells. *PLoS pathogens*. **10**(5), p.e1004098.

Jeong, J.H., Orvis, J., Kim, J.W., McMurtrey, C.P., Renne, R. and Dittmer, D.P. 2004. Regulation and autoregulation of the promoter for the latency-associated nuclear antigen of Kaposi's sarcoma-associated herpesvirus. *The Journal of biological chemistry*. **279**(16), pp.16822–31.

Johannsen, E., Luftig, M., Chase, M.R., Weicksel, S., Cahir-McFarland, E., Illanes, D., Sarracino, D. and Kieff, E. 2004. Proteins of purified Epstein-Barr virus. *Proceedings of the National Academy of Sciences of the United States of America*. **101**(46), pp.16286–91.

Jopling, C.L., Yi, M., Lancaster, A.M., Lemon, S.M. and Sarnow, P. 2005. Modulation of hepatitis C virus RNA abundance by a liver-specific MicroRNA. *Science (New York, N.Y.)*. **309**(5740), pp.1577–81.

Juźwik, C.A., S Drake, S., Zhang, Y., Paradis-Isler, N., Sylvester, A., Amar-Zifkin, A., Douglas, C., Morquette, B., Moore, C.S. and Fournier, A.E. 2019. microRNA dysregulation in neurodegenerative diseases: A systematic review. *Progress in neurobiology*. **182**, p.101664.

Kang, D., Skalsky, R.L. and Cullen, B.R. 2015. EBV BART MicroRNAs Target Multiple Pro-apoptotic Cellular Genes to Promote Epithelial Cell Survival. *PLoS pathogens*. **11**(6), p.e1004979.

Kang, J.-G., Pripuzova, N., Majerciak, V., Kruhlak, M., Le, S.-Y. and Zheng, Z.-M. 2011. Kaposi's sarcoma-associated herpesvirus ORF57 promotes escape of viral and human interleukin-6 from microRNA-mediated suppression. *Journal of virology*. **85**(6), pp.2620–30.

Kang, M.-S. and Kieff, E. 2015. Epstein-Barr virus latent genes. *Experimental & molecular medicine*. **47**(1), p.e131.

Kaposi 1872. Idiopathisches multiples Pigmentsarkom der Haut. *Archiv für Dermatologie und Syphilis*. **4**(2), pp.265–273.

Kaschka-Dierich, C., Werner, F.J., Bauer, I. and Fleckenstein, B. 1982. Structure of nonintegrated, circular Herpesvirus saimiri and Herpesvirus ateles genomes in tumor cell lines and in vitro-transformed cells. *Journal of virology*. **44**(1), pp.295–

310.

Kaul, D., Ahlawat, A. and Gupta, S.D. 2009. HIV-1 genome-encoded hiv1-mir-H1 impairs cellular responses to infection. *Molecular and cellular biochemistry*. **323**(1–2), pp.143–8.

Kawa, K., Okamura, T., Yagi, K., Takeuchi, M., Nakayama, M. and Inoue, M. 2001. Mosquito allergy and Epstein-Barr virus-associated T/natural killer-cell lymphoproliferative disease. *Blood*. **98**(10), pp.3173–4.

Kawahara, Y., Zinshteyn, B., Chendrimada, T.P., Shiekhattar, R. and Nishikura, K. 2007. RNA editing of the microRNA-151 precursor blocks cleavage by the Dicer-TRBP complex. *EMBO reports*. **8**(8), pp.763–9.

Kawahara, Y., Zinshteyn, B., Sethupathy, P., Iizasa, H., Hatzigeorgiou, A.G. and Nishikura, K. 2007. Redirection of silencing targets by adenosine-to-inosine editing of miRNAs. *Science (New York, N.Y.)*. **315**(5815), pp.1137–40.

Kedes, D.H., Operskalski, E., Busch, M., Kohn, R., Flood, J. and Ganem, D. 1996. The seroepidemiology of human herpesvirus 8 (Kaposi's sarcoma-associated herpesvirus): distribution of infection in KS risk groups and evidence for sexual transmission. *Nature medicine*. **2**(8), pp.918–24.

Kelly, B.J., Fraefel, C., Cunningham, A.L. and Diefenbach, R.J. 2009. Functional roles of the tegument proteins of herpes simplex virus type 1. *Virus research*. **145**(2), pp.173–86.

Khoury, J., Willner, C.A., Gbadamosi, B., Gaikazian, S. and Jaiyesimi, I. 2018. Demographics and Survival in Primary Effusion Lymphoma: SEER Database Analysis. *Blood*. **132**(Supplement 1), pp.5397–5397.

Kieffer-Kwon, P., Happel, C., Uldrick, T.S., Ramalingam, D. and Ziegelbauer, J.M. 2015. KSHV MicroRNAs Repress Tropomyosin 1 and Increase Anchorage-Independent Growth and Endothelial Tube Formation. *PloS one*. **10**(8), p.e0135560.

Kim, J., Inoue, K., Ishii, J., Vanti, W.B., Voronov, S. V, Murchison, E., Hannon, G. and Abeliovich, A. 2007. A MicroRNA feedback circuit in midbrain dopamine neurons. *Science (New York, N.Y.)*. **317**(5842), pp.1220–4.

Klase, Z., Winograd, R., Davis, J., Carpio, L., Hildreth, R., Heydarian, M., Fu, S., McCaffrey, T., Meiri, E., Ayash-Rashkovsky, M., Gilad, S., Bentwich, Z. and Kashanchi, F. 2009. HIV-1 TAR miRNA protects against apoptosis by altering cellular gene expression. *Retrovirology*. **6**, p.18.

Konno, M., Koseki, J., Asai, A., Yamagata, A., Shimamura, T., Motooka, D., Okuzaki, D., Kawamoto, K., Mizushima, T., Eguchi, H., Takiguchi, S., Satoh, T., Mimori, K., Ochiya, T., Doki, Y., Ofusa, K., Mori, M. and Ishii, H. 2019. Distinct methylation levels of mature microRNAs in gastrointestinal cancers. *Nature communications*. **10**(1),

p.3888.

Krol, J., Loedige, I. and Filipowicz, W. 2010. The widespread regulation of microRNA biogenesis, function and decay. *Nature reviews. Genetics*. **11**(9), pp.597–610.

Kurth, J., Spieker, T., Wustrow, J., Strickler, G.J., Hansmann, L.M., Rajewsky, K. and Küppers, R. 2000. EBV-infected B cells in infectious mononucleosis: viral strategies for spreading in the B cell compartment and establishing latency. *Immunity*. **13**(4), pp.485–95.

de la Mata, M., Gaidatzis, D., Vitanescu, M., Stadler, M.B., Wentzel, C., Scheiffele, P., Filipowicz, W. and Großhans, H. 2015. Potent degradation of neuronal miRNAs induced by highly complementary targets. *EMBO reports*. **16**(4), pp.500–11.

Lane, C.A., Hardy, J. and Schott, J.M. 2018. Alzheimer's disease. *European journal of neurology*. **25**(1), pp.59–70.

Langhorst, M.F., Solis, G.P., Hannbeck, S., Plattner, H. and Stuermer, C.A.O. 2007. Linking membrane microdomains to the cytoskeleton: regulation of the lateral mobility of reggie-1/flotillin-2 by interaction with actin. *FEBS letters*. **581**(24), pp.4697–703.

Langmead, B. and Salzberg, S.L. 2012. Fast gapped-read alignment with Bowtie 2. *Nature methods*. **9**(4), pp.357–9.

Lee, H.Y., Zhou, K., Smith, A.M., Noland, C.L. and Doudna, J.A. 2013. Differential roles of human Dicer-binding proteins TRBP and PACT in small RNA processing. *Nucleic acids research*. **41**(13), pp.6568–76.

Lee, I., Ajay, S.S., Yook, J.I., Kim, H.S., Hong, S.H., Kim, N.H., Dhanasekaran, S.M., Chinnaiyan, A.M. and Athey, B.D. 2009. New class of microRNA targets containing simultaneous 5'-UTR and 3'-UTR interaction sites. *Genome research*. **19**(7), pp.1175–83.

Lee, R.C., Feinbaum, R.L. and Ambros, V. 1993. The C. elegans heterochronic gene lin-4 encodes small RNAs with antisense complementarity to lin-14. *Cell*. **75**(5), pp.843–54.

Lee, S., Song, J., Kim, S., Kim, J., Hong, Y., Kim, Y., Kim, D., Baek, D. and Ahn, K. 2013. Selective degradation of host MicroRNAs by an intergenic HCMV noncoding RNA accelerates virus production. *Cell host & microbe*. **13**(6), pp.678–90.

Lee, Y., Ahn, C., Han, J., Choi, H., Kim, J., Yim, J., Lee, J., Provost, P., Rådmark, O., Kim, S. and Kim, V.N. 2003. The nuclear RNase III Drosha initiates microRNA processing. *Nature*. **425**(6956), pp.415–9.

Lee, Y., Kim, M., Han, J., Yeom, K.-H., Lee, S., Baek, S.H. and Kim, V.N. 2004. MicroRNA genes are transcribed by RNA polymerase II. *The EMBO journal*. **23**(20), pp.4051–60.

Lei, X., Bai, Z., Ye, F., Xie, J., Kim, C.-G., Huang, Y. and Gao, S.-J. 2010. Regulation of NF-kappaB inhibitor IkappaBalpha and viral replication by a KSHV microRNA. *Nature cell biology*. **12**(2), pp.193–9.

Letang, E., Lewis, J.J., Bower, M., Mosam, A., Borok, M., Campbell, T.B., Naniche, D., Newsom-Davis, T., Shaik, F., Fiorillo, S., Miro, J.M., Schellenberg, D. and Easterbrook, P.J. 2013. Immune reconstitution inflammatory syndrome associated with Kaposi sarcoma: higher incidence and mortality in Africa than in the UK. *AIDS (London, England)*. **27**(10), pp.1603–13.

Leuschner, P.J.F., Ameres, S.L., Kueng, S. and Martinez, J. 2006. Cleavage of the siRNA passenger strand during RISC assembly in human cells. *EMBO reports*. **7**(3), pp.314–20.

Lewis, B.P., Shih, I., Jones-Rhoades, M.W., Bartel, D.P. and Burge, C.B. 2003. Prediction of mammalian microRNA targets. *Cell*. **115**(7), pp.787–98.

Li, Q., Turk, S.M. and Hutt-Fletcher, L.M. 1995. The Epstein-Barr virus (EBV) BZLF2 gene product associates with the gH and gL homologs of EBV and carries an epitope critical to infection of B cells but not of epithelial cells. *Journal of virology*. **69**(7), pp.3987–94.

Li, Q.X., Young, L.S., Niedobitek, G., Dawson, C.W., Birkenbach, M., Wang, F. and Rickinson, A.B. 1992. Epstein-Barr virus infection and replication in a human epithelial cell system. *Nature*. **356**(6367), pp.347–50.

Li, T. and Gao, S.-J. 2021. Metabolic reprogramming and metabolic sensors in KSHV-induced cancers and KSHV infection. *Cell & bioscience*. **11**(1), p.176.

Li, X., Fu, Z., Liang, H., Wang, Y., Qi, X., Ding, M., Sun, X., Zhou, Z., Huang, Y., Gu, H., Li, L., Chen, X., Li, D., Zhao, Q., Liu, F., Wang, H., Wang, J., Zen, K. and Zhang, C.-Y. 2018. H5N1 influenza virus-specific miRNA-like small RNA increases cytokine production and mouse mortality via targeting poly(rC)-binding protein 2. *Cell research*. **28**(2), pp.157–171.

Liang, D., Gao, Y., Lin, X., He, Z., Zhao, Q., Deng, Q. and Lan, K. 2011. A human herpesvirus miRNA attenuates interferon signaling and contributes to maintenance of viral latency by targeting IKKε. *Cell research*. **21**(5), pp.793–806.

Liang, H., Jiao, Z., Rong, W., Qu, S., Liao, Z., Sun, X., Wei, Y., Zhao, Q., Wang, J., Liu, Y., Chen, X., Wang, T., Zhang, C.-Y. and Zen, K. 2020. 3'-Terminal 2'-O-methylation of lung cancer miR-21-5p enhances its stability and association with Argonaute 2. *Nucleic acids research*. **48**(13), pp.7027–7040.

Liang, Y., Chang, J., Lynch, S.J., Lukac, D.M. and Ganem, D. 2002. The lytic switch protein of KSHV activates gene expression via functional interaction with RBP-Jkappa (CSL), the target of the Notch signaling pathway. *Genes & development*. **16**(15), pp.1977–89.

Libri, V., Helwak, A., Miesen, P., Santhakumar, D., Borger, J.G., Kudla, G., Grey, F., Tollervey, D. and Buck, A.H. 2012. Murine cytomegalovirus encodes a miR-27 inhibitor disguised as a target. *Proceedings of the National Academy of Sciences of the United States of America*. **109**(1), pp.279–84.

Lieberman, P.M. 2016. Epigenetics and Genetics of Viral Latency. *Cell Host & Microbe*. **19**(5), pp.619–628.

Lindquester, G.J. and Pellett, P.E. 1991. Properties of the human herpesvirus 6 strain Z29 genome: G + C content, length, and presence of variable-length directly repeated terminal sequence elements. *Virology*. **182**(1), pp.102–10.

Liu, C., Zhang, L., Xu, R. and Zheng, H. 2018. miR-26b Inhibits Virus Replication Through Positively Regulating Interferon Signaling. *Viral immunology*. **31**(10), pp.676–682.

Liu, J., Li, W., Wang, Siwen, Wu, Y., Li, Z., Wang, W., Liu, R., Ou, J., Zhang, C. and Wang, Shenming 2014. MiR-142-3p attenuates the migration of $CD4^+$ T cells through regulating actin cytoskeleton via RAC1 and ROCK2 in arteriosclerosis obliterans. *PloS one*. **9**(4), p.e95514.

Liu, L., Eby, M.T., Rathore, N., Sinha, S.K., Kumar, A. and Chaudhary, P.M. 2002. The human herpes virus 8-encoded viral FLICE inhibitory protein physically associates with and persistently activates the Ikappa B kinase complex. *The Journal of biological chemistry*. **277**(16), pp.13745–51.

Liu, P., Cao, F., Sui, J., Hong, Y., Liu, Q., Gao, X.H., Gong, H., Hao, L., Lou, Z. and Zhang, W. 2020. MicroRNA-142-3p Inhibits Tumorigenesis of Colorectal Cancer via Suppressing the Activation of Wnt Signaling by Directly Targeting to β-Catenin. *Frontiers in Oncology*. **10**, p.3339.

Liu, Q., Wang, J., Zhao, Y., Li, C.-I., Stengel, K.R., Acharya, P., Johnston, G., Hiebert, S.W. and Shyr, Y. 2017. Identification of active miRNA promoters from nuclear run-on RNA sequencing. *Nucleic acids research*. **45**(13), p.e121.

Liu, W., MacDonald, M. and You, J. 2016. Merkel cell polyomavirus infection and Merkel cell carcinoma. *Current opinion in virology*. **20**, pp.20–27.

Lozano-Romero, A., Astudillo-de la Vega, H., Terrones-Gurrola, M.C.D.R., Marchat, L.A., Hernández-Sotelo, D., Salinas-Vera, Y.M., Ramos-Payan, R., Silva-Cázares, M.B., Nuñez-Olvera, S.I., Hernández-de la Cruz, O.N. and López-Camarillo, C. 2020. HOX Transcript Antisense RNA HOTAIR Abrogates Vasculogenic Mimicry by Targeting the AngiomiR-204/FAK Axis in Triple Negative Breast Cancer Cells. *Non-coding RNA*. **6**(2).

Lu, F., Weidmer, A., Liu, C.-G., Volinia, S., Croce, C.M. and Lieberman, P.M. 2008. Epstein-Barr virus-induced miR-155 attenuates NF-kappaB signaling and stabilizes latent virus persistence. *Journal of virology*. **82**(21), pp.10436–43.

Lu, L.J., Tsai, J.C. and Liu, J. 2017. Novel Pharmacologic Candidates for Treatment of Primary Open-Angle Glaucoma. *The Yale journal of biology and medicine*. **90**(1), pp.111–118.

Lubyova, B. and Pitha, P.M. 2000. Characterization of a novel human herpesvirus 8-encoded protein, vIRF-3, that shows homology to viral and cellular interferon regulatory factors. *Journal of virology*. **74**(17), pp.8194–201.

Ludwig, N., Leidinger, P., Becker, K., Backes, C., Fehlmann, T., Pallasch, C., Rheinheimer, S., Meder, B., Stähler, C., Meese, E. and Keller, A. 2016. Distribution of miRNA expression across human tissues. *Nucleic acids research*. **44**(8), pp.3865–77.

Lukac, D.M., Kirshner, J.R. and Ganem, D. 1999. Transcriptional activation by the product of open reading frame 50 of Kaposi's sarcoma-associated herpesvirus is required for lytic viral reactivation in B cells. *Journal of virology*. **73**(11), pp.9348–61.

Lukac, D.M., Renne, R., Kirshner, J.R. and Ganem, D. 1998. Reactivation of Kaposi's sarcoma-associated herpesvirus infection from latency by expression of the ORF 50 transactivator, a homolog of the EBV R protein. *Virology*. **252**(2), pp.304–12.

Luna, J.M., Scheel, T.K.H., Danino, T., Shaw, K.S., Mele, A., Fak, J.J., Nishiuchi, E., Takacs, C.N., Catanese, M.T., de Jong, Y.P., Jacobson, I.M., Rice, C.M. and Darnell, R.B. 2015. Hepatitis C virus RNA functionally sequesters miR-122. *Cell*. **160**(6), pp.1099–110.

Lund, E., Güttinger, S., Calado, A., Dahlberg, J.E. and Kutay, U. 2004. Nuclear export of microRNA precursors. *Science (New York, N.Y.)*. **303**(5654), pp.95–8.

Lytle, J.R., Yario, T.A. and Steitz, J.A. 2007. Target mRNAs are repressed as efficiently by microRNA-binding sites in the 5' UTR as in the 3' UTR. *Proceedings of the National Academy of Sciences of the United States of America*. **104**(23), pp.9667–72.

Mabit, H., Nakano, M.Y., Prank, U., Saam, B., Döhner, K., Sodeik, B. and Greber, U.F. 2002. Intact microtubules support adenovirus and herpes simplex virus infections. *Journal of virology*. **76**(19), pp.9962–71.

Machlin, E.S., Sarnow, P. and Sagan, S.M. 2011. Masking the 5' terminal nucleotides of the hepatitis C virus genome by an unconventional microRNA-target RNA complex. *Proceedings of the National Academy of Sciences of the United States of America*. **108**(8), pp.3193–8.

Majerciak, V., Lu, M., Li, X. and Zheng, Z.-M. 2014. Attenuation of the suppressive activity of cellular splicing factor SRSF3 by Kaposi sarcoma-associated herpesvirus ORF57 protein is required for RNA splicing. *RNA (New York, N.Y.)*. **20**(11), pp.1747–58.

Majerciak, V., Yamanegi, K., Allemand, E., Kruhlak, M., Krainer, A.R. and Zheng, Z.-M. 2008. Kaposi's sarcoma-associated herpesvirus ORF57 functions as a viral splicing factor and promotes expression of intron-containing viral lytic genes in spliceosome-mediated RNA splicing. *Journal of virology*. **82**(6), pp.2792–801.

Majerciak, V. and Zheng, Z.-M. 2015. KSHV ORF57, a protein of many faces. *Viruses*. **7**(2), pp.604–33.

Mansoori, B., Mohammadi, A., Ghasabi, M., Shirjang, S., Dehghan, R., Montazeri, V., Holmskov, U., Kazemi, T., Duijf, P., Gjerstorff, M. and Baradaran, B. 2019. miR-142-3p as tumor suppressor miRNA in the regulation of tumorigenicity, invasion and migration of human breast cancer by targeting Bach-1 expression. *Journal of cellular physiology*. **234**(6), pp.9816–9825.

Martinez, V., Caumes, E., Gambotti, L., Ittah, H., Morini, J.-P., Deleuze, J., Gorin, I., Katlama, C., Bricaire, F. and Dupin, N. 2006. Remission from Kaposi's sarcoma on HAART is associated with suppression of HIV replication and is independent of protease inhibitor therapy. *British journal of cancer*. **94**(7), pp.1000–6.

Masaki, T., Arend, K.C., Li, Y., Yamane, D., McGivern, D.R., Kato, T., Wakita, T., Moorman, N.J. and Lemon, S.M. 2015. miR-122 stimulates hepatitis C virus RNA synthesis by altering the balance of viral RNAs engaged in replication versus translation. *Cell host & microbe*. **17**(2), pp.217–28.

Massimelli, M.J., Kang, J.-G., Majerciak, V., Le, S.-Y., Liewehr, D.J., Steinberg, S.M. and Zheng, Z.-M. 2011. Stability of a long noncoding viral RNA depends on a 9-nt core element at the RNA 5' end to interact with viral ORF57 and cellular PABPC1. *International journal of biological sciences*. **7**(8), pp.1145–60.

Matta, H., Sun, Q., Moses, G. and Chaudhary, P.M. 2003. Molecular genetic analysis of human herpes virus 8-encoded viral FLICE inhibitory protein-induced NF-kappaB activation. *The Journal of biological chemistry*. **278**(52), pp.52406–11.

Matthews, R.E. 1979. Third report of the International Committee on Taxonomy of Viruses. Classification and nomenclature of viruses. *Intervirology*. **12**(3–5), pp.129–296.

Maurer, T., Ponte, M. and Leslie, K. 2007. HIV-associated Kaposi's sarcoma with a high CD4 count and a low viral load. *The New England journal of medicine*. **357**(13), pp.1352–3.

McCormick, C. and Ganem, D. 2005. The kaposin B protein of KSHV activates the p38/MK2 pathway and stabilizes cytokine mRNAs. *Science (New York, N.Y.)*. **307**(5710), pp.739–41.

McGeoch, D.J., Cook, S., Dolan, A., Jamieson, F.E. and Telford, E.A. 1995. Molecular phylogeny and evolutionary timescale for the family of mammalian herpesviruses. *Journal of molecular biology*. **247**(3), pp.443–58.

McGeoch, D.J., Davison, A.J., Dolan, A., Gatherer, D. and Sevilla-Reyes, E.E. 2008. Molecular Evolution of the Herpesvirales. *Origin and Evolution of Viruses*., pp.447–475.

Mehta, A. and Baltimore, D. 2016. MicroRNAs as regulatory elements in immune system logic. *Nature reviews. Immunology*. **16**(5), pp.279–94.

Meijer, H.A., Smith, E.M. and Bushell, M. 2014. Regulation of miRNA strand selection: follow the leader? *Biochemical Society transactions*. **42**(4), pp.1135–40.

Mettenleiter, T.C. 2002. Herpesvirus assembly and egress. *Journal of virology*. **76**(4), pp.1537–47.

Mettenleiter, T.C., Klupp, B.G. and Granzow, H. 2009. Herpesvirus assembly: an update. *Virus research*. **143**(2), pp.222–34.

Miller, N. and Hutt-Fletcher, L.M. 1992. Epstein-Barr virus enters B cells and epithelial cells by different routes. *Journal of virology*. **66**(6), pp.3409–14.

Möhl, B.S., Chen, J. and Longnecker, R. 2019. Gammaherpesvirus entry and fusion: A tale how two human pathogenic viruses enter their host cells. *Advances in virus research*. **104**, pp.313–343.

Morales, S., Monzo, M. and Navarro, A. 2017. Epigenetic regulation mechanisms of microRNA expression. *Biomolecular concepts*. **8**(5–6), pp.203–212.

Moron-Lopez, S., Bernal, S., Wong, J.K., Martinez-Picado, J. and Yukl, S.A. 2021. ABX464 Decreases the Total Human Immunodeficiency Virus (HIV) Reservoir and HIV Transcription Initiation in CD4+ T Cells From Antiretroviral Therapy–Suppressed Individuals Living With HIV. *Clinical Infectious Diseases*.

Muralidhar, S., Pumfery, A.M., Hassani, M., Sadaie, M.R., Kishishita, M., Brady, J.N., Doniger, J., Medveczky, P. and Rosenthal, L.J. 1998. Identification of kaposin (open reading frame K12) as a human herpesvirus 8 (Kaposi's sarcoma-associated herpesvirus) transforming gene. *Journal of virology*. **72**(6), pp.4980–8.

Nador, R.G., Cesarman, E., Chadburn, A., Dawson, D.B., Ansari, M.Q., Said, J. and Knowles, D.M. 1996. Primary Effusion Lymphoma: A Distinct Clinicopathologic Entity Associated With the Kaposi's Sarcoma-Associated Herpes Virus. *Blood*. **88**(2), pp.645–656.

Nam, J.-W., Rissland, O.S., Koppstein, D., Abreu-Goodger, C., Jan, C.H., Agarwal, V., Yildirim, M.A., Rodriguez, A. and Bartel, D.P. 2014. Global analyses of the effect of different cellular contexts on microRNA targeting. *Molecular cell*. **53**(6), pp.1031–1043.

Nicholas, J. 2007. Human herpesvirus 8-encoded proteins with potential roles in virus-associated neoplasia. *Frontiers in bioscience : a journal and virtual library*. **12**(1), pp.265–81.

Nishimura, M. and Mori, Y. 2019. Entry of betaherpesviruses. *Advances in virus research*. **104**, pp.283–312.

Ohsaki, E., Suzuki, T., Karayama, M. and Ueda, K. 2009. Accumulation of LANA at nuclear matrix fraction is important for Kaposi's sarcoma-associated herpesvirus replication in latency. *Virus research*. **139**(1), pp.74–84.

Okada, S., Ueda, H., Noda, Y. and Suzuki, T. 2019. Transcriptome-wide identification of A-to-I RNA editing sites using ICE-seq. *Methods*. **156**, pp.66–78.

Oksenhendler, E., Carcelain, G., Aoki, Y., Boulanger, E., Maillard, A., Clauvel, J.P. and Agbalika, F. 2000. High levels of human herpesvirus 8 viral load, human interleukin-6, interleukin-10, and C reactive protein correlate with exacerbation of multicentric Castleman disease in HIV-infected patients. *Blood*. **96**(6), pp.2069–2073.

Omoto, S., Ito, M., Tsutsumi, Y., Ichikawa, Y., Okuyama, H., Brisibe, E.A., Saksena, N.K. and Fujii, Y.R. 2004. HIV-1 nef suppression by virally encoded microRNA. *Retrovirology*. **1**, p.44.

Otto, G.A. and Puglisi, J.D. 2004. The pathway of HCV IRES-mediated translation initiation. *Cell*. **119**(3), pp.369–80.

Otto, G.P. and Nichols, B.J. 2011. The roles of flotillin microdomains--endocytosis and beyond. *Journal of cell science*. **124**(Pt 23), pp.3933–40.

Ouellet, D.L., Plante, I., Landry, P., Barat, C., Janelle, M.-E., Flamand, L., Tremblay, M.J. and Provost, P. 2008. Identification of functional microRNAs released through asymmetrical processing of HIV-1 TAR element. *Nucleic acids research*. **36**(7), pp.2353–65.

Owen, C.B. 2015. Utilising Omics Approaches to Understand Kaposi's Sarcoma-associated Herpesvirus. *White Rose eTheses Online. University of Leeds*.

Ozsolak, F., Poling, L.L., Wang, Z., Liu, H., Liu, X.S., Roeder, R.G., Zhang, X., Song, J.S. and Fisher, D.E. 2008. Chromatin structure analyses identify miRNA promoters. *Genes & development*. **22**(22), pp.3172–83.

Pallesen, G., Hamilton-Dutoit, S.J., Rowe, M. and Young, L.S. 1991. Expression of Epstein-Barr virus latent gene products in tumour cells of Hodgkin's disease. *Lancet (London, England)*. **337**(8737), pp.320–2.

Pan, D., Flores, O., Umbach, J.L., Pesola, J.M., Bentley, P., Rosato, P.C., Leib, D.A., Cullen, B.R. and Coen, D.M. 2014. A neuron-specific host microRNA targets herpes simplex virus-1 ICP0 expression and promotes latency. *Cell host & microbe*. **15**(4), pp.446–56.

Panda, A.C. 2018. Circular RNAs Act as miRNA Sponges. *Advances in experimental medicine and biology*. **1087**, pp.67–79.

Park, J.-E., Heo, I., Tian, Y., Simanshu, D.K., Chang, H., Jee, D., Patel, D.J. and Kim, V.N. 2011. Dicer recognizes the 5' end of RNA for efficient and accurate processing. *Nature*. **475**(7355), pp.201–5.

Parkin, D.M., Sitas, F., Chirenje, M., Stein, L., Abratt, R. and Wabinga, H. 2008. Part I: Cancer in Indigenous Africans--burden, distribution, and trends. *The Lancet. Oncology*. **9**(7), pp.683–92.

De Paschale, M. and Clerici, P. 2012. Serological diagnosis of Epstein-Barr virus infection: Problems and solutions. *World journal of virology*. **1**(1), pp.31–43.

Pauk, J., Huang, M.L., Brodie, S.J., Wald, A., Koelle, D.M., Schacker, T., Celum, C., Selke, S. and Corey, L. 2000. Mucosal shedding of human herpesvirus 8 in men. *The New England journal of medicine*. **343**(19), pp.1369–77.

Paul, P., Chakraborty, A., Sarkar, D., Langthasa, M., Rahman, M., Bari, M., Singha, R.S., Malakar, A.K. and Chakraborty, S. 2018. Interplay between miRNAs and human diseases. *Journal of cellular physiology*. **233**(3), pp.2007–2018.

Peng, Y. and Croce, C.M. 2016. The role of MicroRNAs in human cancer. *Signal transduction and targeted therapy*. **1**.

Petersen, C.P., Bordeleau, M.-E., Pelletier, J. and Sharp, P.A. 2006. Short RNAs repress translation after initiation in mammalian cells. *Molecular cell*. **21**(4), pp.533–42.

Pfaller, C.K., Donohue, R.C., Nersisyan, S., Brodsky, L. and Cattaneo, R. 2018. Extensive editing of cellular and viral double-stranded RNA structures accounts for innate immunity suppression and the proviral activity of ADAR1p150. *PLoS biology*. **16**(11), p.e2006577.

Pfeffer, S., Sewer, A., Lagos-Quintana, M., Sheridan, R., Sander, C., Grässer, F.A., van Dyk, L.F., Ho, C.K., Shuman, S., Chien, M., Russo, J.J., Ju, J., Randall, G., Lindenbach, B.D., Rice, C.M., Simon, V., Ho, D.D., Zavolan, M. and Tuschl, T. 2005. Identification of microRNAs of the herpesvirus family. *Nature methods*. **2**(4), pp.269–76.

Pfeffer, S., Zavolan, M., Grässer, F.A., Chien, M., Russo, J.J., Ju, J., John, B., Enright, A.J., Marks, D., Sander, C. and Tuschl, T. 2004. Identification of virus-encoded microRNAs. *Science (New York, N.Y.)*. **304**(5671), pp.734–6.

Pietrek, M., Brinkmann, M.M., Glowacka, I., Enlund, A., Hävemeier, A., Dittrich-Breiholz, O., Kracht, M., Lewitzky, M., Saksela, K., Feller, S.M. and Schulz, T.F. 2010. Role of the Kaposi's sarcoma-associated herpesvirus K15 SH3 binding site in inflammatory signaling and B-cell activation. *Journal of virology*. **84**(16), pp.8231–40.

Polizzotto, M.N., Uldrick, T.S., Wyvill, K.M., Aleman, K., Marshall, V., Wang, V., Whitby, D., Pittaluga, S., Jaffe, E.S., Millo, C., Tosato, G., Little, R.F., Steinberg, S.M., Sereti, I. and Yarchoan, R. 2016. Clinical Features and Outcomes of Patients With Symptomatic Kaposi Sarcoma Herpesvirus (KSHV)-associated Inflammation: Prospective Characterization of KSHV Inflammatory Cytokine Syndrome (KICS). *Clinical infectious diseases : an official publication of the Infectious Diseases Society of America*. **62**(6), pp.730–738.

Polizzotto, M.N., Uldrick, T.S., Wyvill, K.M., Aleman, K., Peer, C.J., Bevans, M., Sereti, I., Maldarelli, F., Whitby, D., Marshall, V., Goncalves, P.H., Khetani, V., Figg, W.D., Steinberg, S.M., Zeldis, J.B. and Yarchoan, R. 2016. Pomalidomide for Symptomatic Kaposi's Sarcoma in People With and Without HIV Infection: A Phase I/II Study. *Journal of clinical oncology : official journal of the American Society of Clinical Oncology*. **34**(34), pp.4125–4131.

Qin, H., Ni, H., Liu, Y., Yuan, Y., Xi, T., Li, X. and Zheng, L. 2020. RNA-binding proteins in tumor progression. *Journal of hematology & oncology*. **13**(1), p.90.

Ramírez-Moya, J., Baker, A.R., Slack, F.J. and Santisteban, P. 2020. ADAR1-mediated RNA editing is a novel oncogenic process in thyroid cancer and regulates miR-200 activity. *Oncogene*. **39**(18), pp.3738–3753.

Ramkissoon, S.H., Mainwaring, L.A., Ogasawara, Y., Keyvanfar, K., McCoy, J.P., Sloand, E.M., Kajigaya, S. and Young, N.S. 2006. Hematopoietic-specific microRNA expression in human cells. *Leukemia research*. **30**(5), pp.643–7.

Rappocciolo, G., Hensler, H.R., Jais, M., Reinhart, T.A., Pegu, A., Jenkins, F.J. and Rinaldo, C.R. 2008. Human herpesvirus 8 infects and replicates in primary cultures of activated B lymphocytes through DC-SIGN. *Journal of virology*. **82**(10), pp.4793–806.

van der Ree, M.H., van der Meer, A.J., de Bruijne, J., Maan, R., van Vliet, A., Welzel, T.M., Zeuzem, S., Lawitz, E.J., Rodriguez-Torres, M., Kupcova, V., Wiercinska-Drapalo, A., Hodges, M.R., Janssen, H.L.A. and Reesink, H.W. 2014. Long-term safety and efficacy of microRNA-targeted therapy in chronic hepatitis C patients. *Antiviral research*. **111**, pp.53–9.

van der Ree, M.H., van der Meer, A.J., van Nuenen, A.C., de Bruijne, J., Ottosen, S., Janssen, H.L., Kootstra, N.A. and Reesink, H.W. 2016. Miravirsen dosing in chronic hepatitis C patients results in decreased microRNA-122 levels without affecting other microRNAs in plasma. *Alimentary pharmacology & therapeutics*. **43**(1), pp.102–13.

Reed, R. and Hurt, E. 2002. A conserved mRNA export machinery coupled to pre-mRNA splicing. *Cell*. **108**(4), pp.523–31.

Renne, R., Barry, C., Dittmer, D., Compitello, N., Brown, P.O. and Ganem, D. 2001. Modulation of cellular and viral gene expression by the latency-associated nuclear antigen of Kaposi's sarcoma-associated herpesvirus. *Journal of virology*. **75**(1), pp.458–68.

Rivas, C., Thlick, A.E., Parravicini, C., Moore, P.S. and Chang, Y. 2001. Kaposi's sarcoma-associated herpesvirus LANA2 is a B-cell-specific latent viral protein that inhibits p53. *Journal of virology*. **75**(1), pp.429–38.

Rodríguez-Galán, A., Dosil, S.G., Gómez, M.J., Fernández-Delgado, I., Fernández-Messina,

L., Sánchez-Cabo, F. and Sánchez-Madrid, F. 2021. MiRNA post-transcriptional modification dynamics in T cell activation. *iScience*. **24**(6), p.102530.

Roizman, B., Carmichael, L.E., Deinhardt, F., De-The, G., Nahmias, A.J., Plowright, W., Rapp, F., Sheldrick, P., Takahashi, M. and Wolf, K. 1981. Herpesviridae. Definition, provisional nomenclature, and taxonomy. The Herpesvirus Study Group, the International Committee on Taxonomy of Viruses. *Intervirology*. **16**(4), pp.201–17.

Roizmann, B., Desrosiers, R.C., Fleckenstein, B., Lopez, C., Minson, A.C. and Studdert, M.J. 1992. The family Herpesviridae: an update. The Herpesvirus Study Group of the International Committee on Taxonomy of Viruses. *Archives of virology*. **123**(3–4), pp.425–49.

Rosato, P., Anastasiadou, E., Garg, N., Lenze, D., Boccellato, F., Vincenti, S., Severa, M., Coccia, E.M., Bigi, R., Cirone, M., Ferretti, E., Campese, A.F., Hummel, M., Frati, L., Presutti, C., Faggioni, A. and Trivedi, P. 2012. Differential regulation of miR-21 and miR-146a by Epstein-Barr virus-encoded EBNA2. *Leukemia*. **26**(11), pp.2343–52.

Rossetto, C.C., Tarrant-Elorza, M., Verma, S., Purushothaman, P. and Pari, G.S. 2013. Regulation of viral and cellular gene expression by Kaposi's sarcoma-associated herpesvirus polyadenylated nuclear RNA. *Journal of virology*. **87**(10), pp.5540–53.

Rowe, M., Rowe, D.T., Gregory, C.D., Young, L.S., Farrell, P.J., Rupani, H. and Rickinson, A.B. 1987. Differences in B cell growth phenotype reflect novel patterns of Epstein-Barr virus latent gene expression in Burkitt's lymphoma cells. *The EMBO Journal*. **6**(9), pp.2743–2751.

Ru, J., Sun, H., Fan, H., Wang, C., Li, Y., Liu, M. and Tang, H. 2014. MiR-23a facilitates the replication of HSV-1 through the suppression of interferon regulatory factor 1. *PloS one*. **9**(12), p.e114021.

Russo, J.J., Bohenzky, R.A., Chien, M.C., Chen, J., Yan, M., Maddalena, D., Parry, J.P., Peruzzi, D., Edelman, I.S., Chang, Y. and Moore, P.S. 1996. Nucleotide sequence of the Kaposi sarcoma-associated herpesvirus (HHV8). *Proceedings of the National Academy of Sciences of the United States of America*. **93**(25), pp.14862–7.

Sagan, S.M., Sarnow, P. and Wilson, J.A. 2013. Modulation of GB virus B RNA abundance by microRNA-122: dependence on and escape from microRNA-122 restriction. *Journal of virology*. **87**(13), pp.7338–47.

Sakakibara, S. and Tosato, G. 2014. Contribution of viral mimics of cellular genes to KSHV infection and disease. *Viruses*. **6**(9), pp.3472–86.

Sakurai, M., Yano, T., Kawabata, H., Ueda, H. and Suzuki, T. 2010. Inosine cyanoethylation identifies A-to-I RNA editing sites in the human transcriptome. *Nature chemical biology*. **6**(10), pp.733–40.

Salinas-Vera, Y.M., Gallardo-Rincón, D., García-Vázquez, R., Hernández-de la Cruz, O.N.,

Marchat, L.A., González-Barrios, J.A., Ruíz-García, E., Vázquez-Calzada, C., Contreras-Sanzón, E., Resendiz-Hernández, M., Astudillo-de la Vega, H., Cruz-Colin, J.L., Campos-Parra, A.D. and López-Camarillo, C. 2019. HypoxamiRs Profiling Identify miR-765 as a Regulator of the Early Stages of Vasculogenic Mimicry in SKOV3 Ovarian Cancer Cells. *Frontiers in oncology*. **9**(MAY), p.381.

Sanchez, E.L., Pulliam, T.H., Dimaio, T.A., Thalhofer, A.B., Delgado, T. and Lagunoff, M. 2017. Glycolysis, Glutaminolysis, and Fatty Acid Synthesis Are Required for Distinct Stages of Kaposi's Sarcoma-Associated Herpesvirus Lytic Replication. *Journal of virology*. **91**(10).

Sattentau, Q. 2008. Avoiding the void: cell-to-cell spread of human viruses. *Nature reviews. Microbiology*. **6**(11), pp.815–26.

Sayed, D. and Abdellatif, M. 2011. MicroRNAs in development and disease. *Physiological reviews*. **91**(3), pp.827–87.

Scadden, A.D.J. 2005. The RISC subunit Tudor-SN binds to hyper-edited double-stranded RNA and promotes its cleavage. *Nature structural & molecular biology*. **12**(6), pp.489–96.

Scheel, T.K.H., Luna, J.M., Liniger, M., Nishiuchi, E., Rozen-Gagnon, K., Shlomai, A., Auray, G., Gerber, M., Fak, J., Keller, I., Bruggmann, R., Darnell, R.B., Ruggli, N. and Rice, C.M. 2016. A Broad RNA Virus Survey Reveals Both miRNA Dependence and Functional Sequestration. *Cell host & microbe*. **19**(3), pp.409–23.

Schult, P., Roth, H., Adams, R.L., Mas, C., Imbert, L., Orlik, C., Ruggieri, A., Pyle, A.M. and Lohmann, V. 2018. microRNA-122 amplifies hepatitis C virus translation by shaping the structure of the internal ribosomal entry site. *Nature communications*. **9**(1), p.2613.

Sedano, C.D. and Sarnow, P. 2014. Hepatitis C virus subverts liver-specific miR-122 to protect the viral genome from exoribonuclease Xrn2. *Cell host & microbe*. **16**(2), pp.257–264.

Seo, G.J., Chen, C.J. and Sullivan, C.S. 2009. Merkel cell polyomavirus encodes a microRNA with the ability to autoregulate viral gene expression. *Virology*. **383**(2), pp.183–7.

Sharma, N., Verma, R., Kumawat, K.L., Basu, A. and Singh, S.K. 2015. miR-146a suppresses cellular immune response during Japanese encephalitis virus JaOArS982 strain infection in human microglial cells. *Journal of neuroinflammation*. **12**(1), p.30.

Sheldrick, P. and Berthelot, N. 1975. Inverted repetitions in the chromosome of herpes simplex virus. *Cold Spring Harbor symposia on quantitative biology*. **39 Pt 2**(2), pp.667–78.

Shen, H., An, O., Ren, X., Song, Y., Tang, S.J., Ke, X.-Y., Han, J., Tay, D.J.T., Ng, V.H.E.,

Molias, F.B., Pitcheshwar, P., Leong, K.W., Tan, K.-K., Yang, H. and Chen, L. 2022. ADARs act as potent regulators of circular transcriptome in cancer. *Nature communications*. **13**(1), p.1508.

Shen, W.-W., Zeng, Z., Zhu, W.-X. and Fu, G.-H. 2013. MiR-142-3p functions as a tumor suppressor by targeting CD133, ABCG2, and Lgr5 in colon cancer cells. *Journal of molecular medicine (Berlin, Germany)*. **91**(8), pp.989–1000.

Sinclair, A.J. 2003. bZIP proteins of human gammaherpesviruses. *The Journal of general virology*. **84**(Pt 8), pp.1941–1949.

Skalsky, R.L. and Cullen, B.R. 2010. Viruses, microRNAs, and host interactions. *Annual review of microbiology*. **64**, pp.123–41.

Skårn, M., Barøy, T., Stratford, E.W. and Myklebost, O. 2013. Epigenetic regulation and functional characterization of microRNA-142 in mesenchymal cells. *PloS one*. **8**(11), p.e79231.

Sodeik, B., Ebersold, M.W. and Helenius, A. 1997. Microtubule-mediated transport of incoming herpes simplex virus 1 capsids to the nucleus. *Journal of Cell Biology*. **136**(5), pp.1007–1021.

Song, J.-J., Smith, S.K., Hannon, G.J. and Joshua-Tor, L. 2004. Crystal structure of Argonaute and its implications for RISC slicer activity. *Science (New York, N.Y.)*. **305**(5689), pp.1434–7.

Soulier, J., Grollet, L., Oksenhendler, E., Cacoub, P., Cazals-Hatem, D., Babinet, P., D'Agay, M.F., Clauvel, J.P., Raphael, M., Degos, L. and Sigaux, F. 1995. Kaposi's Sarcoma-Associated Herpesvirus-Like DNA Sequences in Multicentric Castleman's Disease. *Blood*. **86**(4), pp.1276–1280.

Stallone, G., Schena, A., Infante, B., Di Paolo, S., Loverre, A., Maggio, G., Ranieri, E., Gesualdo, L., Schena, F.P. and Grandaliano, G. 2005. Sirolimus for Kaposi's sarcoma in renal-transplant recipients. *The New England journal of medicine*. **352**(13), pp.1317–23.

Staskus, K.A., Zhong, W., Gebhard, K., Herndier, B., Wang, H., Renne, R., Beneke, J., Pudney, J., Anderson, D.J., Ganem, D. and Haase, A.T. 1997. Kaposi's sarcoma-associated herpesvirus gene expression in endothelial (spindle) tumor cells. *Journal of virology*. **71**(1), pp.715–9.

Stevens, J.G. and Cook, M.L. 1971. Latent herpes simplex virus in spinal ganglia of mice. *Science (New York, N.Y.)*. **173**(3999), pp.843–5.

Su, S., Zhao, Q., He, C., Huang, D., Liu, J., Chen, F., Chen, J., Liao, J.-Y., Cui, X., Zeng, Y., Yao, H., Su, F., Liu, Q., Jiang, S. and Song, E. 2015. miR-142-5p and miR-130a-3p are regulated by IL-4 and IL-13 and control profibrogenic macrophage program. *Nature communications*. **6**, p.8523.

Sugawara, Y., Nishii, H., Takahashi, T., Yamauchi, J., Mizuno, N., Tago, K. and Itoh, H. 2007. The lipid raft proteins flotillins/reggies interact with Galphaq and are involved in Gq-mediated p38 mitogen-activated protein kinase activation through tyrosine kinase. *Cellular signalling*. **19**(6), pp.1301–8.

Sugiura, M., Imai, S., Tokunaga, M., Koizumi, S., Uchizawa, M., Okamoto, K. and Osato, T. 1996. Transcriptional analysis of Epstein-Barr virus gene expression in EBV-positive gastric carcinoma: unique viral latency in the tumour cells. *British journal of cancer*. **74**(4), pp.625–31.

Sung, H., Ferlay, J., Siegel, R.L., Laversanne, M., Soerjomataram, I., Jemal, A. and Bray, F. 2021. Global Cancer Statistics 2020: GLOBOCAN Estimates of Incidence and Mortality Worldwide for 36 Cancers in 185 Countries. *CA: a cancer journal for clinicians*. **71**(3), pp.209–249.

Suthaus, J., Stuhlmann-Laeisz, C., Tompkins, V.S., Rosean, T.R., Klapper, W., Tosato, G., Janz, S., Scheller, J. and Rose-John, S. 2012. HHV-8-encoded viral IL-6 collaborates with mouse IL-6 in the development of multicentric Castleman disease in mice. *Blood*. **119**(22), pp.5173–81.

Suzuki, T., Ueda, H., Okada, S. and Sakurai, M. 2015. Transcriptome-wide identification of adenosine-to-inosine editing using the ICE-seq method. *Nature protocols*. **10**(5), pp.715–32.

Syrovatkina, V., Alegre, K.O., Dey, R. and Huang, X.-Y. 2016. Regulation, Signaling, and Physiological Functions of G-Proteins. *Journal of molecular biology*. **428**(19), pp.3850–68.

Tang, S., Yamanegi, K. and Zheng, Z.-M. 2004. Requirement of a 12-base-pair TATT-containing sequence and viral lytic DNA replication in activation of the Kaposi's sarcoma-associated herpesvirus K8.1 late promoter. *Journal of virology*. **78**(5), pp.2609–14.

Tang, X., Wen, S., Zheng, D., Tucker, L., Cao, L., Pantazatos, D., Moss, S.F. and Ramratnam, B. 2013. Acetylation of drosha on the N-terminus inhibits its degradation by ubiquitination. *PloS one*. **8**(8), p.e72503.

Tang, X., Zhang, Y., Tucker, L. and Ramratnam, B. 2010. Phosphorylation of the RNase III enzyme Drosha at Serine300 or Serine302 is required for its nuclear localization. *Nucleic acids research*. **38**(19), pp.6610–9.

Taylor, G.S. and Blackbourn, D.J. 2011. Infectious agents in human cancers: lessons in immunity and immunomodulation from gammaherpesviruses EBV and KSHV. *Cancer letters*. **305**(2), pp.263–78.

Taylor, M.P., Koyuncu, O.O. and Enquist, L.W. 2011. Subversion of the actin cytoskeleton during viral infection. *Nature reviews. Microbiology*. **9**(6), pp.427–39.

Tempera, I. and Lieberman, P.M. 2014. Epigenetic regulation of EBV persistence and oncogenesis. *Seminars in cancer biology*. **26**, pp.22–9.

Thorley-Lawson, D.A. and Gross, A. 2004. Persistence of the Epstein-Barr virus and the origins of associated lymphomas. *The New England journal of medicine*. **350**(13), pp.1328–37.

Tian, Y., Simanshu, D.K., Ma, J.-B., Park, J.-E., Heo, I., Kim, V.N. and Patel, D.J. 2014. A phosphate-binding pocket within the platform-PAZ-connector helix cassette of human Dicer. *Molecular cell*. **53**(4), pp.606–16.

Tong, Z., Cui, Q., Wang, J. and Zhou, Y. 2019. TransmiR v2.0: an updated transcription factor-microRNA regulation database. *Nucleic acids research*. **47**(D1), pp.D253–D258.

Tsutsumi, A., Kawamata, T., Izumi, N., Seitz, H. and Tomari, Y. 2011. Recognition of the pre-miRNA structure by Drosophila Dicer-1. *Nature structural & molecular biology*. **18**(10), pp.1153–8.

Tu, C.-C., Zhong, Y., Nguyen, L., Tsai, A., Sridevi, P., Tarn, W.-Y. and Wang, J.Y.J. 2015. The kinase ABL phosphorylates the microprocessor subunit DGCR8 to stimulate primary microRNA processing in response to DNA damage. *Science signaling*. **8**(383), p.ra64.

Tüfekci, K.U., Meuwissen, R.L.J. and Genç, S. 2014. The role of microRNAs in biological processes. *Methods in molecular biology (Clifton, N.J.)*. **1107**, pp.15–31.

Tugizov, S.M., Berline, J.W. and Palefsky, J.M. 2003. Epstein-Barr virus infection of polarized tongue and nasopharyngeal epithelial cells. *Nature medicine*. **9**(3), pp.307–14.

Turunen, T., Hernández de Sande, A., Pölönen, P. and Heinäniemi, M. 2021. Genome-wide analysis of primary microRNA expression using H3K36me3 ChIP-seq data. *Computational and structural biotechnology journal*. **19**, pp.1944–1955.

Uldrick, T.S., Wang, V., O'Mahony, D., Aleman, K., Wyvill, K.M., Marshall, V., Steinberg, S.M., Pittaluga, S., Maric, I., Whitby, D., Tosato, G., Little, R.F. and Yarchoan, R. 2010. An interleukin-6-related systemic inflammatory syndrome in patients co-infected with Kaposi sarcoma-associated herpesvirus and HIV but without Multicentric Castleman disease. *Clinical infectious diseases : an official publication of the Infectious Diseases Society of America*. **51**(3), pp.350–8.

Uldrick, T.S. and Whitby, D. 2011. Update on KSHV epidemiology, Kaposi Sarcoma pathogenesis, and treatment of Kaposi Sarcoma. *Cancer letters*. **305**(2), pp.150–62.

Vasudevan, S. and Steitz, J.A. 2007. AU-rich-element-mediated upregulation of translation by FXR1 and Argonaute 2. *Cell*. **128**(6), pp.1105–18.

Wang, H., Peng, R., Wang, J., Qin, Z. and Xue, L. 2018. Circulating microRNAs as potential cancer biomarkers: the advantage and disadvantage. *Clinical epigenetics*. **10**(1),

p.59.

Wang, Man, Gu, B., Chen, X., Wang, Y., Li, P. and Wang, K. 2019. The Function and Therapeutic Potential of Epstein-Barr Virus-Encoded MicroRNAs in Cancer. *Molecular therapy. Nucleic acids*. **17**, pp.657–668.

Wang, Mengli, Qin, L. and Tang, B. 2019. MicroRNAs in Alzheimer's disease. *Frontiers in Genetics*. **10**(MAR), p.153.

Wang, Q., Hui, H., Guo, Z., Zhang, W., Hu, Y., He, T., Tai, Y., Peng, P. and Wang, L. 2013. ADAR1 regulates ARHGAP26 gene expression through RNA editing by disrupting miR-30b-3p and miR-573 binding. *RNA (New York, N.Y.)*. **19**(11), pp.1525–36.

Wang, S., Talukder, A., Cha, M., Li, X. and Hu, H. 2021. Computational annotation of miRNA transcription start sites. *Briefings in bioinformatics*. **22**(1), pp.380–392.

Wang, S.E., Wu, F.Y., Chen, H., Shamay, M., Zheng, Q. and Hayward, G.S. 2004. Early activation of the Kaposi's sarcoma-associated herpesvirus RTA, RAP, and MTA promoters by the tetradecanoyl phorbol acetate-induced AP1 pathway. *Journal of virology*. **78**(8), pp.4248–67.

Wang, S.E., Wu, F.Y., Fujimuro, M., Zong, J., Hayward, S.D. and Hayward, G.S. 2003. Role of CCAAT/enhancer-binding protein alpha (C/EBPalpha) in activation of the Kaposi's sarcoma-associated herpesvirus (KSHV) lytic-cycle replication-associated protein (RAP) promoter in cooperation with the KSHV replication and transcription activator (R. *Journal of virology*. **77**(1), pp.600–23.

Wang, X., Diao, C., Yang, X., Yang, Z., Liu, M., Li, X. and Tang, H. 2021. Author Correction: ICP4-induced miR-101 attenuates HSV-1 replication. *Scientific reports*. **11**(1), p.16389.

Wang, X., Wang, H.-K., McCoy, J.P., Banerjee, N.S., Rader, J.S., Broker, T.R., Meyers, C., Chow, L.T. and Zheng, Z.-M. 2009. Oncogenic HPV infection interrupts the expression of tumor-suppressive miR-34a through viral oncoprotein E6. *RNA (New York, N.Y.)*. **15**(4), pp.637–47.

Wang, X., Zhu, N., Li, W., Zhu, F., Wang, Y. and Yuan, Y. 2015. Mono-ubiquitylated ORF45 Mediates Association of KSHV Particles with Internal Lipid Rafts for Viral Assembly and Egress. *PLoS pathogens*. **11**(12), p.e1005332.

Wang, Y., Li, H., Chan, M.Y., Zhu, F.X., Lukac, D.M. and Yuan, Y. 2004. Kaposi's sarcoma-associated herpesvirus ori-Lyt-dependent DNA replication: cis-acting requirements for replication and ori-Lyt-associated RNA transcription. *Journal of virology*. **78**(16), pp.8615–29.

Wang, Z.-X., Lu, B.-B., Wang, H., Cheng, Z.-X. and Yin, Y.-M. 2011. MicroRNA-21 modulates chemosensitivity of breast cancer cells to doxorubicin by targeting PTEN. *Archives of medical research*. **42**(4), pp.281–90.

Wang, Z., Liu, Z., Fang, X. and Yang, H. 2017. MiR-142-5p Suppresses Tumorigenesis by Targeting PIK3CA in Non-Small Cell Lung Cancer. *Cellular physiology and biochemistry : international journal of experimental cellular physiology, biochemistry, and pharmacology*. **43**(6), pp.2505–2515.

Watanabe, Y., Ibrahim, M.S., Suzuki, Y. and Ikuta, K. 2012. The changing nature of avian influenza A virus (H5N1). *Trends in microbiology*. **20**(1), pp.11–20.

Webster-Cyriaque, J., Duus, K., Cooper, C. and Duncan, M. 2006. Oral EBV and KSHV infection in HIV. *Advances in dental research*. **19**(1), pp.91–5.

Whitby, D., Howard, M.R., Tenant-Flowers, M., Brink, N.S., Copas, A., Boshoff, C., Hatzioannou, T., Suggett, F.E., Aldam, D.M. and Denton, A.S. 1995. Detection of Kaposi sarcoma associated herpesvirus in peripheral blood of HIV-infected individuals and progression to Kaposi's sarcoma. *Lancet (London, England)*. **346**(8978), pp.799–802.

Whitley, R.J. 1996. *Herpesviruses* [Online]. Elsevier. [Accessed 7 April 2020]. Available from: http://www.ncbi.nlm.nih.gov/pubmed/21413307.

Whitley, R.J. and Roizman, B. 2001. Herpes simplex virus infections. *Lancet (London, England)*. **357**(9267), pp.1513–8.

Wilson, A.C. and Mohr, I. 2012. A cultured affair: HSV latency and reactivation in neurons. *Trends in microbiology*. **20**(12), pp.604–11.

Wilson, S.J., Tsao, E.H., Webb, B.L.J., Ye, H., Dalton-Griffin, L., Tsantoulas, C., Gale, C. V, Du, M.-Q., Whitehouse, A. and Kellam, P. 2007. X box binding protein XBP-1s transactivates the Kaposi's sarcoma-associated herpesvirus (KSHV) ORF50 promoter, linking plasma cell differentiation to KSHV reactivation from latency. *Journal of virology*. **81**(24), pp.13578–86.

Winkle, M., El-Daly, S.M., Fabbri, M. and Calin, G.A. 2021. Noncoding RNA therapeutics - challenges and potential solutions. *Nature reviews. Drug discovery*. **20**(8), pp.629–651.

Wu, F.Y., Ahn, J.H., Alcendor, D.J., Jang, W.J., Xiao, J., Hayward, S.D. and Hayward, G.S. 2001. Origin-independent assembly of Kaposi's sarcoma-associated herpesvirus DNA replication compartments in transient cotransfection assays and association with the ORF-K8 protein and cellular PML. *Journal of virology*. **75**(3), pp.1487–506.

Wu, S., He, L., Li, Y., Wang, T., Feng, L., Jiang, L., Zhang, P. and Huang, X. 2013. miR-146a facilitates replication of dengue virus by dampening interferon induction by targeting TRAF6. *The Journal of infection*. **67**(4), pp.329–41.

Xiao, M., Li, J., Li, W., Wang, Y., Wu, F., Xi, Y., Zhang, L., Ding, C., Luo, H., Li, Y., Peng, L., Zhao, L., Peng, S., Xiao, Y., Dong, S., Cao, J. and Yu, W. 2017. MicroRNAs activate gene transcription epigenetically as an enhancer trigger. *RNA biology*. **14**(10),

pp.1326–1334.

Xu, T., He, B.-S., Pan, B., Pan, Y.-Q., Sun, H.-L., Liu, X.-X., Xu, X.-N., Chen, X.-X., Zeng, K.-X., Xu, M. and Wang, S.-K. 2020. MiR-142-3p functions as a tumor suppressor by targeting RAC1/PAK1 pathway in breast cancer. *Journal of cellular physiology*. **235**(5), pp.4928–4940.

Yan, Q., Li, W., Tang, Q., Yao, S., Lv, Z., Feng, N., Ma, X., Bai, Z., Zeng, Y., Qin, D. and Lu, C. 2013. Cellular microRNAs 498 and 320d regulate herpes simplex virus 1 induction of Kaposi's sarcoma-associated herpesvirus lytic replication by targeting RTA. *PloS one*. **8**(2), p.e55832.

Yan, Q., Ma, X., Shen, C., Cao, X., Feng, N., Qin, D., Zeng, Y., Zhu, J., Gao, S.-J. and Lu, C. 2014. Inhibition of Kaposi's sarcoma-associated herpesvirus lytic replication by HIV-1 Nef and cellular microRNA hsa-miR-1258. *Journal of virology*. **88**(9), pp.4987–5000.

Yang, W., Chendrimada, T.P., Wang, Q., Higuchi, M., Seeburg, P.H., Shiekhattar, R. and Nishikura, K. 2006. Modulation of microRNA processing and expression through RNA editing by ADAR deaminases. *Nature structural & molecular biology*. **13**(1), pp.13–21.

Yang, Z., Yan, Z. and Wood, C. 2008. Kaposi's sarcoma-associated herpesvirus transactivator RTA promotes degradation of the repressors to regulate viral lytic replication. *Journal of virology*. **82**(7), pp.3590–603.

Ye, F., Lei, X. and Gao, S.-J. 2011. Mechanisms of Kaposi's Sarcoma-Associated Herpesvirus Latency and Reactivation. *Advances in virology*. **2011**.

Ye, X., Huang, N., Liu, Y., Paroo, Z., Huerta, C., Li, P., Chen, S., Liu, Q. and Zhang, H. 2011. Structure of C3PO and mechanism of human RISC activation. *Nature structural & molecular biology*. **18**(6), pp.650–7.

Yi, R., Qin, Y., Macara, I.G. and Cullen, B.R. 2003. Exportin-5 mediates the nuclear export of pre-microRNAs and short hairpin RNAs. *Genes & development*. **17**(24), pp.3011–6.

Yoda, M., Kawamata, T., Paroo, Z., Ye, X., Iwasaki, S., Liu, Q. and Tomari, Y. 2010. ATP-dependent human RISC assembly pathways. *Nature structural & molecular biology*. **17**(1), pp.17–23.

Young, L.S. and Rickinson, A.B. 2004. Epstein-Barr virus: 40 years on. *Nature reviews. Cancer*. **4**(10), pp.757–68.

Yuan, W., Sun, W., Yang, S., Du, J., Zhai, C.-L., Wang, Z.-Q., Zhang, J. and Zhu, T.-H. 2008. Downregulation of microRNA-142 by proto-oncogene LMO2 and its co-factors. *Leukemia*. **22**(5), pp.1067–71.

van Zandwijk, N., Pavlakis, N., Kao, S.C., Linton, A., Boyer, M.J., Clarke, S., Huynh, Y.,

Chrzanowska, A., Fulham, M.J., Bailey, D.L., Cooper, W.A., Kritharides, L., Ridley, L., Pattison, S.T., MacDiarmid, J., Brahmbhatt, H. and Reid, G. 2017. Safety and activity of microRNA-loaded minicells in patients with recurrent malignant pleural mesothelioma: a first-in-man, phase 1, open-label, dose-escalation study. *The Lancet. Oncology*. **18**(10), pp.1386–1396.

Zhang, H., Ni, G. and Damania, B. 2020. ADAR1 Facilitates KSHV Lytic Reactivation by Modulating the RLR-Dependent Signaling Pathway. *Cell reports*. **31**(4), p.107564.

Zhang, Y., Qian, H., Xu, J. and Gao, W. 2019. ADAR, the carcinogenesis mechanisms of ADAR and related clinical applications. *Annals of translational medicine*. **7**(22), p.686.

Zhao, J., Liu, X., Xia, W., Zhang, Y. and Wang, C. 2020. Targeting Amyloidogenic Processing of APP in Alzheimer's Disease. *Frontiers in molecular neuroscience*. **13**, p.137.

Zheng, S., Li, Y., Zhang, Y., Li, X. and Tang, H. 2011. MiR-101 regulates HSV-1 replication by targeting ATP5B. *Antiviral research*. **89**(3), pp.219–26.

Zhou, H. and Rigoutsos, I. 2014. The emerging roles of GPRC5A in diseases. *Oncoscience*. **1**(12), pp.765–76.

Zhou, S., Yang, C., Zhao, F., Huang, Y., Lin, Y., Huang, C., Ma, X., Du, J., Wang, Y., Long, G., He, J., Liu, C. and Zhang, P. 2019. Double-stranded RNA deaminase ADAR1 promotes the Zika virus replication by inhibiting the activation of protein kinase PKR. *The Journal of biological chemistry*. **294**(48), pp.18168–18180.

Zhu, F.X., Cusano, T. and Yuan, Y. 1999. Identification of the immediate-early transcripts of Kaposi's sarcoma-associated herpesvirus. *Journal of virology*. **73**(7), pp.5556–67.